

Micro/Nanoencapsulation of Active Food Ingredients

ACS SYMPOSIUM SERIES **1007**

Micro/Nanoencapsulation of Active Food Ingredients

Qingrong Huang, Editor

Rutgers, The State University of New Jersey

Peter Given, Editor

Pepsi-Cola Company

Michael Qian, Editor

Oregon State University

**Sponsored by the
ACS Division of Agricultural and Food Chemistry, Inc.**



American Chemical Society, Washington, DC



The paper used in this publication meets the minimum requirements of American National Standard for Information Sciences—Permanence of Paper for Printed Library Materials, ANSI Z39.48 1984.

ISBN: 978-0-8412-6964-4

Copyright © 2009 American Chemical Society

Distributed by Oxford University Press

All Rights Reserved. Reprographic copying beyond that permitted by Sections 107 or 108 of the U.S. Copyright Act is allowed for internal use only, provided that a per-chapter fee of \$40.25 plus \$0.75 per page is paid to the Copyright Clearance Center, Inc., 222 Rosewood Drive, Danvers, MA 01923, USA. Republication or reproduction for sale of pages in this book is permitted only under license from ACS. Direct these and other permission requests to ACS Copyright Office, Publications Division, 1155 16th Street, N.W., Washington, DC 20036.

The citation of trade names and/or names of manufacturers in this publication is not to be construed as an endorsement or as approval by ACS of the commercial products or services referenced herein; nor should the mere reference herein to any drawing, specification, chemical process, or other data be regarded as a license or as a conveyance of any right or permission to the holder, reader, or any other person or corporation, to manufacture, reproduce, use, or sell any patented invention or copyrighted work that may in any way be related thereto. Registered names, trademarks, etc., used in this publication, even without specific indication thereof, are not to be considered unprotected by law.

PRINTED IN THE UNITED STATES OF AMERICA

Foreword

The ACS Symposium Series was first published in 1974 to provide a mechanism for publishing symposia quickly in book form. The purpose of the series is to publish timely, comprehensive books developed from ACS sponsored symposia based on current scientific research. Occasionally, books are developed from symposia sponsored by other organizations when the topic is of keen interest to the chemistry audience.

Before agreeing to publish a book, the proposed table of contents is reviewed for appropriate and comprehensive coverage and for interest to the audience. Some papers may be excluded to better focus the book; others may be added to provide comprehensiveness. When appropriate, overview or introductory chapters are added. Drafts of chapters are peer-reviewed prior to final acceptance or rejection, and manuscripts are prepared in camera-ready format.

As a rule, only original research papers and original review papers are included in the volumes. Verbatim reproductions of previously published papers are not accepted.

ACS Books Department

Preface

The functional food market value worldwide is now worth more than \$72 billion. Driven by the increasing consumer demand for novel food products, as well as increased fortification with healthy food ingredients, the functional food market is expected to increase at an annual growth rate of 5.7% between 2007 and 2012 (<http://www.foodsciencecentral.com>). However, many volatile flavors and health promoting ingredients, such as conjugated linoleic acid, and Omega-3 fatty acids are not stable during processing and handling. To enhance ingredient stability and nutritional quality of functional foods, an option is to encapsulate the functional ingredients using food-grade materials that can exhibit controlled release. Traditional encapsulation techniques, such as spray drying, spray chilling and cooling, fluidized bed coating, rotational suspension separation, extrusion, and inclusion complexation, have been developed and widely used in food or pharmaceutical industries. However, traditional encapsulation technologies still have many limitations. Continuous innovation in delivery systems for active ingredients will enable novel food product development that includes value-added ingredients, foods with extended shelf-life, or novel food materials with improved functionality that also meet or exceed consumer taste expectations.

Food Nanotechnology implies (1) novel phenomena, properties, and functions at nanoscale; and (2) the ability to manipulate matter at the nanoscale in order to provide beneficial properties and functions. Encapsulation and controlled-release of active food ingredients are important applications in food science that can be attained with either micro- or nanotechnological approaches. Micro- and nanoencapsulation technologies continue to grow in both

scope and potential in recent years, driven mainly by the pharmaceutical and cosmetic industries. Adoption and applications of these technologies in food systems have led the way to many innovations such as enhancing the bioavailability of nutraceuticals and other nutrients which have poor body-absorption in their original forms, preserving flavor profiles during food processing, and providing mechanisms for targeted release of beneficial ingredients at specific sites of the human gastrointestinal tract, etc.

This book originated from a symposium titled, *Micro/Nano Encapsulation of Active Food Ingredients*, sponsored by the American Chemical Society (ACS) Division of Agricultural and Food Chemistry, Inc. and 21 sponsor companies. The goal of this symposium series is to bring together prominent scientists in the fields of flavors, nutraceuticals, emulsions, and food biopolymers to share their insights and approaches, and highlight the most up-to-date knowledge in encapsulation and controlled release technologies for food applications. In addition, the fundamental science behind capsule design and formation is also included in this book. In Chapters 1–3, structural design principles, assembly and disassembly, and theoretical simulation method for multilayer biopolymer capsules are reported. In Chapters 4–9, and chapter 12, various new proteins (i.e., milk proteins and corn zein), lipid, and surfactant-based delivery systems have been developed to encapsulate active food ingredients. In Chapters 10 and 11, state-of-the-art characterization methods, such as diffusion wave spectroscopy and small-angle X-ray scattering have been used to monitor either interactions or lipid crystallization in oil-in-water (O/W) emulsions. From Chapters 13–18, various micro- and nanoencapsulation technologies have been developed to address the practical problems of poor oral bioavailability of nutraceuticals and low stability of flavors. This book will serve as a useful reference for scientists and students in a variety of disciplines, including food science and engineering, physical chemistry, materials science, chemical engineering, and colloid chemistry. Researchers in the universities, industry, and government laboratories will find the book of particular interest as it provides a cross section of the most up-to-date progress in this fast-growing area.

We are indebted to the authors who contributed to this book and shared their vast knowledge in preparing a state-of-the art infor-

mation package for those interested in the area of micro- and nanoencapsulation, and the sponsor companies for their financial support.

Qingrong Huang

Department of Food Science
Rutgers University,
65 Dudley Road, New Brunswick,
New Jersey 08901.

Peter Given

Pepsi-Cola Company
100 Stevens Ave.
Valhalla, New York 10595

Michael Qian

Department of Food Science
Oregon State University
Corvallis, Oregon 97331

Acknowledgments

- (1) All of the presenters
- (2) Agnes Rimando—AgFd Program Chair
- (3) Wally Yokoyama—organizer of special award speaker roster
- (4) Cynthia Mussinan—AgFd Treasurer

Symposium Organizers

Qingrong (Ron) Huang, Rutgers University
Michael Qian, Oregon State University
Peter Given, Pepsi-Cola Company

Corporate Sponsors

ADM
Bunge
Cargill
Denomega
Firmenich
Frito-Lay
GAT
IFF
Mastertaste
McCormick
National Starch

Pepperidge Farm
Pepsi-Cola
Robertet
San-Ei Gen
Symrise
Takasago
Unilever
Virginia Dare
Wild Flavours
Wrigley

New Strategies of Designing Micro- and Nanoencapsulation Systems

Chapter 1

Structural Design Principles for Improved Food Performance: Nanolaminated Biopolymer Structures in Foods

David Julian McClements

Biopolymers and Colloids Research Laboratory, Department of Food Science, University of Massachusetts, Amherst, MA 01003

The bulk physicochemical, sensory and physiological attributes of most foods are determined by the characteristics, interactions and structural organization of the various ingredients they contain. Biopolymers are important functional ingredients in many foods, contributing to their overall texture, stability, appearance, flavor and nutritional quality. An improved understanding of the molecular and physicochemical basis of biopolymer functionality in foods can lead to the design of improved or novel functional attributes into foods. This chapter describes how nanolaminated layers can be formed from food biopolymers, and highlights their potential applications within the food industry. Electrostatic layer-by-layer (LbL) deposition of charged biopolymers can be used to form nano-structured interfacial layers with specific properties, *e.g.*, charge, thickness, porosity, permeability, responsiveness. These layers may be formed around macroscopic, microscopic or nanoscopic materials, and are therefore applicable to a wide range of food categories. Systematic manipulation of interfacial properties can be used to create materials with novel functional attributes, *e.g.*, improved stability to environmental stresses or controlled release characteristics. The potential of this technique is highlighted using recent studies on the formation of nanolaminated coatings on microscopic lipid droplets and macroscopic hydrogel surfaces.

Introduction

There are a wide number of different lipophilic components within the food industry that need to be delivered in an edible form, including bioactive lipids, vitamins, flavors, antimicrobials and antioxidants *e.g.*, ω -3 fatty acids, phytosterols, lycopene, lutein, β -carotene, coenzyme A, vitamins A and D, citrus oils, essential oils [1-4]. In many cases, it is advantageous to deliver these lipophilic components in an aqueous medium because this increases their stability, palatability, desirability and bioactivity. For example, an active lipophilic component might be incorporated into a beverage or food that could easily be consumed by drinking or eating. Nevertheless, there are often a variety of technical challenges that need to be overcome before an active lipophilic component can be successfully incorporated into an aqueous-based delivery system. Lipophilic active components come in a wide variety of different molecular forms, which lead to differences in their physicochemical and physiological properties, such as chemical stability, physical state, solubility, rheology, optical properties, and bioactivity. Consequently, different delivery systems are usually needed to address specific molecular, physicochemical and physiological concerns associated with each active component. In general, an edible delivery system must have a number of attributes:

- It must be capable of efficiently encapsulating an appreciable amount of functional agent and keeping it entrapped.
- It may have to protect the functional agent from chemical degradation so that it remains in its active state.
- It may have to control the release of the functional agent, *e.g.*, the release rate or the specific environmental stimuli that triggers release.
- It may have to be compatible with the surrounding food or beverage matrix, without causing any adverse effects on product appearance, rheology, mouth feel, flavor or shelf life.
- It may have to resist the environmental stresses foods or beverages experience during their production, storage, transport and utilization *e.g.*, heating, chilling, freezing, dehydration, or shearing.
- It should be prepared completely from generally recognized as safe (GRAS) ingredients using simple cost-effective processing operations.
- It should not adversely impact the bioavailability of the encapsulated material.

A wide variety of different types of delivery system have been developed to encapsulate lipophilic functional agents, including simple solutions, association colloids, emulsions, biopolymer matrices, powders, *etc.* Each type of delivery system has its own advantages and disadvantages for encapsulation, protection

and delivery of functional agents, as well as in its cost, regulatory status, ease of use, biodegradability, biocompatibility *etc.*

This chapter will begin by introducing the basic principles of structural design for creating delivery systems with improved stability and novel functional performance. We will then focus on a particular structural design principle based on layer-by-layer (LbL) electrostatic deposition that can be used to form nanolaminated coatings around microscopic and macroscopic objects. The potential of this method for creating emulsion-based delivery systems with improved stability to environmental stresses will then be demonstrated. Finally, the potential of using the LbL technique to form laminated functional coatings on macroscopic food surfaces (such as fruits, vegetables, fish and meats) will be highlighted.

Structural Design Principles

In this section, a brief outline of the major building blocks available to create food grade delivery systems, as well as the major molecular interactions and structural design principles that can be used to assemble them into functional systems is given.

Building Blocks

The major building blocks that can be used to assemble food-grade delivery systems are outlined below:

- *Lipids*. Lipids are predominantly non-polar substances that are highly hydrophobic. In the food industry, the main sources of lipids are triacylglycerols, which may come from animal, fish, or plant origins. Lipids can be used to solubilize non-polar lipophilic components in foods, and are commonly used in delivery systems based on emulsions or microemulsions.
- *Surfactants*. Surfactants are surface-active molecules that consist of a hydrophilic head group and a lipophilic tail group. The functional performance of a specific surfactant depends on the molecular characteristics of its head and tail groups. Food-grade surfactants come in a variety of different molecular structures. Their head groups may vary in physical dimensions and electrical charge (positive, negative, zwitterionic or non-ionic), while their tail groups may vary in number (typically one or two), length (typically 10 to 20 carbons per chain) and degree of saturation (saturated or unsaturated). Surfactants are typically used to form emulsions,

association colloids or biopolymer complexes that are suitable for use as delivery systems.

- *Biopolymers.* The two most common classes of biopolymer used as structure forming materials in the food industry are proteins and polysaccharides. Ultimately, the functional performance of food biopolymers (*e.g.*, solubility, self-association, binding and surface activity) is determined by their unique molecular characteristics (*e.g.*, molecular weight, conformation, flexibility, polarity, hydrophobicity and interactions). These molecular characteristics are determined by the type, number and sequence of the monomers that make up the polymer chain. The monomers vary according to their polarity, charge, physical dimensions, molecular interactions and chemical reactivity. Biopolymers may adopt a variety of conformations in food systems, which can be conveniently divided into three broad categories: globular, rod-like or random coil. Globular biopolymers have fairly rigid compact structures, rod-like biopolymers have fairly rigid extended structures (usually helical), and random-coil biopolymers have highly dynamic and flexible structures. In practice, many biopolymers do not have exclusively one type of conformation, but have some regions that are random coil, some that are rod-like and some that are globular. Biopolymers can also be classified according to the degree of branching of the chain. Most proteins have linear chains, whereas polysaccharides can have either linear or branched chains. In solution, biopolymers may be present as individual molecules or they may be present as supra-molecular structures where they are associated with one or more molecules of the same or different kind. Finally, it should be mentioned that biopolymers may undergo transitions from one conformation to another, or from one aggregation state to another, if their environment is altered, *e.g.*, pH, ionic strength, solvent composition or temperature. The conformation and interactions of biopolymers play a major role in determining their ability to form structured delivery systems.

Some of the most important food-grade components that are available as building blocks to form structured delivery systems are listed in Table 1. The choice of a particular food-grade component depends on the type of structure that needs to be formed, as well as its legal status, cost, usage levels, ingredient compatibility, stability and ease of utilization.

Molecular Interactions

Knowledge of the origin and nature of the various molecular forces that act between food components is also important for understanding how to assemble delivery systems with specific structures from food grade ingredients:

Table 1. Major food-grade structural components that can be used to construct delivery systems for nutraceuticals.

Name	Important Characteristics	Examples
<i>Lipids</i>	Chemical stability Melting profile Polarity	<i>Animal fats:</i> beef, pork, chicken <i>Fish oils:</i> cod liver, menhedan, salmon, tuna <i>Plant oils:</i> palm, coconut, sunflower, safflower, corn, flax seed, soybean <i>Flavor oils:</i> lemon, orange
<i>Surfactants</i>	Solubility (HLB) Charge Molecular geometry Surface load	<i>Non-ionic:</i> Tween, Span <i>Anionic:</i> SLS, DATEM, CITREM <i>Cationic:</i> Lauric Arginate <i>Zwitterionic:</i> lecithin
<i>Biopolymers</i>	Molar Mass Conformation Charge Hydrophobicity Flexibility	<i>Globular Proteins:</i> whey, soy, egg <i>Flexible Proteins:</i> casein, gelatin <i>Non-ionic Polysaccharides:</i> Starch, Dextran, Agar, Galactomannans, Cellulose <i>Anionic Polysaccharides:</i> Alginate, Pectin, Xanthan, Carrageenan, Gellan, Gum Arabic <i>Cationic Polysaccharides:</i> Chitosan

- *Electrostatic interactions.* Electrostatic interactions are important for food components that have an electrical charge under the utilization conditions, e.g., proteins, ionic polysaccharides, ionic surfactants, phospholipids, mineral ions, acids and bases. Electrostatic interactions may be either attractive or repulsive depending on whether the charge groups involved have opposite or similar signs. The sign and magnitude of the charge on food components usually depends on solution pH, since they have weak acid or base groups. The strength and range of electrostatic interactions decreases with increasing ionic strength due to electrostatic screening effects. The most common means of manipulating the electrostatic interactions between food components are therefore to alter the pH and/or ionic strength of the aqueous solution. Alternatively, electrostatic bridging interactions may be used to assemble food components.
- *Hydrophobic interactions.* Hydrophobic interactions are important for food components that have appreciable amounts of non-polar groups, and they manifest themselves as a tendency for the non-polar groups to associate with each other in water. Hydrophobic interactions may be manipulated somewhat by altering the temperature or changing the polarity of an aqueous solution (e.g., by adding alcohol).
- *Hydrogen bonding.* Hydrogen bonding is important for food components that have polar groups that are capable of forming relatively strong hydrogen bonds with other polar groups on the same or on different molecules. Hydrogen bonds tend to decrease in strength as the temperature is increased, and they often form between helical or sheet-like structures on the same or different biopolymers.
- *Steric exclusion.* Steric exclusion effects are important for food components that occupy relatively large volumes within a system, because they exclude other components from occupying the same volume, thereby altering the configurational and/or conformational entropy of the system.

The relative importance of these interactions in a particular system depends on the types of food components involved (e.g., molecular weight, charge density vs. pH profile, flexibility, hydrophobicity), the solution composition (e.g., pH, ionic strength and dielectric constant) and the environmental conditions, (e.g., temperature, shearing). By modulating these parameters it is possible to control the interactions between the food components and therefore assemble novel structures that can be used as delivery systems.

Structural Design Principles

In this section, some of the major structural design principles that can be used to assemble novel structures from food components are highlighted.

- *Phase separation.* When two different materials are mixed together they may be completely miscible and form a single phase, or they may separate into a number of different phases, depending on the relative strength of the interactions between the different types of molecules present (compared to the thermal energy). There are a number of examples of phase separation involving food components that can be used to create novel structures. The most common example is the phase separation of oil and water due to the fact that oil-water interactions are strongly unfavorable (compared to the average of water-water and oil-oil interactions), which is the basis for the formation of emulsion systems. Another example is the phase separation of mixed biopolymer solutions as a result of relatively strong thermodynamically unfavorable interactions between the different types of biopolymers (e.g., electrostatic repulsion and/or steric exclusion). As a result of this type of phase separation the mixed biopolymer system separates into two different phases: one phase is enriched with one type of biopolymer and depleted with the other type, while the opposite situation occurs in the other phase.
- *Spontaneous Self-assembly.* Under appropriate environmental conditions, certain types of food components spontaneously assemble into well-defined structures since this minimizes the free energy of the system, e.g., micelles, vesicles, fibers, tubes, liquid crystals. The driving force for self-assembly is system dependent, but often involves hydrophobic attraction, electrostatic interactions and/or hydrogen bond formation. Association colloids, such as micelles, vesicles and microemulsions, are some of the most common types of self-assembled structures in food materials. The primary driving force for the spontaneous formation of these structures is the hydrophobic effect, which causes the system to adopt a molecular organization that minimizes the unfavorable contact area between the non-polar tails of the surfactant molecules and water.
- *Directed self-assembly.* Directed self-assembled systems do not form spontaneously if all the components are simply mixed together. Instead, the preparation conditions (e.g., order of mixing, temperature-, pH- or ionic strength-time profiles) must be carefully *controlled* to direct the different components so that they are assembled into a particular metastable structure. The driving force for directed-assembly of food structures is also system-dependent, but again hydrophobic, electrostatic and hydrogen bonding interactions are common. A widely used directed self-assembly method is layer-by-layer (LbL) electrostatic deposition of polyelectrolytes and other charged substances onto oppositely charged surfaces due to electrostatic attraction (which will be covered in this chapter). Another example of this method is the formation of hydrogels from biopolymers. For example, when a solution of gelatin is cooled below a certain temperature a coil-to-helix transition occurs, which is followed by extensive hydrogen bond formation

between helices on different gelatin molecules. These hydrogen bonded regions act as physical cross-links between the gelatin molecules that may eventually lead to gelation. The gelatin molecules therefore self-assemble under the prevailing environmental conditions, but the precise details of the structures formed (*i.e.*, the number, position and length of the cross-links) depends on the specific preparation conditions used (*e.g.*, time-temperature profile, shearing).

- *Directed assembly.* In principle, it is also possible to form structured delivery systems by physically bringing molecules together in well-defined ways, *e.g.*, by micro-manipulation methods. Nevertheless, most of these technologies are unlikely to find widespread use in the food industry, at least in the foreseeable future, due to a variety of economic and practical constraints, such as the fact that expensive equipment is needed to fabricate and characterize the structures formed, and the throughput of fabricated structures is likely to be extremely low.

Structured Delivery Systems

Structural design principles can be used to create a variety of different delivery systems that can be utilized to encapsulate lipophilic components. Some structured delivery systems that can be created using food-grade ingredients and common unit operations that are based on emulsion technology are highlighted in Figure 1.

- *Conventional Emulsions.* Conventional oil-in-water (O/W) emulsions consist of emulsifier-coated lipid droplets dispersed in an aqueous continuous phase. They are formed by homogenizing an oil and water phase together in the presence of a hydrophilic emulsifier.
- *Multiple Emulsions.* Multiple water-in-oil-in-water (W/O/W) emulsions consist of small water droplets contained within larger oil droplets that are dispersed in an aqueous continuous phase. They are normally produced using a two-step procedure. First, a W/O emulsion is produced by homogenizing water, oil and an oil-soluble emulsifier. Second, a W/O/W emulsion is then produced by homogenizing the W/O emulsion with an aqueous solution containing a water-soluble emulsifier.
- *Multilayer Emulsions.* Multilayer oil-in-water (M-O/W) emulsions consist of small oil droplets dispersed in an aqueous medium, with each oil droplet being surrounded by a nano-laminated interfacial layer, which usually consists of emulsifier and biopolymer molecules. They are normally formed using a multiple-step procedure. First, an oil-in-water emulsion is prepared by homogenizing an oil and aqueous phase together in the presence of an ionized water-soluble emulsifier. Second, an oppositely charged polyelectrolyte is added to the system so that it adsorbs to the droplet

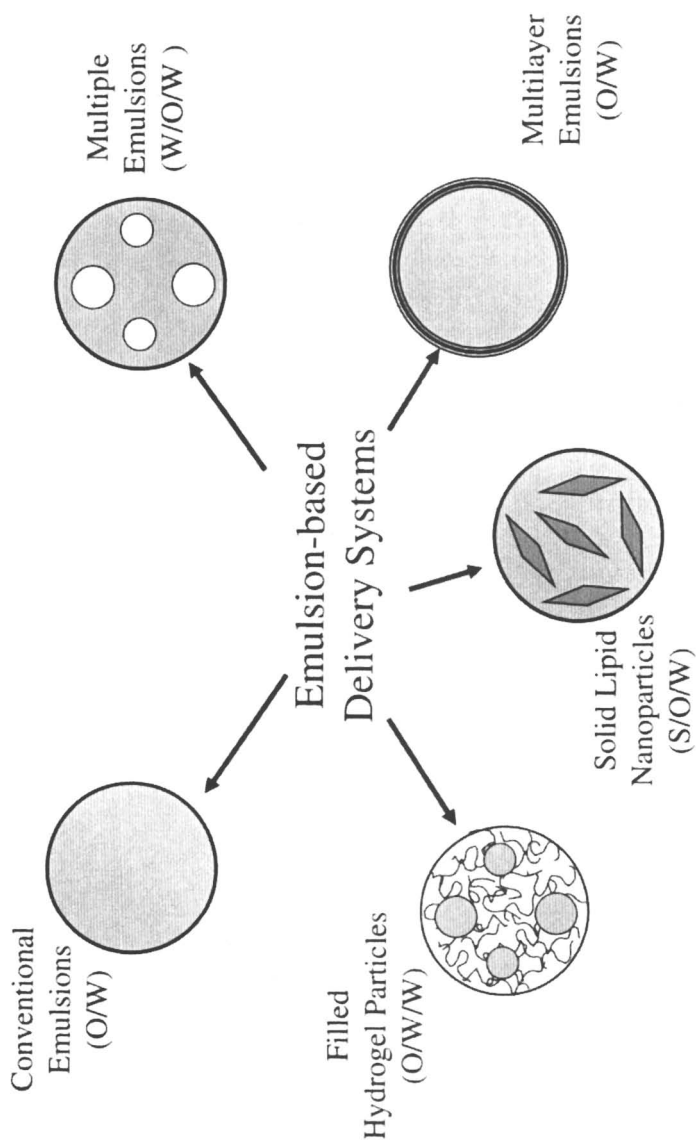


Figure 1. Some emulsion-based structured delivery systems that could potentially be used to encapsulate and delivery lipophilic functional agents.

surfaces and forms a two-layer coating around the droplets. This procedure can be repeated to form oil droplets coated by nano-laminated interfaces containing three or more layers by successively adding polyelectrolytes with opposite charges.

- **Solid Lipid Nanoparticles.** Solid lipid nanoparticles (SLN) are similar to conventional emulsions consisting of emulsifier-coated lipid droplets dispersed in an aqueous continuous phase. However, the lipid phase is either fully or partially solidified, and the morphology and packing of the crystals within the lipid phase may be controlled. SLN are formed by homogenizing an oil and water phase together in the presence of a hydrophilic emulsifier at a temperature above the melting point of the lipid phase. The emulsion is then cooled (usually in a controlled manner) so that some or all of the lipids within the droplets crystallize.
- **Filled Hydrogel Particles.** Filled hydrogel particle emulsions consist of oil droplets contained within hydrogel particles that are dispersed within an aqueous continuous phase. They can therefore be considered to be a type of oil-in-water-in-water (O/W1/W2) emulsion. There are a number of different ways to form this kind of system based on aggregative or segregative phase separation of biopolymers in solution.

The functional performance of a particular delivery system can be controlled by varying the properties of the structured particles (Figure 1): composition (*e.g.*, ratio of oil, water and biopolymer, oil type, biopolymer type); dimensions (*e.g.*, particle radii, film thicknesses), physical state (*e.g.*, solid or liquid); permeability; polarity *etc.*

Multilayer Emulsion-based Delivery Systems: Lipid Droplets Coated by Nanolaminated Coatings

In this section, the focus will be on the development of multilayer emulsions that could be used as delivery systems for lipophilic functional components. Conventionally, oil-in-water (O/W) emulsions are created by homogenizing oil and aqueous phases together in the presence of an emulsifier [5, 6]. The emulsifier adsorbs to the surfaces of the droplets formed during homogenization, where it reduces the interfacial tension and facilitates further droplet disruption. In addition, the adsorbed emulsifier forms a protective coating around the droplets that prevents them from aggregating. Many different kinds of emulsifiers are available for utilization in food products, with the most important being small molecule surfactants, phospholipids, proteins, and polysaccharides. Each type of emulsifier varies in its effectiveness at producing small droplets during homogenization, and its ability to prevent droplet aggregation under different environmental stresses, such as pH, ionic strength,

heating, freezing and drying. Food emulsifiers also differ in their cost, reliability, ease of utilization, ingredient compatibility, label friendliness and legal status. For these reasons, there is no single emulsifier that is ideal for use in every type of food product. Instead, the selection of a particular emulsifier (or combination of emulsifiers) for a specific food product depends on the type and concentration of other ingredients that it contains, the homogenization conditions used to produce it, and the environmental stresses that it experiences during its manufacture, storage and utilization.

Using conventional food emulsifiers and homogenization techniques there are only a limited range of functional attributes that can be achieved in emulsion-based delivery systems. This has motivated a number of researchers to examine alternative means of improving emulsion stability and performance. One strategy has been to create oil-in-water emulsions containing lipid droplets surrounded by multi-component nano-laminated interfacial coatings consisting of emulsifiers and/or biopolymers [7-23]. In this “layer-by-layer” (*LbL*) electrostatic deposition approach, an ionic emulsifier that rapidly adsorbs to the surface of lipid droplets during homogenization is used to produce a *primary* emulsion containing small droplets, then an oppositely charged biopolymer is added to the system that adsorbs to the droplet surfaces and produces *secondary* emulsions containing droplets coated with an emulsifier-biopolymer interfacial layer (Figure 2). This latter procedure can be repeated to form lipid droplets covered by coatings consisting of three or more layers, *e.g.*, emulsifier – biopolymer 1 – biopolymer 2. Emulsions containing lipid droplets surrounded by multi-layered interfacial coatings have been found to have better stability to environmental stresses than conventional oil-in-water emulsions under certain circumstances (18-22). They can also be used to protect lipophilic functional components within lipid droplets from chemical degradation [16, 17], or to develop controlled or triggered release systems [8, 21].

The *LbL*-electrostatic deposition method therefore offers a promising way to improve the stability and performance of emulsion-based delivery systems. Nevertheless, the choice of an appropriate combination of emulsifier and biopolymers is essential to the success of this approach, as well as determination of the optimum preparation conditions (*e.g.*, droplet concentration, biopolymer concentration, pH, ionic strength, order of addition, stirring speed, washing, floc disruption, and temperature) [18, 20, 22]. The purpose of this section is to provide an overview of recent research that has been carried out in our laboratory on the development, characterization and application of O/W emulsions containing lipid droplets surrounded by nanolaminated coatings of emulsifier and biopolymer. In particular, we will focus on the use of the *LbL* electrostatic deposition technique to create emulsions with improved resistance to environmental stresses, such as pH, ionic strength, thermal processing, freezing, dehydration, and lipid oxidation. These multilayer emulsions may be useful for the encapsulation and delivery of lipophilic functional ingredients.

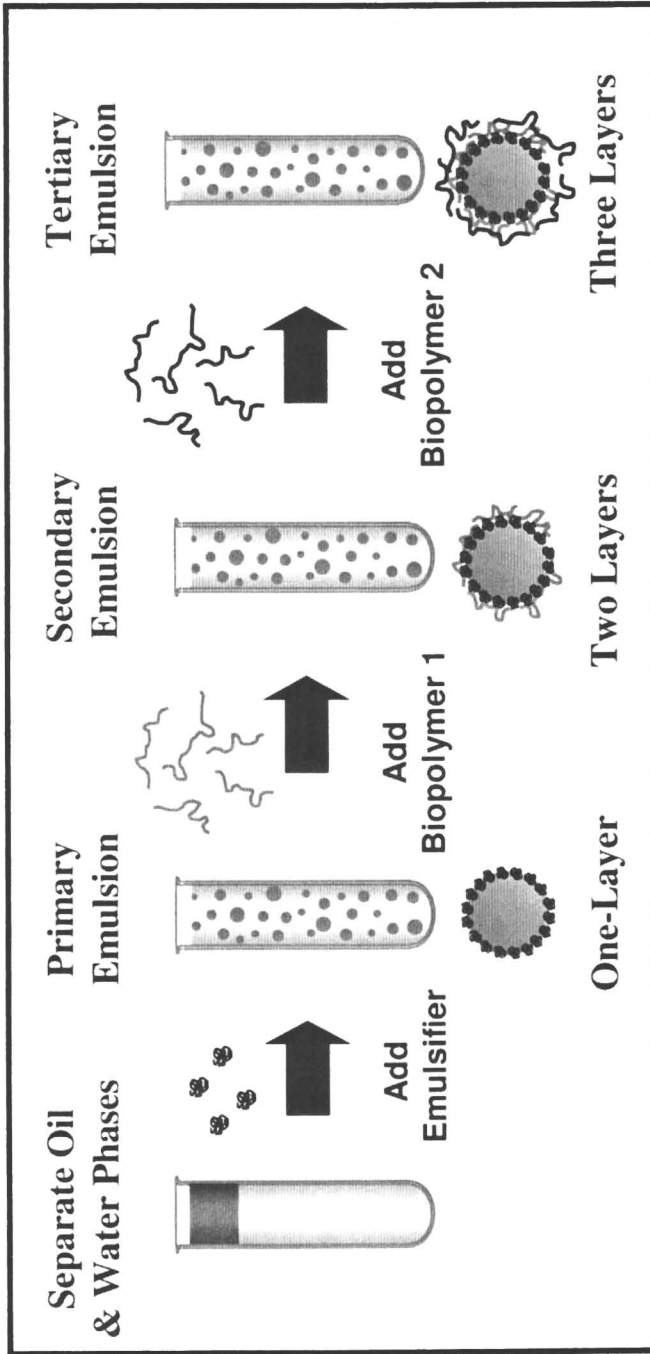


Figure 2. Schematic representation of coating lipid droplets in oil-in-water emulsions with laminated coatings using the layer-by-layer electrostatic deposition method.

Preparation of multilayered emulsions

Oil-in-water emulsions containing oil droplets surrounded by multi-layered interfacial coatings can be prepared using a multiple-step process [12, 18]. For example, the following procedure could be used to create emulsion droplets coated by three layers, *e.g.*, emulsifier-biopolymer 1-biopolymer 2 (Figure 2). First, a *primary* emulsion containing electrically charged droplets surrounded by a layer of emulsifier is prepared by homogenizing oil, aqueous phase and a water-soluble ionic emulsifier together. Second, a *secondary* emulsion containing charged droplets stabilized by emulsifier-biopolymer 1 layers is formed by incorporating biopolymer 1 into the primary emulsion. Biopolymer 1 normally has to have an opposite electrical charge than the droplets in the primary emulsion (although this is not always necessary if there are significantly big patches of opposite charge on the droplet surface). If necessary mechanical agitation is applied to the secondary emulsion to disrupt any flocs formed because of bridging of droplets by biopolymer molecules. In addition, the secondary emulsion may be washed (*e.g.*, by filtration or centrifugation) to remove any free biopolymer remaining in the continuous phase. Third, *tertiary* emulsions containing droplets stabilized by emulsifier-biopolymer 1-biopolymer 2 interfacial layers are formed by incorporating biopolymer 2 into the secondary emulsion. Biopolymer 2 normally has to have an opposite electrical charge than the droplets in the secondary emulsion (but see above). If necessary mechanical agitation is applied to the tertiary emulsion to disrupt any flocs formed, and the emulsion may be washed to remove any non-adsorbed biopolymer. This procedure can be continued to add more layers to the interfacial coating. The adsorption of the biopolymers to the droplet surfaces can be conveniently monitored using ζ -potential measurements (Figures 3 and 4), whereas the stability of the emulsions to flocculation can be monitored by light scattering, microscopy or creaming stability measurements (Figures 3 and 4) [12-14, 20]. Since the major driving force for adsorption of biopolymers to the droplet surfaces is electrostatic in origin, it is important to control the pH and ionic strength of the mixing solution.

Unless stated otherwise, the results reported below are for oil-in-water emulsions containing lipid droplets coated by interfacial layers comprising of β -lactoglobulin (primary) and β -lactoglobulin-pectin (secondary). These emulsions were formed by mixing a β -lactoglobulin-stabilized emulsion with a pectin solution at pH 7 where the protein and polysaccharide were both negatively charged so that no adsorption occurred. Then, the pH of the solution was adjusted so that the protein-coated droplets became positively charged (or had positive patches), which promoted pectin adsorption [11, 19, 24]. The pectin concentration was controlled to avoid both bridging and depletion flocculation [11, 18, 19].

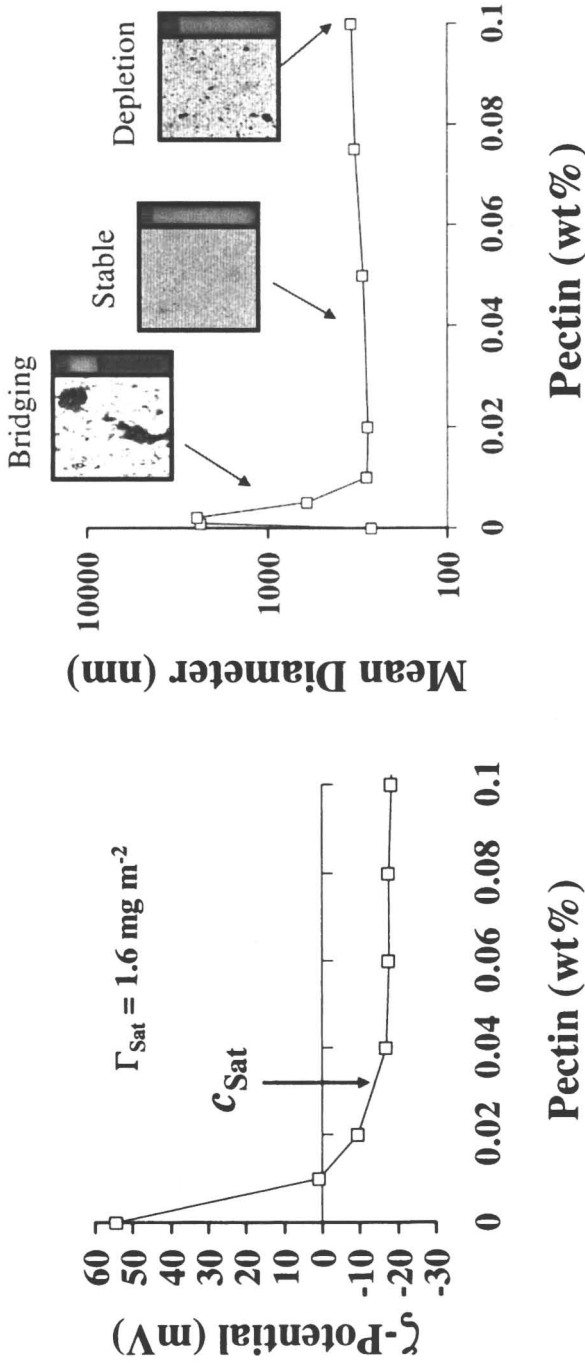


Figure 3. The formation of stable multilayer emulsions can be conveniently monitored using ζ -potential, particle size and microscopy measurements.

Improved Stability to Environmental Stresses

Food emulsions experience a variety of different environmental stresses during their manufacture, storage, transport and utilization, including pH extremes, high ionic strengths, thermal processing, freeze-thaw cycling, dehydration, and mechanical agitation [5]. Many of the emulsifiers currently available for utilization within the food industry provide limited stability to these environmental stresses. In this section, some of the recent work carried out in our laboratories on utilizing the *LbL*-electrostatic deposition technique to improve emulsion stability to various environmental stresses is reviewed.

pH

The influence of pH on the ζ -potential, mean particle diameter and creaming stability of primary (β -lactoglobulin) and secondary (β -lactoglobulin-pectin) emulsions was measured (Figure 4). The ζ -potential of the protein-coated droplets in the primary emulsions changed from negative to positive as the pH decreased from 7 to 3, with the point of zero charge being around pH 5 (Figure 4). This can be attributed to the fact that the isoelectric point of the adsorbed proteins is around pH 5. The ζ -potential of the β -lactoglobulin-pectin coated droplets in the secondary emulsions had a similar negative charge as the β -lactoglobulin-coated droplets in the primary emulsions at pH values > 6 , which indicates that the anionic pectin molecules did not adsorb to the anionic droplets. When the pH was decreased below 6 the charge on the secondary emulsion droplets was more negative than that on the primary emulsion droplets, which indicated pectin adsorption. Indeed, the primary emulsion droplets were cationic at low pH, whereas the secondary emulsion droplets were anionic. This may be important for designing delivery systems that have tunable charge characteristics so that they can adsorb to specific charged sites, or to alter the mouthfeel of delivery systems.

The influence of pH on the mean particle diameter and creaming stability of the droplets in the primary and secondary emulsions is also shown in Figure 4. The primary emulsion was stable to flocculation and creaming at low and high pH due to the strong electrostatic repulsion between the droplets, but was unstable to flocculation and creaming around the isoelectric point of the adsorbed protein because of the relatively low net charge on the droplets. On the other hand, the secondary emulsions were stable across the whole pH range, which can be attributed to the increased electrostatic and steric repulsion between the droplets, and the decreased van der Waals attraction [11, 18, 19]. These results clearly show that the multilayer technique can be used to improve the pH stability of protein-coated droplets, which may be useful in developing delivery systems for lipophilic functional components that can be used in a wider range of products than is currently possible using only protein-coated droplets.

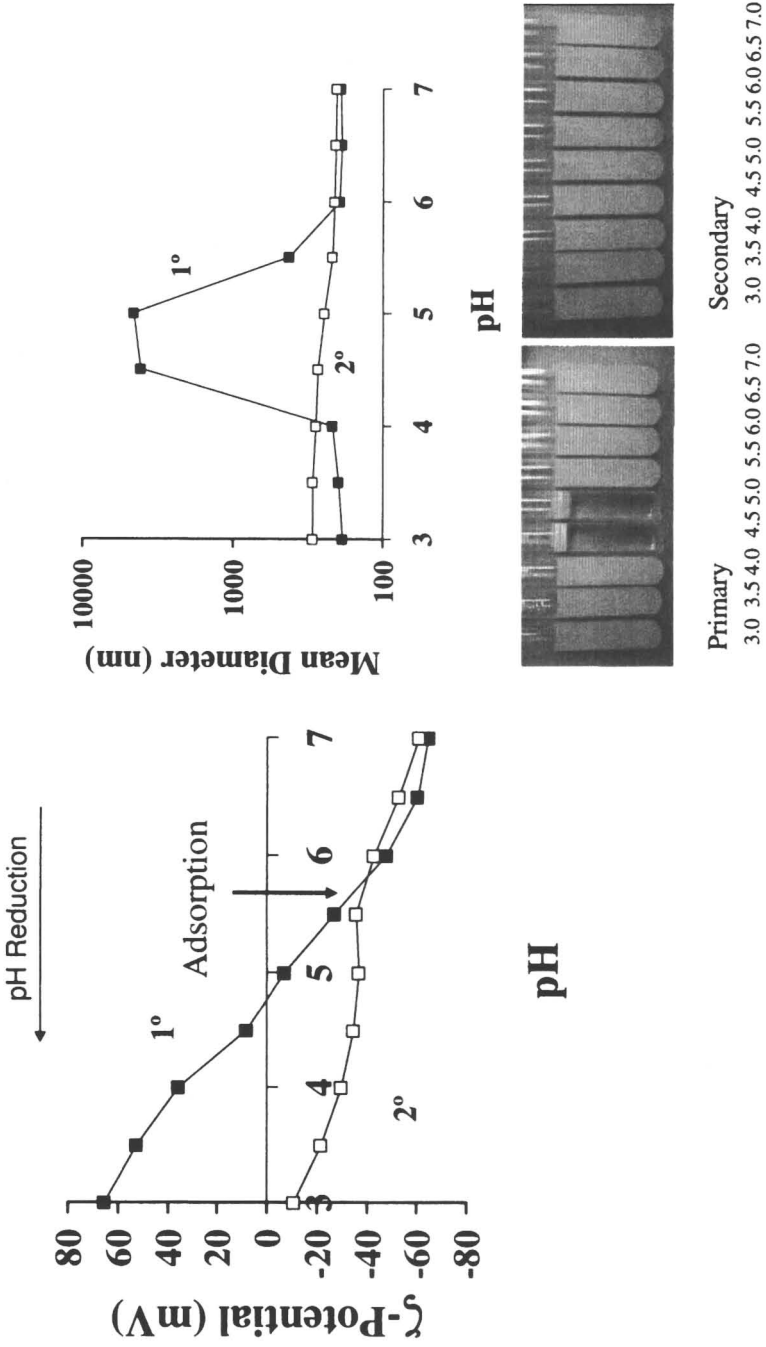


Figure 4. The pH-dependence of the ζ -potential, mean particle diameter and creaming stability of primary (β -lactoglobulin) and secondary (β lactoglobulin-pectin) emulsions.

NaCl

Many food systems contain significant amounts of mineral ions in them, which can negatively impact the physical stability of emulsion-based delivery systems. The influence of NaCl concentration (0 to 300 mM) on the mean particle diameter and creaming stability of diluted primary and secondary emulsions at pH 3.5 has been measured [24]. The primary emulsions were unstable to droplet aggregation and creaming when the salt concentration was \geq 50 mM (Figure 5), which can be attributed to screening of the electrostatic repulsion between the droplets. On the other hand, the secondary emulsions were relatively stable to droplet aggregation up to 200 mM NaCl (Figure 5), which can be attributed to the increased electrostatic and steric repulsion, and decreased van der Waals attraction [11, 18, 19, 24]. These results show that the multilayer technique can be used to improve the salt stability of protein-coated lipid droplets, thus extending the range of food matrices that this kind of delivery system could be used in.

Thermal Processing

The influence of thermal processing on the stability of primary (β -lactoglobulin) and secondary (β -lactoglobulin-carrageenan) emulsions has been studied at pH 6 [8, 10]. These emulsions were held isothermally at temperatures ranging from 30 to 90 °C, cooled to room temperature, and then stored for 24 hours. The ζ -potential, mean particle diameter and creaming stability of the emulsions were then measured (data not shown). In the absence of added salt, there was no significant change in the ζ -potential or mean particle diameter of the secondary emulsions upon heating, and there was no evidence of creaming, which indicated that they were stable to thermal processing in the temperature range used. Nevertheless, at 150 mM NaCl, there was evidence of desorption of carrageenan from the droplet surfaces at temperatures exceeding the thermal denaturation of the adsorbed protein molecules [8, 10]. This suggested that the conformational change of the adsorbed globular protein caused by heating weakened the attraction between the carrageenan and β -lactoglobulin molecules leading to polysaccharide desorption. The emulsions where the carrageenan molecules became detached from the droplet surfaces were more unstable to flocculation after heating.

Freeze-Thaw Cycling

Primary (β -lactoglobulin) and secondary (β -lactoglobulin-pectin) emulsion samples (2 wt% oil, pH 3.5) were transferred into cryogenic test tubes and incubated in a -20 °C freezer for 22 hours. After incubation the emulsion samples were thawed by incubating them in a water bath at 30 °C for 2 hours.

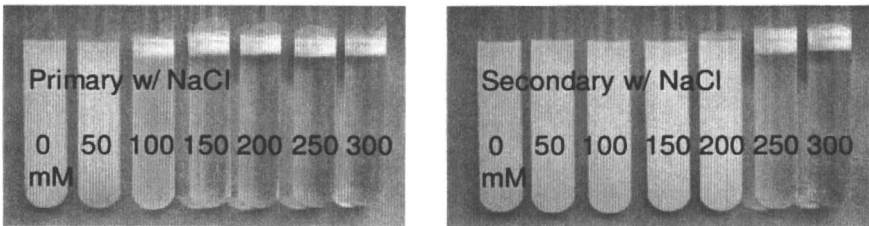
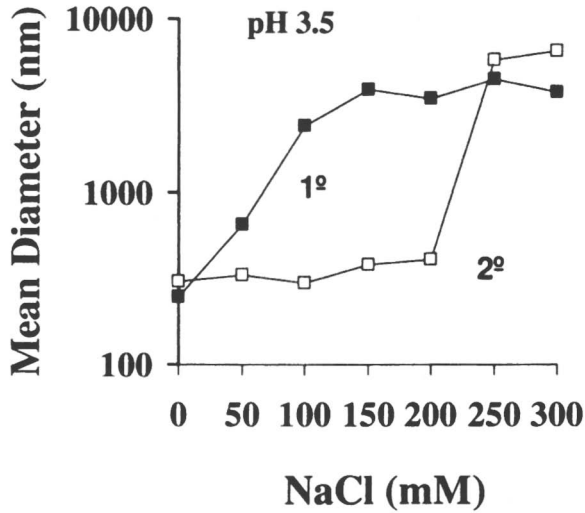


Figure 5. The salt-dependence of the mean particle diameter and creaming stability of primary (β -lactoglobulin) and secondary (β -lactoglobulin-pectin) emulsions. The primary emulsion flocculates at lower salt concentrations than the secondary emulsion.

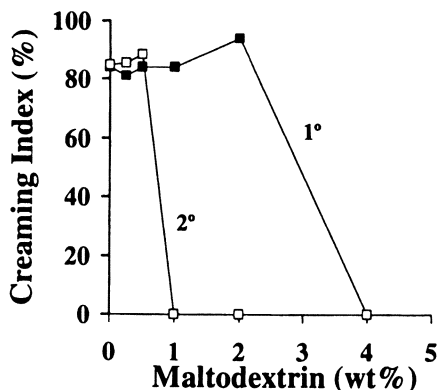


Figure 6. Impact of added maltodextrin on the creaming stability of primary (β -lactoglobulin) and secondary (β -lactoglobulin-pectin) emulsions after freezing and thawing (3 cycles). Less maltodextrin is required to stabilize the secondary emulsion than the primary emulsion.

This freeze-thaw cycle was repeated two times and its influence on emulsion stability (creaming index) was measured (Figure 6). The emulsions were all unstable to droplet aggregation in the absence of maltodextrin. We therefore carried out experiments to determine the minimum amount of maltodextrin required to stabilize the primary and secondary emulsions against droplet aggregation during freezing and thawing. We found that secondary emulsions containing pectin required only 1 wt% maltodextrin to stabilize them against aggregation, whereas the primary emulsions required 4 wt% maltodextrin. We also found that there were differences between polysaccharides, with pectin being more effective than carrageenan. Hence, the multilayer technique may be useful for reducing the amount of sugars that are needed in frozen products to protect lipid droplets against aggregation.

Freeze Drying

We have recently carried out preliminary experiments comparing the stability of primary (β -lactoglobulin) and secondary (β -lactoglobulin-pectin) emulsions to freeze-drying at pH 3.5 [25]. Emulsion samples (30 mL) were transferred into Petri dishes and frozen by placing them overnight in a -40 °C freezer. A laboratory scale freeze-drying device (Virtis, the Virtis Company, Gardiner, NY) was used to dry the frozen emulsions. After finishing the drying process the dried products were ground using a mechanical device (Handy Chopper, Black & Decker Inc., Shelton, CT). The secondary emulsions had a much better stability to droplet aggregation than the primary emulsions after

freeze-drying and reconstitution in buffer solution, especially when maltodextrin was incorporated into the emulsions. For example, we found that secondary emulsions containing pectin were stable to aggregation at maltodextrin concentrations of 2 wt% and higher, whereas more than 8 wt% maltodextrin was required to stabilize primary emulsions. The multilayer technique may therefore prove useful for increasing the lipid load of dehydrated emulsions that could be used as powdered delivery systems.

Lipid Oxidation

We have recently compared the oxidative stability of primary (β -lactoglobulin) and secondary (β -lactoglobulin-pectin) emulsions at pH 3.5. The primary emulsion droplets were cationic, whereas the secondary emulsion droplets were anionic, so we would have expected the primary emulsions to have been more oxidatively stable due to repulsion of the positively charged iron ions from the positively charged protein-coated droplets [26]. Nevertheless, we found that secondary emulsions containing lipid droplets coated by citrus pectin actually had slightly better oxidative stability (data not shown). This suggests that the relatively thick polysaccharide layer may have been able to prevent the iron ions from reaching the lipid surfaces.

Other Systems

In addition to the systems described above we have examined the suitability of other types of emulsifier and biopolymer combinations for preparing stable oil-in-water emulsions containing droplets surrounded by multi-layered interfacial layers. We have shown that laminated lipid droplets can be formed using a variety of different emulsifiers (lecithin, SDS, β -lactoglobulin, caseinate) and biopolymers (chitosan, gelatin, pectin, carrageenan, alginate, gum arabic) [8, 9, 11, 15-20, 27-31]. Recently we have used a similar technique to prepare “colloidosomes”, which consist of large oil droplets surrounded by a layer of small oil droplets [32].

Nano-laminated Coatings on Macroscopic Objects

Applications of Laminated Edible Coatings

Potentially, the LbL deposition technology can also be used to form multifunctional laminated coatings on macroscopic objects, such as fruit, vegetables, meat and fish. For example, there is currently a need for high-performance edible coatings for application on fresh-cut fruits & vegetables that

are capable of exhibiting a variety of different functions, *e.g.*, control of moisture or gas migration; anti-microbial, anti-oxidant and anti-browning activity; prevention of textural degradation; encapsulation of nutraceuticals, colors or flavors; controlled or triggered release of active components [33-36]. Conventional technologies used by the food industry have limited scope for precise engineering of novel functionalities into edible coatings. The LbL deposition technique could be used to design and fabricate laminated edible coatings with greatly improved functional properties. These coatings could be created from food-grade ingredients (*e.g.*, proteins, polysaccharides and lipids) using simple and inexpensive processing operations (*e.g.*, dipping, spraying and washing). In addition, they could be designed to have a range of functional attributes that are difficult to achieve using conventional coating methods, such as selective permeability to water and other volatile components; encapsulation of active components (such as antioxidants, antimicrobials, anti-browning agents, colors, flavors or nutraceuticals); and texture stabilization.

Formation of Laminated Edible Coatings

The principle of using the LbL technique to coat macroscopic objects is highlighted in Figure 7. The object to be coated is dipped sequentially into a series of solutions containing substances that adsorb to its surface. (Alternatively, the solutions containing the adsorbing substances could be sprayed onto the surface of the object). Between each dipping step it may be necessary to have a washing and/or drying step to remove the excess solution attached to the surface prior to introduction of the object into the next dipping solution. The composition, thickness, structure and properties of the laminated coating formed around the object could be controlled in a number of ways, including: (i) changing the type of adsorbing substances in the dipping solutions; (ii) changing the total number of dipping steps used; (iii) changing the order that the object is introduced into the various dipping solutions; (iv) changing the solution and environmental conditions used, such as pH, ionic strength, solvent, temperature, dipping time, stirring speed *etc.* The driving force for adsorption of a substance to a surface would depend on the nature of the surface and the nature of the adsorbing substance, and could be electrostatic, hydrogen bonding, hydrophobic interactions, *etc.* Nevertheless, the major driving force utilized by the LbL deposition method is **electrostatic attraction** between electrically charged substances.

In general, a variety of different adsorbing substances could be used to create the different layers (Figure 8), including:

- *Natural Polyelectrolytes.* Any food-grade polyelectrolyte that is capable of adsorbing to the exposed surface of the object could be used, such as proteins (*e.g.*, whey, casein, soy) or polysaccharides (*e.g.*, pectin, alginate, xanthan, carrageenan, chitosan).

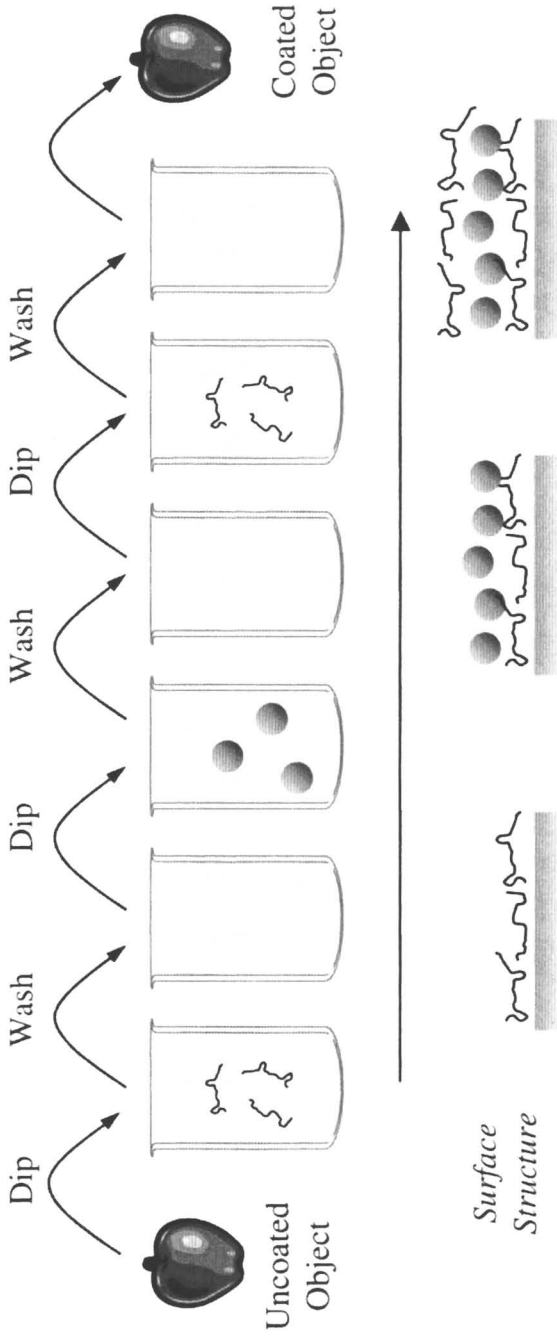


Figure 7. Schematic representation of coating a fruit with multiple layers using a successive dipping and washing procedure. Each dipping solution contains a component that will adsorb to the surface of the material to form a laminated coating around the fruit.

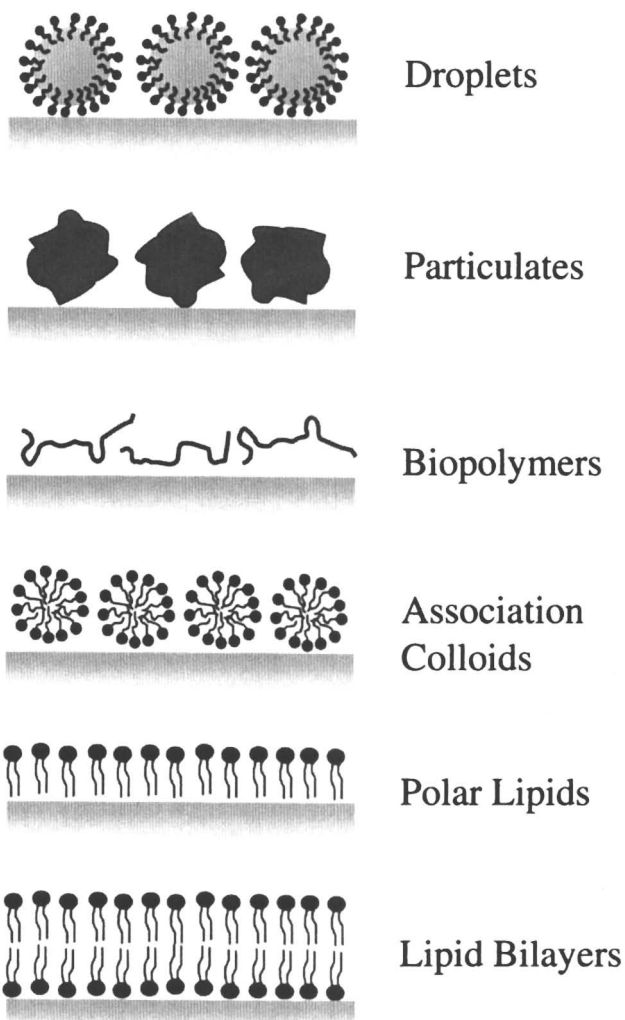


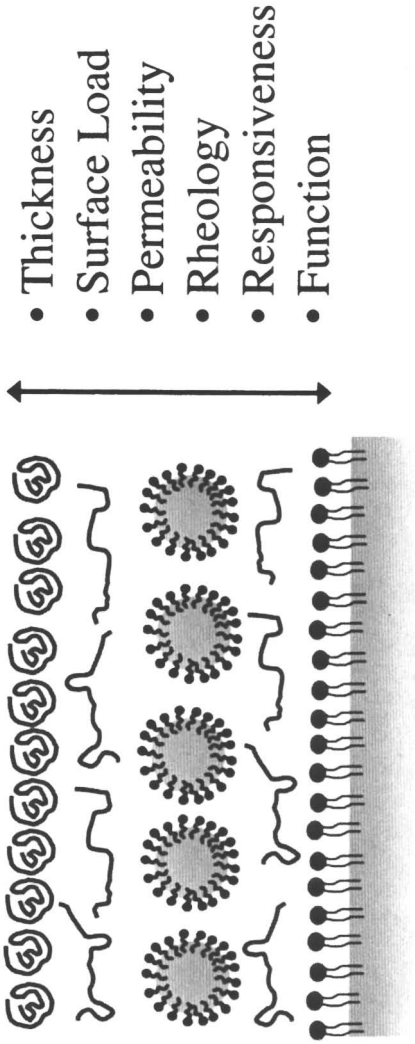
Figure 8. Possible components that could be used to assemble multilayered edible films or coatings

- *Surface-Active Lipids.* Any food-grade lipid that is capable of adsorbing to the exposed surface of the object, *e.g.* phospholipids and small molecule surfactants. These surface active lipids could form single layers, bi-layers, multiple layers, micelles, vesicles or other association colloids at the surface.
- *Lipid Droplets.* Any food-grade lipid droplet that is capable of adsorbing to the exposed surface on the object. The emulsion droplet would usually consist of a liquid oil droplet coated by a food grade emulsifier, but it could also be a partly or fully crystallized oil droplet, or an oil droplet containing small water droplets or other material.

The choice of the type of adsorbing substances used to create each layer, the total number of layers incorporated into the overall coating, the sequence of the different layers, and the preparation conditions used to prepare each layer will determine the functional performance of the final coatings: permeability (*e.g.*, to gasses, organic substances, minerals or water); mechanical properties (*e.g.*, rigidity, flexibility, brittleness); swelling and wetting characteristics; environmental sensitivity (*e.g.*, to pH, ionic strength and temperature). In addition, the above procedure enables one to encapsulate various hydrophilic, amphiphilic or lipophilic substances within the coatings, *e.g.*, non-polar substances could be incorporated in micelles or lipid droplets, while polar substances could be incorporated in biopolymer layers. Thus, it would be possible to incorporate active functional agents such as antimicrobials, anti-browning agents, antioxidants, enzymes, flavors, colors and nutraceuticals into the coatings. These functional agents could be used to increase the shelf-life and quality of the coated fresh-cut fruit and vegetables. An example of a possible multi-component, multi-layered coating is shown in Figure 9.

Preliminary Studies

Recently, we have carried out studies that have shown that the electrostatic layer-by-layer technique can be used to form laminated coatings on planar hydrogels (agar-pectin) that were designed to mimic cut-fruit surfaces (which contain a significant amount of pectin) [37]. However, we have also observed some interesting physicochemical phenomena that need to be considered when forming these coatings on macroscopic objects. An anionic hydrogel was prepared in a Petri dish and then cationic protein-coated droplets were brought into contact with the hydrogel for a specified period. The contact emulsion was then removed and the plate was washed with buffer solution (Figure 10). The turbidity of the plates was measured to monitor the adsorption of droplets to the hydrogel surfaces (Figure 11), and the charge and size of the droplets in the contact emulsion removed from the hydrogel surfaces were measured (Figure 12). The turbidity measurements indicated that the lipid droplets did adsorb to the droplet surfaces fairly rapidly, but the results were not what would be



- Thickness
- Surface Load
- Permeability
- Rheology
- Responsiveness
- Function

Figure 9. Example of possible multilayered edible film containing different functional layers.

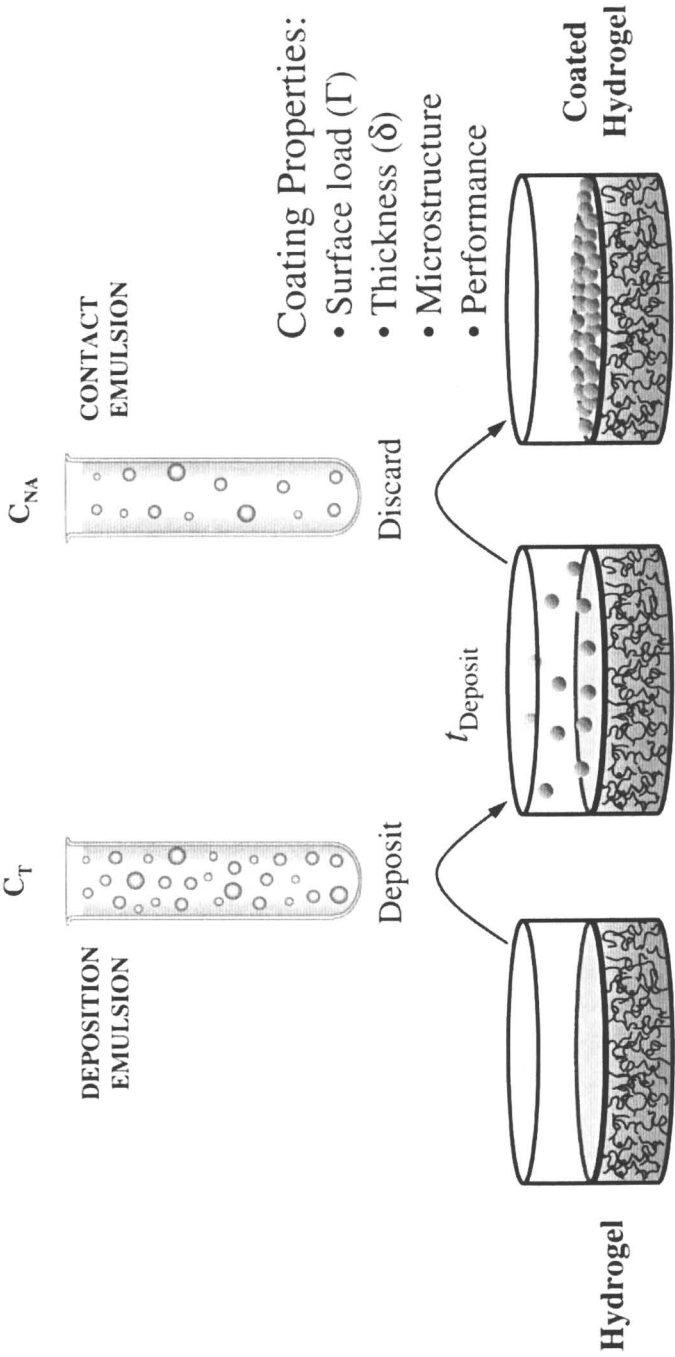


Figure 10. Schematic representation of coating a hydrogel surface with lipid droplets.

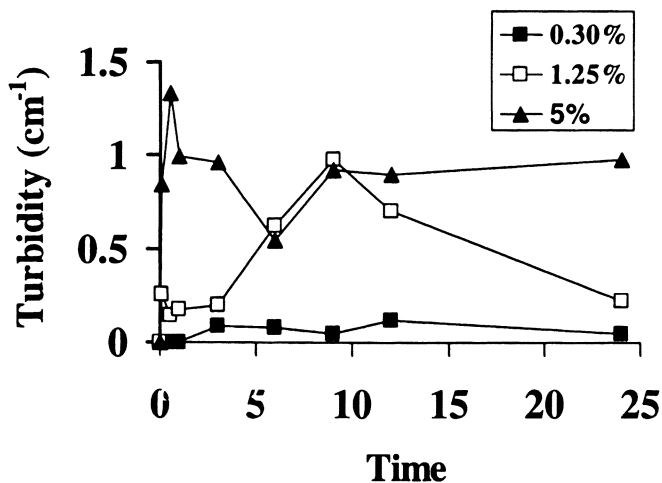


Figure 11. Turbidity of emulsions over time.

expected for a simple adsorption process (e.g., a Langmuir isotherm). For example, we observed increases and then decreases in plate turbidity over time, and no clear dependence of plate turbidity on the initial droplet concentration in the deposition emulsion. In addition, the droplets in the contact emulsion removed from the hydrogel plates became increasingly negative and aggregated over time, with the effect being more pronounced in the more dilute emulsions (Figure 12). We postulate that anionic pectin molecules diffused out of the hydrogels and adsorbed onto the surfaces of the cationic protein-coated droplets, which made them become more negative and aggregate. Indeed, spectrophotometry measurements indicated that the pectin molecules did diffuse out of the hydrogels over time. The diffusion of biopolymers out of macroscopic surfaces may be an important consideration when forming laminated coatings on fruits and vegetables.

In other preliminary studies, we have examined the impact of biopolymer type, pH, contact time, stirring speed, salt concentration and surfactants on the formation of edible coatings on hydrogel surfaces. For example, Figure 13 shows the turbidity of anionic hydrogels (carrageenan/agar) when they have been brought into contact with emulsions containing whey protein coated droplets at different pH values. The droplets only stick to the hydrogel surfaces when the droplets are positively charged ($\text{pH} < \text{pI}$), *i.e.*, they have opposite charges to the hydrogel surfaces. Recently, we have shown that laminated coatings (chitosan and/or eugenol droplets) can be formed on fruit (strawberry and cantaloupe) and vegetable (sweet potatoes) surfaces, and that these provide protection against microbial growth.

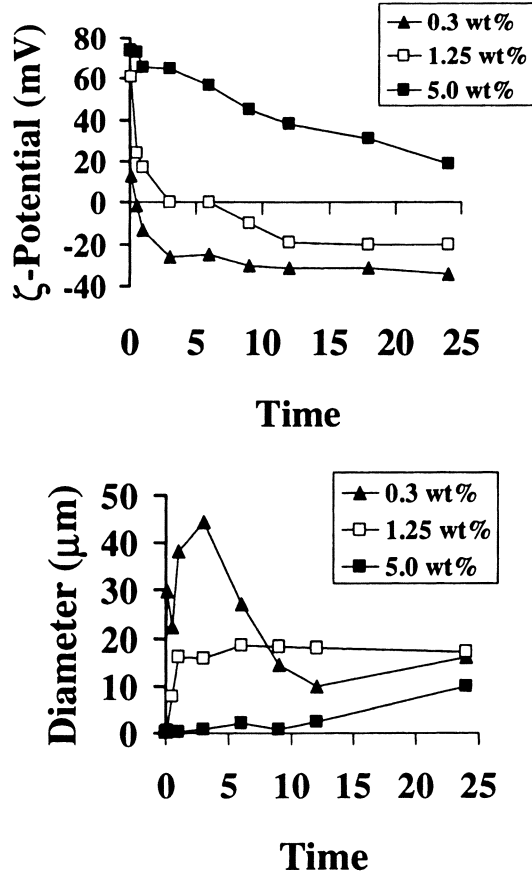


Figure 12. ζ -potential and mean particle diameter of droplets present in the contact emulsion removed from the surfaces of hydrogels. The droplets became more negative over time and aggregated, which can be attributed to diffusion of pectin out of the hydrogels and onto the droplet surfaces.

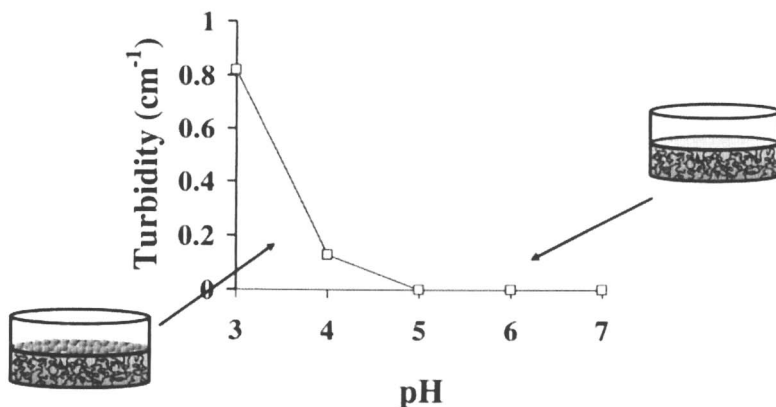


Figure 13. Turbidity of anionic hydrogels (carrageenan/agar) in contact with emulsions containing whey protein coated droplets at different pH values.

Conclusion

Our work so far has shown that stable emulsions containing multi-layered lipid droplets can be prepared using a simple cost-effective method and food grade ingredients. These multilayered emulsions have better stability to environmental stresses than conventional emulsions under certain conditions. More research is still needed to establish, at a fundamental level, the factors that influence the preparation of stable multilayered emulsions with specific functional attributes, including emulsifier characteristics (*e.g.*, sign and magnitude of droplet charge), biopolymer characteristics (*e.g.*, molecular weight, charge density and flexibility), mixing conditions (*e.g.*, order of addition, stirring speed) and washing solution composition (*e.g.*, ionic strength and pH). In addition, research needs to be carried out to establish where these multilayered emulsions can be practically used within the food industry as delivery systems. We have also carried out preliminary experiments showing that the LbL technique may be useful for coating macroscopic objects, such as meat, fish, fruit and vegetables.

References

1. Shefer, A. and S. Shefer, *Novel encapsulation system provides controlled release of ingredients*. Food Technology, 2003. 57: p. 40-43.
2. Ubbink, J., *Flavor delivery systems: Trends, technologies and applications*. Abstracts of Papers of the American Chemical Society, 2002. 223: p. U34-U34.

3. Ubbink, J. and J. Kruger, *Physical approaches for the delivery of active ingredients in foods*. Trends in Food Science & Technology, 2006. 17(5): p. 244-254.
4. Chen, L.Y., G.E. Remondetto, and M. Subirade, *Food protein-based materials as nutraceutical delivery systems*. Trends in Food Science & Technology, 2006. 17(5): p. 272-283.
5. McClements, D.J., *Food Emulsions: Principles, Practice, and Techniques*. 2nd ed. CRC series in contemporary food science. 2005, Boca Raton: CRC Press.
6. Friberg, S., K. Larsson, and J. Sjoblom, *Food Emulsions*. 4 ed. 2004, New York: Marcel Dekker.
7. Aoki, T., E.A. Decker, and D.J. McClements, *Influence of environmental stresses on stability of O/W emulsions containing droplets stabilized by multilayered membranes produced by a layer-by-layer electrostatic deposition technique*. Food Hydrocolloids, 2005. 19(2): p. 209-220.
8. Gu, Y., E. Decker, and D. McClements, *Irreversible thermal denaturation of beta-lactoglobulin retards adsorption of carrageenan onto beta-lactoglobulin-coated droplets* Langmuir, 2006. 22 p. 7480-7486
9. Gu, Y.S., A.E. Decker, and D.J. McClements, *Production and characterization of oil-in-water emulsions containing droplets stabilized by multilayer membranes consisting of beta-lactoglobulin, iota-carrageenan and gelatin*. Langmuir, 2005. 21(13): p. 5752-5760.
10. Gu, Y.S., E.A. Decker, and D.J. McClements, *Influence of iota-carrageenan on droplet flocculation of beta-lactoglobulin-stabilized oil-in-water emulsions during thermal processing*. Langmuir, 2004. 20(22): p. 9565-9570.
11. Guzey, D., H.J. Kim, and D.J. McClements, *Factors influencing the production of O/W emulsions stabilized by beta-lactoglobulin-pectin membranes*. Food Hydrocolloids, 2004. 18(6): p. 967-975.
12. Guzey, D. and D.J. McClements, *Influence of Environmental Stresses on O/W Emulsions Stabilized by β -Lactoglobulin-Pectin and β -Lactoglobulin-Pectin-Chitosan Membranes Produced by the Electrostatic Layer-by-Layer Deposition Technique*. Food Biophysics, 2006. 1(1): p. 30-40.
13. Harnsilawat, T., R. Pongsawatmanit, and D. McClements, *Characterization of β -lactoglobulin-sodium alginate interactions in aqueous solutions: A calorimetry, light scattering, electrophoretic mobility and solubility study*, Food Hydrocolloids, 2006. 20 p. 577-585.
14. Harnsilawat, T., R. Pongsawatmanit, and D. McClements, *Stabilization of model beverage cloud emulsions using protein-polysaccharide electrostatic complexes formed at the oil-water interface* Journal of Agricultural and Food Chemistry, 2006. 54 p. 5540-5547
15. Klinkesorn, U., et al., *Encapsulation of emulsified tuna oil in two-layered interfacial membranes prepared using electrostatic layer-by-layer deposition*. Food Hydrocolloids, 2005. 19(6): p. 1044-1053.

16. Klinkesorn, U., et al., *Stability of spray-dried tuna oil emulsions encapsulated with two-layered interfacial membranes*. Journal of Agricultural and Food Chemistry, 2005. **53**(21): p. 8365-8371.
17. Klinkesorn, U., et al., *Increasing the oxidative stability of liquid and dried tuna oil-in-water emulsions with electrostatic layer-by-layer deposition technology*. Journal of Agricultural and Food Chemistry, 2005. **53**(11): p. 4561-4566.
18. McClements, D.J., *Theoretical analysis of factors affecting the formation and stability of multilayered colloidal dispersions*. Langmuir, 2005. **21**(21): p. 9777-9785.
19. Moreau, L., et al., *Production and characterization of oil-in-water emulsions containing droplets stabilized by beta-lactoglobulin-pectin membranes*. Journal of Agricultural and Food Chemistry, 2003. **51**(22): p. 6612-6617.
20. Mun, S., E.A. Decker, and D.J. McClements, *Influence of droplet characteristics on the formation of oil-in-water emulsions stabilized by surfactant-chitosan layers*. Langmuir, 2005. **21**(14): p. 6228-6234.
21. Ogawa, S., E.A. Decker, and D.J. McClements, *Influence of environmental conditions on the stability of oil in water emulsions containing droplets stabilized by lecithin-chitosan membranes*. Journal of Agricultural and Food Chemistry, 2003. **51**(18): p. 5522-5527.
22. Ogawa, S., E.A. Decker, and D.J. McClements, *Production and characterization of O/W emulsions containing cationic droplets stabilized by lecithin-chitosan membranes*. Journal of Agricultural and Food Chemistry, 2003. **51**(9): p. 2806-2812.
23. Ogawa, S., E.A. Decker, and D.J. McClements, *Production and characterization of O/W emulsions containing droplets stabilized by lecithin-chitosan-pectin multilayered membranes*. Journal of Agricultural and Food Chemistry, 2004. **52**(11): p. 3595-3600.
24. Guzey, D. and D.J. McClements, *Impact of electrostatic interactions on formation and stability of emulsions containing oil droplets coated by beta-lactoglobulin-pectin complexes*. Journal of Agricultural and Food Chemistry, 2007. **55**(2): p. 475-485.
25. Mun, S., E.A. Decker, and D.J. McClements, *Influence of Freeze-Thaw and Freeze-Dry Processes on Stability of Lipid Droplets Coated by Protein-Polysaccharide Layers* In preparation, 2007.
26. McClements, D.J. and E.A. Decker, *Lipid oxidation in oil-in-water emulsions: Impact of molecular environment on chemical reactions in heterogeneous food systems*. Journal of Food Science, 2000. **65**(8): p. 1270-1282.
27. Gu, Y.S., E.A. Decker, and D.J. McClements, *Influence of pH and iota-carrageenan concentration on physicochemical properties and stability of beta-lactoglobulin-stabilized oil-in-water emulsions*. Journal of Agricultural and Food Chemistry, 2004. **52**(11): p. 3626-3632.

28. Gu, Y.S., L. Regnier, and D.J. McClements, *Influence of environmental stresses on stability of oil-in-water emulsions containing droplets stabilized by beta-lactoglobulin-*iota*-carrageenan membranes*. Journal of Colloid and Interface Science, 2005. **286**(2): p. 551-558.
29. Gu, Y.S., E.A. Decker, and D.J. McClements, *Influence of pH and carrageenan type on properties of beta-lactoglobulin stabilized oil-in-water emulsions*. Food Hydrocolloids, 2005. **19**(1): p. 83-91.
30. Harnsilawat, T., R. Pongsawatmanit, and D. McClements, *Influence of pH and ionic strength on formation and stability of emulsions containing oil droplets coated by beta-lactoglobulin-alginate interfaces*. Biomacromolecules, 2006. **7**: p. 2052-2058.
31. Mun, S.H. and D.J. McClements, *Influence of interfacial characteristics on Ostwald ripening in hydrocarbon oil-in-water emulsions*. Langmuir, 2006. **22**(4): p. 1551-1554.
32. Gu, Y.S., E.A. Decker, and D.J. McClements, *Formation of colloidosomes by adsorption of small charged oil droplets onto the surface of large oppositely charged oil droplets*. Food Hydrocolloids, 2006. **20**(1): p. In Press.
33. Krochta, J.M. and C. DeMulderJohnston, *Edible and biodegradable polymer films: Challenges and opportunities*. Food Technology, 1997. **51**(2): p. 61-74.
34. Olivas, G.I. and G.V. Barbosa-Canovas, *Edible coatings for fresh-cut fruits*. Critical Reviews in Food Science and Nutrition, 2005. **45**(7-8): p. 657-670.
35. Krochta, J.M. and C.L. Demulder, *Biodegradable Polymer-Films from Agricultural Products*. Abstracts of Papers of the American Chemical Society, 1995. **209**: p. 61-Btec.
36. Debeaufort, F., M. Martinpolo, and A. Voilley, *Polarity Homogeneity and Structure Affect Water-Vapor Permeability of Model Edible Films*. Journal of Food Science, 1993. **58**(2): p. 426.
37. Vargas, M., J. Weiss, and D.J. McClements, *Adsorption of Protein-Coated Lipid Droplets to Mixed Biopolymer Hydrogel Surfaces: Role of Biopolymer Diffusion*. In preparation, 2007.

Chapter 2

The Assembly and Disassembly of Biopolyelectrolyte Multilayers and Their Potential in the Encapsulation and Controlled Release of Active Ingredients from Foods

J. Moffat, R. Parker, T. R. Noel, D. Duta, and S. G. Ring

**Institute of Food Research, Norwich Research Park, Colney,
Norwich NR4 7UA, United Kingdom**

The assembly of multilayers using layer-by-layer (LbL) deposition of oppositely charged biopolyelectrolytes has the potential to form novel barriers with applications in controlled delivery in the food and pharmaceutical industries. Multilayer assembly was studied using FTIR-ATR and a quartz crystal microbalance to give information on the mass of the deposited layers, their chemical characteristics and hydration. The polyanions examined were pectins of varying degrees of esterification, while chitosan, poly-L-lysine and, at a pH below its pI, β -lactoglobulin were the polycations. Multilayer formation occurred at pH's when both anionic and cationic polyelectrolytes carried a charge. The hydration of the structures was sensitive to variations in pH and ionic strength, resulting in environmentally responsive behavior. Disassembly could be triggered by change in pH, or pH history, resulting in an initial weakening of attractive interactions and subsequent solubilisation of the components. A centrifugation technique for applying a chitosan/pectin multilayer coating to emulsion droplets is also described.

Introduction

The structure and composition of foods affect the site and rate of release of their components and, if manipulated in a rational way, offers the opportunity for foods with controlled or modified release functionalities. Multiple phases are present in foods (1); both in foods themselves and when they are mixed with digestive fluids and so interfacial processes assume a key role in the science of the release process. In pharmaceutical technology there are many types of functional coatings and structures for achieving controlled and modified release of bioactive compounds (2). Designing foods as delivery systems, however, presents a number of distinctly different challenges.

Polyelectrolyte multilayer approaches offer a means of structuring interfaces with potentially useful functionalities (3). The majority of research has been on synthetic polyelectrolyte multilayers (3, 4) but more recent studies have reported results for biopolyelectrolytes (5, 6) including food biopolymers (7, 8).

In previous work we have studied the assembly of biopolyelectrolyte multilayers comprising anionic polysaccharides with cationic polysaccharides, polyamino acids or globular proteins using a range of complementary techniques (9, 10, 11). Surface plasmon resonance was used to follow the sequential layer by layer deposition of pectin and chitosan in real-time under conditions of continuous flow (9). The stoichiometry of pectin/poly-L-lysine multilayers was such that the polymers carry a net positive charge contrary to the common assumption of intrinsic charge balance (11).

In the present work the aim was to identify the factors underlying the disassembly of multilayers in response to changing environmental conditions. In order to test whether multilayer environmental responsiveness investigated upon plane surfaces can be related to release characteristics in three dimensional systems, the multilayers need to be deposited on disperse systems. A centrifugation method for achieving this is also described.

Materials and Methods

Materials

Poly-L-lysine hydrobromide (PLL) with a mean degree of polymerization of 70 and β -lactoglobulin (BLG) were obtained from Sigma, low molecular weight chitosan (nominal degree of acetylation 75-85%) was obtained from Aldrich, citrus pectins with degrees of esterification 51% and 71% were obtained from CP Kelco (Denmark) and citrus polygalacturonic acid (PGA) was obtained from Fluka. D₂O (99.9%), hexadecane, L- α -phosphatidylcholine, sucrose and buffer salts were also obtained from Sigma. Chemical and physicochemical

characterisation of the pectins has been reported previously (11, 12). For multilayer deposition polymers were dissolved at a concentration of 0.6 mg mL^{-1} in 10 mM buffer solution with 30 mM NaCl. For base layers PLL was dissolved at a concentration of 0.08 mg mL^{-1} .

Multilayer-coated emulsion preparation

Five g of hexadecane was blended for 3 min with 95 g of 1% w/w L- α -phosphatidylcholine in 100 mM pH 3.0 acetate buffer using an ultra Turrax T25 fitted with an S-25N head. 1 mL of the emulsion was then dispersed in 40 mL of 25% w/w sucrose. A gradient was formed in a 15 mL centrifuge tube in the order: emulsion/25% w/w sucrose; chitosan/20% w/w sucrose; pectin (or PGA)/15% w/w sucrose; chitosan/10% w/w sucrose; pectin (or PGA)/5% w/w sucrose. The polymer concentration was 0.08 mg/mL in pH 3.6 acetate buffer. Each layer was separated by a layer of buffer containing sucrose of the appropriate concentration. After centrifugation at 2000 g for 30 min, emulsion droplets were harvested from each of the buffer layers.

Fourier Transform Infrared-Attenuated Total Reflection (FTIR-ATR) Spectroscopy

Infrared spectra were collected, over the range $2000\text{-}1500 \text{ cm}^{-1}$, on a Nicolet 860 FTIR spectrometer (Thermo Electron Corporation, Madison, USA) fitted with a silicon cylindrical ATR crystal in a MicroCircle liquid ATR cell (SpectraTech, Warrington, UK). Methods used were as detailed in Krzeminski *et al.* (11). The silicon crystal presented a silica surface for multilayer deposition. The multilayer was deposited by a layer-by-layer (LbL) procedure (3). A base layer of the cationic polyamino acid PLL is first deposited on the silica surface of the ATR crystal of the FTIR by injecting PLL solution into the sample cell. After an adsorption time of 3 min, the excess solution is washed off by injecting buffer solution (as used to dissolve the PLL). This is followed by injecting a polyanion solution, followed by a buffer wash, a polycation solution, a buffer wash and so on until the required number of layers has been deposited. Absorbances were measured relative to a baseline at 1800 cm^{-1} and quantitative analysis was based on methods of Sperline *et al.* (13).

Quartz Crystal Microbalance

Measurements were made with a D300 quartz crystal microbalance with dissipation monitoring (QCMD, Q-Sense AB, Västra Frölunda, Sweden) with a

QAFC 302 axial flow measurements chamber as described in Krzeminski *et al.*, (11). The sensing element was a disc-shaped piezoelectric quartz crystal sandwiched between two gold electrodes which presented a gold surface for multilayer deposition. An approximate analysis of the frequency shift of the microbalance can be made using the Sauerbrey approach (14) to give the hydrated mass of the adsorbed layer. A more refined analysis takes the viscoelasticity of the multilayer into account (15) and was performed using QTools software (Q-Sense AB, as above).

Microelectrophoresis

Electrophoretic mobility of the emulsion droplets in pH 5.6 acetate buffer was determined using a Zetasizer 3 (Malvern Instruments) fitted with a AZ4 electrophoresis cell calibrated using a latex electrophoretic mobility standard.

Results

The disassembly of multilayers was studied by first assembling multilayers directly on the surface of the sensing element of the spectrometer or microbalance and then following their behavior as the solvent conditions were changed. Pectin/protein multilayers can be assembled at pH's below the isoelectric point of the protein under conditions under which the pectin carries a negative charge due to its ionized anhydrogalacturonic acid groups and the protein carries a net positive charge because its positively charged residues outnumber its negatively charged residues. Figure 1 shows the result of a pH titration on a 8 layer pectin/ β -lactoglobulin multilayer probed using FTIR-ATR.

The spectrum of the multilayer in the frequency range 1500 – 1800 cm^{-1} is dominated by the amide I band (1635 cm^{-1}) of the BLG with small absorption bands arising from the –COOD stretch vibrations of the anhydrogalacturonic acid groups (1730 cm^{-1}), –C=O uronic acid methyl ester and the asymmetric stretch of –COO⁻ (1612 cm^{-1}) of the pectin (16). The pK_a of the uronic acid of pectin vary in the range 3.5 – 4.5 (17) and so both ionised and unionised species can be expected at pD 3.6. The carboxyl and carboxylate groups of the acidic amino acid residues (aspartic and glutamic acid) of BLG absorb in the region of 1725 cm^{-1} and 1572 cm^{-1} , respectively. Figure 1 shows spectra for the multilayer as it is rinsed with buffers of increasing pH over the range 3.6 – 5.4. Initially, over the range 3.6 – 4.8, the absorbance associated with carboxyl groups of pectin and/or the protein (1725-1730 cm^{-1}) shows a small decrease. Simultaneously there is an increase in the absorbance associated with the aspartate and glutamate residues of the protein (1572 cm^{-1}). This indicates that while there is an increasing number of negative charges on the protein and a

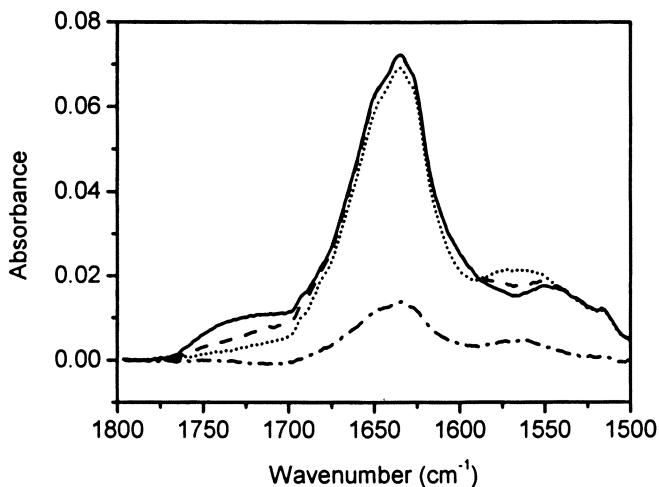


Figure 1. Infrared spectra of a 8 layer pectin (51% DE)/BLG multilayer at pD: 3.6 (—); 4.2 (----); 4.8 (·····); and 5.4 (-·-·-). (Reproduced with permission from reference 16. Copyright 2007).

shifting intrinsic charge balance within the multilayer, it nevertheless maintains its integrity on the ATR crystal. As the pH is further increased there is a marked decrease in the absorbance associated with the amide I band which is shown in Figure 2.

The midpoint of this step decrease is about 5.1 (in a similar experiment using bovine serum albumin the change occurred at pH 5.5 (results not shown)). As the isoionic point of isolated BLG is about 5.1 (18) this shows disassembly is occurring in the region of the isoelectric point of the protein, suggesting that charge interactions are important in stabilising the multilayer and the overall net charge on the protein is a major factor.

The polyamino acid PLL can also be used as the positively charged biopolymer in the assembly of multilayers with pectins of varying degrees of esterification (11). Estimates of the charge balance in these systems showed the net intrinsic charge (that carried by the polymers) in these multilayers was positive and increased with degree of esterification *i. e.* the most highly esterified pectin with the lowest mean charge spacing had the lowest anion/cation charge ratio. This is contrary to the common assumption that the charge on the polymers within the multilayer is balanced ("intrinsic charge balance")(19). By quantifying the relative amounts of galacturonate and ester groups from FTIR studies of the assembly of these multilayers it was found that there was a limited fractionation of the pectins with the more highly esterified (lower mean charge density) pectins absorbing less strongly into the multilayer.

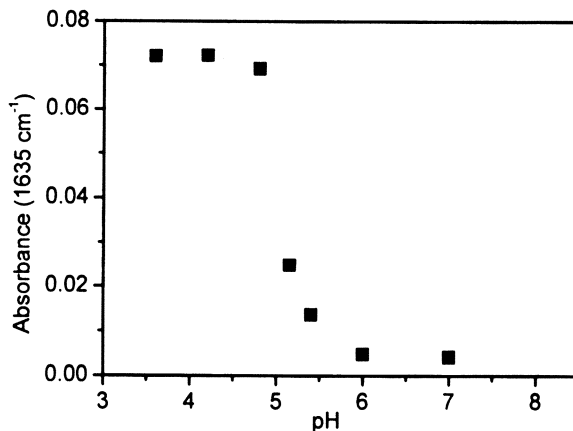


Figure 2. Infrared amide I peak absorbance versus pH for a 8 layer pectin (51% DE)/BLG multilayer. (Reproduced with permission from reference 16. Copyright 2007).

The response of these structures to changing pH has been studied using QCMD and FTIR-ATR (20). The frequency and dissipation changes at the fundamental resonant frequency and three overtones were modeled using a viscoelastic continuum model (15) yielding a hydrated mass for the multilayer. In studying the response of the multilayer to changing environmental conditions the hydrated mass is ratioed to its initial value after assembly to give a swelling ratio. Figure 3 shows the swelling ratio for a 10 layer pectin (71% DE)/PLL multilayer assembled in 10 mM pH 7.0 phosphate buffer containing 30 mM NaCl.

As the pH decreases from 7.0 to 5.0 there is a shrinkage of the multilayer, followed by a reswelling of the multilayer as the pH further decreases from 3.6 to 2.0 and 1.5 (pHs which might be encountered in the stomach). FTIR-ATR measurements (Figure 4) on the effects of these lower pH's on the multilayer show solubilisation of polymer. As the pH is reduced from 7.0 to 2.0 and then 1.5 there is a decrease in absorbance at 1650 cm⁻¹ (amide I of PLL) and 1610 cm⁻¹ (anhydrogalacturonate component of pectin) and a relatively small increase at 1730 cm⁻¹ (anhydrogalacturonic acid component of pectin). As the pectin binds protons (strictly deuterons) with decreasing pH both PLL and pectin are being solubilised. When the system was returned to pH 7.0 (results not shown) it was found that about 80% of the PLL and 85% of the pectin had been solubilised.

In combination the results suggest that as the pH is decreased from 3.6 to 2.0 there is a reduction in PLL cross-linking and the system swells to form a more open structure. On return to pH 7.0 the loss of PLL cross-linker and reionisation of the pectin result in its partial solubilisation. The residual structure has less than 50% of its original hydrated mass (QCMD result, not shown).

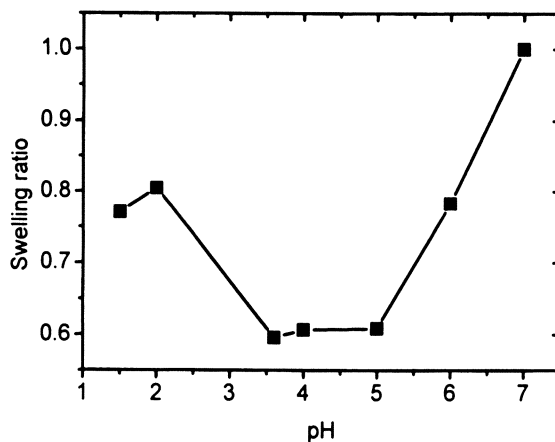


Figure 3. Swelling ratio as a function of pH in the range 7.0 to 1.5 for a 10 layer pectin (71% DE)/PLL multilayer formed at pH 7.0 measured using QCMD. (Reproduced with permission from reference 20. Copyright 2007).

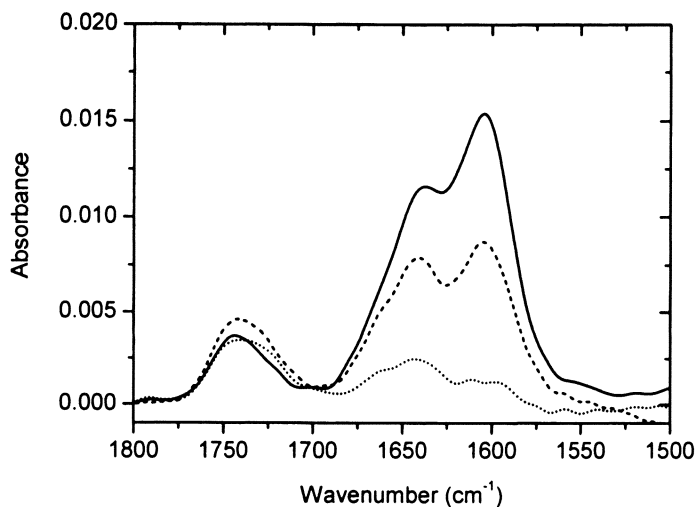


Figure 4. Infrared spectra of a 10 layer pectin (71% DE)/PLL multilayer formed at pH 7.0 as a function of pH. At pH: 7.0 (—), 2.0 (-----) and 1.5 (.....). (Reproduced with permission from reference 20. Copyright 2007).

The above results show that food biopolymer multilayers may be deposited on macroscopic solid surfaces but for some practical applications deposition upon the surface of solid or liquid disperse systems is required. While at the molecular length scale the elementary polymer adsorption/desorption steps depend upon diffusion, in order to exchange the bulk polymer and buffer solutions for the LbL process, relative motion of the dispersed particles and fluid dispersion medium is required. Using centrifugation and a sucrose density gradient this can be achieved in a "one pot" method. Firstly, the appropriate sequence of uncoated emulsion, polymer and buffer solutions of decreasing density are layered into a centrifuge tube. Centrifuging the tube causes the emulsion droplets to cream through the sequence of layers. The ζ -potential of the emulsion droplets recovered from the buffer layers are shown in Figure 5.

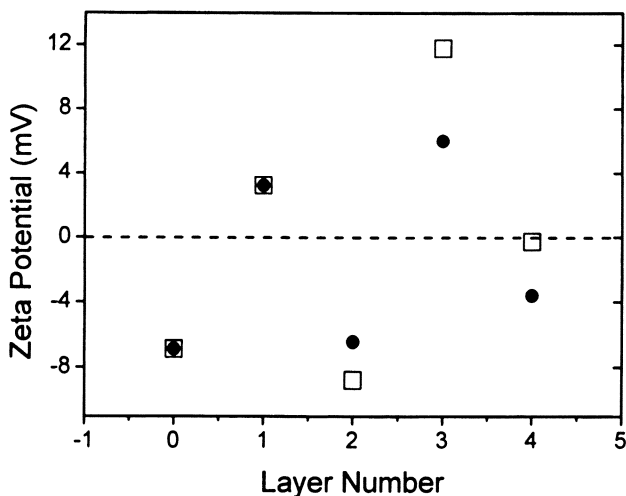


Figure 5. ζ -potential of emulsion droplets at pH 5.6 as a function of layer number after their coating with chitosan and pectin (71% DE) (\square), or polygalacturonic acid (\bullet) layers.

The changing sign of the ζ -potential reflects the changing sign of the charge at the hydrodynamic plane of shear as probed through measurements of the droplet's electrophoretic mobility. The initial negative charge on the droplets originates from the phospholipid used to emulsify the hexadecane. After the droplets have passed through a chitosan layer they have a positive charge (Layer 1 and 3) and after the droplets have passed through a pectin or polygalacturonic acid layer they have a negative charge (Layer 2 and 4). The degree of esterification of the pectin has only minor effects on the ζ -potential of the droplets.

Discussion and Conclusions

Multilayers could affect the release of active ingredients from foods by several mechanisms. If particles or droplets were coated they could modify the flavour or taste of a food through an effect on interfacial transport. The multilayers may act in a similar way to a pharmaceutical enteric coatings *i. e.* by encapsulating materials, separating them from the stomach contents and wall, and then allowing them to be released further down the GI tract. Release from multilayer-coated systems could be by diffusion through the coating and/or erosion of the coating by digestive processes in the small intestine or fermentation in the colon (21). Multilayers could have adhesive or lubricating properties thus affecting rates of transport. In the present study we have examined multilayers for environmentally responsive behaviour, focusing on responses to changes in pH. Future work will examine whether these responses relate to changes in release.

Our results show that, by using a globular protein (in reality a polyampholyte) as the polycation, a layer which will solubilise in the vicinity of the pI of the protein can be made. This result is perhaps not surprising as related dissociation or phase coalescence can be observed for electrostatic complexes (22) and coacervates (23) comprised of (nominally) the same molecules. The same electrostatic interactions underlie each phenomenon though there may be non-equilibrium factors which differentiate the behaviour of multilayers. Experiments using a true polycation (poly-L-lysine) allowed multilayers to be deposited at neutral pH's. On subjecting these to pH changes which might be experienced in the stomach a limited solubilisation of multilayer resulted. In conjunction with the processes mentioned above these responses could potentially modulate rates of release. It is worth noting that in both these systems the pH sensitivity results from the weakly acidic character of carboxyl groups whether they are the anhydrogalacturonic acid residues of pectin and those on aspartic and glutamic acid residues of the protein.

The homogeneity of the multilayers is an important aspect which has not yet been examined sufficiently. In the synthetic multilayer literature there are examples of systems in which the degree of heterogeneity can be switched with pH variation (24). Whether these structures can be maintained on liquid-liquid interfaces rather than solid-liquid interfaces also needs to be established.

In a many practical situations these coating would need to be applied to disperse systems. Methods for applying coatings to alginate-based gel particles are well developed (25). If particles are sufficiently robust filtration and redispersion processes can be used during the LbL deposition process. For particles susceptible to irreversible aggregation and coalescence alternative methods may be required. In principle droplets could be processed singly in a microfluidic device or, as shown practically in this study, centrifugation can be used to transfer droplets between phases.

Acknowledgements

The authors thank the UK Biotechnology and Biological Sciences Research Council for supporting this research through the core strategic grant and the award of a studentship to JM (BBSSK200310164) and the EC commission for the award of a Marie Curie fellowship to DD (contract number QLK-1999-50512).

References

1. Walstra, P. *Physical Chemistry of Foods*; Marcel Dekker: New York, 2003; pp 282-315.
2. *Design of Controlled Release Drug Delivery Systems*; Li, X.; Jasti, B. R. Eds.; McGraw-Hill: New York, 2005; pp 1-435.
3. Decher, G. *Science* **1997**, *277*, 1232.
4. *Multilayer Thin Films, Sequential Assembly of Nanocomposite Materials*; Decher, G.; Schlenoff, J. B. Eds.; Wiley: Weinheim, 2003.
5. Elbert, D. L.; Herbert, C. B.; Hubbell, J. A. *Langmuir* **1999**, *15*, 5355.
6. Richert, L.; Lavallo, P.; Payan, E.; Shu, X. Z.; Prestwich, G. D.; Stoltz, J. F.; Schaaf, P.; Voegel, J. C.; Picart, C. *Langmuir* **2004**, *20*, 448.
7. Ogawa, S.; Decker, E. A.; McClements, D. J. *J. Agric. Food Chem.* **2004**, *52*, 3595.
8. Guzey, D.; McClements, D. J. *Adv. Coll. Int. Sci.* **2006**, *128*, 227.
9. Marudova, M., Lang, S., Brownsey, G. J.; Ring, S. G. *Carbohydr. Res.* **2005**, *340*, 2144.
10. Laos, K.; Parker, R.; Moffat, J.; Wellner, N.; Ring, S. G. *Carbohydr. Polym.* **2006**, *65*, 235.
11. Krzeminski, A.; Marudova, M.; Moffat, J.; Noel, T. R.; Parker, R.; Wellner, N.; Ring, S. G. *Biomacromolecules* **2006**, *7*, 498.
12. Marudova, M.; MacDougall, A. J.; Ring, S. G. *Carbohydr. Res.* **2004**, *339*, 209.
13. Sperline, R. P.; Muralidharan, S.; Freiser, H. *Langmuir* **1987**, *3*, 198.
14. Sauerbrey, G. *Zeitschrift Für Physik* **1959**, *155*, 206.
15. Voinova, M. V. ; Rodahl, M.; Jonson, M.; Kasemo, B. *Phys. Scr.* **1999**, *103*, 472.
16. Noel, T. R.; Krzeminski, A.; Moffat, J.; Parker, R.; Wellner, N.; Ring, S. G. *Carbohydr. Polym.* **2007**, *70*, 393.
17. Ralet, M. C.; Dronnet, V.; Buchholt, H. C.; Thibault, J. F. *Carbohydr. Res.* **2001**, *336*, 117.
18. Cannan, R. K.; Palmer, A. H.; Kibrick, A. C. *J. Biol. Chem.* **1942**, *142*, 803.

19. Schlenoff, J. B. in *Multilayer Thin Films, Sequential Assembly of Nanocomposite Materials*; Decher, G.; Schlenoff, J. B. Eds.; Wiley: Weinheim, 2003, pp 99-132.
20. Moffat, J.; Noel, T. R.; Parker, R.; Wellner, N.; Ring, S. G. *Carbohydr. Polym.* **2007**, *70*, 422.
21. Milojevic, S.; Newton, J. M.; Cummings, J. H.; Gibson, G. R.; Botham, R. L.; Ring, S. G.; Stockham, M.; Allwood, C. J. *Controlled Release* **1996**, *38*, 75.
22. Girard, M.; Turgeon, S. L.; Gauthier, S. F. *Food Hydrocolloids* **2002**, *16*, 585.
23. Girard, M.; Sanchez, C.; Laneuville, S. I.; Turgeon, S. L.; Gauthier, S. E. *Colloids Surfaces B Biointerfaces* **2004**, *35*, 15.
24. Rubner, M. F. in *Multilayer Thin Films, Sequential Assembly of Nanocomposite Materials*; Decher, G.; Schlenoff, J. B. Eds.; Wiley: Weinheim, 2003, pp139-141.
25. Pommersheim, R.; Schrezenmeir, J.; Vogt, W. *Macromol. Chem. Phys.* **1994**, *195*, 1557.

Chapter 3

A Theoretical Self-Consistent Field Study of Mixed Interfacial Biopolymer Films

Rammile Ettelaie, Anna Akinshina, and Eric Dickinson

**Procter Department of Food Science, University of Leeds,
Leeds LS2 9JT, United Kingdom**

The adsorption of a linear polyelectrolyte onto an existing layer of protein at an interface has been investigated. Calculations using a simple model, involving only the short range interactions, show that the polyelectrolyte forms a more extended distinct secondary layer if only certain sections of the molecule interact with the protein layer. These results are also confirmed for a more sophisticated model that accounts for the electrostatic interactions between the two biopolymers. It is found that there is a maximum level of adsorption of polyelectrolyte as the number of charged segments of the chains is varied. The peak occurs at higher levels of charging as the background salt concentration is increased. We also consider the effects of pH on the adsorption. The influence of the structure of the mixed layers on colloidal forces, mediated between two surfaces covered by such films, is also discussed.

Introduction

Proteins and polysaccharides constitute two of the most important functional ingredients in foods. Polysaccharides are by and large high-molecular-weight hydrophilic molecules and as such do not show any tendency for adsorption onto hydrophobic interfaces. They are commonly added to food products as rheology modifiers, thickeners and for their excellent waterholding properties (1). In contrast, the simultaneous presence of both hydrophobic and hydrophilic amino acid groups in the primary structure of proteins makes these molecules surface-active. Most of the important functional properties of proteins in food colloids are the direct consequence of the amphiphilic nature of these molecules. Thus, proteins are widely used as foaming agents, emulsifiers and in particular as colloidal stabilisers in foods (2,3).

The presence of both polysaccharide and protein, in many food colloid formulations, gives rise to the inevitable possibility of these different species interacting with each other. In most cases, where the polysaccharides contain charged groups, these interactions are electrostatic in origin. However, shorter range interactions such as bridging by specific ions and hydrogen bonding can also be present (4). When strong enough, and at sufficient concentrations of the two biopolymers, these interactions can lead to the phase separation of the system into separate regions. The type of phase separation occurring depends on whether the interactions are synergistic or repulsive (4-7). In the latter case the system breaks up into two separate solutions, one rich in protein and the other in polysaccharide. Associative interactions on the other hand result in the phenomenon of coacervation, where one of the resulting phases has a high concentration of both biopolymers and the other is depleted in both.

Despite receiving a great deal of interest (5,6) in the past, the interactions between proteins and polysaccharides in food system were often seen as an unwanted complication. However, in recent years it has been recognised that such interactions provide interesting routes to design of a variety of foods with novel textures and structures (4,8-10). It is predicted that such structures will lead to significant possibilities for better control of the release profile of flavours during consumption of foods, for improving the mouthfeel of the products, for microencapsulation of nutrients and flavours, and for inhibiting the digestion of lipids in the design of healthier food emulsion systems, to name but a few applications.

In choosing the most appropriate structure for each type of application it is useful to broadly distinguish between two different types of structures that occur in the context of such mixed biopolymer systems. The first type involves the entire bulk of the system. An example is the kinetic trapping of a desired structure, at an intermediate stage in the phase separation of the protein and polysaccharide, as a result of gelation of one or both sets of the biopolymers

(9,11). The second type of mixed structures comprises those that are formed specifically at surfaces, and in particular hydrophobic-hydrophilic interfaces (12-15). Such surface structures rely on the amphiphilic nature of proteins to form a primary layer at the interface, with a secondary layer of polysaccharide then being adsorbed on top of the primary one. By suitable adjustment of pH, and alternating the solution, with which the interface is in contact, between one containing anionic to one with cationic polyelectrolytes or *visa versa*, several biopolymer layers can be deposited on the surface to form a multi-layered film at the interface. A number of recent studies on oil-in-water emulsions suggest that, compared to simple protein stabilised emulsions, the coverage of the droplets by these multi-layer films can provide significantly superior stability against pH changes, thermal cycles and increase in background electrolyte concentrations (12,16).

In conjunction with the experimental work there has also been a great deal of interest in theoretical modelling of the process of polyelectrolyte-protein complexation in recent years (7). Most of the work has focused on formation of complexes in bulk systems (17-21) where only one polysaccharide chain interacts with one or a small number of protein molecules. In contrast to these studies, theoretical investigation of the structure of mixed polysaccharide-protein layers has received relatively less attention in the literature (23). Within the interfacial region, the concentration of the biopolymers can be far higher than that in bulk, even for very dilute systems (3,24). Given the additional configurational restrictions that the presence of a surface imposes on the macromolecules, a polyelectrolyte adsorbed at the interface will interact with many more protein molecules. Additionally there will be strong interactions, at very least through the excluded volume and the electrostatic repulsion forces, with the neighbouring polyelectrolyte chains. Thus, under the influence of these forces, even complexes formed in the bulk in the first instance, may have a very different structure once adsorbed on the surface. However, one simplifying consequence of the high concentration of macromolecules at the interface is that the surface becomes increasing more homogenous. This is particularly the case for more flexible or highly denatured proteins, or those with disordered coil-like structures. An archetypal example of the latter is the heterogeneous milk protein casein. In particular, α_{s1} -casein and β -casein are known to have no tertiary and very little secondary structure (25).

The current study focuses on the formation of mixed interfacial layers of flexible disordered protein and polyelectrolyte using the method of Self Consistent Field (SCF) calculations (26,27). Like Monte Carlo simulations, the method only deals with the equilibrium properties of the interfacial film. However, being a numerical calculation, it has the advantage that the presence of a large number of chains can be accounted for. We begin by first giving a brief outline of the SCF methodology in the next section. We then consider a simple model consisting of mixtures of amphiphilic and hydrophilic chain species.

Initially we only introduce short range interactions between the chains. Even at this level of approximation certain interesting features of the mixed interfacial film become evident. We then extend our calculations to surface layers formed by protein-like and polysaccharide-like chains in which the electrostatic interaction play the dominant role. Our model for the protein is roughly based on the primary structure of α_{s1} -casein. We investigate the influence of pH, salt concentration and distribution of charge groups of the polyelectrolyte on the degree of adsorption of these chains and its consequence for the structure of the resulting interfacial layers.

Another possible route for achieving protein-polysaccharide mixed films is to have covalently bonded complexes of these molecules adsorb at the surface (28,29). In the present work we shall not study such systems, deferring the discussion to future publications.

Self Consistent Field Calculations and the Methodology

The theoretical basis of the SCF theory and the details of its implementation have been extensively described in the literature (26, 27, 30). Therefore, in this section we shall confine ourselves to presenting an outline of the key aspects of the method relevant to the present study. In SCF theories all molecular species, including biopolymers, salt ions and solvents are considered to be made from interconnection of a set of equal sized segments. While the salt ions and the solvent molecules only consist of one segment, the biopolymer chains have an appropriately large number of connected units, reflecting their polymeric nature. The monomeric segments on a chain may all be identical, representing a homopolymer, or they may be chosen to have different properties, as would be the case for protein chains consisting of many different types of amino acids. The central quantities of interest to be obtained from SCF calculations are the spatial variation of a set of density profiles between two approaching interfaces. These density profiles, $\phi^{\alpha}(z)$, are determined as functions of perpendicular distance, z , away from one of the interfaces, for each type of segment α , belonging to each kind of biopolymer species i that is present in the solution. The interfaces are taken to be sharply defined, flat surfaces. Units interact with the solvent molecules, the surface and other neighbouring segments through short range interactions. The strength of such interactions between any two different segment types α and β , as well as those with the surface and the solvent, are specified by a set of Flory-Huggins parameters $\chi_{\alpha\beta}$. As usual, a negative value of the Flory-Huggins parameter between two segment types indicates an affinity between the two, while positive values represent an unfavourable interaction. Similarly, we have a good solvent for any given kind of segment, if the solvent-segment χ parameter between the two is less than 0.5,

and a poor solvent if χ is larger than this value (31). Each segment, depending on its type and its location, experiences a potential that in parts is due to the above short range interactions with the neighbouring units. However, there are also two further terms contributing to this potential. The first of these is a hard core potential, $\psi_{hd}(z)$, that enforces the incompressibility condition

$$\sum_i \sum_\alpha \phi_i^\alpha(z) = \sum_i \sum_\alpha \Phi_i^\alpha \quad (1)$$

In the above equation the quantity Φ_i^α refers to the bulk concentration of segments of kind α , belonging to species of type i . The hard core potential term ensures that the total concentration of all segments, including ions and solvent molecules, adds up to the same value everywhere in the system. It can be shown (26,27), that at any given location, this hard component is the same for all segments, irrespective of their type. The second additional contribution to the overall potential only arises for those monomeric groups that are charged. In that case a charged group also interacts with ions and other charged segments through the longer range electrostatic forces. This can easily be accounted for if the local electric potential, $\psi_{el}(z)$, at the location of the charged unit is known. The overall potential resulting from addition of all the three different components mentioned above, for a segment of type α with a net electric charge of q_α , placed at location z , is given by the following expression:

$$\psi^\alpha(z) = \psi_{hd}(z) + \sum_i \sum_\beta \chi_{\alpha\beta} (\phi_i^\beta(z) - \Phi_i^\beta) + q_\alpha \psi_{el}(z) \quad (2)$$

An important assumption in SCF theory is that chains can adopt all configurations available to them. Therefore, the properties related to any given biopolymer species, such as its segment density profile, can be obtained by appropriate statistical mechanics averaging of the quantities of interest over all possible configurations of the chains. This requires the calculation of the Boltzmann factor associated with each configuration, which in turn can only be done if the segment potentials are known. Since these potentials are related to the concentration profiles of the segments in the first place, we have a situation where in order to calculate the desired density profiles one requires a prior knowledge of such profiles. The problem is resolved through an iterative scheme. One begins by choosing a rough initial guess of the concentration profile for each segment type. With the distribution of all groups, including the charged ones now specified, the segment potentials can be calculated from equation 2. For the electric potential term this is made marginally more

complicated by the fact that one first has to solve the Poisson equation $-\nabla^2\psi_{el} = \rho(z)/\epsilon$, where $\rho(z)$ is the charge density at point z and ϵ is the dielectric constant of the solution. Using the segment potentials, a new set of density profiles can be calculated by averaging the segment distribution functions over all configurations available to each molecular species present in the solution. Despite the huge number of internal configurations available to polymeric chains, this procedure can be carried out very efficiently using the numerical scheme originally proposed by Scheutjens and Fleer (26,27). The newly obtained density profiles are next used to recalculate the segment potentials and the whole process is repeated until convergence is obtained.

The resulting self-consistent concentration profiles can also be used to obtain the free energy of the system. It can be shown that the set of density profiles computed through the SCF procedure are precisely those that minimise the free energy of the system (32). In particular, by considering changes in the free energy of the system, as the separation distance between two surfaces is altered, the colloidal interaction forces mediated by the biopolymers between two particles can be computed.

It must be emphasised that, while the assumption regarding the chains adopting all configurations available to them is broadly true of disordered proteins (25,33), that is not true of globular proteins. These, in their native states, only sample a very small number of states available to them. For this reason, the current work will primarily focus on coil-like proteins. Application of self consistent field theories to adsorbed films of the disordered milk protein β -casein (25,30,33), has already been shown to produce results which are in good agreement with the neutron reflectivity experiments on the same protein. Such studies have also been successful in providing a clear explanation for the observed differences in salt-dependent emulsion stability behaviour of droplets stabilised by α_{s1} - and β -casein (33).

Results and Discussion

Simple Model Involving Short Range Interactions

Before we consider the issue of electrostatic interactions and other features arising from the primary structure of protein chains, it is instructive first to study a very simple model. This involves considering a mixture of amphiphilic and hydrophilic polymers. For the amphiphilic molecules we assume a diblock structure, consisting of 100 hydrophobic and 100 hydrophilic segments. We shall refer to these as monomer type A and B, respectively. The hydrophilic polymer will initially be taken as a homopolymer made from $N = 1500$

monomers of type C. The large value of N is to reflect the fact that polysaccharide chains are usually considerably larger than their protein counterparts. The interaction χ parameter for the solvent-hydrophobic monomers is set at 1 (in units of kT). These groups also have an affinity for the surface with an adsorption energy of $-1 kT$ per monomer. Hydrophilic segments, belonging to both species, have no tendency to adsorb at the interface and the solvent is assumed to be athermal ($\chi = 0$) for these. Thus, only in the presence of a favourable interaction between the hydrophilic and amphiphilic chains, is the former expected to adsorb at a hydrophilic-hydrophobic interface.

It is known that homopolymers will adsorb at a flat well defined solid interface only if the magnitude of the adsorption energy per monomer exceeds a certain critical value (26). This critical adsorption energy is required to compensate for the configurational entropy loss suffered by the chains residing in the interfacial region. It is useful to consider whether the same is also true of adsorption of one species of polymer on top of a layer of another polymer. We have used our SCF calculations to predict the variation in the excess amount of hydrophilic polymers at the interface. The number of amphiphilic chains on the surface is kept constant at 0.001 chains per unit monomer area, a_0^2 . This is ensured by having the end monomer, on the hydrophobic side for each chain, tethered to the surface. Unless stated otherwise we shall take a_0 as being 0.3 nm throughout this work. The bulk volume fraction of the hydrophilic chains is set at 0.01 %.

The results presented in Figure 1 show the excess amount, θ^{ex} , of homopolymer at the surface, plotted as a function of the strength of the short range interactions between these chains and the B segments of the diblock polymer. Note that the excess amount is calculated by integrating the volume fraction of the homopolymer, up and beyond its bulk value, over the entire interfacial region. For large polymers, this interfacial region can extend some distance away from the solid surface. It is seen that below the critical interaction strength of around $1.5kT$, the hydrophobic chains are not adsorbed at the surface. Although not very clearly seen on the scale used in the graph, the value of θ^{ex} is in fact negative for $|\chi| < 1.5kT$. This indicates a depletion of the chains from the interfacial region. Above the critical value, the adsorbed amount increases rapidly as the interaction between the B segments of the amphiphilic molecules and the free hydrophilic chains is made stronger.

The thermodynamic similarity of homopolymer chains adsorbing onto a primary layer of polymer to that where they adsorb directly onto a solid surface also extends to the actual configurations adopted by the homopolymer. In Figure 2 we present the calculated density profiles for both the amphiphilic and the hydrophilic chains in our simple model system described above. The bulk concentration of the hydrophilic homopolymer is now set at 0.1% and the interaction parameter χ between B and C segments is -3 . The density variations

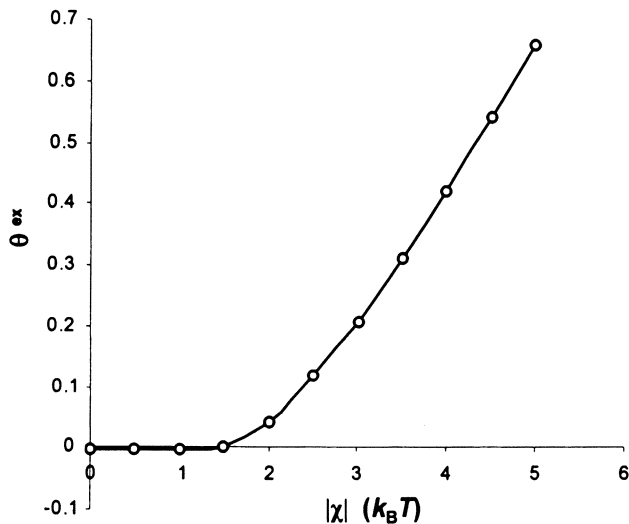


Figure 1. The excess amount of hydrophilic polymers in the interfacial region, θ^{ex} , plotted as a function of the strength of interaction, χ , between these and the B segments of the amphiphilic chains.

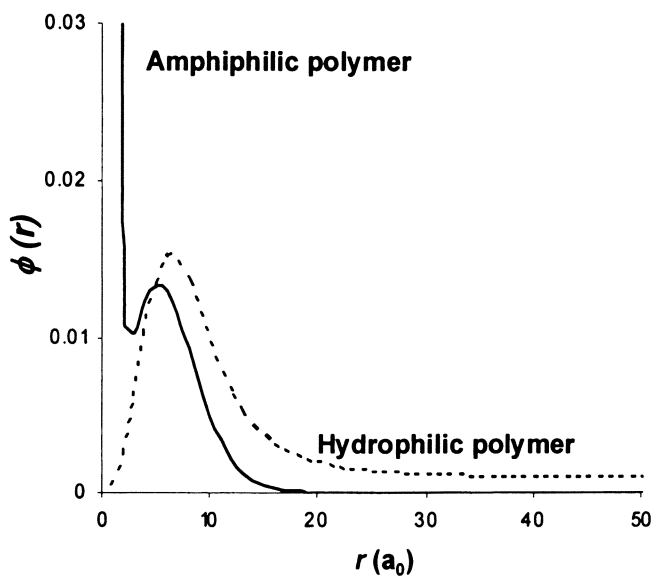


Figure 2. Variation of the density profile $\phi(r)$ of the hydrophilic (--) and amphiphilic (—) chains as a function of distance, r , away from a solid surface.

are plotted against the distance into the bulk, away from the solid interface. There is a large concentration of the amphiphilic diblock species, nearly all consisting of the hydrophobic A segments, in direct contact with the wall. As expected, the hydrophilic part of the molecules protrudes further into the bulk. What is more interesting is the presence of the homopolymer, drawn to the interfacial region, through the favourable interactions with the diblock chains. However, it is also quite evident that the homopolymer molecules do not form a clear distinct secondary layer of their own. Instead, they lie relatively flat at the interface, with a large degree of overlap with the hydrophilic B segments of the amphiphilic polymer.

The above situation is drastically altered if only certain segments or parts of the homopolymer were allowed to interact with the diblock molecules. In Figure 3 we have presented the results of our calculations for such a case. Now only 500 out of the total 1500 monomers of the hydrophilic chains have a favourable interaction with the B segments of the diblock chains, but with a slightly higher strength of $-5kT$. For the rest, this interaction is switched off by setting the appropriate χ values to zero. All other parameters are kept exactly the same as those in Figure 2. The graph of the density profile for the hydrophilic chains in Figure 3 now shows the emergence of a distinct secondary layer. This predominately consists of the non-interacting groups of the hydrophilic polymer. The layer is also seen to extend well into the aqueous phase, far beyond the initial primary layer. As we shall see in the next section, the differences exhibited between these two simple models, as presented in Figures 2 and 3, remain true even when the short range interactions are replaced by long range electrostatic ones.

Mixed Layers of α_{s1} -Casein and Polyelectrolyte

In this section we shall consider a more realistic model for our amphiphilic molecules based on the known primary structure of the milk protein α_{s1} -casein. We also account for the presence of individual salt ions, as well as the charge groups on both the polyelectrolyte and our α_{s1} -casein-like chains. These charge groups interact with each other via the usual electrostatic forces. Previous SCF calculations (25,33) have shown that many of the features of the adsorbed layers of α_{s1} or β -casein can be reproduced using a model in which the various type of amino acid residues making up the proteins can be divided into a relatively small number of groups. In the calculations presented here we shall use six types of distinct residue units. The first two of these are the non-charged hydrophobic and polar segments. Histidine and phosphoserine are given their own separate groups, but otherwise all the other charge-carrying residues are grouped together into either the negative or the positively charged groups. The charge on these

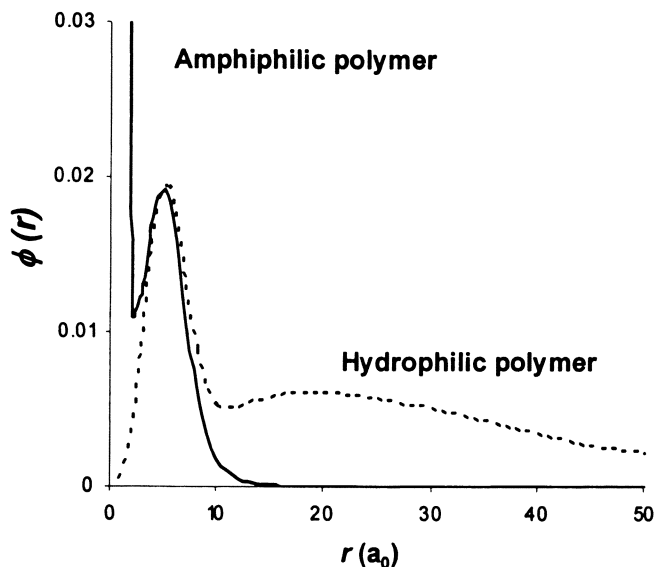


Figure 3. Same results as those in Figure 2, but now with only 500 out of a total of 1500 segments of the hydrophilic chains having an attractive interaction with the amphiphilic polymer molecules.

groups can change according to the value of the pK_a and the bulk pH. The primary structure of α_{s1} -casein, consisting of 199 amino acid residues, on which the sequence of different monomers types in our model protein is based, can be found elsewhere (25). We begin by representing the polyelectrolyte as a homopolymer of size $N = 1500$ units, with each unit carrying a fixed charge of $-2e$. The pK_a values for the charge-carrying units of the protein, as well as the χ parameters for the short range interactions between different groups, those with the salt ions and the ones with the surface, are all listed in Table 1. It is seen that apart from the hydrophobic segments, all the other groups, including the solvent, have no affinity for adsorption onto the solid surface. The solvent is assumed to be a poor one for the hydrophobic segments ($\chi = 2.5$), while there is some degree of affinity between the salt ions and the solvent molecules ($\chi = -1$). This is to capture the tendency of the salt ions to become hydrated. As for the rest of the segment types, the solvent is assumed to be athermal ($\chi = 0$). In contrast to the case studied in the previous section, there are now no favourable short range forces between our α_{s1} -casein-like molecule and the polyelectrolyte. This leaves the electrostatics as the sole possible source of attractive interaction between the two.

In what follows we shall present the results of our self consistent field calculation for systems involving a polyelectrolyte, at a bulk volume fraction of 0.01%, adsorbing from the solution onto an already existing interfacial protein film. The surface coverage for the protein film is set to 0.001 chains per monomer square area (a_0^2). With a molecular weight of around 24 kDa for the α_{s1} -casein, and assuming $a_0 = 0.3$ nm, this translates to a protein surface coverage of 0.44 mg m^{-2} . Once again, we ensure that this degree of coverage remains constant in the calculations by having the C-terminal end of the protein chains grafted onto the surface.

Table I. The Flory-Huggins interaction parameters, χ ($k_B T$), between different monomer types and pK_a values for charged amino acids used in the model.

Type	0	1	2	3	4	5	6	7	8	9
0 – Solvent	0	1	0	0	0	0	0	0	-1	-1
1 – Hydrophobic	1	0	2.0	2.5	2.5	2.5	2.5	2.5	2.5	2.5
2 – Polar	0	2.0	0	0	0	0	0	0	0	0
3 – Positive residues	0	2.5	0	0	0	0	0	0	0	0
4 – Histidine	0	2.5	0	0	0	0	0	0	0	0
5– Negative residues	0	2.5	0	0	0	0	0	0	0	0
6 – Phosphoserine	0	2.5	0	0	0	0	0	0	0	0
7 – Polyelectrolyte	0	2.5	0	0	0	0	0	0	0	0
8 – Positive ions	-1	2.5	0	0	0	0	0	0	0	0
9 – Negative ions	-1	2.5	0	0	0	0	0	0	0	0
S - Surface	0	-2	0	0	0	0	0	0	0	0
pK_{a1}	-	-	-	10	6.75	4.5	3	-	-	-
pK_{a2}	-	-	-	-	-	-	7	-	-	-

In Figures 4a and 4b we present the calculated density profiles of both biopolymers, for two different background salt volume fractions of 0.001 and 0.01, respectively. The pH of the solutions in both cases was chosen to be 4, thus making the net charge of the protein molecules positive. It is seen that there is some adsorption of the negatively charged polyelectrolyte onto the protein layer in both systems, though this is marginally less when the salt concentration is higher. In a similar manner to the homopolymer molecules studied in the simple model of the previous section, we find again that there are no distinct

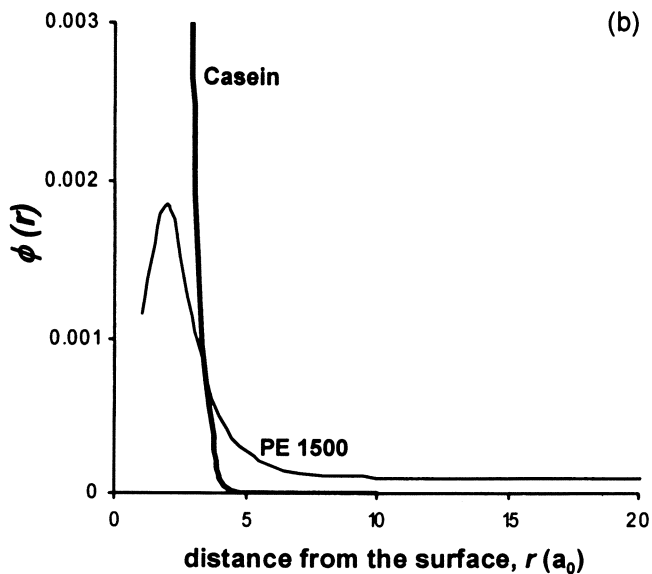
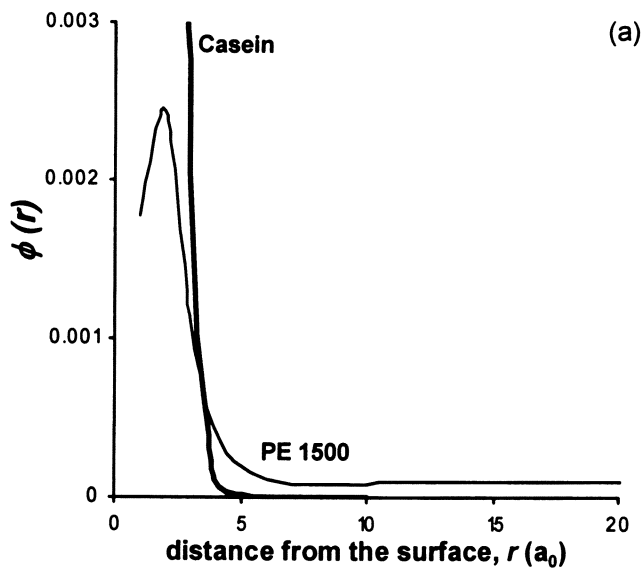


Figure 4. The density profiles of the α_{s1} – casein- like protein and the polyelectrolyte, adsorbed at the interface, at two different background salt volume fractions of a) 0.001 and b) 0.01. The polyelectrolyte (PE) consist of 1500 negatively charged segments.

secondary layers formed. Instead, the protein and the polysaccharide chains strongly overlap, forming what is best described as a mixed single layer. It is also interesting to note that the total amount of polyelectrolyte at the interface is actually rather small. We believe this is due to the very high charge on the polyelectrolyte chains used in these calculations. The picture that emerges then is one in which a relatively few, highly charged, polyelectrolyte chains lie flat at the surface, entangling with the protein layer. In doing so they quickly reverse the charge of the layer, to an extent that any further adsorption of polyelectrolyte chains is inhibited.

Effect of Varying the Charge of the Polyelectrolyte

Some recent experimental studies indicate that the effective charge of polysaccharides such as pectin, can be as low as $-14e$, far smaller than the expected value based on theoretical considerations (13). Reducing the net charge of the polyelectrolyte decreases the strength of the interactions between these chains and the oppositely charged protein layer. On the other hand, it takes a larger number of adsorbed chains to reverse the charge of the primary layer. It is therefore interesting to see how these two potentially competing effects alter the degree of adsorption of the polyelectrolyte chains to the interface. To accomplish this, we change our model such that only a fraction of segments belonging to the polyelectrolyte molecules is now charged. We also assume that these segments are distributed at one end of the chain, giving the polyelectrolyte a more heterogeneous structure. For the units retaining their charge, this is set at $-2e$ per segment as before.

Figure 5 shows the calculated density profile variation of the polyelectrolyte in the interfacial region, obtained for a number of systems involving varying degrees of charging of the chains. This calculation is done at a salt volume fraction of 0.001 and at $\text{pH} = 4$. The labels on the graphs give the number of charged segments, followed by the number of uncharged units, in each case. The density profile for the α_{s1} -casein-like molecules is also included. This shows very little variation from one system to another and is therefore only presented for one of the studied cases. It is very clear that, as the number of charged segments is reduced, the amount of adsorbed polyelectrolyte at the interface increases. Furthermore, with only part of the polyelectrolyte (as opposed to the whole chain) interacting with the protein, a secondary polyelectrolyte layer, distinct from the primary protein layer, now begins to emerge.

Of course, the increase in the amount of adsorbed polyelectrolyte with reduction in the overall charge of the chains cannot continue indefinitely. From Figure 1, we have already seen that there has to be a sufficient degree of attraction between the two biopolymers before any adsorption of the hydrophilic

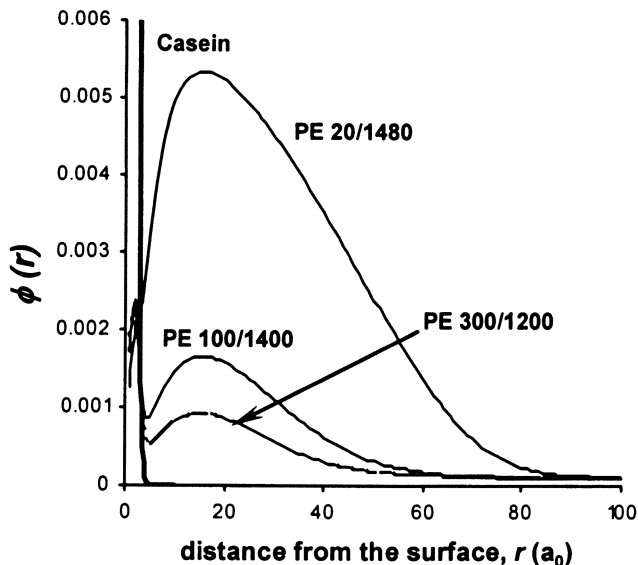


Figure 5. As Figure 4, but now involving polyelectrolytes (PE) carrying different numbers of charge segments. The label on each curve indicates the number of charged segments, followed by uncharged units, for each polyelectrolyte type studied.

chains can take place at all. For electrostatic interactions, when taken together with the above results, this implies that there has to be an optimum level of charge on the polyelectrolyte. The maximum degree of adsorption of polyelectrolyte chains onto the primary protein layer would be expected to occur at this level of charging. This is precisely what has been found here. In Figure 6 we have plotted the amount of excess polyelectrolyte at the interface against the number of charge groups on the chains at $\text{pH} = 4$. For both salt concentrations considered here, there is a peak in the amount of adsorbed polyelectrolyte. The peak occurs at a higher level of charging as the background electrolyte concentration is increased.

Colloidal Interactions Mediated by Mixed Adsorbed Films

The structure of a mixed layer of two biopolymers, adsorbed on the surface of two particles, strongly influences the nature of colloidal interactions between the particles. We have calculated such interactions between two flat surfaces, using SCF theory, for each of the systems considered in Figure 5 and also that of

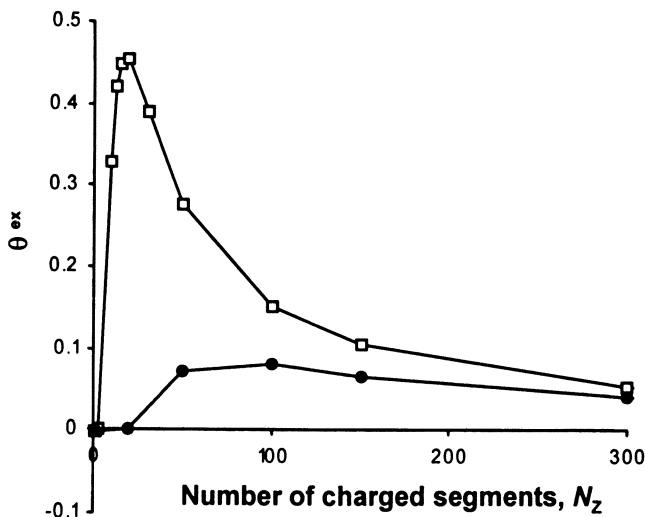


Figure 6. Variation of the adsorbed amount of polyelectrolyte, θ^{ex} , with the number of charged segments on each chain, in two different solutions with electrolyte volume fractions of (\square) 0.001 and (\bullet) 0.01.

Figure 4a. The results are summarised in graphs displayed in Figure 7. These show the interaction potential per unit area (in units of kT/a_0^2) plotted as a function of distance between the two surfaces. The interaction mediated by the pure α_{s1} -casein-like protein layers, in the absence of any polyelectrolyte, is also included for comparison. Both the steric and the electrostatic contributions arising from the mixed layers are taken into account. However, the van der Waals interactions are not included, since these are not significantly affected by the nature of adsorbed biopolymer films. Under the salt concentration and pH conditions studied here, pure α_{s1} -casein layers lead to a repulsive interaction, at all separation distances between the plates. The addition of a highly charged polyelectrolyte, where all segments of the chains are charged, is seen to drastically reduce this repulsion. Indeed, at certain separations, the forces become marginally attractive. The problem of ensuring the stability of the emulsions during the process of layer-by-layer deposition is a rather well known one, and is attributed to possible bridging of the droplets by the polyelectrolyte chains (13). When all segments of the polyelectrolyte are charged, such bridging is more likely. For now, it is more feasible for the polyelectrolyte chains to interact simultaneously with two protein layers on neighbouring surfaces.

Reducing the number of charged segments of the polyelectrolyte from 1500 down to 300, and confining these to one end of the chains, results in a purely repulsive force between the surfaces. However, the net repulsion is still less than

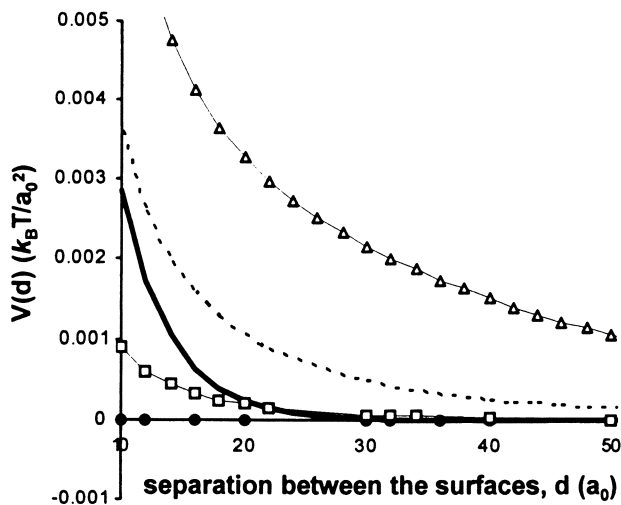


Figure 7. Interaction potential, $v(d)$, between two surfaces, mediated by the mixed protein-polyelectrolyte layers, for a number of polyelectrolytes of the same size but with different degree of charge, (\bullet) 1500; (\square) 300; (---) dashed line 100; and (\triangle) 20 charged segments. The solid line shows the potential resulting from the pure protein layer, in the absence of the polyelectrolyte.

that mediated by the pure protein layers, even though it comes into operation at further surface separations. Only when the number of charged segments is decreased to 100, is a stronger repulsive interaction, operating over longer separation distances, predicted for the mixed layers. This can be understood in terms of the structure of the mixed layers at the interface, as presented in Figure 5. These more lightly charged polymers form more extended secondary layers at the interface. The secondary layers consist mainly of the uncharged segments that have no affinity for the protein layers. The stronger and longer range repulsion results from the steric effects, as two such secondary layers overlap.

Influence of pH and Background Electrolyte

The addition of salt to a solution has the effect of screening the electrostatic interactions between the charged groups. Our calculations indicate that, for polyelectrolyte chains of any charge, the level of adsorption onto the primary protein layer is reduced as the electrolyte volume fraction is increased from 0.001 to 0.01. However, as the graphs in Figure 6 show, the decrease in the amount of excess polyelectrolyte at the interface is far more pronounced for the

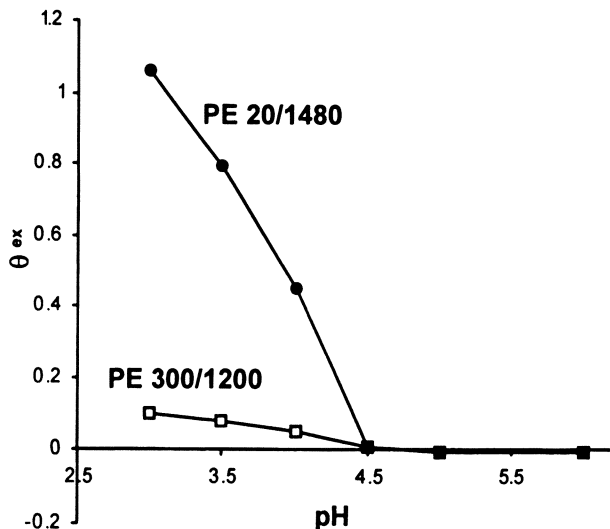


Figure 8. The amount of polyelectrolyte, adsorbed onto a primary protein layer, with the variation in the pH of the solution. The label on each curve indicates the number of charged segments, followed by uncharged segments, for each of the two polyelectrolyte types studied.

lightly charged polymers. Despite their higher level of adsorption at low salt concentrations, each individual chain of a lightly charged polyelectrolyte has a weaker binding to the oppositely charged protein layer. As the background electrolyte is increased, the screening of electrostatic interactions is expected to have a stronger effect on the adsorption of these low charged chains. This also explains the shift in the maximum value of the adsorbed polyelectrolyte, with increasing salt concentration, towards higher charged chains (see Figure 6).

The greater sensitivity of the adsorption of the lightly charged polyelectrolytes, to the weakening of the electrostatic interactions with protein, is also reflected in the manner in which the adsorbed amount varies with changes in the pH of the solution. In Figure 8, we have plotted the excess amount of polyelectrolyte at the interface, as a function of pH, for two different polyelectrolytes. In one case, out of a total of 1500 units, the chains carry 300 charged segments. In the other system, there are only 20 charged units per chain, giving each molecule a total charge of $-40e$. The coverage of the surface by the primary protein layer is fixed at 0.001 chains per unit monomer area. The bulk volume fraction of polyelectrolyte and that of the background electrolyte are 0.01 and 0.001, respectively. As the pH of the solution is reduced, the net charge of the primary protein layer changes from being negative to positive, increasingly further with the lowering of pH. At pH values below

the pI value (~ 4.5) of our α_{s1} -casein-like protein, the amount of adsorbed polyelectrolyte increases as the pH of the solution is decreased. However, the change effect is more pronounced for the lighter charged polyelectrolyte, with only 20 charged segments. At the higher salt volume fraction of 0.01, we found that the excess amount of polyelectrolyte at interface is more comparable for the two polyelectrolytes. Indeed, for this value of background electrolyte concentration, the amount of polyelectrolyte at interface only becomes larger for the lighter charged chain, when pH drops below 3.5.

One noticeable aspect of observed experimental results on such mixed systems is the possibility of binding of polyelectrolyte to the protein layers at pH values above the iso-electric point for the protein (4,7). In these circumstances, the overall charge on the protein has the same sign as the polyelectrolyte. This feature is not reproduced by the SCF calculations here. This might be due to lack of lateral heterogeneity in our model. While such heterogeneities undoubtedly exist at the lower coverage of the surface by the protein molecules, they should tend to average out at higher surface concentrations. This would be expected to be particularly the case for more coil-like disordered proteins, as was argued in the Introduction. There may also exist other kind of short range attraction between protein and polysaccharide molecules, neglected in the present model. These need to be at least as strong as the electrostatic interactions if they are to make any significant difference to the adsorption of the polyelectrolyte at these higher pH values.

Summary and Conclusions

The adsorption behaviour of polysaccharides, onto an existing layer of protein at an interface, is not only determined by protein-polysaccharide interactions but also by interactions between neighbouring polysaccharide chains. We have used Self Consistent Field calculations to study the structure and properties of mixed films of these biopolymers. In the model system considered, it is only the hydrophobic amino acid residues of the protein that have an affinity for adsorption onto a hydrophobic solid surface. The accumulation of the polyelectrolyte at the interface occurs as a result of electrostatic interactions between the positive segments of the protein and the negatively charged polyelectrolyte chains. For the primary structure of our model protein, we have adopted a sequence of amino acids loosely based on the structure of the disordered milk protein α_{s1} -casein.

Our results for the density profile of each biopolymer at the interface show that the adsorption of polysaccharide molecules onto the primary protein film, where all segments of the polyelectrolyte are equally charged, leads to a rather mixed, entangled layer. We find that for this system the polyelectrolyte chains lie rather flat at the interface. Thus, emulsion layers stabilised by these types of

mixed layers are prone to bridging flocculation. Our calculations predict a weakening of colloidal repulsion forces, and even attraction, when compared to those produced by pure protein layers. In contrast, for polyelectrolyte molecules with only certain sections of the chains charged, the adsorption process results in a significantly more extended interfacial film. In this case, a distinct secondary layer is seen to be formed. This predominately consists of hydrophilic uncharged units of the polyelectrolyte. The steric interactions, resulting from the overlap of these secondary layers, greatly enhance the repulsion forces between approaching emulsion droplets stabilised by such interfacial layers. The repulsion is also seen to become longer range, when compared to that mediated by protein layers in the absence of polyelectrolyte. The above results are also found to be true of a much simpler model, where the attractive interactions between the two biopolymer species is assumed to be short range.

We have found that the extent of adsorption of the polyelectrolyte chains onto the protein layer varies greatly with the degree of charging of the polyelectrolyte. Highly charged chains have a stronger affinity for the oppositely charged protein film. However, this also leads to a more effective neutralisation and then reversal of the charge of the interfacial layer as the polyelectrolyte molecules adsorb to the surface. Furthermore, stronger repulsion between neighbouring chains limits the amount of adsorption of the polyelectrolyte. We have shown that these two competing effects result in an optimum level of charging of the chains for which the adsorption level is a maximum. This optimum degree of charging varies with salt concentration and pH of the solution. In particular, for low electrolyte concentrations and low pH values, the adsorption favours lightly charged polyelectrolyte chains. Nevertheless, from a practical point of view, a polyelectrolyte with a higher density of charge segments might be preferable. We find that the amount of adsorption of more highly charged chains show less sensitivity to changes in pH and background salt concentration.

Polyelectrolyte chains in our model are assumed to be flexible. However, many polysaccharide molecules have a rather rigid rod-like backbone. Rigidity of the molecules is known to have important implications for the formation of complexes between protein and polysaccharides in bulk solutions (4,18). The same is expected to be true at the interface. Current work is underway to study adsorption of more rigid polyelectrolyte molecules within the framework of our present model.

References

1. Dickinson, E. *Food Hydrocolloids* **2003**, *17*, 25.
2. McClements, D. J. *Curr. Opin. Colloid Interface Sci.* **2004**, *9*, 305.
3. Walstra, P. *Physical Chemistry of Foods*; Marcel Dekker: New York, 2003.

4. McClements, D. J. *Biotech. Adv.* **2006**, *24*, 621.
5. Turgeon, S.L.; Beaulieu, M.; Schmitt, C.; Sanchez, C. *Curr. Opin. Colloid Interface Sci.* **2003**, *8*, 401.
6. Dickinson, E. In *Food Colloids and Polymers: Stability and Mechanical Properties*; Dickinson, E.; Walstra, P., Eds.; Royal Society of Chemistry: Cambridge, UK, 1993; pp 77-93.
7. Cooper, C.L.; Dubin, P.L.; Kayitmazer, A.B.; Turksen, S. *Curr. Opin. Colloid Interface Sci.* **2005**, *10*, 52.
8. Beysseriat, M.; Decker, E.A.; McClements, D.J. *Food Hydrocolloids* **2006**, *20*, 800.
9. Norton, I.T.; Frith, W.J. In *Food Colloid; Biopolymers and Material*; Dickinson, E.; van Vliet, T., Eds.; Royal Society of Chemistry: Cambridge, UK, 2003; pp 282-297.
10. Weinbreck, F.; Minor, M.; de Kriuf, C.G. *J. Microencapsul.* **2004**, *21*, 667.
11. Norton, I.T.; Frith, W.J. *Food Hydrocolloids* **2001**, *15*, 543.
12. Thanasukran, P.; Pongsawatmanit, R.; McClements, D.J. *Food Res. Int.* **2006**, *39*, 721.
13. Guzey, D.; McClements, D.J. *J. Agric. Food Chem.* **2007**, *55*, 475.
14. Krzeminski, A.; Marudova, M.; Moffat, J.; Noel, T.R.; Parker, R.; Wellner, N.; Ring, S.G. *Biomacromol.* **2006**, *7*, 498.
15. Marudova, M.; Brownsey, G.J.; Ring, S.G. *Carbohydr. Res.* **2005**, *340*, 2144.
16. Harnsilawat, T.; Pongsawatmanit, R.; McClements, D.J. *Biomacromol.* **2006**, *7*, 2052.
17. Jonsson, M.; Linse, P. *J. Chem. Phys.* **2001**, *115*, 10975.
18. Akinchina, A.; Linse, P. *J. Phys. Chem. B* **2003**, *107*, 8011.
19. Carlsson, F.; Linse, P.; Malmsten, M. *J. Chem. Phys. B* **2001**, *105*, 9040.
20. Carlsson, F.; Malmsten, M.; Linse, P. *J. Amer. Chem. Soc.* **2003**, *125*, 3140.
21. Jönsson, B.; Lund, M.; Fernando, L.; da Silva, B. In *Food Colloids: Self-Assembly and Material Science*; Dickinson, E.; Leser, M.E., Eds.; Royal Society of Chemistry: Cambridge, UK, 2007; pp 129-154
22. Seyrek, E.; Dubin, P.L.; Tribet, C.; Gamble, E.A. *Biomacromol.* **2003**, *4*, 273.
23. Dickinson, E.; Euston, S.R. *Food Hydrocolloids* **1992**, *6*, 345.
24. Dickinson, E. *An Introduction to Food Colloids*; Oxford University Press: Oxford, UK, 1992.
25. Dickinson, E.; Horne, D.S.; Pinfield, V.J.; Leermakers, F.A.M. *J. Chem. Soc. Faraday Trans.* **1997**, *93*, 425.
26. Fler, G.J.; Cohen Stuart, M.A.; Scheutjens, J.M.H.M.; Cosgrove, T.; Vincent, B. *Polymers at Interfaces*; Chapman & Hall: London, 1993.
27. Evers, O.A.; Scheutjens, J.M.H.M.; Fler, G.J. *Macromolecules* **1990**, *23*, 5221.
28. Akhtar, M.; Dickinson, E. *Colloids Surf. B* **2003**, *31*, 125.

29. Akhtar, M.; Dickinson, E. *Food Hydrocolloids* **2007**, *21*, 607.
30. Leermakers, F.A.M.; Atkinson, P.J.; Dickinson, E.; Horne, D.S. *J. Colloid Interface Sci.* **1996**, *178*, 681.
31. de Gennes, P.G. *Scaling Concepts in Polymer Physics*; Cornell University Press: Ithaca, New York, 1979.
32. Ettelaie, R.; Murray, B.S.; James, E.L. *Colloids Surf. B* **2003**, *31*, 195.
33. Dickinson, E.; Pinfield, V.J.; Horne, D.S.; Leermakers, F.A.M. *J. Chem. Soc. Faraday Trans.* **1997**, *93*, 1785.

Chapter 4

Modulating Lipid Delivery in Food Emulsions

**Peter J. Wilde, Michael J. Ridout, Alan R. Mackie,
Martin S. J. Wickham, and Richard M. Faulks**

**Institute of Food Research, Norwich Research Park, Colney,
Norwich NR4 7UA, United Kingdom**

Delivering lipids in a controlled manner is one method of modulating dietary fat intake. Rationally designed emulsion microstructures can be exploited to reduce dietary lipid intake either directly (reduced fat foods), or indirectly by modifying the body's response to the food structure. A critical factor is acceptability, therefore the organoleptic properties must be similar to the full fat counterpart. There are three novel approaches that we are currently investigating: The first is to enhance the sensory perception of fat content of emulsions by manipulating the properties of individual lipid droplets; The second is to physically reduce the fat content in the individual lipid droplets, and finally we will describe an approach where we aim to design interfaces which can alter the rate (but not extent) of lipid digestion in order to suppress appetite. We will describe the micro- and nano-structures we are formulating to achieve these objectives.

Introduction

Obesity is a major health concern in westernized society. Obesity and related conditions are a major contributor to adult mortality. Although obesity is symptomatic of a range of lifestyle issues, calorific intake is clearly a contributory factor. Fat has the highest calorific value of the nutritional components of foods and therefore contributes significantly to the calorific intake of a population. Therefore modulating the delivery or impact of dietary fats is an approach to reduce fat intake. Dietary fat in food can take many forms, but in many processed foods, fat is present in the form of an emulsion. A high fat diet contributes to cardiovascular disease (CVD) risk by (a) maintaining high plasma lipid concentrations over prolonged periods (b) obesity through the storage of excess energy, and (c) altering the relative ratios of High and Low Density Lipoproteins (HDL, LDL). In the UK alone, 18 million sick days are taken as a result of obesity related conditions, costing the health service an estimated £0.5 billion per year. Indirect costs (eg lost economic output) are estimated to be over £2 billion pa. Obesity is thought to be the 2nd largest cause of cancer after smoking. Dietary advice is to limit fat intake to not more than 35% of energy. In the UK, about 38% of the population's calorific intake is in the form of fat and this figure is higher in the case of obese subjects. Therefore there has been a drive in recent years to reduce the population's intake of fat, and education & awareness of these issues has been a major government policy for several years. This has had some success in reducing our calorific intake from fat from 42% in the mid 1980's, to present levels of around 38%. However, the desire to consume fat rich foods is strong and certain sectors of the population continue to eat energy-rich foods in spite of the inherent knowledge that these are detrimental to our health. This has resulted in an increase of almost 10% in the number of overweight and obese individuals over the past 7 years, the rise in the number of obese children is of particular concern. Therefore, strategies are required to reduce dietary fat intake, whilst maintaining desirable eating quality to reduce obesity levels within certain sectors of the population. Emulsified fats and oils are present in approximately 50% of processed foods consumed in the UK and make up approximately 40% of the UK population's dietary fat intake. The presence of fat contributes significantly to flavour, texture and other desired sensory properties in products such as milk & cream based products, yoghurts, ice cream, mayonnaise, sauces, dressings and soups. The estimated UK annual market value of some of these product areas are: £200 million for the sauces and dressings sector, £800 million for the ice cream sector, £1.2 billion for the yoghurts & dairy desserts sector and £4 billion for the remainder of the dairy products sector.

The manner in which fat is delivered, digested, absorbed and cleared are all important aspects to consider in effectively controlling fat intake. There are

several stages during the consumption and digestion of fat that could influence affect dietary intake.

There are three strategies that we are currently exploring to deliver reduced dietary fat intake that will be discussed. Two of these involve delivering less fat by manipulating the emulsion structure, and the third involves modulating lipid digestion in order to reduce appetite. The strategies, basic principles involved and some results will be presented below.

Delivering Reduced Fat

Sensory Perception of Fat

The first stage is food intake is consumption, where the food is sensed in the mouth. A complex combination of physical and chemical (and possibly even psychological) sensory events combine to give the overall perception of fat content (1-3). Several studies have shown the importance of rheology (including tribology) (3, 4) on the perception of “creaminess”, and have shown that by enhancing the rheology with gums and stabilisers, certain perceptions associated with emulsions such as creaminess, thickness, smoothness etc., can be improved without the further addition of fat. It is therefore possible to simulate the texture and physical properties of a food emulsion such as cream or mayonnaise without the presence of fat, but matching the full sensory characteristics provided by physical contact of fat with taste receptors is far more difficult. In fact, one problem with reduced fat products is that the perception of the product flavour can be initially quite high, but the intensity soon dissipates, leading to an “unbalanced” flavour. This is because the contribution of fat to flavour perception is dependant on various other factors such as the physical form of the fat (*e.g.* solid/liquid, particle size), the manner in which the fat interacts with taste receptors and the partitioning of flavour molecules between fat & aqueous phases. Strategies have been developed to create structures which prolong the release of flavour in emulsion products (5, 6). In order to produce a good low-fat food emulsion food, the number and size of the fat droplets within the emulsion need to be retained in order to impart the desirable sensory properties.

The food industry has attempted to address fat reduction by producing lower-fat alternatives in a wide range of food types, and it is expected that the demand for such low-fat foods will continue to grow. However, at present, many low-fat alternatives are not perceived as palatable or acceptable by consumers in terms of their sensory characteristics. Fat reduction results in poor texture and flavour characteristics in many low-fat variants and in existing low-fat alternatives, this is often counterbalanced by the addition of thickeners, sugars

and other bulking agents. The result is a reduced-fat product, but still with a high calorific value and reduced organoleptic properties. In addition, many consumers simply have an aversion to low-fat products, assuming that these will be of lower sensory quality to the corresponding conventional products. In order to produce high-quality, low-fat, reduced-calorie products, it would be advantageous if the rheological, sensory and textural characteristics provided by the fat could be retained but at a lower overall fat level. To achieve this, it is important to have a more thorough, fundamental understanding of how the physico-chemical properties of emulsions precisely influence the sensory perception of fat content. In this way, rational designs for emulsion structures can be formulated to exploit this knowledge, and produce fully acceptable reduced fat emulsions based foods to deliver reduced levels of dietary fat.

Role of the Interface

The sensory perception of fat in emulsions is highly complex, but can be influenced by the textural or rheological behaviour. The rheology of emulsions is highly complex and is dependent on numerous parameters such as droplet size, interfacial tension, surface charge, phase volume etc. Some studies have shown that both interfacial tension and droplet radius influence emulsion rheology at high phase volume by changing the Laplace pressure and thus droplet deformability. In a similar manner, interfacial rheology may also influence droplet deformability.

Proteins are often used to stabilise food emulsions against coalescence, as they possess unique interfacial properties that can confer high levels of long term stability (7). Proteins are complex, polyionic, amphiphilic macromolecules, and their unique interfacial properties have been studied for many years (8,9). Following adsorption to the interface they tend to undergo rearrangement and aggregation processes to form an immobile, elastic interfacial film (9). Hence the molecular structure of the proteins can strongly influence their interfacial rheological properties (10,11) which have often been associated with enhanced stability of emulsions and foams (7,9). In contrast, surfactants tend to form a fluid mobile film at the interface. This can infer significant differences in the physical properties of emulsions, and as such, manipulating interfacial composition can be used as a strategy to control emulsion functionality. This is demonstrated in Figure 1 showing the typical interfacial rheological behavior of a protein system (whey protein isolate). As the protein adsorbs, it rearranges and interacts with neighbouring proteins to form a viscoelastic film. However, in the presence of sufficient surfactant to disrupt or displace the protein film, the elasticity can be completely destroyed.

The physical properties of emulsions that are relevant to organoleptic properties are microstructure and rheology (12,13). Apart from the properties of

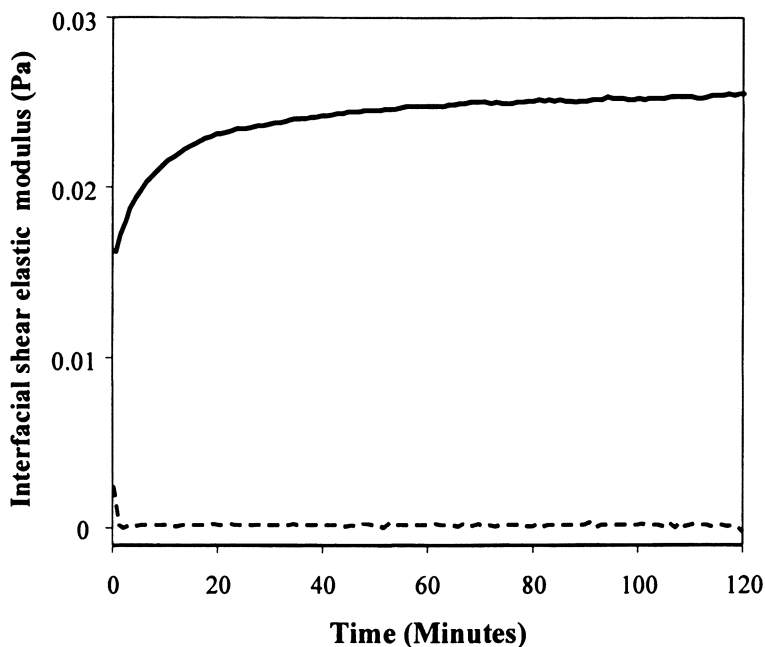


Figure 1. Typical Interfacial shear elastic behavior of protein (whey protein isolate) (solid line). Compared to the same in the presence of a surfactant (0.2% SDS) (dashed line).

the continuous phase, the main factors which govern emulsion rheology are the properties of the dispersed phase droplets (12,14). These include droplet volume fraction, droplet-droplet interactions and droplet viscosity and deformability. Considerable progress has been made in understanding the factors that influence the physical properties of model emulsions. However, our knowledge of the structure and rheology of dispersions containing polydisperse, deformable droplets is still at an elementary stage. Emulsified oil droplets have a fluid internal phase and a flexible interface. The application of stress can cause circulation of the internal phase and may lead to droplet distortion (15). The deformation of the droplets is influenced by the viscosity of the dispersed and continuous phases and the shear field, and this in turn can be influenced by the interfacial tension forces (14,16), and how this changes the internal Laplace pressure of dispersed phase droplets (17,18). An interfacial viscosity parameter has been shown to influence droplet deformation (19) by suppressing interfacial motion and hence reduce the magnitude of the droplet deformation.

It has been shown that the rheology of concentrated emulsions stabilised by proteins tend to have greater elastic moduli than emulsions stabilised by low

molecular weight emulsifiers (13,20-23). Recently we took to studying this in a more controlled fashion by creating sets of emulsions with identical phase volumes and droplet size distributions, but with controlled interfacial properties. Oil-in-water emulsions were prepared initially using 0.43% (w/v) Whey Protein Isolate (Bipro, Davisco Foods International inc. MN) in a Waring blender using a timed shearing cycle. The parent emulsion was then divided into equal parts and to each sample the same amount of buffer solution was added, containing either zero or 2.7% surfactant to displace the protein from the interface. This produced separate emulsions with identical oil phase volumes and droplet size distributions, but one was stabilised by protein and the others by surfactant. The surfactants used were a non-ionic (polyoxyethylene 23 lauryl ether (Brij 35)) and an anionic (Sodium dodecyl sulphate (SDS)) surfactant. Mixtures of these were used to vary the zeta potential in order to match that of the protein stabilized emulsion. Figure 2 shows the concentration of oil in the top of the cream layer as the emulsions were allowed to cream over several days. The three surfactant mixtures were chosen to have a wide range of zeta potentials (-0.4 to -79.9 mV) which spanned that of the protein stabilized emulsion (-28.4mV). The emulsions stabilized by the surfactants are consistently more densely packed than the protein stabilized emulsion. The surface charge on the emulsion droplets can be largely discounted as the zeta potential of the surfactant emulsions spans that of the protein emulsion. The droplet size and phase volume of all the emulsions are identical. The creaming profiles as measured by ultrasound velocity measurements show that the protein stabilized emulsions are capable of supporting the buoyancy of the cream layer with a less dense emulsion. What appears to be happening is that the protein emulsion droplets are interacting to form a less dense, but stronger network.

To test this hypothesis, the rheology of the cream layer can be measured *in situ*, allowing the cream layer to form around the measuring geometry during the creaming process. A 40mm hollow cylinder was used as the measuring geometry, inside a cylinder containing the emulsion. Figure 3 shows the development of the viscoelasticity of cream layers stabilized either by protein or surfactant. The Elasticity of the protein stabilized emulsion is more than an order of magnitude greater than that of the surfactant stabilized emulsion. This is despite the fact that the droplet size distribution is identical and the phase volume of the surfactant stabilized systems is 10% higher than the protein sample (Figure 2).

Our conclusion is that the stabilizing layer surrounding the droplets has a profound influence on the bulk rheological properties of the emulsions. However the mechanism(s) underlying this phenomenon was not entirely clear. There have been some theoretical treatments showing how an elastic interfacial layer can influence droplet deformation (24,25) and emulsion rheology (22), and certainly the elasticity of most globular protein interfaces would induce this effect.

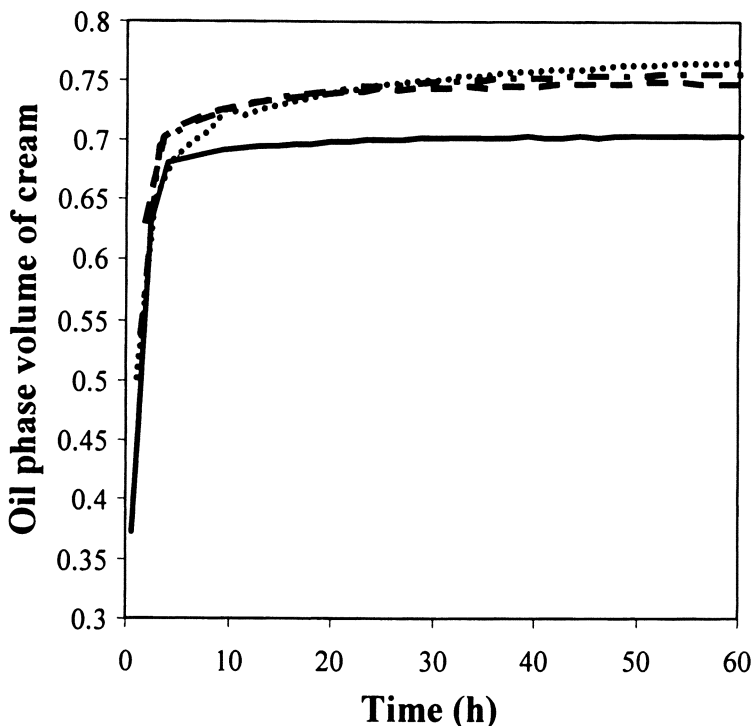


Figure 2. Dispersed phase volume of upper 20mm of cream layer in oil-in-water emulsions as a function of time, for emulsions stabilised by whey protein isolate (solid line) and SDS/Brij 35 mixtures (dashed and dotted lines).

Experimental studies of rheology of protein stabilised emulsions have suggested that the interactions between the protein stabilised droplets may be responsible for the enhanced rheological properties (21). There have been several studies looking at the interactions between protein stabilised droplets and surfaces, and although long range interactions are dominated by electrostatic repulsion (26-28), short range interactions can vary for different proteins (26). Most globular proteins have a large steric repulsion term (26,28), sometimes due to the formation of multilayers (26), or adsorbed protein aggregates (27), but also it has been inferred that non-DLVO hydration forces may also exist (28,29).

We have already shown that the interfacial structure of simple emulsion systems can have a significant effect on the organoleptic properties of emulsions (30). Figure 4 compares the sensory perception of “creaminess” for emulsions stabilized by protein or surfactants.

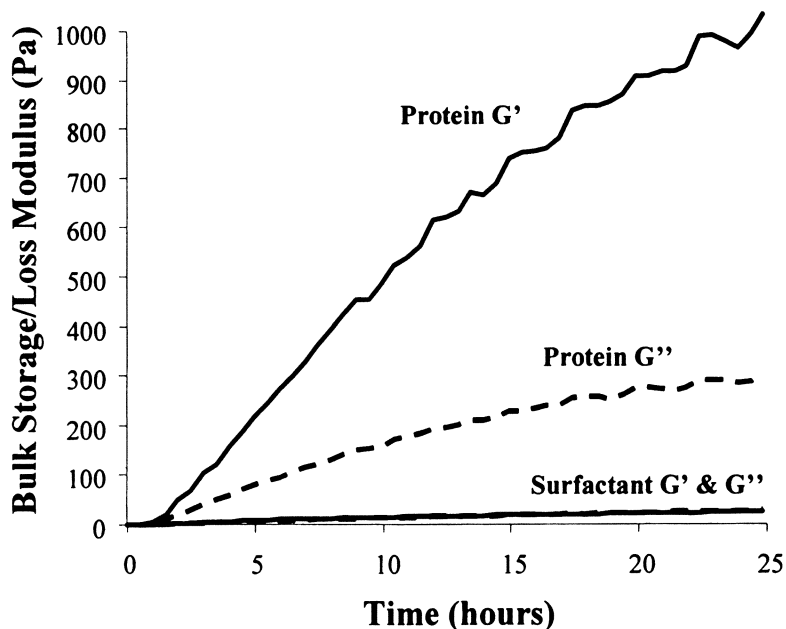


Figure 3. Bulk elastic (G' , solid lines) and viscous (G'' , dashed lines) for near identical emulsions stabilized by whey protein isolate (upper curves) and surfactants (lower curves).

This demonstrated that the interfacial composition of the model emulsions could have a significant influence on the sensory perception of fat content in food emulsions. The findings are consistent with this current study in that the emulsions stabilised by proteins which possessed an enhanced sensory response to fat content also displayed enhanced visco-elastic properties. This therefore demonstrates that by careful formulation, moderate reductions in fat content can be achieved through intelligent design based on an understanding of the fundamental principles underlying emulsion rheological properties.

Multiple Emulsions

Another approach to modulate lipid intake is through the design of complex, low fat emulsion structures that deliver the required sensory properties and acceptability. One approach is to make multiple Water in Oil in Water (WOW) emulsions (31,32). These emulsions are composed of fat droplets, which themselves contain small water droplets. Therefore, theoretically, these droplets should possess the same physical properties (appearance, texture/rheology) as a

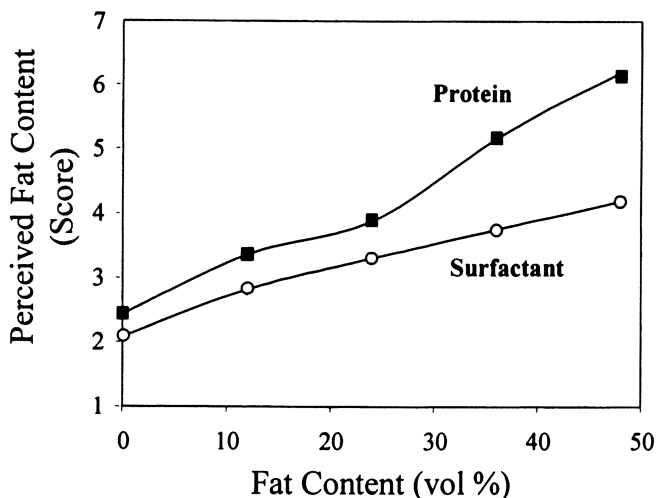


Figure 4. Sensory scores of perceived fat content of model emulsions as a function of actual fat content of emulsions stabilised by either whey protein (filled squares) or sucrose ester surfactant (open circles). (Data from Moore et al 1998).

conventional emulsion, but provide an overall reduced fat content. In addition, the sensory properties should also be similar to that of the full fat emulsion, as fat will still be the primary constituent of each emulsion droplet.

Was a fat reduction strategy in foods, the potential for multiple emulsions has long been recognised, however they have not been manufactured on a large scale. This is mainly due to the difficulties in controlling emulsion formation under the high shear conditions experienced in conventional high-pressure homogenisers and rotor/stator machines (32). The high shear involved disrupts the multiple emulsion droplets to such an extent that the internal water droplets are forced into the external water phase. It is for this reason that, according to recent reviews of multiple emulsions, to date no practical multiple emulsion products exist in the marketplace (32,33). However, crossflow membrane emulsification (XME) techniques have been successfully used to create stable multiple emulsions (32,34). The reason why membrane emulsification can successfully produce stable multiple emulsions is that the technique involves very low shear rates during the emulsification process (32). The process of emulsion formation using XME has been researched on a number of food, pharmaceutical and industrial products at the laboratory scale. An emulsion is created by passing the oil phase of an emulsion through a suitable micro-porous membrane as shown in Figure 5. As the oil phase passes through the membrane pores, individual droplets grow at the membrane surface. The droplets formed

pass directly into the moving continuous phase thus forming the emulsion droplets. Secondly, the previously created water-in-oil emulsion is passed through a membrane into a second continuous phase, creating a multiple emulsion under minimal shear conditions. These multiple emulsions can be either further refined or optimised by incorporating additional treatments. For example, by controlling the osmotic potential of the external water phase, the size of the encapsulated water droplets can be modified (35), leading to further control over droplet size and encapsulated phase volumes.

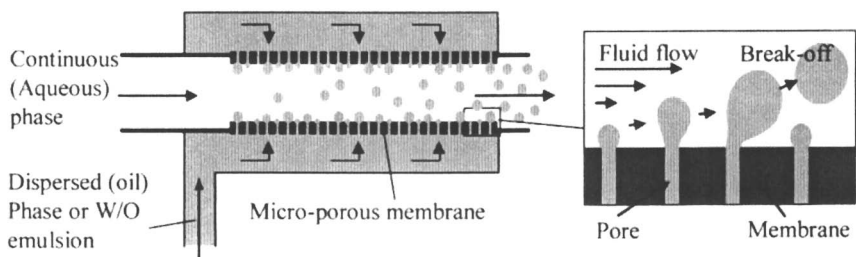


Figure 5. Schematic diagram of cross flow membrane emulsification method. The dispersed phase is forced through a porous membrane into the flowing continuous phase. To make multiple WOW emulsions, the dispersed phase comprises a W/O emulsion.

Membrane emulsification was developed in Japan in the late 1980s based on a microporous glass membrane (36). Subsequent developments included producing water-in-oil emulsions (37), multiple emulsions (34) and the use of PTFE membranes to reduce droplet sizes in coarse emulsions (38). Most recent studies looked at the technical aspects of membrane emulsification such as crossflow hydrodynamics, flux rates, and membrane materials and characteristics (39). In particular, some research on adsorption properties of the emulsifiers themselves has shown the importance of emulsifier adsorption rates (40-42), but additional work is required to define the specific needs of the technology. Ceramic membranes, developed from the membrane filtration industry, have been investigated for formation of food-type emulsions (43-45).

XME is a low shear method reliant on the surface energy of the ingredients. It is therefore regarded as considerably more energy-efficient than conventional homogenisation methods, and therefore incorporation of this technology into current production platforms is likely to have a significant impact on energy consumption, as conventional homogenisation methods such as high pressure homogenisers and high shear blenders often take up a large proportion of the energy consumption during processing.

Although XME lends itself to highly surface active systems, it has been shown that XME can make emulsions using food grade ingredients (43-45). Figure 6 shows a micrograph of a multiple WOW emulsion made by food grade ingredients. More specifically the emulsions were created using proteins, which are the most widely used emulsifying agents within the food and drink industry. Proteins are not as surface active as most small molecule emulsifiers, but they appear to be perfectly capable of creating stable multiple emulsions using XME. The critical factor however is the creation of a stable water in oil emulsion that is used as the dispersed phase for the multiple emulsion. The molecular structure and HLB of the emulsifier are critical to create fine water droplets capable of passing through the membrane, and provide stability to prevent coalescence and loss of the internal water droplets.

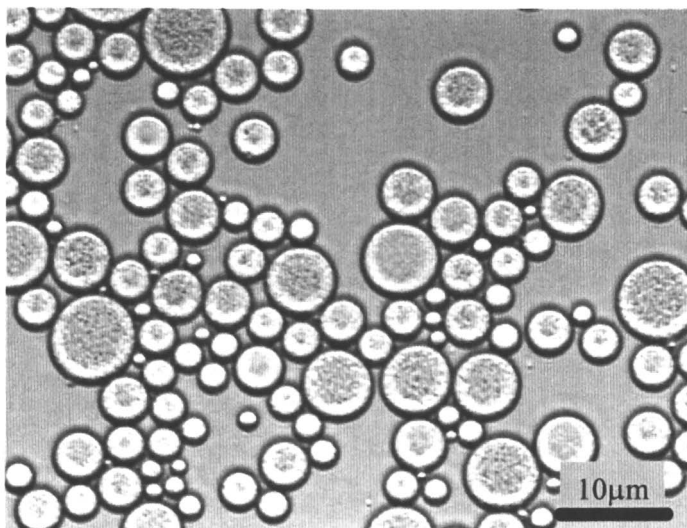


Figure 6. Optical micrograph of a WOW multiple emulsion. The granularity observed in the oil droplets is due to the encapsulated water droplets. The emulsion was formed using XME stabilised by 3 wt% polyglycerol polyricinoleate in the oil phase, and 1 wt% whey protein concentrate in the continuous phase.

The next challenge is to develop the critical design rules for optimisation of the physical structure that will have the most impact on fat reduction, yet retain the sensory impact of conventional high fat counterparts. This will require investigations of a number of factors; for instance, the incorporation of water

droplets within the oil droplets may change droplet deformability, and may therefore impact on sensory perception. Previous work at IFR (30) have shown that the interfacial properties of oil droplets can affect the sensory properties of emulsions. The effect of droplet deformability can be tested by controlling the number, size and rheology of the internal water droplets, and hence allowing for minimisation of any negative effects on sensory perception of fat content. Another approach, could include the incorporation of fatty flavours into the internal water droplets, to improve the sensory impact.

Finally, knowledge of sensory perception of low-fat multiple emulsions compared with equivalent conventional ones is not currently available. To date no commercial multiple emulsion-based products exist (33). However, De Cindio (31) reported that the colloidal and rheological properties of multiple emulsions are similar to the full fat equivalent single emulsion. However, the chemical interactions of the fat and sensory perception of fat in these multiple emulsion systems are not known, and must therefore be determined if multiple emulsions are to be used as a credible fat reduction strategy by the food industry.

Modulating Fat Digestion

Fat Digestion

After ingestion, dietary fat is normally converted into an emulsion comprising fat droplets dispersed in the predominantly aqueous phase of the gastric contents. Therefore for the fat to become available for absorption, it has to be “solubilised”. The digestion and absorption of dietary triglycerides can conveniently be divided into four steps:

- (1) Emulsification in the stomach to increase the surface area available for lipolysis.
- (2) Lipolysis by lipase and co-lipase to convert triglycerides into more absorbable fatty acids and monoglycerides.
- (3) Mixed micelle formation to transport products of lipolysis to gut wall.
- (4) Absorption of fatty acids and monoglycerides.

Emulsification of bulk lipid normally occurs in the antrum (lower stomach chamber) as a result of partial lipolysis (gastric lipase) and gastric secretion of phospholipids together with high rates of shear, dispersing the large insoluble oil masses into finer oil-water emulsion of higher surface area. It is at this interface that the pancreatic lipases act.

Lipolysis by pancreatic lipase begins in the duodenum directly after the stomach begins to empty. Prior to lipolysis, bile salts secreted into the duodenum

adsorb on to the surface of the lipid droplets. Bile salts are highly surface active and can alter the structure and composition of the emulsion interface (46) by displacing water-soluble proteins (including pancreatic lipase). This prevents blocking of the interface by denatured proteins. Bile salts may also prevent further protein adsorption by bestowing a negative charge to the interface, thus repelling negatively charged proteins. Most proteins have an isoelectric point below duodenal pH, and hence possess a net negative charge. However, the negative charge attracts colipase to the surface, which then attaches to the ester bond region of the triglyceride by hydrogen bonding. Lipase then couples tightly with the colipase by electrostatic binding to adopt a suitable configuration for lipolysis. Lipolysis itself involves a reversible penetration of the lipase into the interface where the enzyme undergoes a conformational change. This change allows binding with the substrate to produce the activated complex which decomposes to give the products. Thus it is the interfacial binding which regulates the concentration of lipase at the interface, and hence the rate of lipolysis. A common feature of lipolysis is a characteristic lag time prior to the establishment of steady state hydrolysis. These lag times appear to be due to slow interfacial penetration of the enzyme, which is related to the physicochemical nature and composition of the interface (47). Hence, it has been shown that lipase action is very sensitive to interfacial composition. Some surface active molecules are known to hinder lipolysis, of these, galactolipids are thought to adsorb at the lipid interface and sterically hinder the adsorption of lipase or co-lipase to the droplet surface (48,49). Furthermore, some non-ionic detergents can inhibit the enzyme by binding to the active site (50,51). However, thorough characterisation of the interface in the presence of these lipids and surfactants has yet to be investigated and as such the exact molecular mechanism underlying the effect on lipase activity is still unknown.

Lipolysis products (fatty acids, monoglycerides etc.) are released into the aqueous phase, where they are solubilised by mixed micelles. A dynamic equilibrium of the products between the micelles and the monomers in the aqueous phase facilitates their absorption into the enterocytes (52).

The Role of the GI tract and GI-endocrine feedback:

The gastrointestinal tract is equipped with a number of entero-endocrine feed-back mechanisms that optimise the time required for digestion, absorption and systemic handling of the nutrients. This prevents 'loss' of nutrients to the colon or wasted effort extracting nutrients from indigestible material. Different mechanisms dominate during the ingestion and passage through the GI tract, (about 4-14h duration). Gastric stretch receptors may inhibit the further ingestion of food until the stomach empties, and it is well known that lipid in the small intestine delays gastric emptying and extends duodenal transit time. Lack of

appetite and feelings of satiety beyond about 4h after a meal (i.e. after the stomach has emptied) are mainly due to entero-endocrine responses to the presence of undigested food in the ileum. Infusion of undigested lipid in the jejunum delays chyme transfer through the ileocolonic junction (53) and jejunal motility and transit time are inhibited by ileal lipid infusion (54). Many gut hormones have been identified as playing a role in gastro-intestinal transit and brain responses. Of these, peptide YY (PYY) and cholecystokinin (CCK) have been identified with gastrointestinal handling of lipids. CCK secretion is stimulated by lipid in the proximal ileum and triggers contraction of the gall bladder thus providing the bile salts necessary for lipid digestion, whereas PYY is mainly stimulated by the presence of lipid, such as oleic acid, in the distal ileum (55). The systemic infusion of PYY at physiological doses markedly suppresses appetite (56,57). Therefore, it is this through this feedback mechanism by which retarding lipolysis in the small intestine is likely to influence appetite suppression.

Dietary strategies to reduce fat or energy intake:

Conventional approaches to reduce lipidaemia and obesity by modifying lipid digestion include: increasing the use of low or zero energy fats and to increase the use of short and medium chain triglycerides. Low energy fats, eg, triglycerides where one long chain fatty acid is substituted with a short chain fatty acid, have found limited use but are currently expensive (58). Non-digestible fats have been developed including sucrose ester based lipids, however, their use is restricted due to the adverse side effects of excess lipids in the colon causing steatorrhoea (fatty diarrhoea) (59). Short and medium chain triglycerides, commonly used for enteral nutrition have found limited commercial use. However, because fatty acids of C12 or less are absorbed directly into the portal blood, they do not cause post-prandial hyperlipidaemia. However, their energy value is similar to the conventional long chain triglyceride, and can result in impaired absorption of lipid soluble nutrients (e.g., vitamins A,D,E and carotenoids) (60). The other major source of fat in the diet is baked products where it has not been possible to produce many acceptable low fat or modified fat containing products. It is possible to gain limited health advantage from a pick-and-mix approach using existing technology. However, engineering lipids and lipid containing foods to control the rate of lipolysis and hence the rate of absorption of the lipid and its distribution in the ileum has not received serious attention other than the development of lipase inhibiting drugs.

Emulsions and Satiety

Previous studies carried out using Echo Planar Imaging (EPI) and ^{13}C labelled fatty acid, observed that two identical lipid emulsions produced using different emulsifiers behaved differently in the gastric environment and produced significant differences in appetite and satiety for up to 12h as shown in Figure 7, without causing steatorrhoea (fatty diarrhoea) (59).

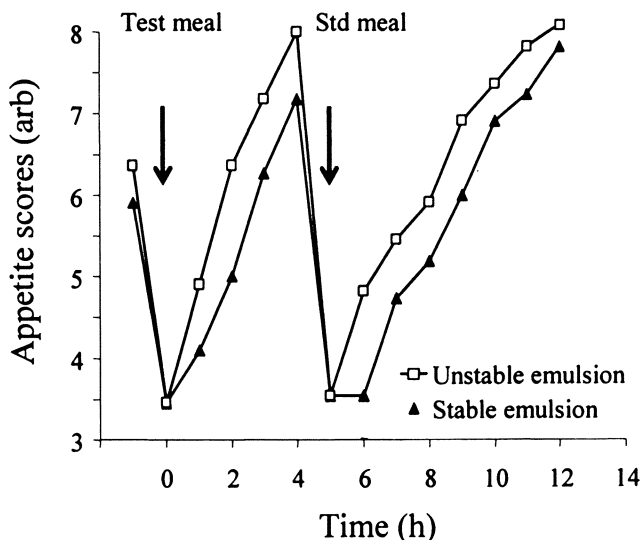


Figure 7. Average appetite scores for individuals fed model stable (Solid triangles) and unstable (Open squares) emulsions as a test meal.

The subsequent reduction in food intake amounted to around 10% which is equivalent to reducing energy intake by around 200kcal/day. This demonstrated the key effects of interfacial composition and the possible presence of unabsorbed lipid in the distal ileum on both lipidaemia and food intake.

Glycolipids

There are literally hundreds of natural and synthetic surfactants and emulsifiers, but those which are acceptable and permitted in foods are more limited. Of the natural surface active agents, lecithin is widely used but is readily

digested by phospholipases and thus does not significantly affect lipolysis. Most food grade non-ionic surfactants and emulsifiers are a form of glycolipids with a glycerol or sugar based headgroup such as sucrose, or sorbitan. There is also a range of ethoxylated surfactants, with large polyoxyethylene headgroups, although not approved for food use, they may prove useful for investigating the mechanism of lipase inhibition as they are available in a wide range of headgroup sizes and acyl chain lengths. Plants and animals also have a range of naturally occurring surface active glycolipids and of these, plant galactolipids are relatively resistant to digestion (61) and persist longer in the GI tract than the phospholipids. Galactolipids are the most abundant lipid group in plants. Up to 70% of structural lipids in plants are composed of mono and di-galacto diacylglycerols (MGDG, DGDG) and they may constitute 10% of plant dry matter. Main sources are green leaf and cereals. As a nutrient they have been ignored but it is estimated we ingest 1-5g/d (more in the case of vegetarians). One of the reasons they attract little attention is that their bioaccessibility is low. This is because they are the major lipid in chloroplast membranes, and hence are trapped within the plant tissue structure and not normally exposed to enzymatic degradation. Both the MGDG and DGDG are amphiphilic surface active agents with known excellent emulsifying activity and ability to prolong release of encapsulated drugs (49). DGDG functions as a conventional surfactant in aqueous solutions producing colloid phases in which they position their hydrophobic regions at the core while the mono-dgag, because of their geometry, prefer a concave interfacial curvature and tend to produce inverted structures with their hydrophobic regions on the outside (62).

Both are resistant to lipolysis by the normal pancreatic lipase in part because co-lipase is not an effective mediator in the hydrolysis reaction and they are only slowly hydrolysed by pancreatic lipase related protein 2 (PLRP2) (61,63). In mixed meals, the galactolipids will migrate to the interface of the triglyceride emulsion droplets. Unlike protein and polysaccharides they are not displaced from the interface by the bile salts and thus theoretically reduce the emulsion surface area at which the pancreatic lipase can act. Slowing lipolysis will allow lipid droplets to persist longer in the small intestine thus reducing post-prandial triglyceridaemia and inducing beneficial changes in appetite and satiety. There is one lipid product, sold as a food ingredient (Olibra[®]) that claims increased satiety at subsequent meals. It is composed of fractionated palm oil (95%) and fractionated oat oil (5%). It is not clear how increased satiety is induced but oat oil contains a high proportion of galactolipids (64-66). Further, oats have documented hypocholesterolaemic effects (67). Green leaves and cereals are rich in galactolipids, thus provide a potential route for exploitation of waste streams.

Current investigations are looking at how the galactolipids compete for interfacial area with other physiologically relevant surface active components. Figure 8 shows the surface elasticity and surface pressure for mixtures of DGDG and phosphatidyl choline (PC).

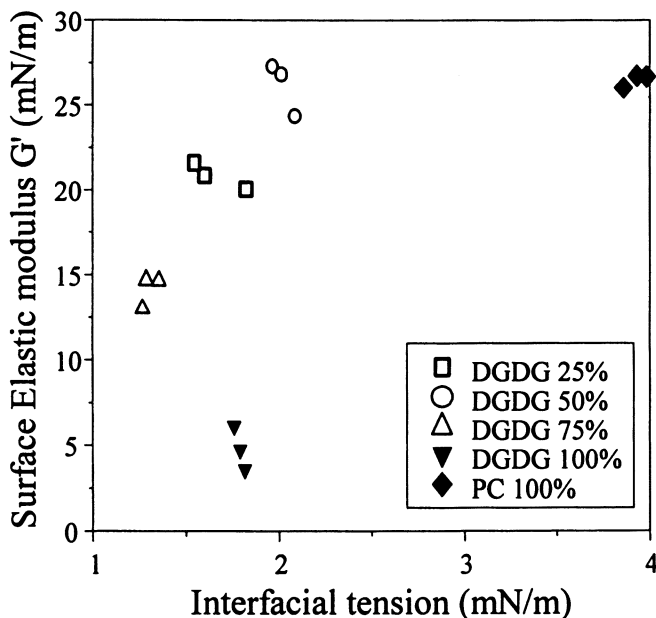


Figure 8. Interfacial elastic modulus as a function of interfacial tension at the olive oil – aqueous phase interface of equimolar mixtures of PC and galactolipids DGDG. Total lipid concentration = 1 wt%.

The competition for the interface between the components results in a surface film with different structures that have different responses to stress, hence revealing a fingerprint which gives us a qualitative indication of the surface composition.

Figure 8 shows that the DGDG itself has a much lower interfacial tension than the PC, however, subsequent measurements also showed that bile salts present in the duodenum during lipolysis, were more surface active than the DGDG. Further investigation of the competitive adsorption of the different surface active species is required to be able to accurately determine the surface composition of mixed interfaces such as these.

Bile salts are very surface active, and one of their roles is thought to be the ability to strip surface active components from the oil surface to allow effective adsorption of lipase and colipase. Figure 9 shows how, by measuring surface dilatational elasticity, how a pre-adsorbed protein film is displaced by subsequent additions of bile salts.

This demonstrates how effective bile salts are at stripping adsorbed components from a surface in preparation for lipolysis. Another technique for looking at surface composition is atomic force microscopy. This has been used

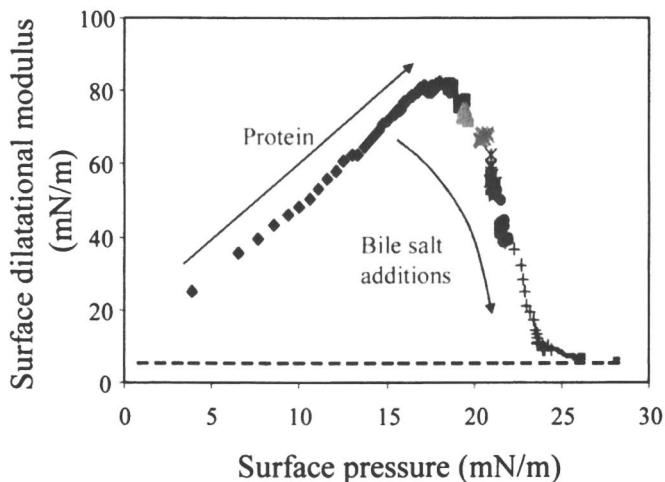


Figure 9. Surface dilatational elastic modulus as a function of surface pressure of $1\ \mu\text{M}$ protein (β -lactoglobulin) adsorption. This is followed with displacement by sequential additions of bile salt into the subphase. Dashed line represents values for bile salt alone at 9mM .

to reveal the nano-scale structure of mixed interfaces (68) and how surfactants can displace proteins and other surface active components from surfaces. This approach can be used to determine which interfacial structures are required to promote or inhibit lipolysis. With this information, it will be possible to intelligently design food ingredients and products with the right interfacial structures necessary to modulate lipolysis and enhance satiety.

Summary

In summary therefore, we have presented three approaches whereby we are trying to design structures that enable the delivery of fat in a way that will reduce overall dietary lipid intake in acceptable forms. The first is to understand in more detail the intrinsic rheological properties of emulsions that contribute to textural perceptions of fat content and how to maximise the impact of these in order to deliver emulsion based products with reduced fat content. The second is to reduce fat content through the design of acceptable, stable multiple WOW emulsions, and to develop the technologies to deliver these structures in an appropriate form. Finally we have described an approach that we intend to use to engineer the interfaces of emulsions to prolong the digestion of fats so as to promote satiety, hence reduce dietary intake in subsequent meals.

It is unlikely that these approaches will, individually, lead to significant reductions in fat content, however, in combination, the application of the knowledge gained from these studies could lead to the development of a new generation of intelligently designed, fully acceptable food products and ingredients that could deliver modest reductions in fat content. It is the modest reduction in dietary fat content for prolonged periods that could, in the medium to long term, result in sustainable weight loss. However, dietary intake is not the only approach that is required to curb the rise in obesity in developed nations, but a change in lifestyle is also required if current trends are to be reversed.

Acknowledgement

The authors would like to acknowledge the BBSRC for funding the Institute through the Core Strategic Grant and through Response Mode Grant number BBD0022731, and to DEFRA for funding through Link project FQ102.

References

1. Phillips, L. G.; McGiff, M. L.; Barbano, D. M.; Lawless, H. T. *J. Dairy Sci.* **1995**, *78*, 1258.
2. Kilcast, D.; Clegg, S. *Food Qual. Preference* **2002**, *13*, 609.
3. Akhtar, M.; Stenzel, J.; Murray, B. S.; Dickinson, E.; *Food Hydrocolloids* **2005**, *19*, 521.
4. Malone, M. E.; Appelqvist, I. A. M.; Norton, I. T. *Food Hydrocolloids* **2003**, *17*, 775.
5. Malone, M. E.; Appelqvist, I. A. M. *J. Controlled Release* **2003**, *90*, 227.
6. Appelqvist, I. A. M. Patent Application "Low-fat food emulsions having controlled flavour release and processes therefore" **2000**, Application no. WO1999EP05041 19990715.
7. Izmailova, V. N.; Yampolskaya, G. P.; Tulovskaya, Z. D. *Colloids Surfaces A: Physicochem. Eng. Aspects* **1999**, *160*, 89.
8. Bos, M. A.; van Vliet, T. *Adv. Colloid Interface Sci.* **2001**, *91*, 437.
9. Dickinson, E. *Colloids Surfaces B: Biointerfaces* **1999**, *15*, 161.
10. Freer, E. M.; Yim, K. S.; Fuller, G. G.; Radke, C. J. *Langmuir* **2004**, *20*, 10159.
11. Ridout, M. J.; Mackie, A. R.; Wilde, P. J. *J. Agric. Food Chem.* **2004**, *52*, 3930.
12. Coke, M.; Wilde, P. J.; Russell, E. J.; Clark, D. C. *J. Colloid Interface Sci.* **1990**, *138*, 489.
13. Lequeux, F. *Curr. Opinion Colloid Interface Sci.* **1998**, *3*, 408.
14. Tadros, T. F. *Colloids Surfaces A-Physicochem. Eng. Aspects* **1994**, *91*, 31.

15. Mason, T. G.; Lacasse, M. D.; Grest, G. S.; Levine, D.; Bibette, J.; Weitz, D. A. *Phys. Rev. E* **1997**, *56*, 3150.
16. Cavallo, R.; Guido, S.; Simeone, M. *Rheologica Acta* **2003**, *42*, 1.
17. Princen, H. M. *J. Colloid Interface Sci.* **1983**, *91*, 160.
18. Mason, T. G. *Curr. Opinion Colloid Interface Sci.* **1999**, *4*, 231.
19. Pozrikidis, C. *J. Eng. Math.* **2004**, *50*, 311.
20. Bressy, L.; Hebraud, P.; Schmitt, V.; Bibette, J. *Langmuir* **2003**, *19*, 598.
21. Danov, K. D. *J. Colloid Interface Sci.* **2001**, *235*, 144.
22. Oosterbroek, M.; Mellema, J. *J. Colloid Interface Sci.* **1981**, *84*, 14.
23. Dimitrova, T. D.; Leal-Calderon, F. *Langmuir* **2002**, *17*, 3235.
24. Nadim, A. *Chem. Eng. Comms.* **1996**, *150*, 391.
25. Pozrikidis, C. *J. Non-Newtonian Fluid Mech.* **1994**, *51*, 161.
26. Dimitrova, T. D.; Leal-Calderon, F.; Gurkov, T. D.; Campbell, B. *Langmuir* **2001**, *17*, 8069.
27. Dimitrova, T. D.; Leal-Calderon, F.; Gurkov, T. D.; Campbell, B. *Adv. Colloid Interface Sci.* **2004**, *108-109*, 73.
28. Valle-Delgado, J. J.; Molina-Bolivar, J. A.; Galisteo-Gonzalez, F.; Galvez-Ruiz, M. J.; Feiler, A.; Rutland, M. W. *J Phys. Chem. B.* **2004**, *108*, 5365.
29. Molina-Bolivar, J. A.; Galisteo-Gonzalez, F.; Hidalgo-Alvarez, R. *Colloids Surfaces B-Biointerfaces* **1999**, *14*, 3.
30. Moore, P. B.; Langley, K.; Wilde, P. J.; Fillery-Travis, A.; Mela, D. J. *J. Sci. Food Agric.* **1998**, *76*, 469.
31. De Cindio, B.; Cacace, D. *Int. J. Food Sci. Technol.* **1995**, *30*, 505.
32. Van der Graaf, S.; Schroen, C. G. P. H.; Boom, R. M. *J. Membrane Sci.* **2005**, *251*, 7.
33. Garti, N.; Benichou, A. in *Food Emulsions 4th Edition* Friberg, S. E.; Larsson, K. and Sjöblom, J. Eds. Marcel Dekker, New York, **2004**; p353.
34. Mine, Y.; Shimizu, M.; Nakashima, T. *Colloids Surfaces B: Biointerfaces*, **1996**, *6*, 261.
35. Mezzenga, R.; Folmer, B. M.; Hughes, E. *Langmuir* **2004**, *20*, 3574.
36. Kandori, K. In *Food Processing: Recent Developments*. Gaonkar, A. G. Ed., Elsevier Science, Amsterdam, **1995**; 113.
37. Kandori, K.; Kishi, K.; Ishikawa T. *Colloids Surfaces* **1991**, *61*, 269-279.
38. Suzuki, K.; Fujiki, I.; Hagura, Y. *Food Sci. Technol Int. Tokyo* **1998**, *4*, 164.
39. Josceline, S.; Tragardh, G. *J. Membrane Sci.* **2000**, *169*, 107.
40. Schroder, V.; Schubert, H. *Proc. 1st Eur. Congress Chem. Eng.* **1997**, *34*, S2491.
41. Schroder, V.; Behrend, O.; Schubert, H. *J. Colloid Interface Sci.* **1998**, *202*, 334.
42. Scherze, I.; Marzilger, K.; Muschiolik, G. *Colloids Surfaces B: Biointerfaces* **1999**, *12*, 213.
43. Joscelyne, S.; Tragardh, G. *J. Food Eng.* **1999**, *39*, 59.

44. Suzuki, K.; Shuto, I.; Hagara, Y. in *Development in Food Engineering Part 1*. Proc. 6th Int Congress Eng. Food **1993**, 107.
45. Katoh, R.; Asano, Y.; Furuya, A.; Sotoyama, K.; Tomita, M. *J. Membrane Sci.* **1996**, *113*, 131.
46. Wickham, M.; Wilde, P.; Fillery-Travis, A. *Biochim. Biophys. Acta* **2002**, *1580*, 110.
47. Wickham, M.; Garrood, M.; Leney, J.; Wilson, P. D. G.; Fillery-Travis A. J. *J. Lipid Res.* **1998**, *39*, 623.
48. Carriere, F.; Withers-Martinez, C.; van Tilbeurgh, H.; Roussel, A.; Cambillau, C.; Verger, R. *Biochim. Biophys. Acta* **1998**, *1376*, 417.
49. Gren, T.; Hutchison, K.; Kaufmann, P. *Drug Delivery Technol.* **2002**, *2*, Article 83, (www.drugdeliverytech.com/cgi-bin?idArticle=83).
50. Borgström, B. *Biochim. Biophys. Acta* **1977**, *488*, 381.
51. Hermoso, J.; Pignol, D.; Kerflecs, B.; Crenon, I.; Chapus, C.; Fontecilla-Camps, J. L. *J. Biol. Chem.* **1995**, *271*, 18007.
52. Tso, P. "Intestinal lipid absorption" in *Physiology of the Gastrointestinal Tract, 3rd edition*, Johnson, L. R. Ed. Raven Press, New York, **1994**; p1867.
53. Hammer, J.; Hammer, K.; Kletter, K. *Gut* **1998**, *43*, 111.
54. Spiller, R. C.; Trotman, I. F.; Higgins, B. E.; Ghatei, M. A.; Grimble, G. K.; Lee, Y. C.; Bloom, S. R.; Misiewicz, J. J.; Silk, D. B. *Gut* **1984**, *25*, 365.
55. Pironi, L.; Stanghellini, V.; Miglioli, M.; Corinaldesi, R.; De Giorgio, R.; Ruggeri, E.; Tosetti, C.; Poggioli, G.; Morselli-Labate, AM.; Monetti, N.; Gozzetti, G.; Barbara, L.; Go, V. L. W. *Gastroenterology* **1993**, *105*, 733.
56. Batterham, R. L.; Cohen, M. A.; Ellis, S. M.; Le Roux, C. W.; Withers, D. J.; Frost, G. S.; Ghatei, M. A.; Bloom, S. R. *N. Engl. J. Med* **2003**, *349*, 926.
57. Batterham, R. L.; Bloom, S. R. *Ann. N.Y. Acad. Sci.* **2003**, *1994*, 941.
58. Høy, C. E.; Xu X. in *Structured and Modified Lipids*. Gunstone, F. Ed. Marcel Dekker, New York, **2001**; p209.
59. Marciani, L.; Wickham, M.; Bush, D.; Faulks, R.; Wright, J.; Fillery-Travis, A. J.; Spiller, R. C.; Gowland, P. A. *Brit. J. Nutr.* **2006**, *95*, 331.
60. Borel, P.; Tyssandier, V.; Mekki, N.; Grolier, P.; Rochette, Y.; Alexandre-Gouabau, M. C.; Lairon, D.; Azais-Braesco V. *J. Nutr.* **1998**, *128*, 1361.
61. Ohlsson L. (2000) PhD Thesis. University of Lund.
62. Brasseur, R.; De Meutter, J.; Goormaghtigh, E.; Ruysschaert J. M. *Biochem. Biophys. Res. Commun.* **1983**, *115*, 666.
63. Andersson, L.; Carriere, F.; Lowe, M. E.; Nilsson, A.; Verger, R. *Biochim. Biophys. Acta.* **1996**, *1302*, 236.
64. Burns, A. A.; Livingstone, M. B. E.; Welch, R. W.; Dunne, A.; Robson, P. J.; Lindmark, L.; Reid, C. A.; Mullaney, U.; Rowland, I. R. *Int. J. Obes. Relat. Metab. Disord.* **2000**, *24*, 1419.
65. Burns, A. A.; Livingstone, M. B. E.; Welch, R. W.; Dunne, A.; Reid, C. A.; Rowland, I. R. *Int. J. Obes Relat Metab Disord.* **2001**, *25*, 1487.

66. Burns, A. A.; Livingstone, M. B. E.; Welch, R. W.; Dunne, A.; Rowland, I. R. *Eur. J. Clin. Nutr.* **2002**, *56*, 368.
67. NOVIS **2004** <http://nutraingredients.com/news/news-NG.asp?id=56299>.
68. Mackie, A. R.; Gunning, A. P.; Wilde, P. J.; Morris, V. J. *Langmuir* **2000**, *16*, 2242.

Chapter 5

Protein Structures as Delivery Vehicles in Foods

Paul Smith^{1,2} and Mark Plunkett¹

**¹YKI Institute for Surface Chemistry, Box 5607, SE 114 86,
Stockholm, Sweden**

**²Current address: Cargill R&D Centre Europe, Havenstraat 84,
B1800 Vilvoorde, Belgium**

Protein structures are important for providing many properties of foods. Hydrophobins have recently been extracted from filamentous fungi. These are amphiphilic molecules with unusual surface-active properties. These can be used in order to make unique nano-structures in foods and also to give different behaviour in other applications. There are a great many opportunities and challenges for food scientists. Structures could be used for incorporation of ingredients or to create novel textures and products.

Introduction

Proteins have many different roles in foods. They are very important nutritional components of the diet. Certain proteins are surface active. They are widely used in food systems where a surface-active component is required. Obvious examples are in milk and dairy products. These are generally low-tech foods and a great deal of specific functionality is not needed. It is the other ingredients that people have looked for in developing newer foods. However specific active proteins exist that can be developed and applied to give new functionalities and opportunities. One such proteins are the hydrophobins.

Hydrophobins are proteins that exist on the outside of filamentous fungi. They were initially discovered because they were stable to boiling during extraction (1). This is very unusual for such a complicated material. The structure of the proteins has been well characterized (2) and reviews of the literature have been published. The hydrophobins tend to be found on the outside of the fungi. The proteins are all about 10kDa in size and contain a large proportion of hydrophobic amino acids. The main unifying feature is the presence of 8 Cys residues.

Study has shown that different hydrophobins are formed and expressed at different stages of the fungi's life. They are expressed all through the life of fungi. The properties and biological roles are fully described in different reviews (3-5). However it can be seen that they have two main roles. They help fungi survive and adapt to the environment and they also have various structural roles.

The 3D structure of a hydrophobin has been discovered relatively recently. The relationship between the structure and the properties is very interesting. The structure is illustrated in Figure 1.

It can be seen that the molecule is amphiphilic with one hydrophobic and one hydrophilic part. This means that when the molecules are placed together they can form different self-assembled structures. This work will describe the properties of the different structures and suggest ways in which they can be incorporated and used in foods.

Experimental

The experimental work was performed using a variety of different pieces of equipment.

Hydrophobin II was extracted and manufactured at VTT Biotechnology, Espoo, Finland. It was supplied as a gift. Sodium caseinate was purchased from Arla Foods, Stockholm, Sweden. Lipids were obtained from Sigma Chemicals.

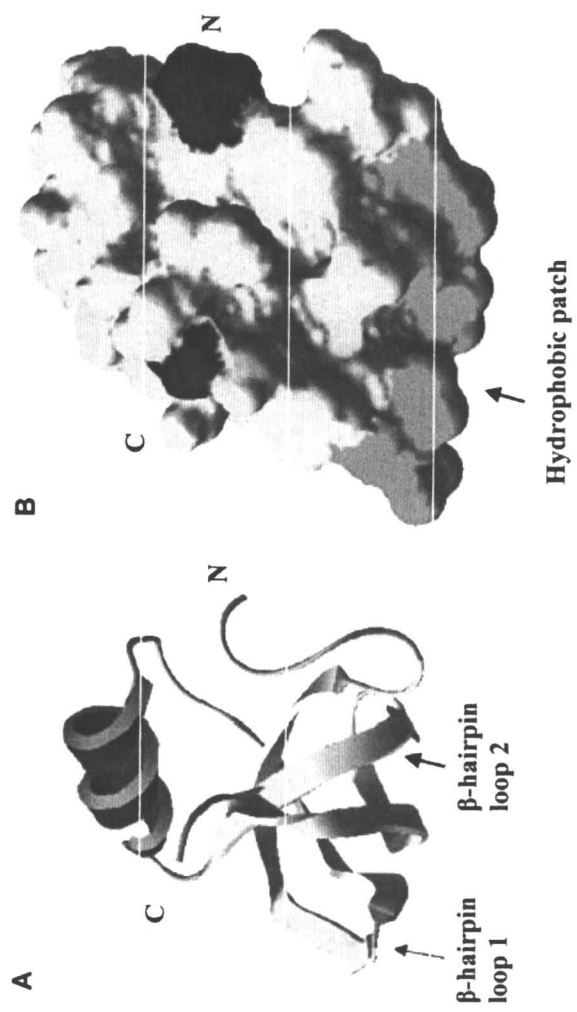


Figure 1. The structure of a hydrophobin 2 molecule (after ref. 1).

Solutions of different quantities of hydrophobin in milli Q water were prepared and degassed. They were used as fresh. Varying concentrations were used up to 5 mg/ml.

Foam stability was measured using a Turbiscan Classic, Formulation, Toulouse, France. Air was bubbled into the solutions and the density of the foam was measured for up to 17 days.

Contact angle measurements on the solutions were performed using the pendant drop technique.

Surface rheology measurements were performed using a surface rheometer from KSV Instruments, Helsinki, Finland. A Langmuir-Blodgett trough was obtained from the same source.

Results

On investigation of the samples by Mastersizer we saw very clear evidence of structuring within the system (Figure 2). This was also apparent after extensive degassing of the system. This was seen repeatedly. If we consider the size of the structures then we see that they appear to be of a scale for small vesicles, which can agglomerate in the system. The larger structures are presumably agglomerations.

Contact angle measurements showed that the hydrophobins were surface active, with surface activity increasing with concentration (Figure 3). Despite this, attempts at using the materials for emulsification were unsuccessful. An extremely large amount of work was given over to the attempt to manufacture emulsions, either water in oil or oil in water, but this was ultimately unsuccessful. In conjunction with other surface-active proteins such as sodium caseinate, emulsification was possible. These emulsions did not differ significantly in character from sodium caseinate stabilized systems and so presumably it is the sodium caseinate that is responsible for the effect.

However it was found that the hydrophobins had very strong foaming effects. Foams made at 5 mg/ml of additive were stable for over a month. Decay was measured with a turbiscan and over 17 days only relatively small changes were seen with the 5 mg/ml solution. Even at lower concentrations, very good and stable foams were seen that lasted for several days at 0.01 mg/ml. This indicates that the hydrophobins have very strong interactions and a profanity for the air / water interface.

Because of this strong foam building ability and the poor emulsification properties it was decided to use surface rheology in order to study the behavior. On performing these measurements it was found that extremely low concentrations of hydrophobin in water were necessary in order to be able to achieve any measurements at all. In fact concentrations lower than 1×10^{-6} mg/ml were needed.



HFB II (050901) 5mg/ml

10 May, 2008

TABNA

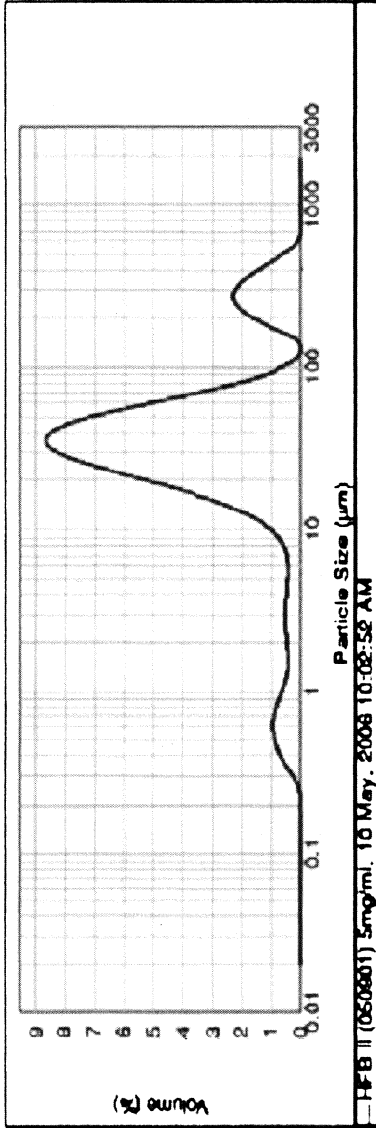
Runs: 8

10 May, 2008 10:02:53

Measurement

Default					
1.520	0.1				5.41 %
Water					1.394 %
1.330					0 Deg. C.
0.0071 %v/d					0.962 mg
6.297					6.237 um
Volume	010.11	3.928 um			um
					60.01: 218.660 um

Figure 2. Particle Sizing Distribution of a Hydrophobin in water. Continued on next page.



3 µm (µm)	5 µm (µm)	10 µm (µm)	20 µm (µm)	40 µm (µm)	80 µm (µm)	150 µm (µm)	300 µm (µm)	600 µm (µm)	1000 µm (µm)	2000 µm (µm)
0.010	0.100	1.000	10.000	100.000	1000.000	10000.000	100000.000	1000000.000	10000000.000	100000000.000
0.011	0.132	1.020	10.100	101.000	1010.000	10100.000	101000.000	1010000.000	10100000.000	101000000.000
0.012	0.168	1.040	10.200	102.000	1020.000	10200.000	102000.000	1020000.000	10200000.000	102000000.000
0.013	0.208	1.060	10.300	103.000	1030.000	10300.000	103000.000	1030000.000	10300000.000	103000000.000
0.014	0.252	1.080	10.400	104.000	1040.000	10400.000	104000.000	1040000.000	10400000.000	104000000.000
0.015	0.300	1.100	10.500	105.000	1050.000	10500.000	105000.000	1050000.000	10500000.000	105000000.000
0.016	0.352	1.120	10.600	106.000	1060.000	10600.000	106000.000	1060000.000	10600000.000	106000000.000
0.017	0.408	1.140	10.700	107.000	1070.000	10700.000	107000.000	1070000.000	10700000.000	107000000.000
0.018	0.468	1.160	10.800	108.000	1080.000	10800.000	108000.000	1080000.000	10800000.000	108000000.000
0.019	0.532	1.180	10.900	109.000	1090.000	10900.000	109000.000	1090000.000	10900000.000	109000000.000
0.020	0.600	1.200	11.000	110.000	1100.000	11000.000	110000.000	1100000.000	11000000.000	110000000.000
0.021	0.672	1.220	11.100	111.000	1110.000	11100.000	111000.000	1110000.000	11100000.000	111000000.000
0.022	0.748	1.240	11.200	112.000	1120.000	11200.000	112000.000	1120000.000	11200000.000	112000000.000
0.023	0.828	1.260	11.300	113.000	1130.000	11300.000	113000.000	1130000.000	11300000.000	113000000.000
0.024	0.912	1.280	11.400	114.000	1140.000	11400.000	114000.000	1140000.000	11400000.000	114000000.000
0.025	1.000	1.300	11.500	115.000	1150.000	11500.000	115000.000	1150000.000	11500000.000	115000000.000
0.026	1.092	1.320	11.600	116.000	1160.000	11600.000	116000.000	1160000.000	11600000.000	116000000.000
0.027	1.188	1.340	11.700	117.000	1170.000	11700.000	117000.000	1170000.000	11700000.000	117000000.000
0.028	1.288	1.360	11.800	118.000	1180.000	11800.000	118000.000	1180000.000	11800000.000	118000000.000
0.029	1.392	1.380	11.900	119.000	1190.000	11900.000	119000.000	1190000.000	11900000.000	119000000.000
0.030	1.500	1.400	12.000	120.000	1200.000	12000.000	120000.000	1200000.000	12000000.000	120000000.000
0.031	1.612	1.420	12.100	121.000	1210.000	12100.000	121000.000	1210000.000	12100000.000	121000000.000
0.032	1.728	1.440	12.200	122.000	1220.000	12200.000	122000.000	1220000.000	12200000.000	122000000.000
0.033	1.848	1.460	12.300	123.000	1230.000	12300.000	123000.000	1230000.000	12300000.000	123000000.000
0.034	1.972	1.480	12.400	124.000	1240.000	12400.000	124000.000	1240000.000	12400000.000	124000000.000
0.035	2.100	1.500	12.500	125.000	1250.000	12500.000	125000.000	1250000.000	12500000.000	125000000.000
0.036	2.232	1.520	12.600	126.000	1260.000	12600.000	126000.000	1260000.000	12600000.000	126000000.000
0.037	2.368	1.540	12.700	127.000	1270.000	12700.000	127000.000	1270000.000	12700000.000	127000000.000
0.038	2.508	1.560	12.800	128.000	1280.000	12800.000	128000.000	1280000.000	12800000.000	128000000.000
0.039	2.652	1.580	12.900	129.000	1290.000	12900.000	129000.000	1290000.000	12900000.000	129000000.000
0.040	2.800	1.600	13.000	130.000	1300.000	13000.000	130000.000	1300000.000	13000000.000	130000000.000
0.041	2.952	1.620	13.100	131.000	1310.000	13100.000	131000.000	1310000.000	13100000.000	131000000.000
0.042	3.108	1.640	13.200	132.000	1320.000	13200.000	132000.000	1320000.000	13200000.000	132000000.000
0.043	3.268	1.660	13.300	133.000	1330.000	13300.000	133000.000	1330000.000	13300000.000	133000000.000
0.044	3.432	1.680	13.400	134.000	1340.000	13400.000	134000.000	1340000.000	13400000.000	134000000.000
0.045	3.600	1.700	13.500	135.000	1350.000	13500.000	135000.000	1350000.000	13500000.000	135000000.000
0.046	3.772	1.720	13.600	136.000	1360.000	13600.000	136000.000	1360000.000	13600000.000	136000000.000
0.047	3.948	1.740	13.700	137.000	1370.000	13700.000	137000.000	1370000.000	13700000.000	137000000.000
0.048	4.128	1.760	13.800	138.000	1380.000	13800.000	138000.000	1380000.000	13800000.000	138000000.000
0.049	4.312	1.780	13.900	139.000	1390.000	13900.000	139000.000	1390000.000	13900000.000	139000000.000
0.050	4.500	1.800	14.000	140.000	1400.000	14000.000	140000.000	1400000.000	14000000.000	140000000.000
0.051	4.692	1.820	14.100	141.000	1410.000	14100.000	141000.000	1410000.000	14100000.000	141000000.000
0.052	4.888	1.840	14.200	142.000	1420.000	14200.000	142000.000	1420000.000	14200000.000	142000000.000
0.053	5.088	1.860	14.300	143.000	1430.000	14300.000	143000.000	1430000.000	14300000.000	143000000.000
0.054	5.292	1.880	14.400	144.000	1440.000	14400.000	144000.000	1440000.000	14400000.000	144000000.000
0.055	5.500	1.900	14.500	145.000	1450.000	14500.000	145000.000	1450000.000	14500000.000	145000000.000
0.056	5.712	1.920	14.600	146.000	1460.000	14600.000	146000.000	1460000.000	14600000.000	146000000.000
0.057	5.928	1.940	14.700	147.000	1470.000	14700.000	147000.000	1470000.000	14700000.000	147000000.000
0.058	6.148	1.960	14.800	148.000	1480.000	14800.000	148000.000	1480000.000	14800000.000	148000000.000
0.059	6.372	1.980	14.900	149.000	1490.000	14900.000	149000.000	1490000.000	14900000.000	149000000.000
0.060	6.600	2.000	15.000	150.000	1500.000	15000.000	150000.000	1500000.000	15000000.000	150000000.000
0.061	6.832	2.020	15.100	151.000	1510.000	15100.000	151000.000	1510000.000	15100000.000	151000000.000
0.062	7.068	2.040	15.200	152.000	1520.000	15200.000	152000.000	1520000.000	15200000.000	152000000.000
0.063	7.308	2.060	15.300	153.000	1530.000	15300.000	153000.000	1530000.000	15300000.000	153000000.000
0.064	7.552	2.080	15.400	154.000	1540.000	15400.000	154000.000	1540000.000	15400000.000	154000000.000
0.065	7.800	2.100	15.500	155.000	1550.000	15500.000	155000.000	1550000.000	15500000.000	155000000.000
0.066	8.052	2.120	15.600	156.000	1560.000	15600.000	156000.000	1560000.000	15600000.000	156000000.000
0.067	8.308	2.140	15.700	157.000	1570.000	15700.000	157000.000	1570000.000	15700000.000	157000000.000
0.068	8.568	2.160	15.800	158.000	1580.000	15800.000	158000.000	1580000.000	15800000.000	158000000.000
0.069	8.832	2.180	15.900	159.000	1590.000	15900.000	159000.000	1590000.000	15900000.000	159000000.000
0.070	9.100	2.200	16.000	160.000	1600.000	16000.000	160000.000	1600000.000	16000000.000	160000000.000

Model: ZONE Ver 9.1
 Seed Number: 34005 67
 10 May 2006 07:45:58 CMT

Model: ZONE Ver 9.1
 Seed Number: 34005 67

Model: ZONE Ver 9.1
 Seed Number: 34005 67
 10 May 2006 07:45:58 CMT

Figure 2. Continued.

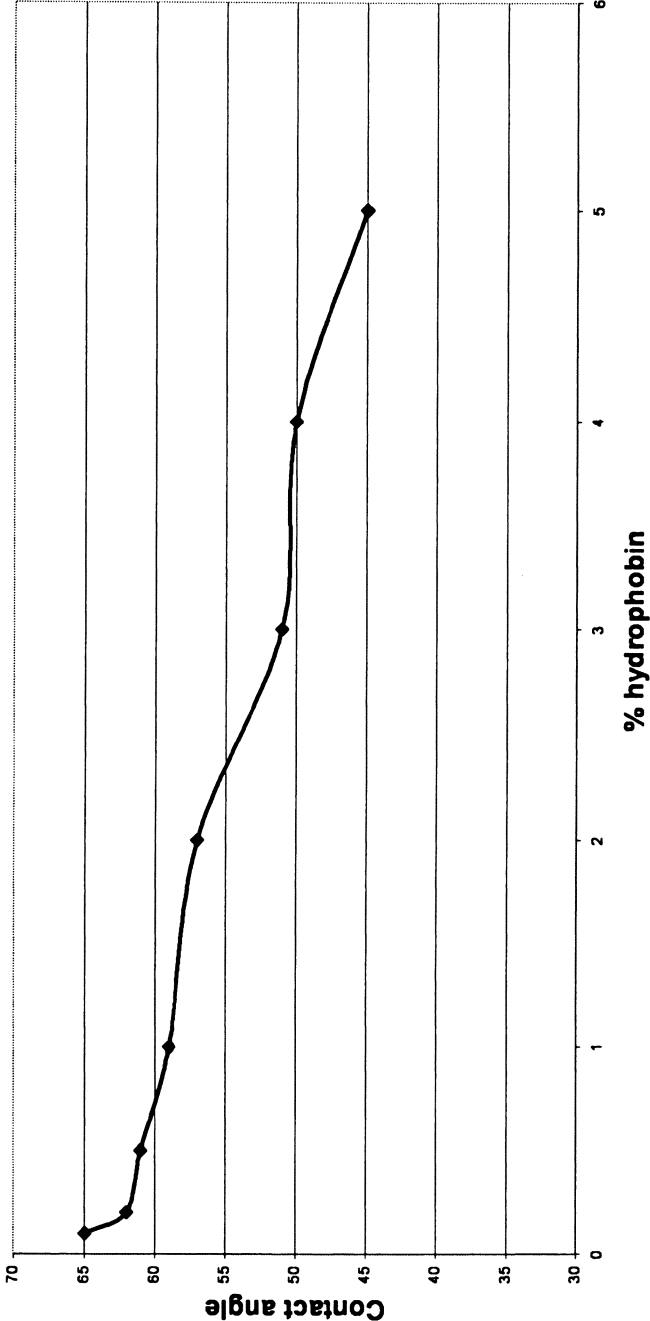
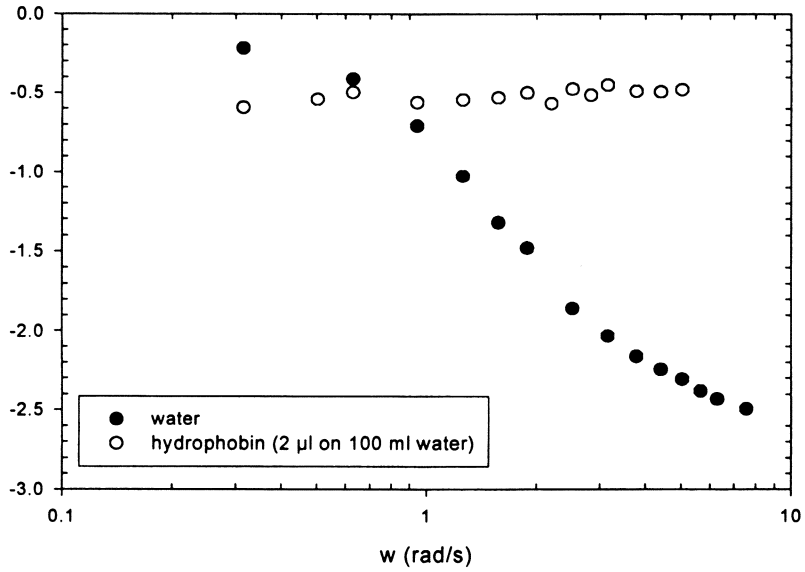


Figure 3. The effect of increasing hydrophobin content on contact angle between water and air.



5 mN/m (2 μ l on 100 ml water trough)

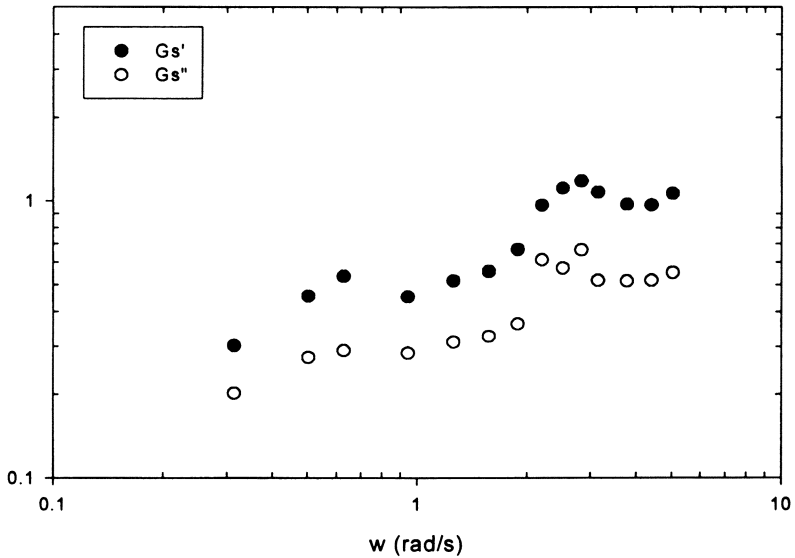


Figure 4. Surface rheology data for hydrophobin gels: a, shear stress ν frequency, b: G' and G'' ν frequency.

At these low concentrations, a two dimensional gel was formed between the particles. These were relatively strong interactions between the individual molecules. These have resulted in the interactions that are seen. As can be deduced from Figure 4 these films are very strong and elastic gel.

Conclusions

We can see that the behavior of the hydrophobins is very interesting. Although the properties that have been studied are bulk ones it is in fact the behavior at the nanoscale that is having a significant effect. The evidence is that small structures of hydrophobins are forming. These can then partition to the air water interface where the amphiphilic nature of the molecule causes them to interact to form strong elastic films. There is clearly little partition to any oil/water interface. This indicates that the specific nano-scale interactions of the particles are important. In order to further establish the use and applicability of these systems further work is needed.

The results also reveal the complexity and functionality of the hydrophobin molecules and their applicability in fungi. It seems that the film building functionality is extremely critical.

Acknowledgements

We would like to thank Rauni Seppanen, Per Claesson and Eva Blomberg for interesting discussions. Hans Ringblom, Annika Dahlman and Anne-Marie Hårdin provided experimental help. We are grateful to VINNOVA and TEKES for financial support.

References

1. Wessels J.G., de Vries O.M., Asgeirsdottir S.A., Springer J. *J. Gen. Microbiol.* **1991**, *137*, 2349-2345.
2. Linder M.B., Szilvay G.R., Nakari-Setälä T, Penttilä M.E., *FEMS Microbiol. Rev.* **2005**, *29*, 879-896.
3. Wösten H.A., van Wetter W.A., Lugones L.G., van der Mei H.C., Burscher H.J., Wessels J.G., *Curr. Biol.*, **1999**, *9*, 85-88.
4. Talbot N.J., *Nature*, **1999**, *398*, 295-296.
5. Scholtmeijer K., Wessels J.G., Wösten H.A., *Appl. Microbiol. Biotechnol.* **2001**, *56*, 1-8.

Chapter 6

Calcium Cross-Linked Soy Protein Beads and Microspheres as Carriers for Nutraceutical Compound Delivery

Lingyun Chen, Gabriel E. Remondetto, and Muriel Subirade*

Canada Research Chair in Proteins, Biosystems and Functional Foods, Nutraceuticals and Functional Foods Institute (INAF/STELA), Université Laval, Laval, Quebec G1K 7P4, Canada

The ongoing identification of compounds with health benefits beyond those of classical nutrients and vitamins, so-called nutraceutical compounds, presents an excellent opportunity for the development of innovative functional foods. However, successful incorporation of these compounds into food systems is often very difficult, due to their sensitivity to environmental factors encountered during food processing, such as light, oxygen and heat, as well as to conditions prevailing in the gastrointestinal tract, such as acidic pH and enzymatic hydrolysis, which limit their activity and potential health benefits. The food industry is thus challenged to develop delivery systems for incorporating nutraceutical compounds into food without reducing their bioavailability or functionality. In this article, we present recent progress in the design, preparation and evaluation of soy protein beads and micro-particles as delivery systems and their potential for the development of innovative functional foods.

Introduction

Avoiding or delaying the onset of chronic diseases has become an attractive strategy for improving the cost-effectiveness of public health spending. Possible health benefits beyond the basic nutritional functions of a wide variety of nutrients have been explored over the past several years. Known as nutraceuticals, this category of compounds has received much attention in recent years from the scientific community, consumers and food manufacturers. The list of potential nutraceutical products (vitamins, probiotics, bioactive peptides, antioxidants and so on) is endless and scientific evidence to support the concept of health promoting food ingredients is growing steadily ¹. Increasing intake of such molecules by consuming so-called functional foods has been proposed as an alternative to classical pharmacology for improving health and wellbeing as well as lessening the burden of disease ². However, development of innovative products for this purpose encounters several obstacles. Because of their sensitivity to environmental factors associated with food processing, such as light, oxygen and high temperatures, in addition to conditions prevailing in the gastrointestinal tract, such as acidic pH and hydrolysis by digestive enzymes, most active food components are susceptible to degradation when incorporated into food formulations for transport from the digestive system to the site of desired action ³⁻⁵. The delivery of these molecules will therefore require food formulators and manufacturers to provide protective mechanisms that 1) maintain the active molecular form until the time of consumption and 2) deliver this form to the physiological target within the organism.

Protein is an essential component of the daily diet. Adult humans must eat dozens of grams of protein every day. It provides energy as well as materials for the synthesis of all bodily structures and enzymes, including all the hydrolases that are secreted daily into the GI tract to digest food ⁶. Most natural foods contain at least some protein and certain by-products of the food-processing industry are rich in protein (whey from cheese production, press cake from vegetable oil production). Proteins are also widely used in formulated foods, partly because of their nutritional value, but especially for their functional properties, which include gelling, foaming and emulsification and underlie many food sensory attributes ⁷⁻¹⁰. Among these functional properties, the abilities to form networks and to adsorb spontaneously to interfaces to stabilize polyphasic systems offer the possibility of developing GRAS biocompatible carriers for oral administration of sensitive nutraceuticals in a wide variety of foods, including nano- and micro-particles ¹¹.

This chapter illustrates the potential of food protein-based matrices to serve as carriers for the controlled release of functional food components. Since the diversity of the systems and production processes under investigation is already vast, this chapter focuses on recent progress in the design, preparation and evaluation of soy protein beads and micro-particles as delivery systems and their potential for the development of innovative functional foods.

Calcium cross-linked soy protein hydrogels

Soy protein is used extensively as a functional ingredient in many different food products, such as baked goods and cured meats. It is composed almost exclusively of two globular protein fractions differentiated by sedimentation coefficient: 7S (β -conglycinin) and 11S (glycinin)^{12,13}. Both fractions are able to aggregate when heated and form three-dimensional gel networks with characteristics dependent on conditions such as pH, ionic strength and temperature¹⁴⁻¹⁸. Examination of the gelling mechanism indicates that intermolecular disulfide, hydrogen and hydrophobic bonds play important roles¹⁹. The gelling properties of soy protein isolate have been of interest for developing hydrogel networks entrapping bioactive molecules. However, the heat needed to produce these gels limits their application to formulations that do not contain heat-sensitive ingredients.

It has been shown recently that cold-induced gelation of soy protein can be achieved by adding Ca^{2+} ions to a preheated soy protein suspension. As adapted from cold gelation of whey proteins²⁰, this method requires a heating step during which proteins are denatured and polymerized into soluble aggregates, followed by a cooling step and subsequent salt addition, which results in the formation of a network²¹. Gel micro-structural analyses have shown that two types of gels may thus be obtained, depending mainly on calcium concentration. Gel prepared at 10mM CaCl_2 (Fig. 1a) exhibits a 'filamentous' character and is composed of very fine strands in a dense arrangement with pores of relatively even size. In contrast, gel formed at 20mM CaCl_2 (Fig. 1b) is particulate, composed of irregularly sized fused masses of bead-like particles. Based on FT-IR spectroscopy and rheological analysis, a two-step mechanism of soy protein cold gelation has been proposed²². Protein molecules first associate upon preheating into aggregates, which constitute the structural units responsible for forming the three-dimensional network. Calcium ions subsequently neutralize the negative charges on the structural unit surface. This electrostatic neutralization enables the formation of a three-dimensional network by two mechanisms, each occurring at a different calcium concentration. At the lower calcium concentration (10mM), the surface charge is partially screened, which keeps the energy barrier between any two units relatively high. However, charge-free hydrophobic patches on structural units can approach one another and link. This type of interaction promotes aggregation growth preferentially along linear paths, leading to filamentous gels. At the higher calcium concentration (20mM), a quasi total screening of repulsive forces between structural units occurs, resulting in random aggregation to form particulate gels.

This method opens interesting opportunities for soy proteins as carriers of thermo-sensitive nutraceutical compounds. Moreover, during the preheating step, proteins denature and polypeptide chains unfold to expose normally buried functional groups and create new interactions, including hydrogen bonds,

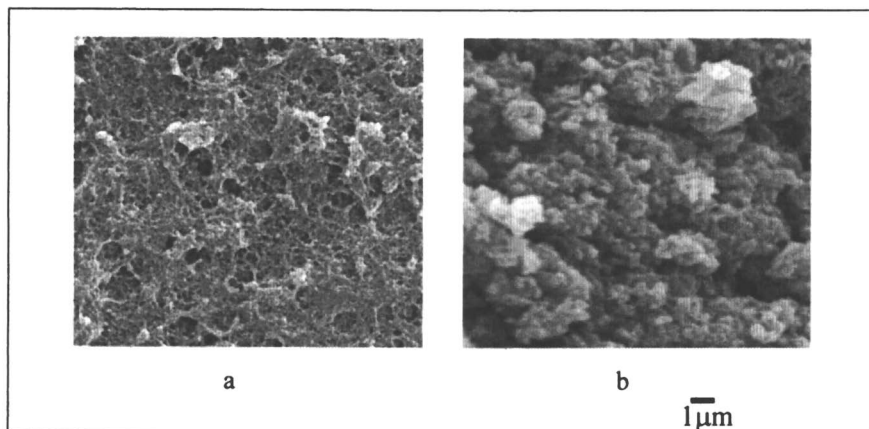


Figure 1. scanning electron micrographs of 8% (w/w) soy protein cold-set gels formed at 10mM CaCl₂ (a) and 20mM CaCl₂ (b).

hydrophobic interactions and electrostatic interactions, to entrap nutraceutical compounds within the three-dimensional gels.

Soy protein beads and microspheres

Thorough knowledge of soy protein network structure and function provides the possibility of developing a wide range of soy protein formulations. Among these, beads and microspheres are of particular interest, due to their ability to control incorporated compound release rate. By formulating the internal composition and the surface coating to control matrix breakdown or by precise control of particle size, it is possible to obtain content release at predetermined times and locations in the digestive tract and thereby mimic different drug administration schedules^{23,24}. However, published studies on soy protein beads and micro-spheres are scarce. We provide below some observations from our examination of the suitability of soy protein isolate for producing calcium cross-linked beads and micro-spheres that could be used as delivery systems for nutraceutical compounds.

Beads

The extrusion technique, a convenient method of encapsulating bioactive compounds in food matrices by injecting protein droplets containing a fixing agent into a solution containing a gelling agent, was chosen to prepare soy

protein beads of 1-2 mm. In summary (Fig.2), soy protein isolate (SPI) powder was added to de-ionized water and the mixture was stirred for 2 h at room temperature to hydrate the protein. After centrifuging at $2,000 \times g$ for 30 min to remove air bubbles, the solution was heated at 105°C for 30 min. The resulting solution was cooled for 1 h at room temperature and then added drop-wise to 150 mL of CaCl_2 solution using a hydraulic pump (Allo Kramer Shear Press, model SP 12, Rockville, MD) equipped with a 0.8 mm (i.d.) needle (Terumo Medical Corp., Elkton, MD). Magnetic stirring was maintained during the gelation. The resulting beads were rinsed with distilled water and dried in P_2O_5 .

The effects of SPI concentration and the gelling bath calcium concentration on bead morphology and physical properties were investigated. The photographs in Figure 2 show beads prepared with 10-14% protein (w/w). The beads are regular and spherical in shape at 12% protein and characterized by a smooth surface. At both 10-11% and 13-14% protein, the beads exhibited irregular shapes. The inset image in Figure 2 shows droplet shape at the end of the extrusion needle, which is an important factor in regulating final bead morphology. At 10-11% and 13-14%, the protein solution viscosity was too low or too high, which prevented the formation of spherical droplets. At the optimal protein concentration (12%), spherical droplets were formed, which then fell by gravity into the gelling bath to produce round beads. The CaCl_2 concentration influenced both bead morphology and strength. Increasing this concentration led to beads with greater sphericity and rupture strength, which may be due to spontaneous formation of salt bridges between adjacent protein molecular chains at the droplet interface to allow formation of a three-dimensional network. Soy protein beads prepared at 12% protein and 3M CaCl_2 demonstrated rupture strength and Young's modulus comparable to that of 1% alginate beads, based on analysis with a texture analyzer TA-XT2 version 5.15 (50 N maximum force, precision of 0.001 N; Stable Micro Systems, Haslemere, Surrey, United Kingdom) as shown in Figure 3.

Microspheres

The food industry is being challenged to develop carriers for controlled delivery of nutraceutical compounds. The advantage of using micro-spheres comes from their small size. Particles $\leq 100 \mu\text{m}$ can be incorporated into most foods, including solid and semi-solid products, without changing their sensory qualities²⁵. Moreover, it has been reported in earlier work that as carrier system diameter decreases, residence time in the gut increases. Therefore, greater residence time may be expected for small micro-particles compared to beads, allowing an increase in bioavailability. Although extrusion methods generally produce beads $\geq 1\text{mm}$, soy protein micro-particles of 50-150 μm were successfully prepared using an Inotech Encapsulator (Inotech Biosystems

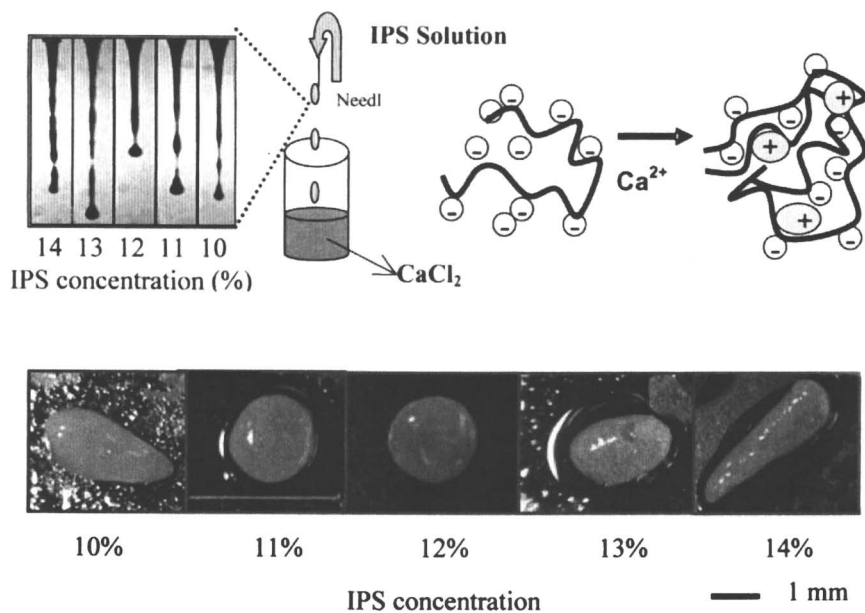


Figure 2. Photographs of soy protein beads prepared by extrusion at various protein concentrations. (See page 1 of color insert.)

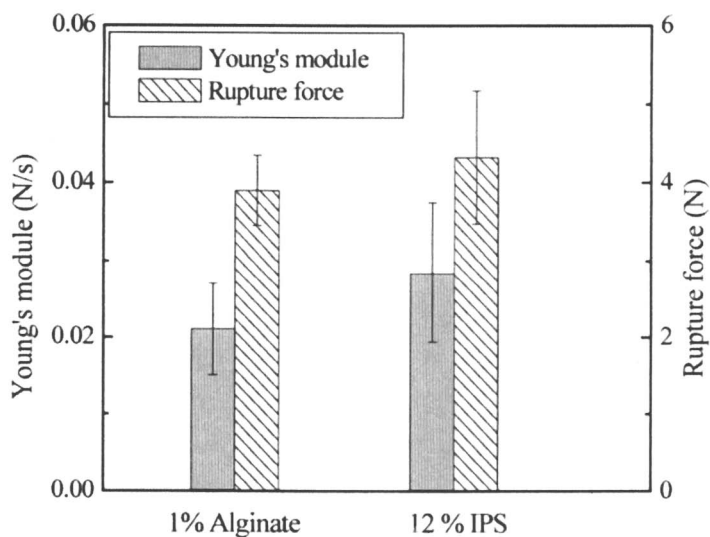


Figure 3. Young's modulus and rupture force of beads prepared with 1% alginate and 13% soy protein isolate.

International, Switzerland) equipped with a harmonically vibrating 100 μm nozzle, which produces round, uniform droplets continually. Figure 4a shows the fluorescence micrograph of these micro-spheres (Olympus BX50WI optical microscope fitted with epi-fluorescence and optical fluorescent filters). The samples were stained with Nile red, which is a fluorescent marker for oil globules incorporated inside protein matrix and visualized as red. The particles exhibited uniform size with spherical shape. As expected, CaCl_2 is involved in the formation of a network by electrostatic attractions between Ca^{2+} and the carboxyl groups in side chains of proteins in solution. However, neither too high nor too low calcium concentration resulted in strong gels. This may be attributed to repulsion of the protein molecular chains when they are negatively charged (bearing $-\text{COO}^-$ groups at low CaCl_2 concentration) or positively charged (saturated with Ca^{2+} at high CaCl_2 concentration) during gelling step. The strongest micro-particles were obtained at a CaCl_2 concentration of 100mM, where the ratio between carboxyl groups and Ca^{2+} ions seemed to be optimal for reinforcing protein intermolecular interactions to form a network.

The emulsification-gelation technique is widely used to prepare micro-spheres. In conventional methods, protein micro-spheres are prepared by emulsifying a protein solution containing the encapsulated substance, followed by particle hardening by protein precipitation using a cross-linking agent such as glutaraldehyde and formaldehyde, or by increasing the temperature to above 90°C. Although gelatin, albumin and other protein micro-spheres have been prepared this way for pharmaceutical applications, these are not suitable for daily consumption and the heating process will rule out their use as carriers for thermo-sensitive nutrients. Recently, soy protein micro-spheres were developed in our group using an emulsification-internal cold gelation method, which is based on the release of calcium ions from an acid-soluble calcium salt in emulsified protein solution. This is achieved by acidification with an oil-soluble acid, which partitions to the dispersed aqueous phase, releasing soluble calcium and initiating gelation. Since neither toxic organic reagents nor heating are used to bring about gelling, this method is regarded as safe for producing protein micro-spheres for food applications. In summary, soy protein powder was hydrated in de-ionized water and denatured at 105°C for 30 min. Calcium carbonate was then added to this solution. The soy protein / CaCO_3 mixture was dispersed in soybean oil and the system was stirred vigorously for 15 min to form a W/O emulsion. During agitation, glacial acetic acid was added to initiate droplet gelation. The suspension of droplets in oil was subsequently added to calcium chloride solution. After complete partitioning of droplets to the aqueous phase, the oil was discarded and the micro-spheres were filtered, washed and lyophilized. The morphology of the micro-spheres was observed using an Olympus BX50WI optical microscope fitted with epi-fluorescence and optical fluorescent filters and a JEOL JSM 35CF scanning electron microscope (SEM). For fluorescence observation, micro-spheres were stained with phen green, which is a fluorescent marker for calcium and visualized as green ²⁶. The

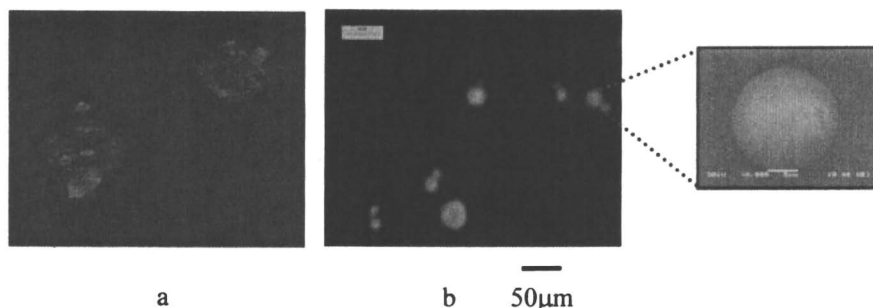


Figure 4. Fluorescence photomicrographs of soy protein micro-spheres prepared by extrusion (a) and emulsification/internal cold gelation (b). Insets show scanning electron microscopic image of micro-spheres in photograph b. (See page 1 of color insert.)

microphotograph in Figure 4b indicates homogenous distribution of Ca^{2+} in the soy protein matrix. The SEM image (inset) shows uniform soy protein micro-spheres of 20 μm in diameter characterized by spherical shape and smooth surface. In fact, by controlling agitation during W/O emulsion formation, micro-spheres with mean diameters ranging from 20 to 100 μm were obtained. Emulsion droplet size and resulting bead diameter are determined by the relationship between the dispersive forces and the surface tension of the discontinuous phase. However, strong dispersive force combined with surfactants (e.g. Span 80), which are usually used to lower the interfacial tension between the water and oil phases and to stabilize emulsion droplets against coalescence, are required to prepare small micro-spheres.

It should be noted that both kinds of protein micro-spheres exhibited high stability. No aggregation was observed in buffers at pH 1-7 over two weeks of storage, as determined by static light scattering using a Mastersizer 2000 (Malvern Instruments, Southborough, MA, USA).

Nutrient encapsulation and release in the gastrointestinal tract

Soy protein has the ability to interact with a wide range of active compounds due to the affinity of these compounds for proteins with gelling properties. These binding properties are dependant on the molecular structure of the protein, which under appropriate conditions (pH, temperature, ionic strength...) can expose multiple functional groups to modulate interactions with active compounds. An active compound having affinity for gelling proteins may therefore be expected to be loaded preferentially into a carrier and be

controllably released. The following section describes the functionality of soy protein micro-particles as delivery systems for hydrophilic and hydrophobic nutrients.

Hydrophilic nutrients

Riboflavin (vitamin B2) is an essential water soluble nutrient in human nutrition, playing a key role in the metabolism of amino acids and fats, the activation of vitamin B6 and folic acid and the conversion of carbohydrates into the energy that powers all bodily functions. But riboflavin is unstable in light and thus riboflavin containing foods subjected to ultraviolet or visible light can show significant losses of riboflavin. Soy protein micro-spheres incorporating riboflavin were prepared by the emulsification-internal cold gelation method described above with incorporation of riboflavin as a model into the soy protein / CaCO₃ mixture before emulsifying. An encapsulation efficiency of 87.8% and a loading efficiency of 14.6% were obtained for these micro-spheres. Figure 5a shows that the yellow crystals of riboflavin were homogeneously distributed in the soy protein spherical matrix. Swelling properties of dried soy protein micro-spheres were investigated at pH 1.2 (gastric pH), pH 4.8 (near the pI of soy protein) and pH 7.5 (normal conditions in the small intestine). Temperature was maintained at 37°C in an incubator. Figure 5b shows that pH has a significant effect on the degree of swelling of soy protein micro-spheres, which was lowest at pH 4.8 and increased with changes in pH (increasing at pH 7.4 or decreased at pH 1.2), suggesting that swelling behavior is mainly governed by the net charge of the protein molecules. At pI, the net charge of the soy protein molecule is minimal, which leads to low electrostatic repulsion between chains and results in a low swelling ratio. However, as the pH deviates from pI, the net charge of the soy protein molecule increases, leading to high electrostatic repulsive forces and an increase in the swelling ratio. At the gastric pH, the beads are the most swollen, suggesting high repulsive interactions between positive charges created by the complete protonation of the amine groups on the polypeptide chains. Riboflavin release from the micro-spheres was examined at pH 1.2, 4.8 and 7.4 and 37°C (Figure 6c). After 1h, almost 80% of the riboflavin was found in the medium at both pH 1.2 and 7.4, suggesting rapid release of riboflavin from soy protein micro-spheres in stomach and intestine pH. However, riboflavin was slowly released at pH 4.8. After a burst release of about 30% at the initial one hour, the release% leveled off. This slow release can be attributed to a shrink status of the micro-particles.

The TNO intestinal model, a sophisticated simulator of the gastrointestinal tract (TIM1, Fig. 6), was applied to provide further investigation of the release properties of soy protein micro-spheres and to estimate the availability of encapsulated riboflavin for absorption in human beings. This system is

composed of four serial compartments simulating the stomach, the duodenum, the jejunum and the ileum. The availability of riboflavin for absorption was estimated by measuring its concentration in the jejunal and ileal dialysis fluids, following its passive diffusion through the hollow fiber membranes connected to the two compartments representing the jejunum and the ileum, respectively ²⁷. Dry protein micro-spheres were introduced into the gastric compartment simultaneously with water (representing the fasting state). Riboflavin dissolved in water (without encapsulation) was compared as a control. The standard fasting state protocol was applied ²⁸. Figure 7 depicts the results expressed as cumulative amounts of riboflavin in the dialysis fluid. They show a profile characteristic of the release and absorption of riboflavin from protein micro-spheres. More than 80% of the riboflavin was absorbed in the jejunum, indicating that this is the main site of absorption, regardless of the nature of the micro-spheres. Both riboflavin encapsulated in micro-spheres and dissolved in water showed very high absorption rates, confirming the rapid release of riboflavin from the micro-spheres, which may be attributed to quick diffusion from the soy protein matrix due to its hydrophilic nature. The potential for soy protein micro-particles as immediate release vehicles for hydrophilic molecules is thus apparent. These micro-particles might be used as encapsulation systems for water soluble vitamins in liquid or semi-liquid foods such as fruit juice and yogurt at pH 4-5 to preserve their bioactivities during storage. After oral administration, they can be released quickly and absorbed in stomach and intestine.

Hydrophobic nutrients

Soy protein is very effective at stabilizing oil-in-water emulsions by adsorbing to the oil droplet surface, lowering interfacial tension, forming protective membranes around the lipid and imparting an electrical charge to the droplet surface when the pH is not near the pI of the interfacial protein. Hydrophobic nutrients such as oil soluble vitamins or unsaturated fatty acid encapsulated in protein micro-particles can thus be converted to a stable form that is more resistant to oxidation. Retinol (vitamin A), is a fat-soluble antioxidant vitamin. It is considered to be essential for proper vision, bone growth and maintenance of healthy skin and the mucous membranes lining the nose, sinuses and mouth. Retinol-loaded beads were prepared by adding retinol to the soybean oil. Prior to preparing the emulsion, the soy protein solution and soybean oil were pre-dispersed using an Ultra-Turrax mixer (Janke & Kunkel, IKALabortechnik, Germany). The dispersion was then homogenized using an Emulsiflex-C5 high-pressure homogenizer (AVESTIN Inc., Ottawa, Canada). Emulsion preparation was initially performed at 150 MPa pressure and then at 3 MPa. The resulting emulsion was added drop-wise to CaCl₂ solution to form protein beads. Figure 8 shows oil globules encapsulated in soy protein micro-

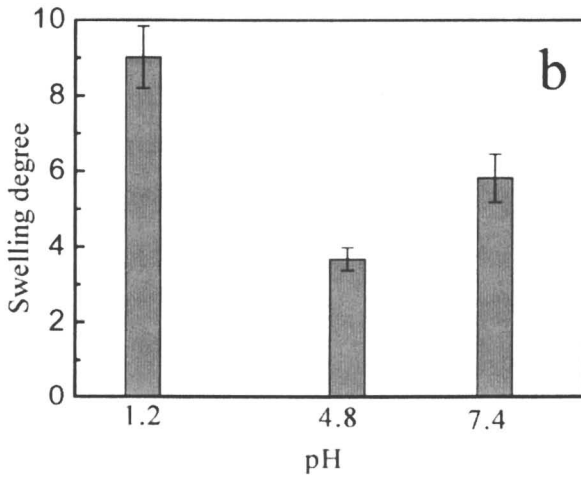
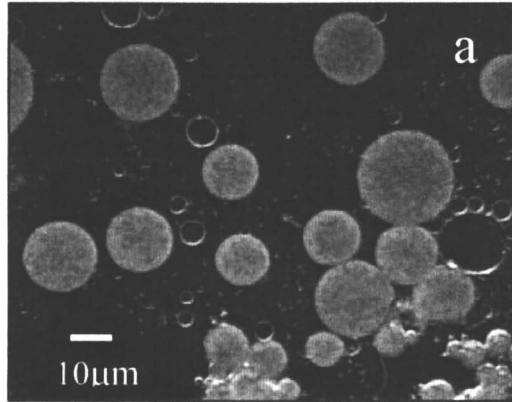


Figure 5. Photomicrograph of soy protein micro-spheres incorporating riboflavin (a); micro-sphere swelling (b); vitamin release profile at different pH (c).

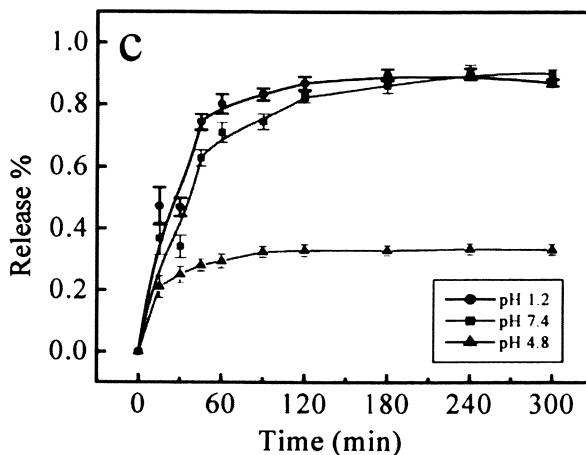


Figure 5. Continued.

particles of 150 μm prepared by extrusion at CaCl_2 concentrations of 0.01M (a), 0.1M (b) and 1M (c). The photomicrographs show uniform and homogeneous distribution of oil globules stabilized by soy protein aggregates layer in the gel networks. During the emulsification step, thermally pre-denatured soy proteins, acting as an emulsifier, rapidly adsorbed to the surface of the oil droplets. In the presence of calcium, protein aggregated to create a stabilizing coating that protects the fine droplets against coalescence and provides physical stability to the emulsion. Increasing the CaCl_2 concentration led to a thicker protein aggregate layer, which should ensure a more stable internal structure. Studies are presently underway in our laboratory on the release properties of retinol from soy protein micro-spheres. Preliminary results suggest that delivery of the hydrophobic nutrient is regulated by gel biodegradation. Further research will be carried out on retinol stability in the protein emulsion and its release profile in the gastrointestinal tract simulator.

As can be inferred from the above examples, soy protein micro-spheres hold promise for providing effective and efficient means of protecting nutrients, peptides and antioxidants and delivering them at the desired site in the human body to enhance their efficacy and bioavailability.

Conclusion

Calcium cross-linked soy protein hydrogels show great potential as new GRAS food matrices with the capacity to incorporate nutraceutical compounds. These matrices can be tailored to formulate beads and micro-spheres as

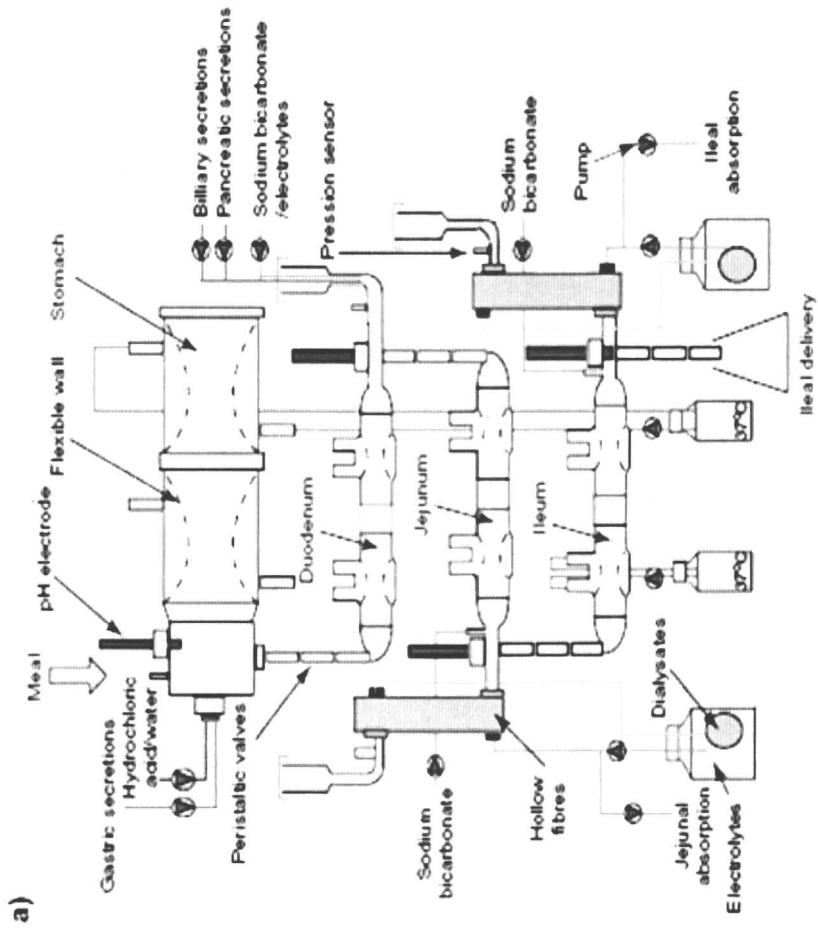


Figure 6. Scheme of Tim1.

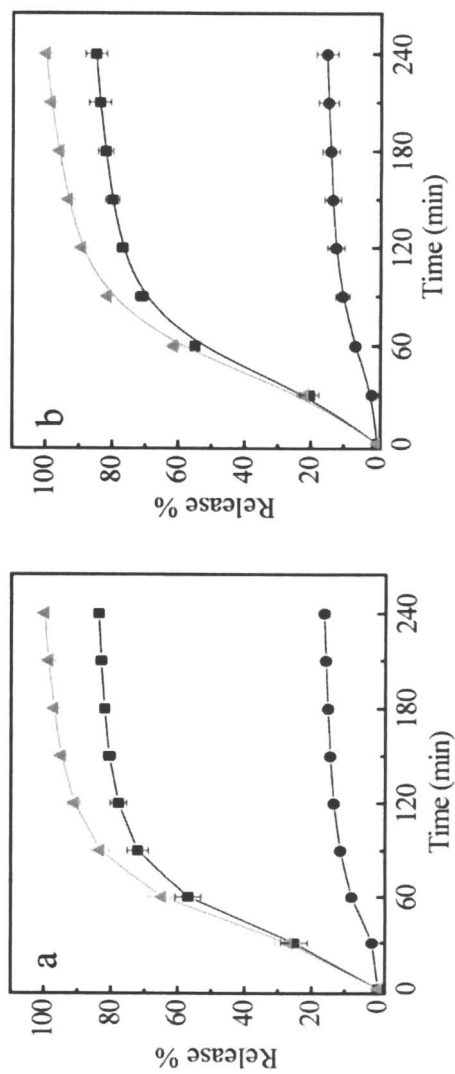


Figure 7. Cumulative percentage (mean \pm S.D.) of riboflavin absorbed in the TIM1 in the fasting state; Riboflavin incorporated into protein micro-spheres (a); riboflavin dissolved directly in water (b) (■ Absorption from jejunum ● Absorption from ileum ▲ Total absorption: jejunum + ileum).

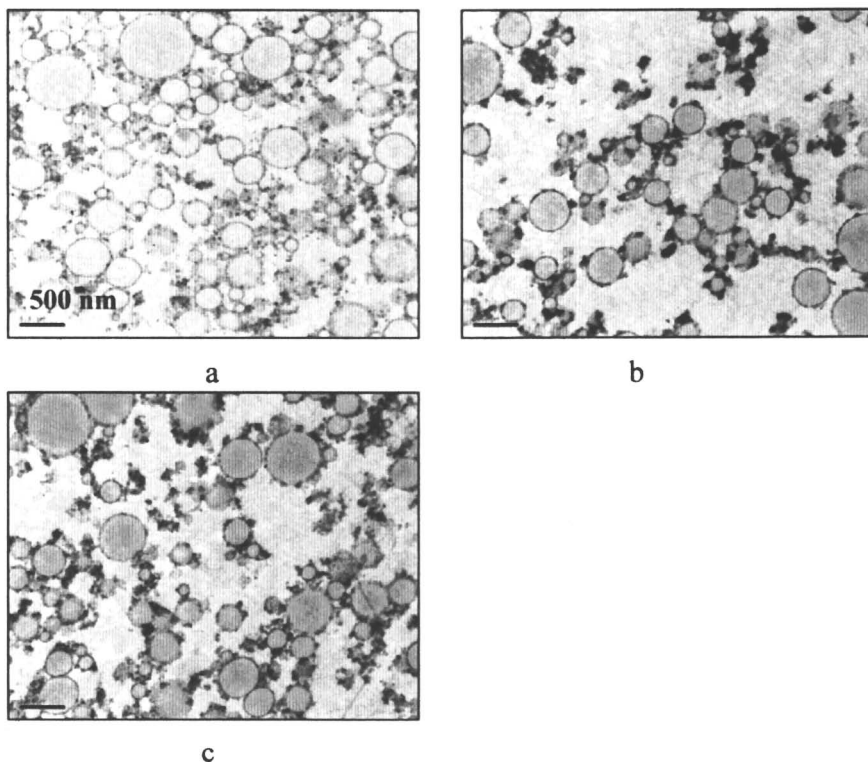


Figure 8. Transmission electron microscopic image of the internal structure of soy protein emulsion micro-spheres incorporating retinol prepared at 0.01M CaCl_2 (a), 0.1 M CaCl_2 (b) and 1M CaCl_2 (c).

described in this chapter and thus provide means of controlling compound release. Although still in the preliminary stages, their application in both food and non-food industries is promising. Further experiments are aimed at fundamental understanding of protein–protein and protein–nutrient interactions at the molecular level and their impact on functional properties of proteins to ensure design of ideal carriers for use with nutraceutical compounds in the food industry.

Acknowledgement

This work was financially supported by the Canada Research Chairs Program (M.S.), the Natural Sciences and Engineering Research Council of Canada (NSERC) and the Canadian Institute of Health Research (CIHR) (Collaborative Health Research Projects Program). The authors would like to thank Dr Eric Beyssac (Faculty of pharmacy, Auvergne University, France) for fruitful discussion on TIM experiments and for the access to TIM instrument. The authors thank P. Giraud and C. Mercier for their technical assistance.

References

1. Wildman, R. E. C. In R. E. C. Wildman (Ed.), *Handbook of nutraceuticals and functional foods*; New York, CRC Press, 2001.
2. Elliott R.; Ong T. J. Science, medicine, and the future of nutritional genomics. *Br. Med. J.* **2002**, *324*, 1438-1442.
3. Bell L. N. Stability testing of nutraceuticals and functional foods, in Wildman R. E. C. *Handbook of nutraceuticals and functional foods*; New York, CRC Press, 2001, p501-551.
4. Shoji, Y.; Nakashima, H. Nutraceuticals and delivery systems. *J. Drug Targets* **2004**, *12*, 385-391.
5. Chen, L.; Subirade, M. Chitosan/b-lactoglobulin core-shell nanoparticles as nutraceutical carriers. *Biomaterials* **2005**, *26*, 6041–6953.
6. Shahidi F.; Mine Y. *Nutraceutical proteins and peptides in health and disease*; Boca Raton, CRC/Taylor and Francis, 2005.
7. Bryant, C. M.; McClement, D. J. Molecular basis of protein functionality with special consideration of cold-set gels derived from heat-denatured whey. *Trends Food Sci. Tech.* **1998**, *9*, 143-151.
8. Clark, A. H. Gelation of globular proteins. In S. E. Hill, D. A. Leward, & J. R. Mitchell (Eds.), *Functional properties of food macromolecules*; Gaithersburg, MD, Aspen, 1998, p 77-142.
9. Dickinson, E. Colloidal aggregation: Mechanism and implications. In E. Dickinson, & T. van Vlie (Eds.), *Food colloids, biopolymers and materials*; Cambridge, Royal Society of Chemistry, 2003, p 68-83.

10. Walstra, P. Studying food colloids: Past, present and future. In E. Dickinson, & T. van Vlie (Eds.), *Food colloids, biopolymers and materials*; Cambridge, Royal Society of Chemistry, 2003, p 391-400.
11. Chen L.; Remondetto G. E.; Subirade M. Food protein-based materials as nutraceutical delivery systems, *Trends in Food Sci Tech*, **2006**, *17*, 272-283.
12. Wolf W. J.; Babcock G. E.; Smith A. K. Ultracentrifugal differences in soybean protein composition. *Nature* **1961**, *191*, 1395-1396.
13. Saio K.; Watanabe T. Differences in functional properties of 7S and 1S soybean protein. *J. Texture Studies* **1978**, *9*, 135-157.
14. German B.; Damodaran S.; Kinsella J. E. Thermal dissociation behavior of soy proteins. *J. Agric. Food Chem.* **1982**, *30*(5), 807-811.
15. Utsumi S.; Kinsella J. E. Forces involved in soy protein gelation: effect of various reagents on the formation; hardness and solubility of heat-induced gels made from 7S, 11S and soy isolate. *J. Food Sci.* **1985**, *50*, 1278-1282.
16. Hermansson A. M. Structure of glycinin and conglycinin gels. *J. Sci. Food Agric.* **1985**, *36*, 822-832.
17. Hermansson A. M. Soy protein gelation. *J. Am. Oil Chem. Soc.* **1986**, *63*(5), 658-666.
18. Renkema J. M. S.; Knabben J. H. M.; van Vliet T. Gel formation by β -conglycinin and glycinin and their mixture. *Food Hydrocolloids* **2001**, *15*, 407-414.
19. Furukawa T.; Ohta S. Mechanical and water-holding properties of heat-induced soy protein gels as related to their structural aspects. *J. Texture Studies* **1982**, *13*, 59-69.
20. Barbut S.; Foegeding E. A. Ca^{2+} -induced gelation of pre-heated whey protein isolate. *J. Food Sci.* **1993**, *58*(4), 867-871.
21. Maltais A.; Remondetto G.; Gonzalez R.; Subirade M. Formation of Soy Protein Isolate Cold-set Gels: Protein and Salt Effects. *J. Food Sci.* **2005**, *70*, 67-73.
22. Maltais A.; Remondetto G.; Gonzalez R.; Subirade M. Mechanisms involved in the formation and structure of soya protein cold-set gels: a molecular and supramolecular investigation, *Food hydrocolloids* **2007**, in press.
23. Schäfer, V.; von Briesen, H.; Andreesen, R.; Steffan, A. M.; Royer, C.; Tröster, S.; et al. Phagocytosis of nanoparticles by human immunodeficiency virus (HIV)-infected macrophages: A possibility for antiviral drug targeting. *Pharm. Res.* **1992**, *9*, 541-546.
24. Chen L.; Subirade M. Alginate-whey protein granular microspheres as oral delivery vehicles for bioactive compounds. *Biomaterials*, **2006**, *27*, 4646-4654.
25. Pothakamury, U. R.; Barbosa-Gnovas, G. V. Fundamental aspects of controlled release in foods. *Trends Food Sci. Tech.* **1995**, *61*, 397-406.
26. Augustin, M. A. The role of microencapsulation in the development of functional dairy foods. *Australian J. Dairy Tech.* **2003**, *58*(2), 156-160.

27. Souliman S.; Blanquet S.; Beyssac E. ; Cardot J. M. A level A in vitro/in vivo correlation in fasted and fed states using different methods: Applied to solid immediate release oral dosage form. *Eur. J. pharm. Sci.* **2006**, *27*, 72-79.
28. Blanquet S.; Marol-Bonnin S.; Beyssac, E.; Pompon D.; Renaud M.; Alric M. The 'biodrug' concept: an innovative approach to therapy, *Trends in Biotech.* **2001**, *19*, 393-400.

Chapter 7

Design of Single Surfactant Microemulsion

Nabil Naouli and Henri L. Rosano

Department of Chemistry, The City College of the City University of New York, New York, NY 10031

A series of microemulsions, both W/O and O/W, based on non-ionic surfactants of the form $(NP(EO)_n)$, were prepared using the titration method. Mixing a constant weight of surfactant with a constant volume of the dispersed phase and an initial volume of continuous phase produces an emulsion, which is titrated to clarity with another surfactant (cosurfactant). Plotting (a) the volume of cosurfactant necessary to transform an emulsion into a microemulsion containing a fixed volume of dispersed phase and constant weight of surfactant versus (b) different initial continuous-phase volumes yields a straight line. Extrapolating from experimentally determined values for the cosurfactant volume to the value corresponding to a zero-volume continuous phase allows the determination of the surfactant molar composition and the average number of ethylene oxides (EO) per nonylphenol adsorbed at the interface. Using a surfactant with the same number of ethylene oxides yields a single-surfactant microemulsion. Measurement of surfactant(s) transmittance in the oil and water phases demonstrates that microemulsification occurs when the surfactant interfacial film is equally soluble in the two phases. Surface pressure measurements reveal that oil penetration impedes the formation of O/W Microemulsion formation with n-tetradecane or n-hexadecane as the dispersed phase.

Introduction

An emulsion is the system that results from the mixing of two immiscible (or partially miscible) liquids, the “phases,” and one or more suitable surfactants (surface active agents) in the proper ratio, so that one phase becomes dispersed in the other—the “continuous” phase—in the form of globules. Usually, one of the phases is aqueous—the so-called “water” phase—and the other an “oil” in the wide sense, i.e., a hydrophobic substance such as an aliphatic or aromatic hydrocarbon (e.g., n-decane, toluene) or a vegetable oil (soybean oil, canola oil). The visual appearance of an emulsion results from the scattering of light by the droplets of the dispersed phase and is dependent on the droplet diameter. As droplet diameter decreases, emulsions range in appearance from a milky-white-opaque solution or “macroemulsion” (in which the droplets, with diameter larger than 0.3 μm , scatter the entire spectrum of incident visible light) through a gray translucent solution or “mini-emulsion” (with diameters between 0.1 μm and 0.3 μm , the droplets are too small to scatter the entire spectrum of incident visible light) and finally to a transparent solution or “microemulsion” (with droplet diameter less than approximately $\frac{1}{4}$ the wavelength of the incident visible light, i.e., less than 0.1 μm). Microemulsions are particularly interesting from the practical viewpoint, since emulsion applications are typically accompanied by stability problems, creaming and flocculation in particular. These problems are obviated if the particle size is sufficiently small.

Despite their structural similarities, microemulsions and macroemulsions (henceforth, “emulsions”) differ substantially in their physical and thermodynamic properties.

In the case of emulsions, the diameter of the droplets grows continuously with time, so that phase separation eventually occurs under gravitational forces; i.e., they are kinetically stable and their formation requires input of work. In the case of microemulsions, once the right conditions are satisfied, microemulsification occurs spontaneously; they are thermodynamically stable and isotropic. Along with “microemulsion”, such other terms as “swollen micellar solution”, “hydrophilic lipomicelles”, “micellar solution”, “middle phase”, “unstable microemulsion”, and “spontaneous transparent emulsion”—transparency is a consequence of the small diameter of the dispersed-phase droplets—have been used to describe these systems.

In principle, three structural types have been shown to exist in such systems.

- oil-in-water (O/W) microemulsions
- water-in-oil (W/O) microemulsions
- bicontinuous structures

All observed O/W and W/O microemulsion systems are characterized by a low relative volume of the inner or dispersed phase, whether this is aqueous or lipophilic. The investigation of the mechanism of microemulsion formation

presented above demonstrated that above a threshold volume Φ of the dispersed phase such a system enters a period of dynamic equilibrium, with droplets merging and re-forming—so-called percolation. An increase in dispersed-phase volume beyond that sufficient to cause percolation leads to destabilization, i.e., the breakdown of the microemulsion system or formation of a bicontinuous microemulsion (1-11).

The aim of the current study is to consider the formation and characteristics of a class of microemulsions containing such non-ionic surfactants as nonylphenoethylene oxide (NP(EO)_n): these are surfactants with a hydrophilic part consisting of a varying number of ethylene oxides and a hydrophobic part consisting of a nonylphenol, as shown in Figure 1. In particular, we develop a technique for producing single-surfactant microemulsions.

The present study, using the "titration method" of microemulsion preparation, includes measurements of transmittance, and surface pressure. The microemulsions studied were of the types W/O—both Water/O and Saline/O—and O/W—in particular, O/Saline. Table I summarizes the composition—hydrocarbon, surfactant, and cosurfactant—of the 18 microemulsions studied.

Nonylphenol Ethoxylates

Igepal	# of (EO)	HLB
210	1.5	4.6
430	4	8.8
520	5	10
530	6	10.8
610	7-8	12.2
630	9	13

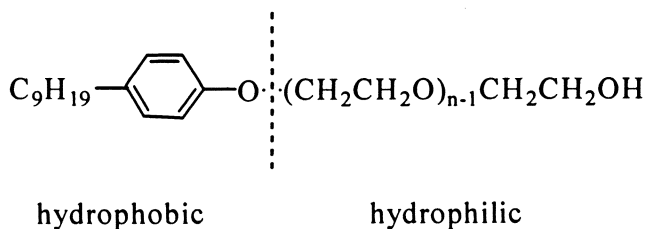


Figure 1. Structure and HLB of Nonylphenol ethylene oxide (NP(EO)_n) surfactants.

Titration Method of Microemulsion Preparation

Calculation of the Minimum Amount of Primary Surfactant Needed

Rosano (12-16) suggested a way to determine the minimum amount of primary surfactant molecules needed for a particular system. This method is based on geometric considerations; in particular, the assumptions that all the surfactant molecules end up at the interface, and that spherical droplets are formed. The total interfacial area A is given by Equation 1.

$$A = n\sigma = 4\pi r^2 \times a \quad [1]$$

where

n = number of surfactant molecules;

σ = area per surfactant molecule adsorbed at the interface ($\text{\AA}^2/\text{molecule}$);

r = radius of the dispersed phase droplet (\AA); and

a = total number of droplets formed by the dispersed phase.

The total volume of the dispersed phase is given by Equation 2.

$$V = \frac{4}{3} \pi r^3 \times a \quad [2]$$

Combining Equations 1 and 2, we have Equation 3, which relates the number of surfactant molecules needed to cover the interfacial area to the volume of the dispersed phase.

$$n = \frac{3V}{r\sigma} \quad [3]$$

The number of grams of surfactant is then given by Equation 4.

$$g = \frac{GMW}{6.02 \times 10^{23} \frac{\text{molecules}}{\text{mole}}} \times n \quad [4]$$

where

g = number of grams of surfactant; and

GMW = gram molecular weight of the surfactant.

Table I. W/O and O/W microemulsions prepared with nonylphenol ethylene oxide NP(EO)_n surfactants

<i>Exp.</i>	<i>Continuous Phase</i>	<i>Dispersed Phase</i>	<i>Primary Surfactant</i>	<i>Cosurfactant</i>	<i>Extrapolated n (EO)</i>
1	n-octane	Water (1mL)	NP-9-EO (1g)	NP-4-EO	5.7
2	n-octane	Water (1mL)	NP-9-EO (1g)	NP-1.5-EO	5.5
3	n-octane	Water (1mL)	NP-6-EO (1g)	NP-4-EO	5.9
4	n-octane	Water (1mL)	NP-6-EO (1g)	NP-1.5-EO	5.4
5	n-heptane	Saline (1mL)	NP-6-EO (1g)	NP-4-EO	5.2
6	n-octane	Saline (1mL)	NP-9-EO (1g)	NP-4-EO	5.3
7	n-decane	Saline (1mL)	NP-9-EO (1g)	NP-4-EO	5.2
8	n-decane	Saline (1mL)	NP-7.5-EO (1g)	NP-4-EO	5.4
9	n-decane	Saline (1mL)	NP-6-EO (1g)	NP-4-EO	5.3
10	n-decane	Saline (1mL)	NP-9-EO (1g)	NP-1.5-EO	5.1
11	n-decane	Saline (1mL)	NP-7.5-EO (1g)	NP-1.5-EO	5.2
12	n-decane	Saline (1mL)	NP-6-EO (1g)	NP-1.5-EO	5.2

13	n-dodecane	Saline (1mL)	NP-9-EO (1g)	NP-4-EO	5.1
14	n-tetradecane	Saline (1mL)	NP-6-EO (1g)	NP-4-EO	5.0
15	n-hexadecane	Saline (1mL)	NP-6-EO (1g)	NP-4-EO	4.9
16	Saline	n-octane (1mL)	NP-5-EO (1g)	NP-9-EO	6.0
17	Saline	n-decane (1mL)	NP-5-EO (1g)	NP-9-EO	6.0
18	Saline	n-dodecane(1mL)	NP-5-EO (1g)	NP-9-EO	6.0

The value of σ can be obtained either from the plot of surface tension vs. log concentration of the surfactant solution or from monolayer measurements. For microemulsions, the upper limit of r is $1/4$ the wavelength of visible light, while the lower limit is set by the surfactant chain length. This simple calculation provides an approximate value for the minimum amount of surfactant necessary to cover the interface. It takes into account neither the amount of surfactant that is dispersed in both the aqueous and oil phases nor any other aggregates that may form in solution.

Titration Method

The titration method of microemulsion formation begins by forming an initial emulsion using the estimated minimum amount of primary surfactant calculated as described in the previous section.

To determine if a transparent dispersion is possible, a cosurfactant is gradually added to the coarse emulsion. If the system does not turn clear after the amount of added cosurfactant is equal to the amount of the primary surfactant used, the system can be considered unenviable. In this case, one of the components must be replaced to form a microemulsion. Since the cosurfactant is usually the nonspecific component of the system, it is the first to be altered.

The next option available, once the range of possible cosurfactants is exhausted, is to consider a new primary surfactant. A fresh calculation is made to determine the minimum amount of the new surfactant, and repeat titrations are carried out with the various cosurfactants until a successful result is obtained.

As a last resource, if none of the primary surfactant/cosurfactant pairs can be made to work, the dispersed phase in an O/W system can be altered and the entire procedure repeated. In the case of a W/O system, no change in the dispersed phase is possible. In the case of a hydrocarbon dispersed phase, for example, the chain length can be systematically increased or decreased, depending on the requirement of the formulation.

When microemulsions are prepared by the titration method various changes are often noted. Sometimes there are dramatic viscosity increases just before the mixture becomes transparent. Also, mixtures may progress from lactescent to clear, rapidly or slowly, as drops of cosurfactant are added.

Aronson's experimental results (17) show that, above a certain concentration of surfactant molecules, we observe a phenomenon of creamage—due to reversible flocculation by free surfactant—rather than a smooth transition to smaller particle sizes.

Giustini et al. (1) published a paper entitled "Does the Schulman's Titration of Microemulsion Really Provide Meaningful Parameters?" in which they demonstrated, based on results from pulsed gradient spin-echo NMR, that

Schulman's titration method quantitatively describes the cosurfactant partition in a microemulsion system. They concluded that analysis of the data obtained from the classic Schulman titration effectively describes the microemulsion behavior along a path where the self-assembled aggregates are separated by increasing inter-aggregate distances with the composition of both the aggregates and the continuous phase remaining unchanged.

Applying the Titration Method

Each of the 18 systems shown in Table I started with an identical dispersed-phase volume of 1 mL. Using the minimum primary surfactant calculation, an estimated value of g (minimum number of grams of primary surfactant) was calculated for each case; these values were all close to 1. To facilitate comparisons among the various systems, the amount of primary surfactant was set at 1 g throughout.

All microemulsions were prepared using the titration method (also known as "point method"). The W/O and Saline/O systems used a nonylphenoethylene oxide NP(EO)_n surfactant (HLB greater than 9; see Table I) dispersed in the aqueous phase and a hydrocarbon as the continuous phase, in a 30°C water-jacket beaker. (Since viscosity levels are always quite low with these systems, simple mixing equipment is sufficient.) The emulsions were then titrated to clarity (% transmittance > 95 % at 520 nm), using another NP(EO)_n with an HLB less than 9 as cosurfactant. Continuous stirring was maintained throughout the titration process to ensure homogeneous mixing. (Most of these cosurfactants are liquids and can easily be titrated into the emulsion with gentle mixing.)

One example of the Saline/O microemulsions prepared in this way used 1 mL of saline (1% NaCl), 1 g of NP-6-EO (Igepal CO-530), and 20 mL of n-decane. The emulsion was titrated to clarity with, as cosurfactant, either NP-4-EO (Igepal CO-430) or NP-1.5-EO (Igepal CO-210). In the case of O/Saline systems, the phases are reversed; the surfactant chosen had HLB less than 9, and titration was with NP-9-EO (Table I, Experiments 16-18).

Determination of the Surfactant Molar Composition at the O/W Interface

Mixing a constant weight of surfactant with a constant volume of the dispersed phase and an initial volume of the continuous phase produces an optically opaque emulsion. Titrating this emulsion to clarity with cosurfactant produces a microemulsion. The minimum volume of cosurfactant needed to titrate the system to clarity versus the volume of the continuous phase was recorded. Additional continuous phase is then added to the system, causing the

system to become optically opaque again. Once more, additional cosurfactant is added to bring the system to clarity; the minimum volume of cosurfactant needed is recorded. This procedure—adding more continuous phase and titrating with additional cosurfactant—is repeated so as to generate numerous data points. Plotting these data points, and applying a linear regression formula, yields a straight line and allows its slope and intercept to be determined. Figure 2 demonstrates the volume of the cosurfactant plotted against the volume of the continuous phase. Finding the cosurfactant volume at the interface, which is given by the extrapolated intercept (and which corresponds to an idealized zero-volume continuous phase), it is possible to determine the composition of the interface—the surfactant/cosurfactant ratio—assuming that both surfactants are adsorbed at the interface. Also, for a given volume of the continuous phase, the difference between the total amount of cosurfactant and the amount of cosurfactant at the interface represents the amount of cosurfactant at equilibrium in the continuous phase. Knowing the relative amounts of surfactant and cosurfactant enables us to calculate the average number of ethylene oxide (EO) per nonylphenol adsorbed at the O/W interface.

The following algorithm allows us to use Figure 2's interpolated y-intercept (cosurfactant volume at zero volume of continuous phase) to determine the number of ethylene oxides per molecule at the interface. The molar ratio ρ_i of the cosurfactant at the interface can be determined from Equation [5]:

$$\rho_i = \frac{b \times d_{\text{cosurf}}}{M_{\text{cosurf}}} \times \frac{M_{\text{surf}}}{V_{\text{surf}} \times d_{\text{surf}}} \quad [5]$$

where b is the amount in mL of cosurfactant at the interface; V_{surf} is the total amount in mL of primary surfactant; d_{cosurf} and d_{surf} are the densities of the cosurfactant and the primary surfactant, respectively; and M_{cosurf} and M_{surf} are the molar masses of the cosurfactant and the primary surfactant, respectively. From this molar ratio ρ_i , the average number of ethylene oxides per molecule at the interface ($n(\text{EO})$) can be calculated using Equation [6]:

$$n(\text{EO}) = \frac{\rho_i \text{EO}_{\text{cosurf}} + \text{EO}_{\text{surf}}}{1 + \rho_i} \quad [6]$$

where $\text{EO}_{\text{cosurf}}$ and EO_{surf} are the average number of EO for the cosurfactant and the primary surfactant, respectively.

Each microemulsion studied was titrated to clarity (transmission greater than 95% at 520 nm) at 30°C, with constant surfactant concentration and constant volume of the dispersed phase, for various volumes of continuous phase.

Table I, listing the 18 microemulsion formulations studied, also shows the extrapolated EO value for each one. Experiments 1-4, all water-in-n-octane W/O microemulsions, yielded an average extrapolated EO value of 5.6. Experiments 5-15, microemulsions of saline in various hydrocarbons, showed average extrapolated EO values of 5.1. Experiments 16, 17, and 18 are, respectively, n-octane-, n-decane, and n-dodecane-in-saline, with an average extrapolated EO value of 6.

The greater value calculated for EO at the interface in O/Saline microemulsions (Experiments 16-18) as compared to Saline/O microemulsions (Experiments 5-15) is due to the bending of the interface (steric hindrance). In contrast, the lower average EO value for Saline/O microemulsions (Experiments 5-15) as compared with W/O microemulsions (Experiments 1-4) is due to the presence of NaCl, which competes for the water of hydration. Moreover, for W/O microemulsions in general, as the chain length of the hydrocarbon increases, more cosurfactant is needed to clear the system. Note that Table I does not include O/Saline microemulsion formulations for n-tetradecane or n-hexadecane; our attempts to form such microemulsions were unsuccessful, owing to the excess length of the hydrocarbon chain compared to the 12 carbon chain of the nonylphenol.

Using an NP-5.6-EO surfactant blend—i.e., a mixture of surfactants with an average EO number of 5.6—yields single surfactant water-in-oil microemulsions for systems corresponding to Experiments 1-4 (same dispersed and continuous phases, no cosurfactant required). Similarly, preparing a single-surfactant oil-in-water microemulsion was possible for systems corresponding to Experiments 16-18 if an NP-6-EO surfactant is used.

The greater value calculated for EO at the interface in O/Saline microemulsions (Experiments 16-18) as compared to Saline/O microemulsions (Experiments 5-15) is due to the bending of the interface (steric hindrance). In contrast, the lower average EO value for Saline/O microemulsions (Experiments 5-15) as compared with W/O microemulsions (Experiments 1-4) is due to the presence of NaCl, which competes for the water of hydration. Moreover, for W/O microemulsions in general, as the chain length of the hydrocarbon increases, more cosurfactant is needed to clear the system. Note that Table I does not include O/Saline microemulsion formulations for n-tetradecane or n-hexadecane; attempts to form such microemulsions were unsuccessful, owing to the excess length of the hydrocarbon chain compared to the 12 carbon chain of the nonylphenol. A long hydrocarbon chain (n-tetradecane or n-hexadecane) penetrates to the surfactant monolayer, with the resultant formation of a structure that is difficult to bend; this in turn impedes the formation of the microemulsion. These results indicate that the structure of the interface plays a significant role in the formation of these systems.

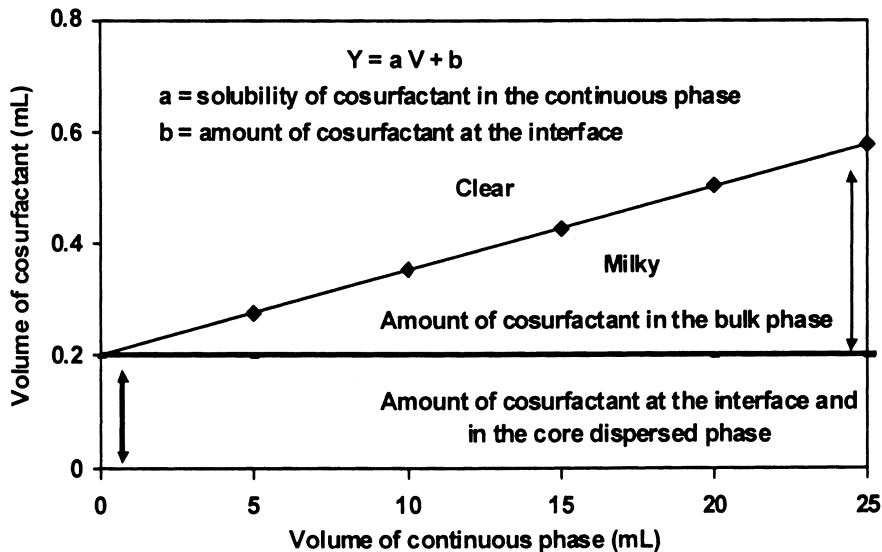


Figure 2. Typical graph of microemulsion titration

Role of the Surfactant Solubility at the O/W Interface

As depicted in Figure 3, the percent transmittance, whether in water or in oil, is somewhat related to the solubility of the NP(EO)_n. For EO ranging between 5 and 6 a domain of equal solubility exists, in both the oil phase and the aqueous phase. These results lead us to suggest that when the surfactant interfacial film around the droplets is equally soluble in the two phases, microemulsions will form. Since a surfactant capable of forming W/O or O/W microemulsions will have borderline solubility in each phase, it will stay at the interface. This analysis differs fundamentally from the conclusion reached by Rosano in 1973 [18]; at that time he identified low surface tension as fundamental to spontaneous emulsification, with the surfactant serving merely to stabilize the system against coalescence. With the NP(EO)_n systems considered in the current investigation, the corresponding EO values range from 5.1 for Saline/O, through 5.6 for W/O, to 6.0 EO for O/Saline systems—which is precisely the zone of equal solubility of NP(EO)_n in both water and oil phases. In short: when the interfacial film is equally soluble in both phases, the system spontaneously forms a microemulsion.

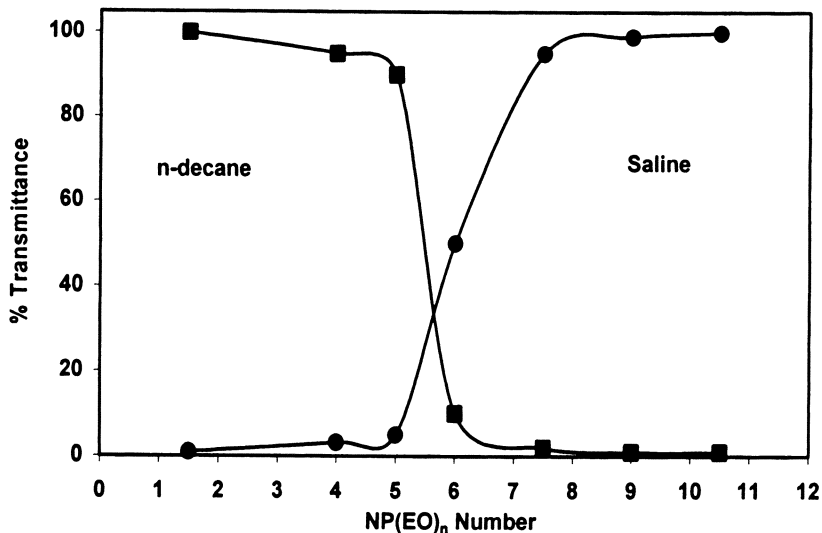


Figure 3. Solubility of NP(EO)_n surfactant in n-decane and saline solution

Effect of Oil Penetration on Microemulsion Formation

Analysis of Figures 4, showing surface pressure and potential for NP(EO)₅ surfactants, shows that the NP(EO)₅ is an expanded film, and that the area per molecule of NP(EO)₅ surfactant at the oil/water interface is higher than the area per molecule at the air/water interface as a result of the oil penetration to the surfactant monolayer. This hydrocarbon chain length penetration to the surfactant monolayer is responsible for the high extrapolated value of ethylene oxide (EO) at the interface for the O/W microemulsions listed in Table I (Experiments 16, 17, and 18), which is due to the bending of the interface in the case of O/W microemulsions in general. Moreover, oil penetration to the surfactant monolayer in the case of n-tetradecane and n-hexadecane as the dispersed phase prevents the formation of such O/W microemulsions. These results indicate that the structure of the interface plays a significant role in the formation of these systems. The effect of oil penetration (also referred to as oil uptake in surfactant tail) on microemulsion formation has also been demonstrated by Chen et al. (19-20), who found that n-hexadecane does not form microemulsion with didodecyldimethyl ammonium bromide (DDAB) as a surfactant; they concluded that curvature of the surfactant film is a major determinant of microemulsion structure.

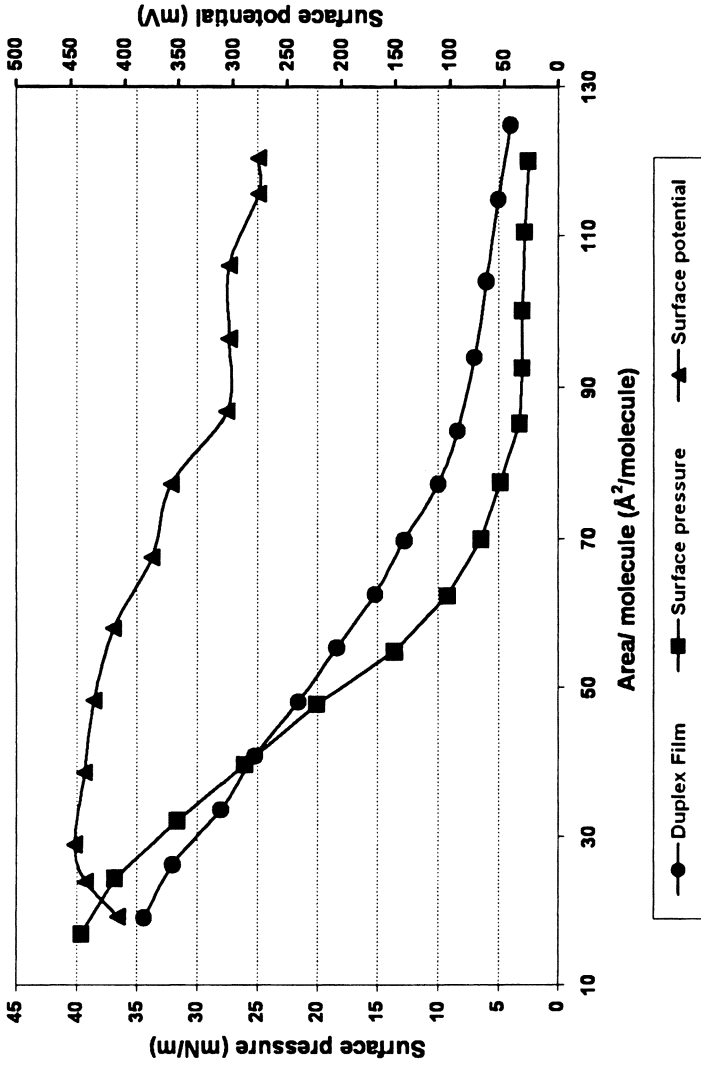


Figure 4. Surface pressure of NP-5-EO surfactant at the water/oil and water/air interfaces

Conclusions

Taken together, these results suggest that several conditions must be met simultaneously for the formation and stability of a microemulsion based on the non-ionic surfactants under consideration. First, the amount of surfactant(s) used must be sufficient to cover the total interfacial area of the droplets, and the volume of dispersed phase adequate to accommodate the hydrophilic groups of the surfactant. Second, the chain length of the oil must be compatible with the hydrophobic part of the surfactants to facilitate the formation of O/W microemulsions. Finally, the interfacial mixed film of non-ionic surfactant(s) must be of equal solubility in both the oil and the aqueous phase. We showed that determination of surfactant/cosurfactant molar compositions at the interface using the titration method—elaborated on the basis of Schulman's pioneering titration—permits the formulation of single surfactant microemulsions.

References

1. Giustini, M.; Murgia, S.; Palazzo, G. *Langmuir*. **2004**, *20*, 7381.
2. Kahlweit, M.; Lessner, E.; Haase, D. *J. Phys. Chem.* **1985**, *89*, 163.
3. Moulik, S. P.; Paul, B. K. *Adv. Colloid Interface Sci.* **1998**, *78*, 99.
4. Ruckenstein, E.; Chi, C. J. *J. Chem. Soc., Faraday Trans.* **1975**, *71*, 1960.
5. De Gennes, P. G.; Taupin, C. *J. Phys. Chem.* **1982**, *86*, 2294.
6. Safran, S. A. In *Micellar Solutions and Microemulsions: Structure, Dynamics and Statistical Thermodynamics*. Chen, S. H.; Rajagopalan, R., eds. New York: Springer-Verlag, 1990; p. 165.
7. Stoeckenius, W.; Schulman, J. H.; Prince, L. M. *Kolloid-Z.* **1960**, *169*, 170.
8. Shinoda, K.; Kunieda, H. *J. Colloid Interface Sci.* **1973**, *42*, 381.
9. Hoar, T. P.; Schulman, J. H. *Nature (London)*. **1943**, *152*, 102.
10. Adamson, A.W. *J. Colloid Interface Sci.* **1960**, *29*, 261.
11. Naouli, N. Ph.D. thesis, The City University of New York, New York, NY, 2005.
12. Rosano, H. L.; Lan, T.; Weiss, A.; Whittam, J. H.; Gerbacia, W. E. F. *J. Phys. Chem.* **1981**, *85*, 468.
13. Rosano, L. H.; Lan, T.; Weiss, A.; Gerbacia, W. E. F.; Whittam, J. H. *J. Colloid Interface Sci.* **1979**, *72*, 233.
14. Rosano, H. L.; Nixon, A. L.; Cavallo, J. L. *J. Phys. Chem.* **1989**, *93*, 4536.
15. Rosano, H. L. *J. Soc. Cosmetic Chem.* **1974**, *25*, 609.
16. Kanouni, M.; Rosano, H. L.; Naouli, N. *Adv. Colloid Interface Sci.* **2002**, *99*, 229.

17. Aronson, P. M. *Colloids and surfaces*. **1991**, 58, 195.
18. Gerbacia, W. E. F.; Rosano, H. L. *J. Colloid Interface Sci.* **1973**, 44, 242.
19. Chen, S. J.; Evans, D. F.; Ninham, B.W.; Mitchell, D. J.; Blum, F. D.; Pickup, S. *J. Phys. Chem.* **1986**, 90, 842.
20. Chen, S. J.; Evans, D. F.; Ninham, B. W. *J. Phys. Chem.* **1984**, 88, 1621.

Chapter 8

Nanoencapsulation Systems Based on Milk Proteins and Phospholipids

Harjinder Singh¹, Aiqain Ye^{1,2}, and Abby Thompson¹

¹Riddet Centre, Massey University, Private Bag 11 222, Palmerston North, New Zealand

²Current address: Fonterra Co-operative Limited, Palmerston North, New Zealand

Milk contains several components that can be utilized to make nanoparticles for encapsulation and delivery of bioactive compounds. Caseins in milk are essentially natural nanoparticles, designed to deliver essential nutrients, in particular calcium. Similarly, whey proteins, particularly β -lactoglobulin, have been designed by nature to bind and transport hydrophobic molecules. The ability of milk proteins to interact strongly with charged polysaccharides opens up further possibilities for making novel hybrid nanoparticles. Phospholipid-rich fractions, extracted from fat globule membranes, can be used to form liposomes. Due to their high sphingomyelin content, these liposomes have some unique stability and entrapment characteristics.

Since the end of the 20th century, there has been a growing realization of the pivotal link between diet and human health. Consequently, the food industry has created a new category of foods, the so-called functional foods. To fully realize this opportunity the food industry must address several critical challenges, including discovering the potential bioactivity of beneficial compounds, establishing optimal intake levels, and developing adequate food delivering matrix and product formulations.

Traditionally, microencapsulation can be used for many applications in the food industry including stabilizing the core material, controlling the oxidative reaction, providing sustained or controlled release, masking flavors, colors or odors, to extend shelf life or protect components against nutritional loss. In recent years, there is considerable interest in developing high performance delivery vehicles for encapsulation and protection of biologically active substances of food origin. Nanosciences, which investigates how to build matter on nanometer scale, usually between 1 and 100 nm, by manipulating individual molecules or atoms, has the potential to provide new solutions in many of these fronts. Certainly nanoparticles may seem attractive as delivery vehicles. By carefully choosing the molecular components, it seems possible to design particles with different surface properties. These nanoparticles are able to encapsulate and deliver the active compounds directly to appropriate sites, maintain their concentration at suitable levels for long periods of time, and prevent their premature degradation. Research efforts are already being made to develop food-based delivery vehicles, such as protein-polysaccharide coacervates, multiple emulsions, liposomes and cochleates.

Milk contains several components that can be utilized to make nanoparticles for encapsulation and delivery of bioactive compounds. Caseins in milk are essentially natural nanoparticles, designed to deliver essential nutrients, in particular calcium. Similarly, whey proteins, particularly β -lactoglobulin, have been designed by nature to bind and transport hydrophobic molecules. Milk proteins interact strongly with charged polysaccharides, creating possibilities for novel hybrid nanoparticles. Phospholipid-rich fractions, extracted from fat globule membranes, can be used to form liposomes. These liposomes have some unique stability and entrapment characteristics for both hydrophobic and hydrophilic molecules.

This paper provides an overview of potential nanoparticle-based delivery systems, based on milk proteins and phospholipids. A particular focus is placed on recent work in the area of protein-polysaccharide nanoparticles and liposomes carried out in our laboratory at Massey University in New Zealand.

Milk Proteins as Potential Nano-encapsulation Systems

Normal bovine milk contains about 3.5% protein which can be separated into caseins and whey proteins (1). Caseins can be fractionated into four distinct

proteins, α_{s1} -, α_{s2} -, β - and κ - caseins; these represent approximately 38%, 10%, 36% and 12% of whole caseins, respectively. The structures and properties of caseins have been extensively studied (2). In comparison with typical globular proteins, the structures of caseins are quite unique. The most unusual feature is the amphiphilicity of their primary structure. The hydrophobic residues and many of the charged residues, particularly the phosphoserine residues, in the caseins are not uniformly distributed along the polypeptide chain. Therefore, all four caseins have a distinctly amphipathic character with separate hydrophobic and hydrophilic domains, with relatively open and unordered secondary structures. As an example, the distribution of charged residues and hydrophobicity as a function of sequence position of β -casein is shown in Figure 1. β -Casein has two large hydrophobic regions (55-90 and 130-209). The N-terminal 21-residue sequence has a net charge of -12, while the rest of the molecule has no net charge.

Because the casein monomers cannot sufficiently remove their hydrophobic surfaces from contact with water, the caseins tend to associate with themselves and with each other. In addition, all caseins are able to bind calcium with the extent of binding being proportional to the number of phosphoserine residues in the molecule. α_{s1} - and α_{s2} -caseins are most sensitive to calcium followed by β -casein while κ -casein is insensitive to calcium. κ -Casein is capable of stabilising other caseins against calcium-induced precipitation and allows the formation of colloidal size aggregates.

The unique physio-chemical properties of caseins have been traditionally exploited to modify and enhance textural and sensory characteristics of foods (3). Casein and caseinates can bind water, stabilise foams, emulsify fat and control viscosity in formulated foods, in addition to providing high nutritional value. Caseins also possess many of the properties required of a good wall material for encapsulation (4). The ability of caseins to self-assemble into particles of varying sizes with different stability characteristics offers opportunities for nanoencapsulation for the delivery of bioactive compounds. A recent study (5) showed that hydrophobic compounds, such as vitamin D2, can be incorporated into casein particles, formed by the re-assembly of caseins. These reassembled casein particles can provide partial protection against UV-light-induced degradation of vitamin D2 entrapped in them. Further understanding of "surfactant-like" self-assembly properties of caseins would allow us to create novel nanometer-scale structures suitable for delivery of bioactive compounds.

The principal fractions of whey proteins are β -lactoglobulin, bovine serum albumin, α -lactalbumin and immunoglobulins (1). In contrast to caseins, the whey proteins possess high levels of secondary, tertiary and, in most cases, quaternary structures. β -Lg is built up of two β -sheets, formed from nine strands converging at one end to form a hydrophobic calyx or pocket, and a flanking three-turn α -helix (6). This pocket serves as a binding locus for apolar

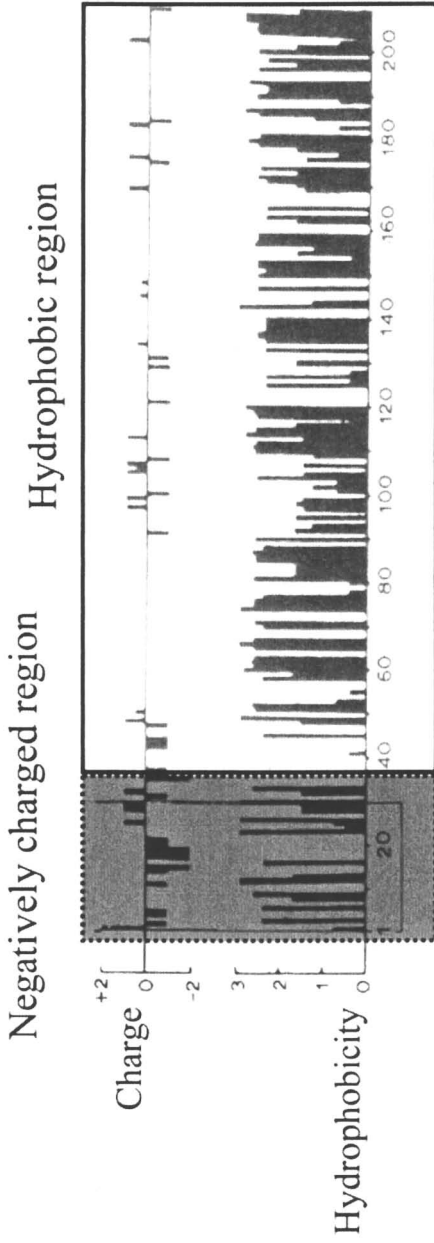


Figure 1. Distribution of charged residues and hydrophobicity as a function of sequence position of β -casein.

molecules such as retinol (7) and long-chain fatty acids (8). Similarly, bovine serum albumin binds a large variety of compounds, including retinol and long-chain fatty acids (9). The concept of using ligand-selective whey proteins for delivery and protection of active agents is relatively new, and such systems need further development.

The ability of whey proteins to aggregate and form gels during heat treatment is of considerable importance (1,3). By controlling the assembly of protein molecules during the aggregation process, hydrogels, micro- and nanoparticles suitable for the delivery of bioactive compounds can be produced. For example, a monodisperse dispersion of 40 nm whey protein nanospheres was obtained by Chen et al. (10) by heating whey proteins at relatively low protein concentration and ionic strength and a temperature around 55°C. The potential of these nanospheres as carriers of nutraceutical agents was studied *in vitro*; it appears that protein nanoparticles could be internalized by cells and degraded therein to release nutraceutical compounds.

Partial hydrolysis of whey protein, α -lactalbumin, by a protease from *Bacillus licheniformis* has been shown to produce peptides that self-assemble into nanometer-sized tubular structures under certain conditions (11). These micrometer long hollow tubes, with a diameter of only 20 nm, have potential applications in the delivery of nutraceuticals.

Milk Proteins-Polysaccharide Composite Systems

Protein structure can be modified through processing treatments or change of solution conditions to allow formation of complexes with polysaccharides. A wide variety of nutrients can be incorporated into these complexes by relatively non-specific means. Specific binding of a nutrient to amino acid side chains can also be achieved in some cases.

At pH values below their isoelectric points (pI), proteins carry positive charges and can interact with polysaccharides bearing carboxylic, phosphate, or sulfate groups. This inter-biopolymer complexation of positively charged proteins and anionic polysaccharides can lead to the formation of soluble and insoluble complexes (12). Interbiopolymer complexes can be regarded as a new type of food biopolymer whose functional properties differ strongly from those of the macromolecular reactants. The complex coacervation of globular proteins and polyelectrolytes, e.g., gelatin, β -lactoglobulin, bovine serum albumin, egg albumin, and soy protein, has been extensively studied (13-14).

Recently, we have observed the formation of soluble and stable complexes on the mixing of gum arabic and sodium caseinate at a wide pH range (pH 4 to 5.4); the complexes resulted in stable dispersions with particle size between 100 to 200 nm (15).

Mixtures containing 0.1% sodium caseinate and 0.5% gum arabic were acidified by dropwise addition of HCl from pH 7.0 to pH 2.0 and samples were stored for 24 h at 20°C. The absorbance profiles of mixtures are shown in Figure 2. The absorbance values of 0.1% sodium caseinate solution abruptly increased at pH 5.4 and reached a maximum at pH 5.0 (Figure 2). Further decrease in pH caused a decrease in absorbance due to large-scale aggregation and subsequent precipitation of the caseins around their pI. In contrast, the absorbance of sodium caseinate/gum arabic mixtures increased slightly at pH 5.4 (pH_c) but remained almost constant between pH 5.4 and pH 3.0. No phase separation occurred in this pH range (see photographs of 0.1% sodium caseinate/0.5% gum arabic mixtures at different pH values in Figure 2). On decreasing the pH below pH 3.0, the absorbance values increased and phase separation took place subsequently. At pH 2.0, the absorbance values of the sodium caseinate/gum arabic mixture decreased.

Particle sizes of these stable dispersions in the pH range from 5.4 to pH 3.0, measured using dynamic light scattering, showed that the average diameter of the particles in the sodium caseinate/gum arabic mixtures remained stable at approximately 110 nm as the pH was decreased from pH 5.4 to pH 3.0 and increased to very large values ($> 10 \mu\text{m}$) when the pH was reduced further. Electron microscopy confirmed the presence of these composite nanoparticles between pH 5.4 to pH 3.0 (15).

The mechanism of the formation of these nanoparticles based around the self-aggregation of casein and the electrostatic interaction between the aggregated particles of casein and gum arabic molecules has been proposed (15, Figure 2). As the pH of the mixture decreases below pH 5.4, the caseinate molecules tend to undergo small-scale aggregation prior to large-scale aggregation and precipitation at pH values closer to their pI (pH 4.6). In this case, the gum arabic molecules may attach to the outside of these small-scale aggregates in the early stages of aggregation through electrostatic interactions between negatively charged gum arabic and exposed positive patches on the surface of the caseinate aggregates. The presence of hydrophilic gum arabic molecules on the outside of the caseinate aggregate may be enough to sterically stabilise these nano-particles and consequently prevent self-aggregation. As the charge on the nano-particles is quite low, for example, $\sim 15\text{mV}$ at pH 4.0, steric stabilisation is probably important.

Effect of NaCl and CaCl₂ on the properties of nanoparticles

Different amounts of NaCl or CaCl₂ were added to the stable nanoparticle dispersion of caseinate/gum arabic at pH 4.6. The changes in the absorbance and average particle size of mixtures, which were measured after storage for 24 h, are shown in Figure 3. The absorbance value of the dispersions increased with

increasing NaCl concentration upon to 45 mM but decreased abruptly at higher NaCl concentrations (Figure 3A). The average particle size of particles increased from ~105 nm to ~450 nm at 40 mM added NaCl. It also was noted that the dispersions containing 0 to 40 mM added NaCl were stable (no phase separation) after 7 days, whereas precipitation occurred at added NaCl > 40 mM (Figure 3A). The analysis of these precipitated samples showed that there was no protein and nearly 100% of gum arabic remained at the top clear layer (data not shown). This indicated that the precipitation was due to self-association of caseinate molecules, and the association of gum arabic with the casein aggregates was prevented by the added NaCl. This is consistent with our previous work (15) that showed that the complexes can not be formed between the sodium caseinate and gum arabic in the presence of NaCl > 50 mM.

At added NaCl < 50 mM, the size of stable complex particles increased with increasing the concentration of NaCl. This could be due to the dissociation of some of the gum arabic molecules from the casein aggregate surface. The amount of gum Arabic remaining is probably sufficient to prevent large scale aggregation and precipitation of casein.

The caseinate-gum arabic mixture began to precipitate when the concentration of added CaCl₂ were higher than 3 mM (Figure 3B). At CaCl₂ added < 3mM, the absorbance the nanoparticle dispersions increased with increasing the concentration of added CaCl₂. The average particle size increased from ~105 nm to ~220 nm at 3 mM added CaCl₂. The behaviour of dispersions after addition of CaCl₂ was similar to that after addition of NaCl. This indicated that the effect of added CaCl₂ was because of change in the ionic strength of system. In addition, It was ion bridging that could take place between the divalent calcium ion and the negatively charged casein molecules in the complexes. This may result in an increase in the size of complex particles and precipitation above certain CaCl₂ concentration.

Milk Phospholipids as Potential Nanoencapsulation Systems

Milk contains 0.13-0.34 mg mg⁻¹ protein phospholipids of which about 60% are associated with milk fat globule membrane (MFGM) (16). The most abundant phospholipids are phosphatidylcholine (PC), phosphatidylethanolamine (PE) and sphingomyelin, while phosphatidylserine (PS) and phosphatidylinositol (PI) are present in low amounts (16-17). The MFGM phospholipids contain high levels of long chain fatty acids, such as palmitic (16:0), stearate (18:0), tricosanoate (23:0) while the short- and medium-chain fatty acids are present in very low levels. The composition of the MFGM phospholipid is very different from the commonly used soy- or egg-derived phospholipids (16). These differences would be expected to influence the self-assembly characteristics of phospholipids produced from the MFGM. It should

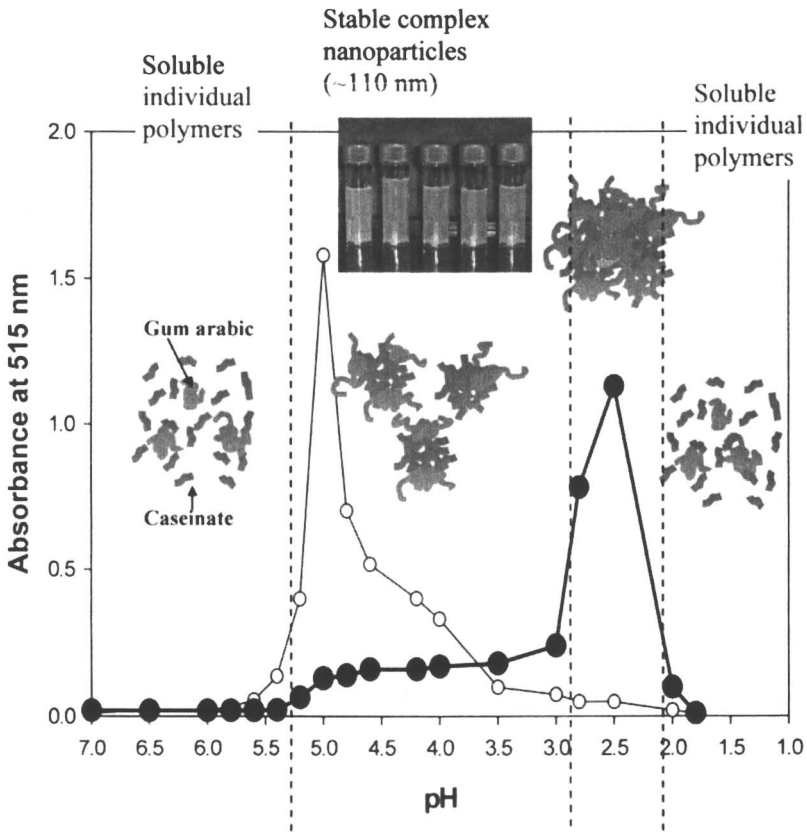


Figure 2. Absorbance as a function of pH of 0.1% sodium caseinate solution (○) and mixtures (●) of 0.1% sodium caseinate and 0.5% gum arabic at 20 °C. The mixtures were acidified using HCl and then stored at 4 °C for 24 h. The proposed model of Ye et al (15) for the formation of nanoparticles is also depicted. Pictures of 0.1% sodium caseinate and 0.5% gum arabic mixtures at different pH values are also shown.

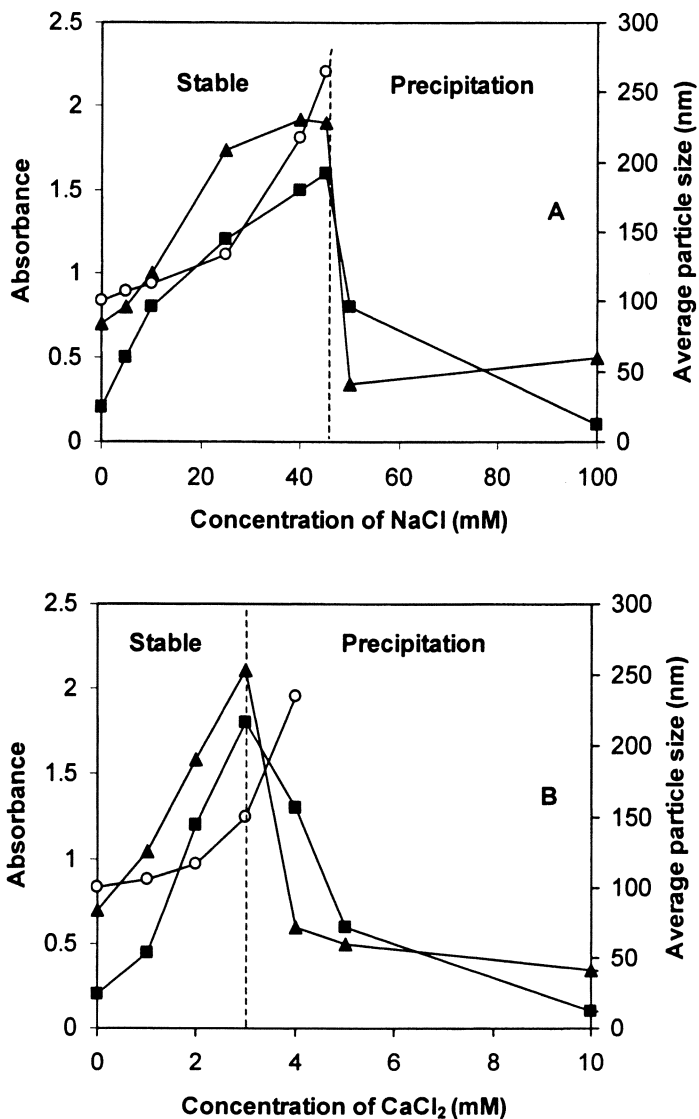


Figure 3. Absorbance at 515 nm of 0.1% sodium caseinate and 0.5% gum arabic mixtures (■) or absorbance at 810nm of 0.5% sodium caseinate and 0.5% gum arabic mixture (▲) at pH 4.6 as a function of concentration of added NaCl (A) or added CaCl₂ (B). The average size (○) of 0.1% sodium caseinate and 0.5% gum arabic mixtures at pH 4.6 at different concentrations of added NaCl is also shown. The samples precipitated when the concentrations of added NaCl or CaCl₂ were over the dashed line.

be possible to exploit the unique composition of the MFGM phospholipid fraction in the delivery of bioactive compounds.

Formation of Liposomes from MFGM-phospholipids

Liposomes are spherical structures, with diameters ranging from 20 nm to several microns, formed through the self-assembly of amphiphilic molecules, usually phospholipids. They consist of one or more phospholipid bilayers enclosing an aqueous core. During the formation process, hydrophobic molecules can be incorporated in the lipid bilayers and hydrophilic molecules become entrapped in the aqueous core. The three most common types of liposomes, namely small unilamellar vesicles, large unilamellar vesicles and multi-lamellar vesicles, have different properties in terms of stability, entrapment and release of encapsulated materials. Release of the entrapped material can be either a gradual process resulting from diffusion through the membranes, or almost instantaneous following membrane disruption caused by changes in pH or temperatures.

Liposomes are used by the pharmaceutical and cosmetic industries for the entrapment and controlled release of drugs or nutraceuticals, as model membranes or cells, and even for specialist techniques such as gene delivery. There are many potential applications for liposomes in the food industry, ranging from protecting sensitive ingredients, to increasing the efficacy of food additives and to confining undesirable flavours. However, the high cost of the purified soy and egg phospholipids, combined with problems finding a large-scale, continuous production method suitable for use in the food industry, has limited the use of liposomes in foods. Many of the standard methods for liposome formation are slow and difficult to scale up and many of these use detergents and organic solvents, which are undesirable in food products. The relatively recent development of techniques using high-pressure homogenizers, e.g. microfluidization offers a possible solution to many of the processing problems, and large volumes of liposomes can be produced in a continuous and a reproducible manner without the use of detergents and solvents.

We have recently shown that liposomes can be produced from milk-derived phospholipids, using a microfluidization technique (18-20). Typical electron micrograph of a liposome dispersion prepared using MFGM by this technique is shown in Figure 4. The liposomes could be seen as roughly spherical particles and the outer layer surrounding the internal aqueous space could be observed in many of the liposomes. There appeared to be a large number of very small particles (≤ 40 nm) interspersed with much larger particles (100–200 nm). Some of the liposome dispersions appeared to have irregular membranous structures trapped inside the outer bilayer and non-spherical shapes.

The liposomes prepared from the milk phospholipid material have been shown to have a significantly higher phase transition temperature, thicker membrane and lower membrane permeability than liposomes prepared from a non-hydrogenated soy phospholipid fraction (19).

Experiments comparing the stability of the liposome dispersions found that the milk phospholipid liposome dispersions showed significantly better stability during storage at temperatures in the range 4-35 °C. The milk phospholipid dispersions were also more stable during a wide range of heat treatments and ionic environments. We are currently determining the potential for use of such liposomes for the delivery of bioactive material in food systems in terms of encapsulation and release of hydrophobic and hydrophilic materials within the liposomes.

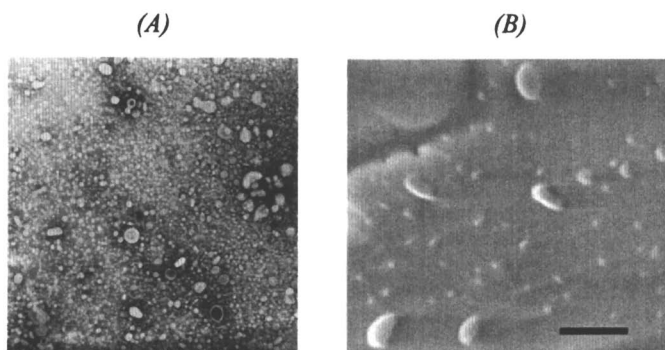


Figure 4. Negative staining TEM (A) or Scanning electron micrographs (B) of liposomes produced via microfluidization from the milk phospholipids.
Bar = 1.0 μm .

References

1. Fox, P.F. 2003. In *Advanced Dairy Chemistry-Vol. 1; Proteins*; P.F. Fox and P.L.H. McSweeney Eds; Kluwer Academic/Plenum Publishers, London, 2003, pp 1-48.
2. Swaisgood, H.E. In *Advanced Dairy Chemistry-Vol. 1; Proteins*; P.F. Fox and P.L.H. McSweeney Eds. Kluwer Academic/Plenum Publishers, London, 2003, pp 139-187.
3. Singh, H.; Flanagan, J. *Handbook of Food Science and Technology*; Y.H. Hui, Ed; Taylor and Francis, New York, 2006, pp 26-1-26-23.
4. Hogan, S.A.; McNamee, B.F., O'Riordan, E.D.; O'Sullivan, M. *J. Agric. Food Chem.*, 2001, 49, 1934-1938.

5. Semo, E.; Kesselman, E., Danino, D.; Liveny, Y.D. *Food Hydrocolloids*, **2007**, 936-942.
6. Sawyer L.; Papiz M.Z.; North A.C.T.; Eliopoulos E.E. *Biochem. Soc. Trans*, **1985**, 13, 265-266.
7. Fugate, R.D.; Song, P.S. *Biochim. Biophys. Acta*, **1980**, 625, 28-42.
8. Ragona, L.; Fogolari, F.; Zetta, L.; Perez, D.M.; Puyol, P. de Kruif, K.; Lohr, F.; Ruterjans, H.; Molinari, H. *Prot. Sc.* **2000**, 9, 1347-1356.
9. Pérez, M.D.; Díaz de Villegas, M.C.; Sánchez, L.; Aranda, P.; Ena, J.M.; Calvo, M.. *J. Biochem.* **1989**, 106, 1094-1097.
10. Chen, L; Remondetto, G.E. ; Subirade, M. *Trends Food Sci. Technol.* **2006**, 17, 272-283.
11. Graveland-Bikker, J.F.; de Kruif, C.G. *Trends Food Sci. Technol.* **2006**, 17, 196-203.
12. Doublier, J. L., Garnier, C., Renard D, Snachez, C. *Curr. Opin. Colloid Interf. Sci.*, **2000**, 5(3-4), 202-214.
13. Schmitt C; Sanchez C; Desobry-Banon S; Hardy, J, *Crit. Rev.Food Sci. Nutr.* **1998**, 38 (8), 689-753.
14. Weinbreck, F.; de Vries, R.; Schrooyen, P.; de Kruif, C. G. *Biomacromolecules*, **2003**, 4(2), 293-303.
15. Ye, A.; Flanagan, J.; Singh, H. *Biopolymers*, **2006**, 82, 121-133,
16. Singh, H.; Bennett, R.J.. In *Dairy Microbiology Handbook*. Robinson, R.K.(ed) Willey-Interscience, New York, **2002**, pp. 1-35.
17. Walstra, P., Geurts, T.J., Noomen, A., Jellema, A. & van Boekel M.A.J.S. *Dairy Technology: Principles of Milk Properties and Processes*. **1999**, Marcel Dekker Inc. New York.
18. Thompson, A. K.; Singh, H. Preparation of liposomes from milk fat globule membrane phospholipids using a microfluidiser. *J. Dairy Sci.*, **2006**, 89, 410-419.
19. Thompson, A.K.; Hindmarsh, J.P.; Haisman, D.; Rades, T.; Singh, H. *J. Agric. Food Chem.* **2006**, 54, 3704-3711.
20. Thompson, A.K.; Haisman, D.; Singh, H. *J. Agric. Food Chem.* **2006**, 54, 6390-6397.

Chapter 9

Controlled Self-Organization of Zein Nanostructures for Encapsulation of Food Ingredients

Graciela W. Padua and Qin Wang

Department of Food Science and Human Nutrition, University of Illinois
at Urbana-Champaign, 382/D AESB, 1304 West Pennsylvania Avenue,
Urbana, IL 61801

Micro/nano-encapsulation technologies have the potential to meet food industry challenges concerning the effective delivery of health functional ingredients and controlled release of flavor compounds. The inherent complexity of food systems has translated into an intensive search for novel functional shell materials. Understanding their structure has become critical for the design of effective carriers. Nanotechnology methods may prove useful in the construction of food delivery systems. Zein, the prolamine in corn endosperm, has long been recognized for its coating ability. Zein has a marked amphiphilic character. It is soluble in alcohol-water mixtures. It contains more than 50% nonpolar amino acids arranged in unique spatial disposition consisting of tandem repeats of α -helix segments aligned parallel to each other forming a ribbon or prism. This structure gives rise to well defined hydrophobic and hydrophilic domains at the protein surface. Zein can bind and enrobe lipids, keeping them from deteriorative changes. Zein has been shown to adsorb fatty acids and produce periodic structures, most interestingly, nanoscale layers of cooperatively assembled fatty acid and zein sheets. Other experiments have detected the formation of nanoscale “tubes” of zein formed upon adsorption of the protein on hydrophilic surfaces. Lamellar structures detected by x-ray diffraction, formation of zein “tubes” observed by AFM, and the long rod-like structures observed by SEM may

be explained in terms of the formation of liquid crystalline phases. Effort has been invested in tracking the self-organization and characterizing resulting tertiary structures formed by zein. The goal is to produce nanostructures of controlled geometry, useful as microencapsulation materials for fatty acids, flavors, oleoresins, vitamins, and peptides.

Introduction

Better, widespread information on the impact of diets on health and well being has raised consumers' expectations from the foods they eat. Nutrient and bioactive content, avoidance of food components associated with health risks, and food safety have an increasing impact on consumers' choices. Quality demands are also on the rise, prompted by an increase in trade and availability of wider selections. The food industry has responded by looking into the incorporation of health functional ingredients, food component replacement, and controlled release of flavors and aromas. Major challenges to this effort are effective ingredient delivery without compromising sensory quality, and sustained bioactivity. Micro/nano-encapsulation technologies have the potential to meet these challenges.

Encapsulation involves surrounding a core compound with a suitable shell material which carries, protects, and delivers the core in a controlled fashion. For example, in the pharmaceutical industry poly (lactic-co-glycolic acid) (PLGA) is used to encapsulate proteins (i.e. human growth hormone) (1,2). The food industry has seen the micro-encapsulation of antioxidants, flavor compounds, natural extracts, vitamins, probiotic bacteria and others. Conjugated linoleic acid was encapsulated in whey protein concentrate (3). Microcapsules containing short chain fatty acids were produced using gum arabic and maltodextrins as wall materials (4). Desai and Park (5) studied the stabilization of vitamin C in chitosan microspheres cross-linked with tripolyphosphate. Probiotic bacteria (*Lactobacillus acidophilus* and *Bifidobacterium lactis*) were encapsulated in calcium-induced alginate-starch shells to enhance the survival of probiotic bacteria in yogurt during storage (6).

The variety of shell materials and encapsulation processes reflects the inherent complexity of food systems, which seems to require *ad-hoc* solutions for every problem. This was translated into an intensive search for novel functional compounds. Understanding their structure has become the basis for design of effective carriers. Nanotechnology methods may prove useful in the construction of food delivery systems (7,8). Graveland-Bikker and de Kruif (9) observed the self-assembly of α -lactalbumin derived peptides into nano-sized tubular structures. These nanostructures promise various applications in food technology.

Proteins, depending on their amino acid sequence, may acquire distinct spatial conformations and show varied functionalities in response to their environment. Temperature, pH, ionic strength, and the hydrophobic/hydrophilic character of the medium or adsorbing interface affect the 3D structure of individual proteins and the way they interact and associate with each other. Zein, the prolamine in corn endosperm, has long been recognized for its coating ability. Its conventional applications include coating of tablets in the pharmaceutical industry and as a substitute for shellac in candies and confections. New applications include slow release formulations in drug delivery. Zein microspheres were investigated as carriers for ovalbumin and heparin (10,11). Such microspheres were resistant to physical and chemical degradation but degradable by pepsin and pancreatin. Zein also can impart protection as antioxidant. Zein films are reported to have an inherent free radical scavenging activity (12). Zein can also bind and enrobe lipids, keeping them from deteriorative changes. Wang and others (13) reported that zein showed antioxidant activity on methyl linoleate, possibly by binding and physically shielding the lipid. Zein has been shown to adsorb fatty acids and produce periodic structures (14), most interestingly, nanoscale layers of alternating fatty acid and zein sheets. Other experiments have detected the formation of nanoscale “tubes” of zein formed upon adsorption of the protein on hydrophilic surfaces (15). Zein structures have been proposed as encapsulation materials for fatty acids and other lipophilic compounds.

Zein Structure

Zein is not soluble in water but in alcohol-water mixtures (16,17). Its amphiphilic character results from the balance between hydrophobic and hydrophilic amino acids in its sequence and their unique spatial disposition (18). Zein amino acid sequence contains more than 50% nonpolar amino acids including leucine, proline, and alanine (19). The high content of nonpolar amino acids is responsible for the hydrophobic nature of zein and its lack of solubility in water. On the other hand, the high content of glutamine makes it insoluble in alcohol because of the formation of intramolecular hydrogen bonds.

Zein consists of two groups of polypeptides, according to sodium dodecyl sulfate polyacrylamide gel electrophoresis (SDS-PAGE) (18,20) and MALDI results (21), a chain of 23,000-24,000 molecular weight and a second peptide chain of 26,000-27,000 (22,23). Both peptide chains have sequence homology: N-terminals contain 35 to 37 amino acids, C-terminals have 8 amino acids, and central domains consist of 9 (for the 23,000-24,000 chain) or 10 (for the 26,000-27,000) repetitive sequences. The repetitive domains contain blocks of 14 to 25 amino acid residues with an average length of 19-20 (23,24). The secondary structure of zein, as determined by optical rotation, optical rotary dispersion, and

circular dichroism (18), is formed by 50-60% α -helix, mainly existing in the central domains of the peptide chain, 15% of β -sheet, with the rest of the molecule being aperiodic. The tertiary structure of zein consists of asymmetric particles, initially proposed to approximate rods, with axial ratios of 7:1 to 28:1 (17,25,26)

Small-angle x-ray scattering (SAXS) was used to explore the size and shape of zein particles. Matsushima and coworkers (27) reported SAXS measurements on zein in 70% aqueous ethanol over a concentration range of 2-40 mg/mL. They determined R_g and R_c values of 40 and 13.9 Å, respectively, for reduced zein in solutions containing 0.1 or 2% v/v β -mercaptoethanol. For the non-reduced zein, they obtained R_g and R_c values of 49.8 and 19 Å, respectively. From those measurements, they proposed that the reduced zein structural unit has a rectangular prism shape measuring 130 Å for the longest dimension and 34 Å for each of the other two dimensions. For the non-reduced zein the longest dimension was determined at 160 Å and 46 Å for the other two lateral dimensions. Along the short dimension, zein was proposed to consist of four molecules. Therefore, the shortest dimension of the molecule was around 12 Å. Matsushima and coworkers (27) assumed a model (Figure 1), related to an earlier model by Argos (18), consisting of 9 (Z19) or 10 (Z22) helical segments folded in an anti-parallel fashion linked by glutamine-rich turns and held in place by hydrogen bonds. They proposed that the helical segments were aligned to form a compact ribbon. A portion of the N-terminus formed an additional helical segment at the end of the ribbon. Figure 2 shows a transmission electron microscope (TEM) image of critical point freeze dried zein showing particle size grains of 200Å, in relatively close agreement with the measurements above. The structural model in Figure 1 suggests that the location of zein hydrophobic domains lay along the helix surfaces (front and back). Hydrophilic domains would correspond with the glutamine-rich loops (top and bottom).

Zein Adsorption to Hydrophobic and Hydrophilic Surfaces

Zein adsorption to hydrophobic and hydrophilic surfaces was investigated by surface plasmon resonance (SPR) (15). Hydrophilic and hydrophobic surfaces were generated by monolayers of a carboxylic acid terminated thiol, 11-mercaptoundecanoic acid ($\text{COOH}(\text{CH}_2)_{10}\text{SH}$) and a methyl-terminated alkanethiol, 1-octanethiol ($\text{CH}_3(\text{CH}_2)_7\text{SH}$), respectively, fixed on gold-coated glass slides. Figure 3 shows the rate of zein adsorption at various bulk concentration levels (Cb). SPR experiments indicated that zein was adsorbed to 1-octanethiol (hydrophobic) as well as to 11-mercaptoundecanoic acid (hydrophilic) surfaces. However, initial adsorption rate was higher for zein on 11-mercaptoundecanoic acid than on 1-octanethiol suggesting that a different adsorption mechanism for each case.

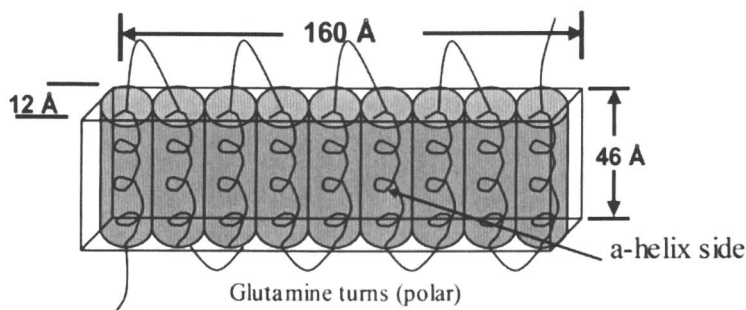


Figure 1. Diagram of zein tertiary structure according to Matsushima et al. (1997).

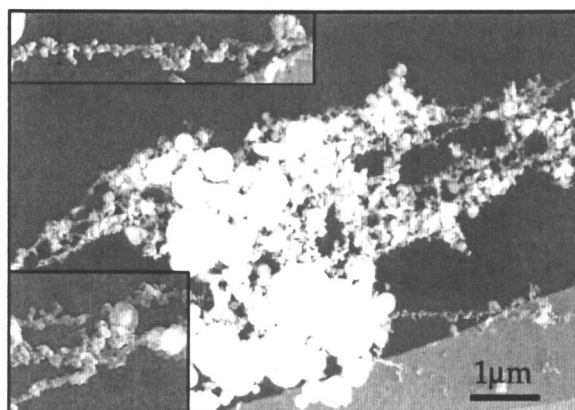


Figure 2. TEM image of critical point freeze dried zein showing particle size grains of 200 Å. Large particles are starch.

In the same experiment, flushing off loosely adsorbed zein allowed the observation of a monolayer, which was thicker for zein on 11-mercaptoundecanoic acid than for zein on 1-octanethiol. Figure 3 shows the desorption effect caused by flushing the SPR cell with 75% 2-propanol (at 1200 sec). Zein adsorption decreased from Γ_{\max} to a lower value, Γ_{flushed} , which was similar for all curves in each figure. Flushing could have removed loosely bound zein adsorbed above surface saturation. The consistency of Γ_{flushed} values suggested that each corresponded to its monolayer. Γ_{flushed} was higher for hydrophilic (0.54 mg/m^2) than for hydrophobic (0.11 mg/m^2) surfaces. The difference in monolayer values was explained in terms of footprint size, which according to the above structural model would be larger for zein on hydrophobic than on hydrophilic surfaces. Matsushima et al (1997) considered that the zein molecule measured $170 \times 46 \times 12$

\AA^3 . The $170 \times 46 \text{\AA}^2$ faces corresponding to the exterior of α -helix segments are largely hydrophobic. The $170 \times 12 \text{\AA}^2$ faces containing glutamine loops or turns are hydrophilic. Zein may have used different faces of its molecule to adsorb on hydrophobic or hydrophilic surfaces, as shown in Figure 4. It was suggested that zein may be induced into anisotropic behavior by controlling the polar character of solvent media or adsorbing surfaces.

Topography of Zein Deposits

The topography of zein deposits after SPR experiments was examined by atomic force microscopy (AFM). Images of zein adsorbed on 11-mercaptoundecanoic acid and 1-octanethiol SAMs fixed on gold-coated slides are shown in Figures 5 and 6, respectively. Section analyses for both images are also presented. Figure 5, zein deposited on 11-mercaptoundecanoic acid, shows a surface populated by distinct tubular structures, 35 nm high. The approximate diameter of those cylinders is 200 nm. Surface roughness was calculated at 13.7 nm. By comparison, in Figure 6, zein adsorbed on a hydrophobic surface appears uniform, nearly featureless, and has a lower calculated roughness of 2.2 nm.

Zein Structured Solids

Zein molecular structure allows it to readily stack and form films on hard surfaces. The formation of free-standing zein films for environmental packaging and other applications has been the focus of intensive research (28-31). Zein films are brittle, necessitating the addition of plasticizers to impart ductility. Zein films were prepared by solubilizing zein and fatty acids (0.5 - 1 g fatty acid/g zein) in aqueous ethanol (70% v/v) followed by the addition of water. The aqueous environment promoted co-precipitation of zein-fatty acid aggregates which were collected as a soft solid (32). The hydrated resin was very ductile and stretchable. Films were drawn from this soft mass and allowed to dry at room conditions. The study of zein plasticization provided the framework for the investigation of the interaction between zein and fatty acids, which will be essential to the development of microencapsulation systems.

The structure of zein-oleic acid films was investigated by x-ray diffraction (14). Wide-angle (WAXS) diffraction patterns showed d -spacings of 4.6 and 10.5 \AA which were attributed to the α -helix backbone distance along the chain and the inter-chain spacing between helices, respectively. Untreated granular zein gave only slightly smaller values. It was concluded that film forming did not affect the basic structure of the α -helix. SAXS results showed a strong periodicity (135 \AA) normal to the film plane which was interpreted in terms of a platelet structure, developed during the resin making process and aligned during

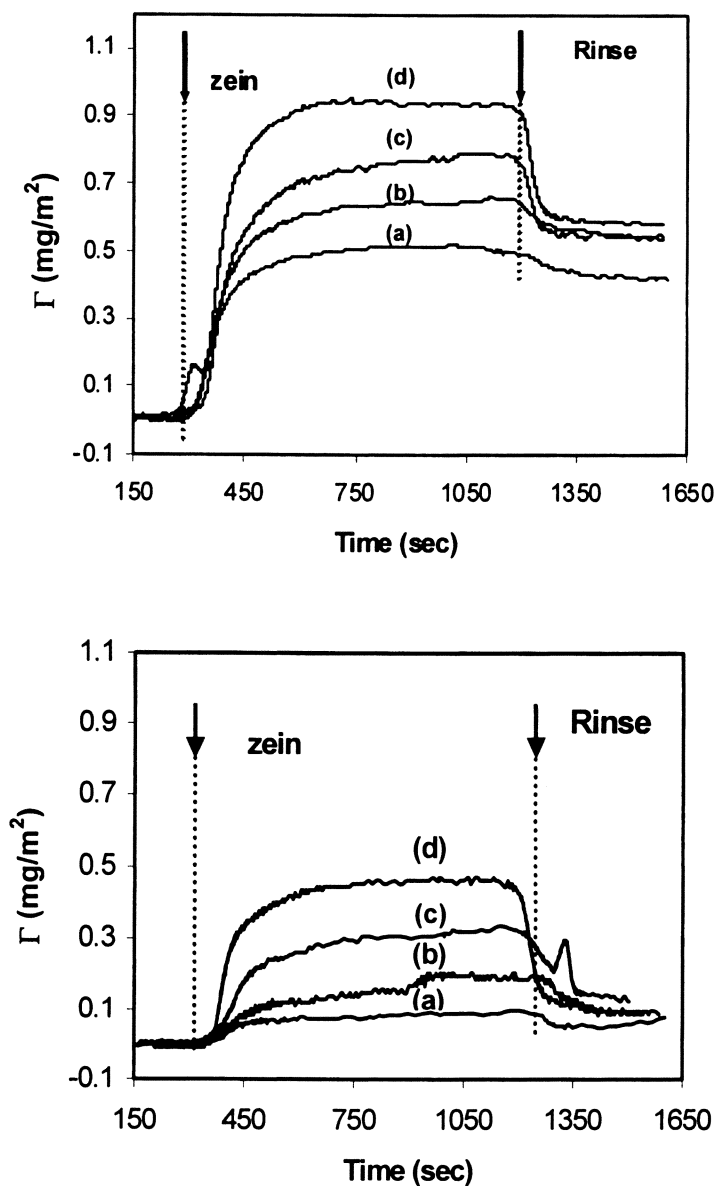


Figure 3. Zein adsorption kinetics from 75% 2-propanol solutions onto surfaces of 11-mercaptoundecanoic acid (up) and 1-octanethiol (bottom) for different zein bulk concentration levels, C_b = (a) 0.05%; (b) 0.1%; (c) 0.3%; (d) 0.5%.

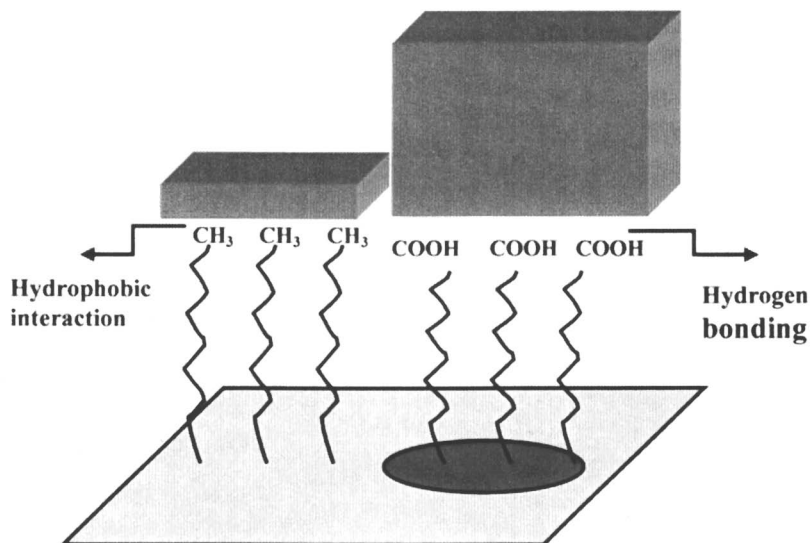


Figure 4. Zein adsorption to carboxylic and methylated surfaces using different faces of its prism-shaped molecule.

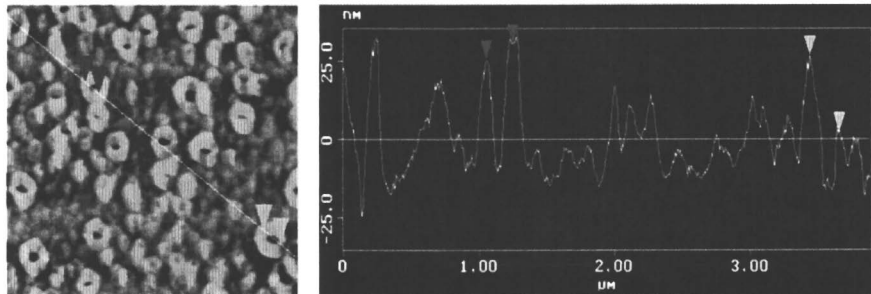


Figure 5. AFM image and section analysis of zein deposited on a hydrophilic surface.

film formation. Experiments using stearic acid also suggested the presence of platelets. Fatty acids seemed to play an important role in the formation of platelet structures. Granular zein did not show any SAXS periodicity.

Lai and coworkers proposed a structural model for zein-oleic acid films (Figure 7) based on x-ray measurements and zein molecular dimensions for non-reduced zein (27). In this model, layers of zein ribbon-like units of $160 \times 46 \times 12 \text{ \AA}$ were double-stacked and alternated with bilayers of oleic acid, measuring 42 \AA . The model suggested that the mechanism for film formation, depicted in

Figure 8, involved the dispersion of zein molecules in aqueous alcohol (8A) followed by electrostatic adsorption of oleic acid to the polar residues on the zein surface (8B). Addition of cold water during resin precipitation resulted in hydrophobic aggregation of zein-oleic acid units. Figure 8C represents associations normal to the film surface and Figure 8D represents the association of those units in the film plane. Zein-to-zein associations represented in 8E can develop curvature as a hydrophobic response to the aqueous medium and roll into “tubes” as shown in 8F. Figure 9 shows an SEM image of the zein-oleic acid film surface. It appears to show an entanglement of fibers or rods, possibly formed as depicted in Figure 8F (also see Figure 5). Figure 10 shows a TEM image of a zein “tube” formed by the curling of a zein film upon itself.

Zein-Fatty Acid Organization

The lamellar structures detected by x-ray diffraction, the formation of zein “tubes” observed by AFM, and the long rod-like structures observed by SEM may be explained in terms of the formation of liquid crystalline phases.

It is known that amphiphilic molecules in aqueous solutions can form a large variety of different aggregates (33). In general, such aggregates can be spherical (micelles), cylindrical (rod-like) and lamellar (disc-like) shapes. These supramolecular arrangements can, in turn, organize themselves on a larger scale, forming structures with long range (liquid crystal phases) or short range order (liquid isotropic phases). In water, the hydrophobic chains of the amphiphile are located in the interior of the aggregates shielded from contact with the polar solvent by the hydrophilic head groups. The micellar phase is composed of amphiphile monolayers, while bilayers build lamellar phases or spherical vesicles. The closed structures of bilayered phases include solvent in their interior. Lyotropic liquid crystalline phases can be formed in concentrated mixtures of amphiphilic molecules and water. The hexagonal and lamellar structures are two such liquid crystalline phases. The hexagonal phase consists of infinite cylindrical micellar rods hexagonally close-packed in the lattice. The rod radius in this phase is usually constant and less than the fully extended hydrophobic chain of the amphiphilic entity. The structural building block of the lamellar phase is the bilayer, the thickness of which is always greater than 1.5 times the length of the fully extended hydrophobic moiety of the amphiphile (34). In this phase, the bilayers are stacked one on top of another, with water in the inter-bilayer region to form a phase of one-dimensional periodicity. The two phases are common to many systems that form lyotropic crystalline phases with the hexagonal phase occurring at lower amphiphilic volume fractions than the lamellar phase. Transitions between phases upon increasing amphiphile concentration are marked by topological transitions from discrete micellar aggregates having positive interfacial curvature to continuous bilayers with zero net curvature.

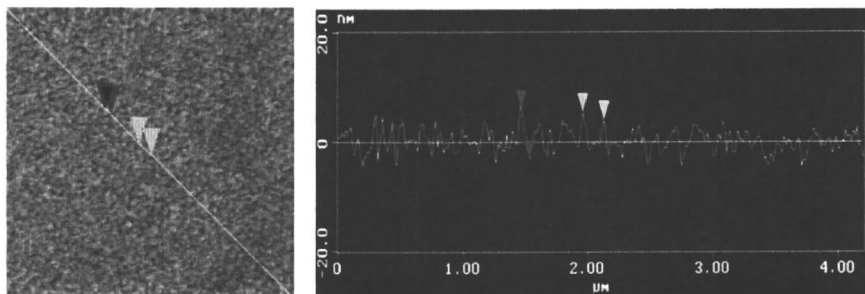


Figure 6. AFM image and section analysis of zein deposited on a hydrophobic surface.

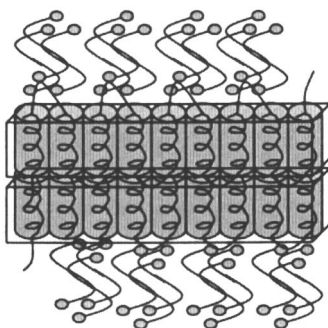


Figure 7. Structure model of zein films proposed by Lai (14).

The self-assembly of amphiphilic molecules in water is driven by two competitive processes, the exclusion of water from the hydrophobic alkyl chain region and the packing of these chains into the volume of the enclosure. The interplay between these two processes dictates the aggregate size and shape in solution. At the molecular level, the closure of the aggregate imposes a curvature in the hydrophilic head group-water interface. The interfacial curvature is controlled by the molecular architecture as well as by the presence of any additional components. Changes in solvent environment may trigger precipitation-driven-assembly. For example, certain silicate and surfactant systems aggregate by this mechanism (35). It is reported that within 3 min after the addition of silicon alkoxide, SAXS measurements show the formation of an ordered phase. Moreover, the formation of reversible thermodynamically stable silicate-surfactant mesophases has been demonstrated. Figure 11 illustrates this mechanism where silicates and surfactants cooperatively assemble in a dilute aqueous phase. Under certain conditions, silicon encapsulated cylindrical micelle "nanotubes" have

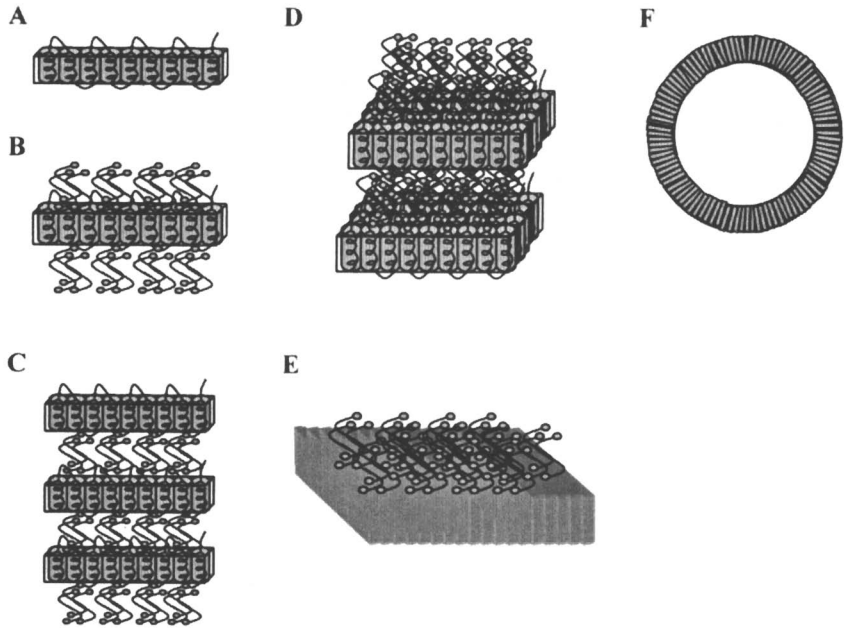


Figure 8. Development of zein-oleic acid structures as a response to the changing character of the solvent. F shows a replica of related “coiled” lamellae in a single disclination domain.

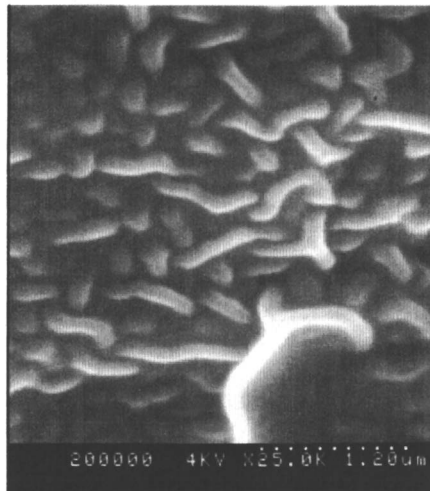


Figure 9. SEM image of zein-oleic acid film.

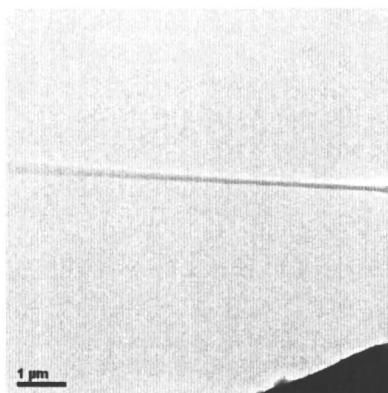


Figure 10. TEM image of a zein “tube” formed by the curling up of a zein film.

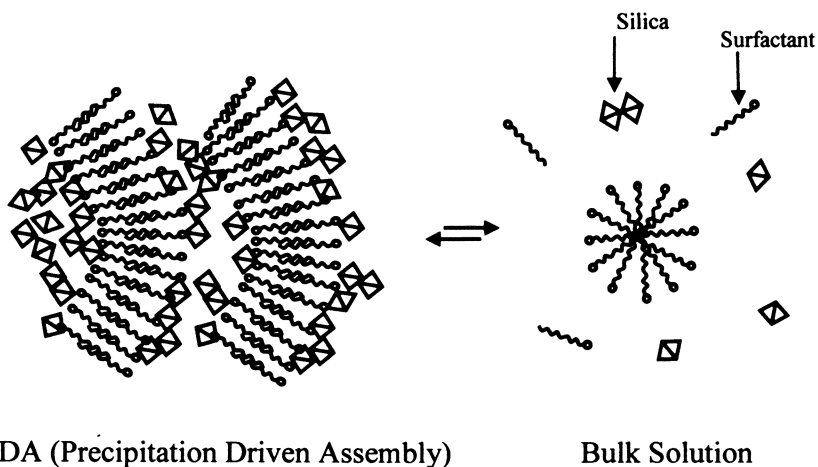


Figure 11. Cooperative assembly of silicate–surfactant mesophases in water.
Illustration based on Rankin (35).

been observed by cryo-TEM. The cooperative crystallization process is dynamic and may involve transformations between silica-surfactant mesophases. For example, a lamellar phase has been observed by x-ray diffraction to re-crystallize into hexagonal close-packed cylindrical channels. Self-assembly of amphiphilic molecules is not only observed in surfactants but also in polymers, biopolymers, and polar lipids. An interesting liquid-crystalline mesophase is the cubic phase. For example, a glycerol based monounsaturated fatty acid ester and water exhibits two main forms of the bicontinuous cubic phase, the gyroid (low hydration) and the diamond (high hydration). The system is a solid-like bicontinuous cubic phase at

water contents between 20 and 40% at room temperature. Such phases are composed of porous matrices (pores of ca. 5 nm) built from bilayer contours into infinite periodic minimal surfaces. The interconnectedness of the surface results in a clear viscous gel similar in macroscopic appearance and rheology to cross-linked polymer hydrogels. Cubic phases have received increased attention in relation to biological lipid/protein structures (36). They were used to prepare crystals of membrane proteins and to demonstrate the role of the lipid matrix in the formation of three-dimensional crystals.

Effort has been invested in tracking the self-organization and characterizing resulting tertiary structures formed by zein. The goal is to produce nanostructures of controlled geometry, useful as microencapsulation materials for fatty acids, flavor compounds, oleoresins and other lipids, vitamins, and peptides. By controlling the chain length and unsaturation level of fatty acids, the hydrophobic/hydrophilic balance of the medium, and physical conditions of the experiment affecting liquid crystalline phases organization and transformations, we can expect to generate a host of nanoscale layered, interpenetrating, and vesicle structures.

Applications of zein-based structured solids may include encasing of omega-3 fatty acids and other lipid nutrients shielding them from deterioration and while keeping a low impact on the sensory quality of foods. Such structures would be amenable with lipid matrices such as chocolate or ice-cream. Another possibility is the encapsulation of binary systems such as enzymes and substrates in compartmentalized nano/microstructures of controlled composition and geometry.

References

1. Johnson, O. L.; Jaworowicz, W.; Cleland, J. L.; Bailey, L.; Charnis, M.; Duenas, E.; Wu, C. C.; Shepard, D.; Magil, S.; Last, T.; Jones, A. J. S.; Putney, S. D. *Pharm. Res.* **1997**, *14*, 730-735.
2. Costantino, H. R.; Johnson, O. L.; Zale, S. E. *J. Pharm. Sci.* **2004**, *93*, 2624-2634.
3. Jimenez, M.; García, H. S.; Beristain, C. I. *J. Sci. Food Agric.* **2006**, *86*, 2431-2437.
4. Teixeira, M. I.; Andrade, L. R.; Farina, M.; Rocha-Leão, M. H. M. *Mater. Sci. Eng. C* **2004**, *24*, 653-658
5. Desai, K. G. H.; Park, H. J. *J. Microencapsul* **2005**, *22*, 179-192.
6. Kailasapathy, K. *LWT* **2006**, *39*, 1221-1227.
7. Weiss, J.; Takhistov, P.; McClements, D. J. *J. Food Sci.* **2006**, *71*, R107-R116.
8. Moraru, C. I.; Panchapakesan, C. P.; Huang, Q. R.; Takhistov, P.; Liu, S.; Kokini, J. L. *Food Tech.* **2003**, *57*, 24-29.
9. Graveland-Bikkera, J. F.; de Kruifa, C. G. *Trends Food Sci. Tech.* **2006**, *17*, 196-203.
10. Hurtado-López, P.; Murdan, S. *J. Microencapsul.* **2006**, *23*, 303-314.

11. Wang, H.-J.; Lin, Z.-X.; Liu, X.-M.; Sheng, S.-Y.; Wang, J.-Y. *J. Controlled Release* **2005**, *105*, 120-131.
12. Güçbilmez, Ç. M.; Yemenicioflu, A.; Arslanoflu, A. *Food Res. Internat.* **2007**, *40*, 80-91.
13. Wang, J.-Y.; Fujimoto, K.; Miyazawa, T.; Endo, Y. *J. Agri. Food Chem.* **1991**, *29*, 351-355.
14. Lai, H.-M.; Geil, P. H.; Padua, G. W. *J. Appl. Polym. Sci.* **1999**, *71*, 1267-1281.
15. Wang, Q.; Wang, J.-F.; Geil, P. H.; Padua, G. W. *Biomacromolecules* **2004**, *5*, 1356.
16. Shotwell, M. A.; Larkins, B. A. 1989. *The Biochemistry of Plants*; Marcus, A., Ed.; Academic Press: New York, NY, 1989; Vol. 15, pp 297-345
17. Tatham, A. S.; Field, J. M.; Morris, V. F.; I'Anson, K. J.; Cardle, L. *J. Biol. Chem.* **1993**, *268*, 26253-26259.
18. Argos, P.; Pederson, K.; Marks, M. D.; Larkins, B. A. *J. Biol. Chem.* **1982**, *257*, 9984-9990.
19. Pomes, A. F. *Encyclopedia of Polymer Science and Technology*; Mark, H., Ed.; Wiley: New York, NY, 1971; Vol. 15, pp 125-132.
20. Esen, A. *Plant Physiol.* **1986**, *80*, 623-627.
21. Wang, J. F.; Geil, P. H.; Kolling, D. R. J.; Padua, G. W. *J. Agri. and Food Chem.* **2003**, *51*, 5849-5852.
22. Pedersen, K.; Devereux, J.; Wilson, D. R.; Sheldon, E.; Larkins, B. A. *Cell* **1982**, *29*, 1015-1026.
23. Heidecker, G.; Chaudhuri, S. *J. Genomics* **1991**, *10*, 719-732.
24. Thompson, G. A.; Siemieniak, D. R.; Sieu, L. C.; Slightom, J. L.; Larkins, B. A. *Plant Mol. Biol.* **1992**, *18*, 827-833.
25. Watson, C. C.; Arrhenius, S.; Williams, J. W. *Nature* **1936**, *137*, 322-323.
26. Foster, J. F.; Edsall, J. T. *J. Amer. Chem. Soc.* **1945**, *61*, 617-624.
27. Matsushima, N.; Danno, G. I.; Takezawa, H.; Izumi, Y. *Biochim. Biophys. Acta* **1997**, *1339*, 14-22.
28. Gennadios, A.; Weller, C. L. *Food Technol.* **1990**, *44*, 63-69.
29. Krochta, J. M.; De Mulder-Johnston, C. *Food Technol.* **1997**, *51*, 61-74.
30. Lai, H.-M.; Padua, G. W. *Cereal Chem.* **1998**, *75*, 194-199.
31. Wang, Y.; Padua, G. W. *Macromol. Mater. Engr.* **2003**, *288*, 886-893.
32. Lai, H.-M.; Padua, G. W. *Cereal Chem.* **1997**, *74*, 771-775.
33. Zana, R. *Dynamicvs of Surfactant Self-Assemblies: Micelles, Micro-emulsions, Vesicles, and Lyotropic Phases*; Zana, R. Ed.; CRC Press: Boca Raton, FL, 2005; pp 37-73.
34. Holmes, M. and Leaver, M. *Bicontinuous Liquid Crystals*; Lynch, M.; Spicer, P., Eds.; CRC Press: Boca Raton, FL, 2005; pp 15-39.
35. Rankin, S. *Bicontinuous Liquid Crystals*; Lynch, M.; Spicer, P., Eds.; CRC Press: Boca Raton, FL, 2005; pp 243-283.
36. Garti, N. *Bicontinuous Liquid Crystals*; Lynch, M.; Spicer, P., Eds.; CRC Press: Boca Raton, FL, 2005; pp 387-423.

Chapter 10

Real Time Monitoring of Interactions in Oil-in-Water Emulsions: Diffusing Wave and Ultrasonic Spectroscopy

M. Alexander, J. Liu, and M. Corredig^{*}

Department of Food Science, University of Guelph, Guelph,
Ontario N1G 2W1, Canada

Diffusing wave and ultrasonic spectroscopy were employed to study the interactions occurring in sodium-caseinate stabilized oil droplets in the presence of two charged polysaccharides (high methoxyl pectin and soy soluble polysaccharide). These mixed systems, studied at high pH or during acidification, offered different model systems with different dynamics: droplet aggregation due to decreased electrostatic and steric interactions, bridging or depletion flocculation. By observing the bulk changes occurring in the system with non-invasive techniques, it was possible not only to measure accurately the point of destabilization, but also identify the changes occurring at the early stages of structure development and the modifications in the spatial arrangement of the droplets in real time.

Food emulsions of the oil-in-water type are often stabilized by protein systems such as sodium caseinate (a mixture of the four principal casein proteins, α_{s1} , α_{s2} , β and κ -caseins). At neutral pH these proteins stabilize the emulsion droplets via steric and electrostatic interactions (1).

When lowering the pH towards the isoelectric point of the proteins, the protein-covered oil droplets lose their stability and droplet flocculation occurs (2).

Charged polysaccharides are often added to control the bulk properties of these emulsions (i.e. viscosity, appearance, microstructure, stability). Understanding the dynamics of the interactions occurring at the interface between the polysaccharides and the adsorbed proteins is of great importance to ensure optimal quality of the final product. Although the molecular mechanisms involved in the interaction of charged polysaccharides and proteins are known, our understanding of the dynamics during structure formation in emulsion systems derives mainly from studies under diluted conditions. Therefore, it is not always possible to predict the bulk properties because these same properties will depend on the concentration of the polymer and the volume fraction of the oil droplets.

In the presence of polysaccharides, changes in the bulk properties of emulsions often occur because of due to phase separation by depletion or bridging mechanisms. When repulsive or attractive forces dominate, structuring of the colloidal system takes place and in most cases the system is in metastable conditions. For this reason, the early stages of these reactions can be easily affected by the measurements themselves. In colloidal systems such as emulsions containing polysaccharides, the dynamics of the interactions are not fully understood and most published work either focused on identifying aggregation and flocculation phenomena (i.e. rheology, microscopy, or simply following macroscopic creaming) or on determining changes occurring to the particle size of the system using traditional light scattering techniques, which require extremely dilute conditions.

In recent years non-invasive techniques such as ultrasonic spectroscopy and diffusing wave spectroscopy have been applied to study the reactions in colloidal systems. These techniques have proven very useful to determine the details of the interactions occurring during flocculation of emulsion droplets.

Effect of Charged Polysaccharides on the Bulk Properties of Protein-stabilized Emulsions

The reactions occurring at the molecular level between charged polysaccharides and proteins are fairly known (3). When both the polysaccharide and the protein are negatively charged (often this is the case in

food emulsions at high pH), electrostatic forces induce repulsion between the molecules. On the other hand, if the polymers have opposite charges, electrostatic interactions will occur, causing the adsorption of the polysaccharide at the interface (4, 5).

This manuscript summarizes our observations on a model system containing sodium-caseinate stabilized oil droplets and two negatively charged polysaccharides, high methoxyl pectin (HMP) and soy soluble polysaccharide (SSPS). HMP is a galacturonic acid-based polysaccharide with a high degree of methylesterification, with branches of neutral sugar (i.e. arabinose, galactose and xylose). HMP has been shown to interact with casein particles in acid milk beverages at $\text{pH} < 5.0$ and to stabilize the suspensions with a combination of electrostatic and steric stabilization (6). At neutral pH and above a critical concentration, HMP causes depletion flocculation of protein-stabilized emulsions (3, 5, 7). SSPS is also an acidic polysaccharide extracted from soy cotyledons, consisting of homogalacturonan and rhamnogalacturonan, branched with galactan and arabinan chains (8). SSPS has also been shown to stabilize casein particles in acidified milk by interacting with proteins at low pH (9). However, SSPS has a different interacting mechanism than HMP, because of the higher amount of branched neutral sugars, the presence of small amounts of protein, its globular structure and its relatively small radius (about 25 nm) (10). For example, when compared to HMP at high pH, SSPS does not cause depletion flocculation of protein-stabilized emulsions at concentrations as high as 0.3% (7).

Ultrasonic Spectroscopy

As an ultrasonic wave propagates through a colloidal sample, the density and compressibility inhomogeneities encountered in its path will cause a change in the intensity and phase of the incoming wave. The changes in phase of the sound wave are related to the velocity of the wave propagating through the system. Ultrasonic velocity is an optimal parameter for characterizing chemical reactions or changes in chemical composition of solutions (11). In colloidal systems more information can be derived from measurements of attenuation of the ultrasonic wave, which is related to the decrease in the intensity of the sound wave during its propagation. This parameter is sensitive to changes in the range of nanometers to micrometers, depending on the range of frequencies tested (12). The attenuation of the ultrasonic wave derives mostly from thermal, visco-inertial and scattering components (12, 13). In food emulsions visco-inertial effects are not as important as thermal effects, as the former are only significant when there is a gradient in density between the dispersed particle and its surroundings. Thermal effects on the other hand depend on the physical properties of the various components in the system, such as thermal expansion,

heat capacity and heat conductance. In oil-in-water emulsions, the thermal attenuation is the main reason for losses in attenuation. The compression and decompression of the ultrasonic wave during propagation cause a heat flow between the colloidal particle and the solvent phase, and a thermal gradient forms at the interface. Total attenuation from scattering, as the ultrasound energy is directed away from its path, becomes increasingly important as the particle size increases (12, 13).

Diffusing Wave Spectroscopy

In DWS the intensity fluctuation of a speckle of scattered light is measured in a multiple scattering regime and a time-resolved correlation function is derived. In contrast with traditional dynamic light scattering, where highly diluted samples are required to avoid multiple scattering, DWS requires turbid systems, as the photon path through the sample is treated as a random walk (14). The parameters derived from DWS experiments can yield not only information on the size of the scatterers, but also on particle interactions. The photon transport mean free path (l^*) is the length over which the direction of the incoming photon is completely randomized. The decorrelation of light is related to the physical properties of the sample as well as their spatial arrangement. The l^* parameter is a function of the scattering form factor $F(q)$ and the structure factor $S(q)$, where $q (=4\pi n/\lambda \sin(\theta/2))$ is the scattering vector, n is the index of refraction of the medium and λ is the wavelength in vacuum (14). $F(q)$ is related to shape, size, refractive index contrast, physical changes in the scattering system, while $S(q)$ is related to the spatial correlation between the particles (14, 15).

The value of l^* can be calculated from static measurements of light transmission (in multiple scattered systems) (14) and once l^* is determined, it is possible to solve the autocorrelation function from the multiple scattered events and calculate the diffusion coefficient and the radius of the scatterer using the Stokes-Einstein relation, knowing the values of viscosity of the solution.

Experimental

Stock emulsions were prepared containing 0.5% (w/w) sodium caseinate in ultrapure water and 10% soybean oil using a high pressure valve homogenizer (Emulsiflex C5, Avestin Inc., Ottawa, ON, Canada) with three passes at 40 MPa. HMP (67.4 % methylation, unstandardized, CpKelco, San Diego, CA, USA) and SSPS (DA 300S, Fuji Oil Co. Ltd, Japan) dispersions were prepared in ultrapure water at 70°C continuously stirring to room temperature. Emulsions and

solutions were stored at 4°C for 24 h, and before mixing the pH was adjusted to pH 6.8 using NaOH.

The viscosity of the polysaccharide solutions was measured using a Ubbelohde viscometer (type A859 size 1B, Industrial Research Glassware, NJ, USA).

The polysaccharides were added to the emulsions to a final oil concentration of 6% (w/w) and varying levels of SSPS or HMP up to 0.2% (w/w). Mixtures were studied at pH 6.8 as well as during acidification. Acidification was induced by slow hydrolysis of 0.3% glucono- δ -lactone (GDL). The pH was continuously measured in parallel with the spectroscopy experiments.

The average apparent diameter of the emulsions with or without polysaccharide at pH 6.8 was measured using dynamic light scattering (DLS) (Zeta Sizer Nano ZS, ZEN 3600, Malvern Inst. Ltd. UK) after extensive dilution in 10 mM imidazole buffer at pH 6.8 filtered through 0.2 μ m.

Transmission DWS measurements were carried out as previously described (15), with a solid-state laser (532 nm, 100 mW, Omnicrome, Chino, CA, USA) and a 5 mm quartz cuvette at 23°C. The laser intensity (for measurement of I*) was determined using 269 nm latex spheres (Portland Duke Scientific, Palo Alto, CA, USA).

A high resolution ultrasonic spectrometer (HR-US102, Ultrasonic Scientific, Dublin, Ireland) was used to measure the changes in velocity and attenuation of sound as described elsewhere (16). The samples were equilibrated and measured at 23°C. In the acidification experiments samples with no GDL were used in the reference cell. The instrument was calibrated with water at 25°C, and tuned to measure six frequencies (3, 5, 8, 11 and 15 MHz).

The results shown are the average of three replicate experiments.

Results and Discussion

At neutral pH, sodium caseinate-stabilized oil droplets are negatively charged. At this pH, both HMP and pectin will not interact with the droplets because of electrostatic repulsion between like-charges. The apparent diameter of the oil droplets was measured using DLS and DWS (Figure 1) as a function of polysaccharide concentration.

Results derived from DLS suggest that the hydrodynamic diameter of the emulsion droplets does not change as a function of HMP or SSPS concentration. These observations are in agreement with previously published research reporting a lack of interactions between the protein surface and SSPS molecules at neutral pH (5, 7). However, DLS experiments are performed after extensive dilution. The diameter values calculated from DWS data on the other hand,

show a constant diameter for emulsions containing SSPS, while indicate an increase in the apparent size of the emulsion droplets in emulsions with >0.07% HMP. Since these apparent diameters are calculated correcting for medium viscosity, change in the apparent size suggest the formation of flocculated clusters. The discrepancies between DLS and DWS data confirm the occurrence of depletion flocculation at high concentration of HMP. The difference in behaviour between HMP and SSPS at high pH, and the lack of depletion flocculation in emulsions containing SSPS has already been shown for soy protein-stabilized emulsions (7) and can be explained by the different structure of SSPS, highly branched and much less elongated than that of HMP (10).

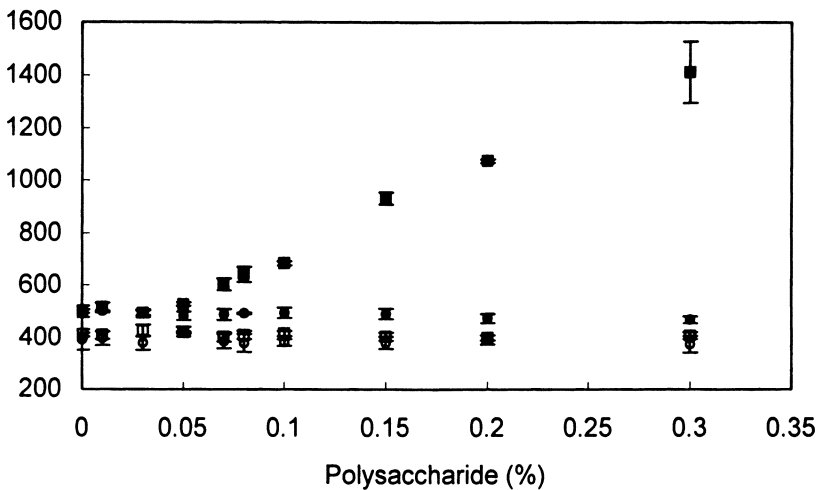


Figure 1. Average diameter as a function of polysaccharide added to sodium caseinate emulsions at pH 6.8, measured using DWS (filled symbols) and dynamic light scattering (empty symbols). Emulsions containing HMP (squares) and SSPS (circles).

Figure 2 illustrates the changes in the $1/l^*$ parameter measured by DWS and the ultrasonic attenuation measured by US in the emulsions at neutral pH as a function of polysaccharide concentration. When HMP is added to the emulsion the ultrasonic attenuation and the $1/l^*$ parameter show a decrease with HMP concentration up to 0.07 before leveling off with increasing concentration of HMP. It is clearly demonstrated that the results obtained from DWS and US are in full agreement.

The changes in $1/l^*$ can be associated to changes in the refractive index of the medium, particle size and spatial correlation between the scatterers. It is

possible to hypothesize that at low HMP concentrations no changes occur to the form factor ($F(q)$) and most of the changes are reflected by a rearrangement of the particles thus affecting ($S(q)$). This hypothesis is confirmed by the results obtained using ultrasonic spectroscopy: a decrease in the attenuation of sound with increasing HMP concentration. The formation of droplet-rich domains will cause an overlap of the viscothermal effects caused by the compression and decompression of the ultrasonic wave. The overlap of the viscothermal effect will decrease the thermal losses and this will be reflected in a decrease in the attenuation of the ultrasonic wave.

As both the $1/l^*$ parameter and the ultrasonic attenuation reflect changes in the arrangement of the colloidal particles in the system, it was concluded that the steep decrease in $1/l^*$ and attenuation at $\text{HMP} < 0.08\%$ was caused by the rearrangement of emulsion droplets in space because of the strong electrostatic repulsion between the HMP molecules and the oil droplets. At higher concentrations of HMP the depleted domains of oil droplets become more defined and macroscopic creaming is observed. At these higher concentrations of HMP the domains are more crowded, with not much difference in the overall spatial distribution, explaining the leveling off of the values of attenuation and $1/l^*$.

Confirming what was observed in Figure 1, the presence of SSPS does not cause restructuring of the emulsion droplets at concentrations as high as 0.3%. The $1/l^*$ parameter and ultrasonic attenuation remain constant as a function of concentration of SSPS. It can be concluded that the droplets' arrangement and

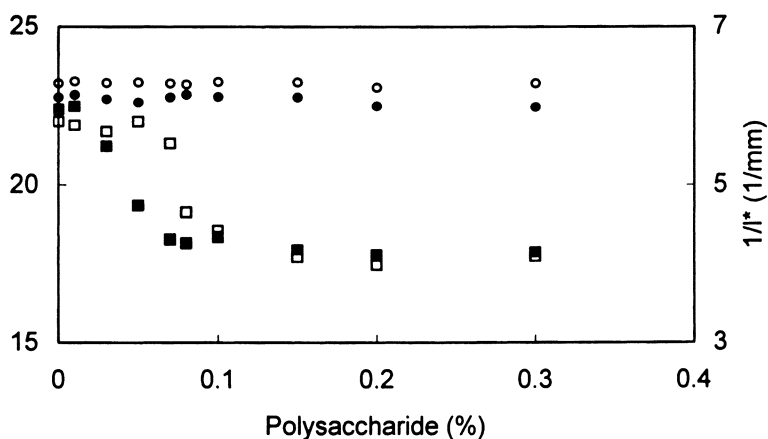


Figure 2. Values of $1/l^*$ measured by DWS (filled symbols) and ultrasonic attenuation at 5 MHz (empty symbols) for emulsions at pH 6.8 as a function of HMP (squares) or SSPS (circles) concentration.

the optical properties of the emulsions containing SSPS are not significantly different from those of the control emulsion with no polysaccharide.

The changes occurring during acidification of emulsions by addition of 0.3% GDL were also observed using DWS and ultrasonic spectroscopy (Figure 3). In control emulsions with no polysaccharide, the pH slowly decreases towards the isoelectric point of the caseins, causing a sol-gel transition at pH 5.6. At this pH the oil droplets aggregate because of the decrease of the electrostatic repulsion on the surface of the oil droplets. The results, shown in Figure 3 confirm previous reports on the acid-induced aggregation of casein emulsions (2, 3).

When the polysaccharides are present with sodium caseinate-stabilized oil droplets, numerous other reactions take place. The addition of 0.05% polysaccharide shifts the aggregation to a lower pH, with a lower pH for emulsions containing HMP (pH 4.5) compared to emulsions containing SSPS (pH 5.0), but in both cases this concentration (0.05%) is insufficient to stabilize the system. When enough SSPS or HMP are added to the mixture, the pH-induced aggregation is inhibited.

It is possible to suggest that both SSPS and HMP interact with positively charged casein patches via electrostatic interaction, as it has already been suggested for casein particles in acid milk dispersions (6, 9).

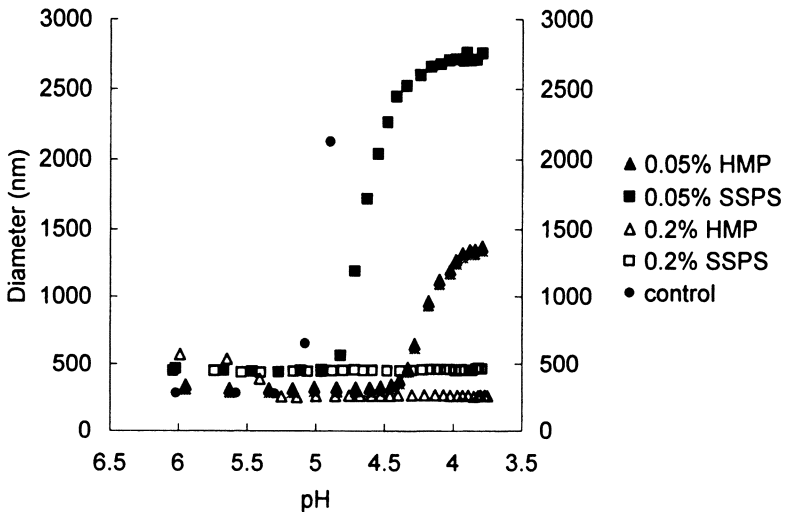


Figure 3. Average diameter as a function of pH during acidification, calculated from DWS measurements for emulsions containing SSPS and HMP.

Both DWS and ultrasonic spectroscopy show significant differences in the dynamics occurring to the emulsions during acidification (Figures 4 and 5) in the presence of the two polysaccharides. The values of $1/l^*$ are in full agreement with values of attenuation of sound.

When 0.2% SSPS was added to sodium caseinate emulsions no decrease in $1/l^*$ and attenuation can be observed (Figure 4). Since SSPS does not cause depletion flocculation and the adsorption of SSPS molecules does not change significantly the size of the emulsion droplets or the index of refraction of the droplets with the wavelength used in this study, no changes were measurable using a static measurement such as $1/l^*$. It may also be concluded that the oil droplets of emulsions containing 0.2% SSPS have a spatial distribution quite similar to that of the original emulsions.

Also in the emulsions containing 0.2% HMP the ultrasonic attenuation data are in full agreement with the light scattering data collected using DWS. In this case though, the presence of HMP in the emulsion causes a decrease of attenuation and $1/l^*$ values as already shown in Figure 2. This indicates that the energy losses of the ultrasonic wave were lower in the emulsion containing HMP, explaining the structuring of the oil droplets at high pH because of charge repulsion between polymers of like-charges. HMP forces the emulsion droplets to rearrange in microdomains at neutral pH, and this is clear from the decrease of $1/l^*$ value and attenuation. At a pH of about 5.6 both $1/l^*$ and attenuation of sound increase steeply reaching a plateau value at pH 5.4.

At this pH, the electrostatic interactions between HMP and the oil droplets cause the oil droplets to redisperse from the microdomains and occupy an average spatial distribution similar to that of the original emulsions at high pH. The $1/l^*$ values for 0.2% HMP emulsions at low pH are similar to those of the emulsions containing SSPS or emulsions with no polysaccharides, indicating that these emulsions with HMP at low pH have similar optical properties and a structural organization.

These results, collected with two techniques probing very different length scales, demonstrate that it is possible to study non-invasively and *in situ* very different interaction dynamics between the emulsion droplets. Both DWS and ultrasonic spectroscopy identify quite well changes in the physical aspects of the particles as well as the state of correlation of the system.

Acknowledgements

The authors would like to acknowledge CpKelco and Fuji Oil for providing research grade polysaccharides and the natural sciences and engineering council of Canada for funding.

References

1. Dickinson, E.; Caseins in emulsions: interfacial properties and interactions. *Int. Dairy J.* **1999**, *9*, 305-312.
2. Bonnet, C.; Corredig, M.; Alexander, M.; Stabilization of caseinate-covered oil droplets during acidification with high methoxyl pectin. *J. Agric. Food Chem.* **2005**, *53*, 8600-8606.
3. Dickinson, E.; Semenova, M.G.; Antipova, A.S.; Pelan, E.G.; Effect of high-methoxyl pectin on properties of casein-stabilized emulsions. *Food Hydrocoll.* **1998**, *12*, 425-432.
4. Moreau, L.; Kim, H.J.; Decker, E.A.; Mc Clements, D.J.; Production and Characterization of oil-in-water emulsions containing droplets stabilized by beta-lactoglobulin-pectin membranes. *J. Agric. Food Chem.* **2003**, *51*, 6612-6617.
5. Gancz, K.; Alexander, M.; Corredig, M.; In situ study of flocculation of whey protein-stabilized emulsions caused by addition of high methoxyl pectin. *Food Hydrocoll.* **2006**, *20*, 293-298.
6. Tromp, R.H.; de Kruif, C.G., van Eijk, M.; Rolin, C.; On the mechanism of stabilization of acidified milk drinks by pectin. *Food Hydrocoll.* **2004**, *18*, 565-572.
7. Roudsari, M.; Nakamura, A.; Smith, A.; Corredig, M.; Stabilizing behavior of soy soluble polysaccharide or high methoxyl pectin in soy protein isolate emulsions at low pH.
8. Nakamura, A.; Furuta, H.; Maeda, H.; Takao, T.; Nagamatsu, Y.; Yoshimoto, A.; Analysis of structural components and molecular construction of soybean soluble polysaccharides by stepwise enzymatic degradation. *BioSci. Biotech. Biochem.* **2001**, *65*, 2249-2258.
9. Nakamura, A.; Furuta, H.; Kato, M.; Maeda, H.; Nagamatsu, Y.; Effect of soybean soluble polysaccharides on the stability of milk protein under acidic conditions. *Food Hydrocoll.* **2003**, *17*, 333-343.
10. Wang, Q.; Huang, X.; Nakamura, A.; Burchard, W.; Hallett, F. R. Molecular characterization of soybean polysaccharides: An approach by size exclusion chromatography, dynamic and static light scattering methods. *Carbohydrates Res.* **2005**, *340*, 2637-2644.
11. Dukhin, A.S.; Goetz, P.J., Travers, B.; Use of ultrasound for characterizing dairy products. *J. Dairy Res.* **2005**, *88*, 1320-1334.
12. Allegra, J.R.; Hawley, S.A. Attenuation of sound in suspensions and emulsions: Theory and experiments. *J. Acoustic Soc.* **1972**, *51*, 1545-1564
13. Dukhin, A.S.; Goetz, P.J.; Wines, T.H.; Somasundaran, P.; Acoustic and electroacoustic spectroscopy. *Coll. Surf. A* **2000**, *173*, 127-158.
14. Weitz, D.A.; Pine, D.J.; In *Dynamic Light Scattering: The Method and Some Applications*. Brown, W. Ed.; Oxford University Press: Oxford, UK, 1993; pp 652-720.

15. Alexander, M.; Dalgleish, D. G.; Application of transmission diffusing wave spectroscopy to the study of gelation of milk by acidification and rennet. *Coll. Surf. B: Bioint.* **2004**, *38*, 83-90.
16. Buckin, V.; Smyth, C.; High-resolution ultrasonic resonator measurements for analysis of liquids. *Seminars Food Analysis*, **1999**, *4*, 113-130.

Chapter 11

Droplet-Size Dependent Solubilization and Crystallization of Lipids in Oil-in-Water Emulsion

N. Hasuo^{1,3}, T. Sonoda², S. Ueno¹, and K. Sato^{1,*}

¹Graduate School of Biosphere Science, Hiroshima University, Higashi, Hiroshima 739-8528, Japan

²Tanabe Pharmaceutical Company Ltd., Osaka 532-8505, Japan

³Current address: Meiji Dairies Company, Odawara 250-0862, Japan

We measured the rate and extent of solubilization and crystallization of lipids (long-chain fatty acids; lauric, myristic and palmitic acids) in oil-in-water emulsion with average oil droplet diameters of 120 nm, 170 nm, and 220 nm. We found that the rate and extent of the solubilized materials increased as the oil concentration in emulsion increased, the diameter of emulsion droplets decreased, the temperature of solubilization increased, and the melting points of the fatty acids decreased. The crystallization temperatures of the fatty acids in emulsion remarkably decreased compared with bulk oil. The present study demonstrated that the fatty acids became more solubilized and less crystallized when they are embedded in the nm-size emulsion droplets.

Introduction

Oil-in-water (O/W) emulsion and microemulsion have been investigated as an advanced delivery tool of pharmaceutical (1, 2, 3), cosmetic (4) and food materials (5) having water-insoluble and oil soluble properties. This is because the O/W emulsion droplets are expected to exhibit multiple functions such as controlled release (6) and high bioavailability (7). In order to make the O/W emulsion droplets more functional and stable in practical uses, various physicochemical studies are needed; e.g., increased solubilization, controlled release, stabilization at elevated temperature for sterilization, and chilled temperatures for storage. In particular, much attention has been paid to highly solubilized lipophilic materials in the O/W emulsion droplets in order to increase loading efficiency of the lipophilic materials in the emulsion. High solubilization is critically important for the oil droplets having diameters around 100 nm, since such droplets are new tools of delivery systems in nanotechnology applicable to food, cosmetics and pharmaceutical industries.

Solubilization of lipophilic molecules in micelle solutions has been thoroughly investigated (8). For solubilization of oil into micelle particles from oil droplets in the O/W emulsion, the solubilization kinetics are thought to be dominated by interfacial transport processes, which are affected by temperature, the nature of the oil/water interface, droplet-micelle interaction, and the chemical structure and molecular volume of the oil and surfactant molecules (9). Nizri and Magdassi studied the solubilization kinetics of small lipophilic molecules into nanoparticles made of surfactants and polymers, and demonstrated that the nanoparticles solubilize the lipophilic molecules at different positions of the particles depending on the polarity or lipophilicity of the molecules (10). The solubilization of oil in microemulsion was also investigated (11). Compared to solubilization in surfactant-based micelle solutions and microemulsion, few studies have been conducted on the effects of droplet sizes on the solubilization kinetics of lipophilic molecules in O/W emulsions.

In the present work, we prepared an O/W emulsion containing oil droplets with different average diameters (120 nm, 170 nm and 220 nm) by changing the high-pressure homogenization conditions. Usually, high-melting-temperature material is solubilized into the oil phase above its melting point. However, this method does not facilitate precise measurement of the time variation of the solubilization and the saturated solubilized quantity in the emulsion. Therefore, we solubilized the solid lipids below their melting point by adding crystal powders to the emulsion. The time variation of the solubilized quantity was thus examined at a constant temperature over 48 hours. Three long-chain fatty acids (lauric acid (LA), myristic acid (MA) and palmitic acid (PA)) were employed to measure the solubilization properties in the emulsion droplets, whereas lauric acid was solely examined in the crystallization experiments.

Materials and methods

Materials

Three fatty acids with purity of 99% were purchased from Sigma Aldrich (Steinheim, Germany), and used without further purification. Nanometer-sized emulsions were made of soybean oil and canola oil mixture as a dispersed oil phase, distilled water as a continuous phase, and polyglycerine fatty acid ester, decaglycerine monostearate (10G1S, Sakamoto Pharmaceutical Co., Osaka, Japan) as an emulsifier. The emulsification was carried out by using a high-pressure homogenizer (DeBEE 2000). The size of the oil droplets was varied by changing the ratio of oil-water-emulsifier (O-W-E, wt.%) and by changing the passing time of the emulsification at different emulsification pressures. The emulsion samples containing the oil droplets with different average diameters (D) were prepared under the following conditions: D~120 ± 30 nm; O-W-E =20-70-10, five passing times at 200 MPa, D~170 ± 30 nm; 20-75-5, five passing times at 138 MPa, and D~220 ± 30 nm; 20-77-3, five passing times at 100 MPa. As shown here, the oil concentration was always kept 20 % of the total emulsion samples. The droplet size was measured with an ELS 8000 (Otsuka Electronics, Tokyo) using dynamic light-scattering methods.

Solubilization

The solubilization experiments were conducted using the following methods. The powder crystal samples of the fatty acid (2 g) were put into the emulsion sample (40 g) placed in a thermostated vessel whose temperature was controlled within ±0.1°C. The emulsion sample containing the crystal powder was stirred with a magnetic stirrer (200 rpm). The solubilized quantity, defined as the fraction (%) of the weight of solubilized materials divided by the total weight of crystal powder, was obtained by weighing the crystal samples present in the vessel, which were separated from the emulsion by vacuum filtration using a membrane filter. Samples were weighed up to 48 hours for varying durations (short periods (minutes) in the initial stage to longer periods (hours) in the later stage of solubilization). The measurements were repeated three times to get the average values. The solubilization temperatures examined were 15 °C, 25 °C and 35 °C for LA (melting point, 44 °C); 25 °C, 35 °C and 45 °C for PA (melting point, 54 °C); and 35 °C, 45 °C and 55 °C for PA (melting point, 63 °C).

For comparison, the solubilities of the fatty acids in the bulk oil were measured at the same temperatures as those of the solubilization experiments in the emulsion. The solubilities of the three fatty acids in the water containing

10G1S of 2.5 wt.% (aqueous micelle solution) were measured. Samples were visually observed to determine the saturated concentration of the fatty acids in the oil phase and water phases at constant temperature.

Crystallization

Crystallization behavior of lauric acid solubilized in the bulk oil and emulsion was observed with DSC by synchrotron radiation X-ray diffraction (SR-XRD). DSC cooling and heating thermopeaks were measured by cooling from 50°C to 0°C, and heating from 0 °C to 50 °C at a rate of 2 °C/min, using Thermoplus 8240 (Rigaku, Tokyo). The SR-XRD measurements were performed in BL-15A stations of the synchrotron radiation facility, Photon Factory, in the High-Energy Accelerator Research Organization (KEK), Tsukuba, Japan. The details of the SAXS/WAXS instrument were reported elsewhere (12). The wavelength was 0.15 nm, and the X-ray beam shape was 1.0 mm (horizontal) x 0.7 mm (vertical). The emulsion samples were set in sample cells with internal dimensions of 5 mm (H) × 5 mm (V) × 1 mm (W), and the cells were immersed in a temperature control system, Linkam THMS600 (Linkam Scientific Instruments, Surrey, United Kingdom). The rate of cooling was 100 °C/min, with which isothermal crystallization was monitored by the SR-XRD technique.

Results and Discussion

Figure 1 illustrates the effect of the oil concentration in the emulsion on the solubilization quantity of LA in the emulsion samples with three average droplet diameters measured after stirring up to 5 hours at 35 °C. The oil concentration was varied by diluting the initially formed emulsion (oil concentration was 20 %) with water containing the same 10G1S concentrations as those of the emulsification. It was evident that the solubilized quantity increased in proportion to the oil concentration increase in the three types of emulsion. This demonstrated that LA was solubilized by the presence of the oil phase of the emulsion, and that the solubilized quantity increased as the droplet diameter decreased at every oil concentration. From this result, we fixed the oil concentration for the solubilization experiments at 5 %.

Figures 2 (a), (b) and (c) plot the time variations of the solubilized quantity of LA, MA and PA in the three types of emulsion measured at 35 °C. The following properties were observed in all cases.

- (a) The solubilized quantity rapidly increased soon after the solubilization started.

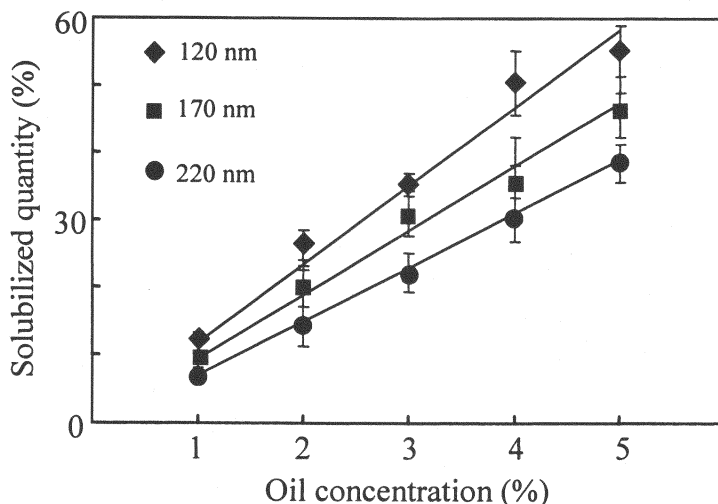


Figure 1. Solubilized quantity of lauric acid with varying oil concentration in emulsion measured after stirring for 5 hours at 35 °C.

- (b) The solubilized quantity increase began to slow down at around 6 hours, reached a saturated value after 12 hours, and remained constant for up to 48 hours.
- (c) The solubilization rate, defined as the time-dependence of solubilization in the initial stage, and the extent defined as saturated quantity of solubilization increased with decreasing diameter of the oil droplets.
- (d) The rate and extent of solubilization decreased as the melting point of fatty acid increased; it was the highest for LA and the lowest for PA.

Although not shown here, the above properties were commonly observed in the solubilization experiments of LA at 15 °C and 25°C, in MA at 25 °C and 45 °C, and in PA at 45 °C and 55 °C.

Table I summarizes the solubilization data of the three fatty acids obtained in the present study. The solubilized quantities after 48 hours are presented as representative data taken in the emulsion. It must be noted that the solubilized data in bulk oil correspond to thermodynamic solubility, whereas the data obtained in the emulsion do not correspond to solubility, since the O/W emulsion is not thermodynamically stable. Therefore, we refer to solubilized quantity for the case of emulsion.

In Table I, the solubilized quantities in emulsion are obviously larger than the solubilities in bulk oil for the three fatty acids at all temperatures and emulsion droplet sizes examined. More interestingly, the difference between them increased when the emulsion solubilization temperature and droplet

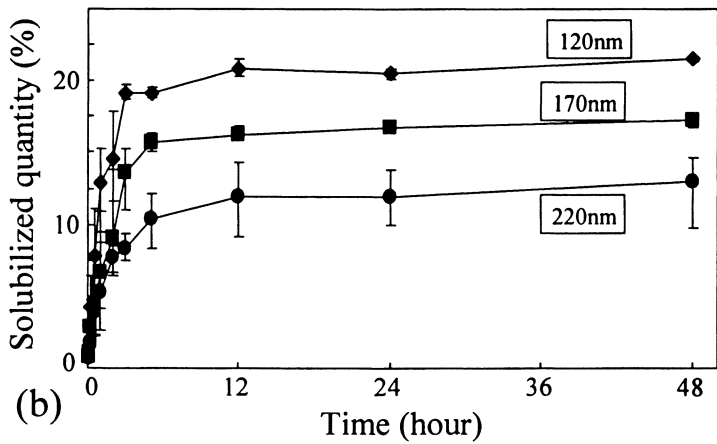
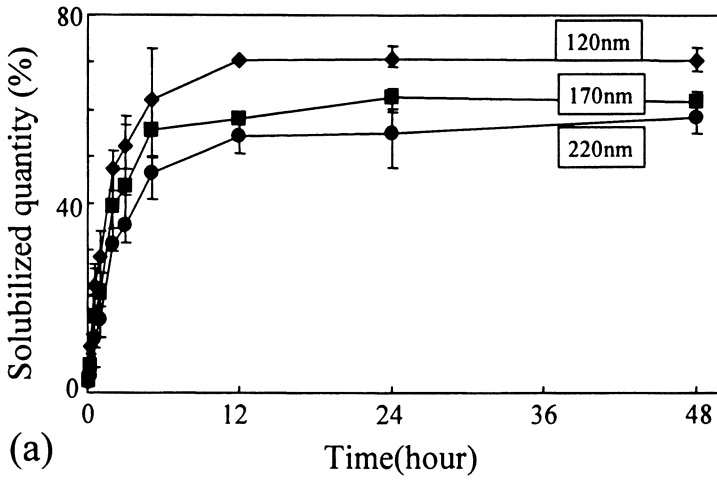


Figure 2. Time variation of solubilized quantity of (a) lauric acid, (b) myristic acid and (c) palmitic acid at 35 °C.

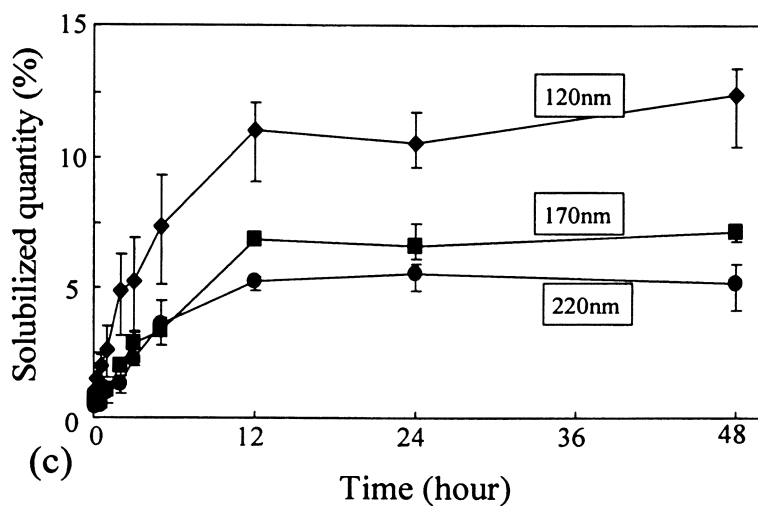


Figure 2. Continued.

Table I. Solubilized quantity (g/100g of salad oil) of fatty acids in emulsion, bulk oil and aqueous micelle solution.

		<i>Lauric acid</i>			<i>Myristic acid</i>			<i>Palmitic acid</i>		
T		15	25	35	25	35	45	35	45	55
D	120	8	18	70	10	21	56	10	19	62
	170	7	16	62	7	17	48	6	16	53
	220	6	14	59	4	13	36	5	11	38
B		3	13	50	2	11	34	2	10	33

NOTE: T; temperature (°C), D; emulsion diameter (nm), B: bulk oil.

diameter decreased. For example, the solubilized quantity of LA with D~220 nm at 25 °C was 14 g, and the solubility in bulk oil was 13.37 g, and the same values of PA at 45°C were 11 g (emulsion with D~220 nm) and 10.67 g (bulk). However, the solubilized quantities exceeded the solubilities of the bulk oil by 2.8 times (LA, D~120nm at 15 °C) and 4 times (MA, D~120 nm at 25 °C and PA, D~120 nm at 35 °C). From the results summarized in Table I, we may conclude that the solubility in the O/W emulsion was remarkably increased by decreasing the emulsion droplet size.

Figure 3 depicts DSC cooling thermopeaks of crystallization of lauric acid solubilized in bulk oil, and in the emulsion (average droplet diameter 120 nm) in which lauric acid was solubilized at 35 °C. In both cases, the solubilized quantity of lauric acid was 50 % with respect to the salad oil. An exothermic peak corresponding to the crystallization of lauric acid appeared at 29.7 °C in the bulk oil, whereas a small exothermic peak appeared at 12.1 °C in emulsion. These results indicate that crystallization of lauric acid was remarkably retarded in emulsion compared with bulk.

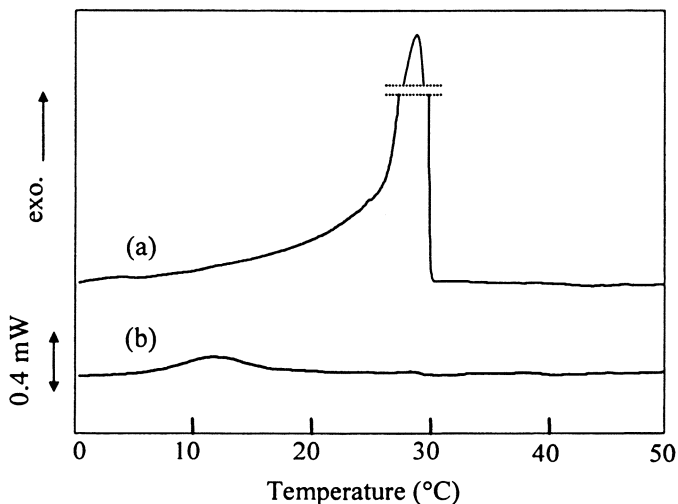


Figure 3. DSC cooling thermopeaks of lauric acid, (a) bulk salad oil and (b) emulsion with average droplet diameter of 120 nm.

Figure 4 illustrates the SR-XRD patterns of lauric acid crystals formed in emulsion (D~120 nm), in which lauric acid was solubilized to the quantity of 50 wt.% with respect to salad oil. The crystallization occurred at 12 °C, and its polymorphic form was C form, as judged from the WAXS pattern of 0.41 nm

and the SAXS pattern of 2.7 nm (13). The C form crystals melted at 34 °C during heating. These SR-XRD patterns were consistent with the DSC measurements. Although not shown here, the reduction in the crystallization temperature of lauric acid in emulsion was confirmed for the emulsion droplets containing different quantities of lauric acid.

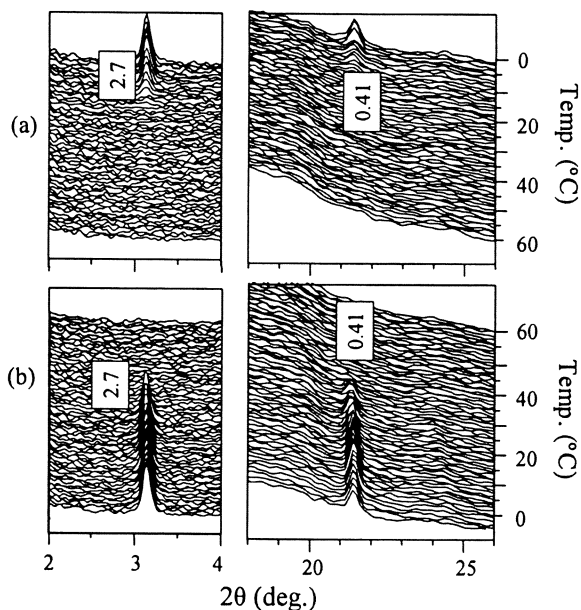


Figure 4. Synchrotron radiation-XRD patterns of bulk lauric acid and emulsion with solubilized lauric acid taken during (a) cooling and (b) heating.

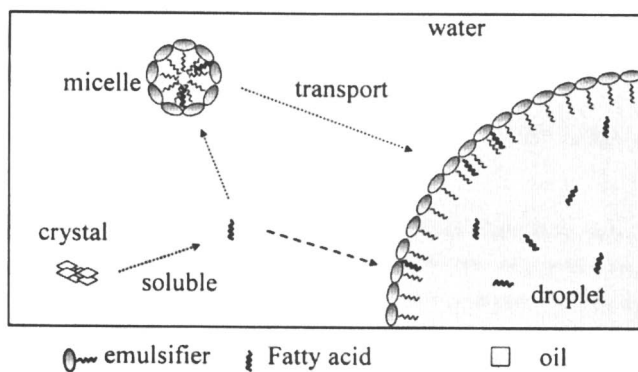


Figure 5. Schematic model of solubilization of lipid into emulsion droplets.

The above results indicate that the solubility of lipids was increased and the crystallization rates in nano-meter size emulsion droplets were retarded compared with the bulk oil. This may be interpreted by taking into account the solubilization mechanisms of lipophilic materials in micelles and emulsions (8) as illustrated in Figure 5. We assumed that the solubilization of the fatty acids from the crystal powders suspended in the aqueous phase in emulsion might first occur through solubilization in the aqueous phase and then through absorption into the emulsion droplets either directly from the aqueous phase and/or through solubilization into the micelle particles made of the emulsifiers, that may transport the fatty acids into the emulsion droplets. In the oil droplets in emulsion, there may be two states of solubilization of the fatty acids: in the oil phase and at the emulsion membrane surface. The latter state may be enabled for the fatty acids because of their amphiphilicity. The excess amount of solubilized quantity of the fatty acids in the emulsion droplets may be ascribed to the solubilization at the membrane interfaces whose relative importance compared with the volume size of the oil droplet increases with decreasing emulsion droplet size. Crystallization in the emulsion may be retarded by the size effects of the droplets as well as by the solubilization at the membrane interface that cause dilution effects of the crystallizing materials. Further precise clarification of these processes is necessary.

Acknowledgements

This work was supported in part by a grant from the Food Nanotechnology Project of the Ministry of Agriculture, Forest and Fisheries.

References

1. Tamilivanan, S. *Prog. Lipid Res.* **2004**, *43*, 489-533.
2. Kogan, A. ; Garti, N. *Adv. Coll. Interface Sci.*, **2006**, *123-126*, 369-385.
3. Bunjes, H.; Unruh, T. *Adv. Drug Deliv. Rev.*, **2007**, *59*, 379-402.
4. Bolzenger, M. A.; Cogne, C.; Lafferrere, I. ; Salvatori, F. ; Ardaud, P. ; Zanetti, M. ; Puel, F. *Coll. Surf. A.*, **2007**, *299*, 93-100.
5. Spemath, A. ; Aserin, A. *Adv. Coll. Interface Sci.*, **2006**, *128-130*, 47-64.
6. Malone, M. E.; Appleqvist, I. A. M. *J. Control. Release*, **2003**, *90*, 227-241.
7. Ton, N. M.; Chang, C.; Carpentier, Y. A. ; Deckelbaum, R. J. *Clin. Nutr.*, **2004**, *24*, 492-501.
8. Dickinson, E.; McClements, D. J. *Advances in Food Colloids*, Blackie Academic Professional, London, 1995, pp. 256-272.
9. McClements, D. J.; Dungan, S. R. *Coll. Surf. A*, **1995**, *104*, 127-135.

10. Nizri, G.; Magdassi, S. *J. Coll. Interface Sci.*, **2005**, *291*, 169-174.
11. Garti, N. ; Yaghmur, A. ; Leser, M. E. ; Clement, V. ; Watzke, H. J. *J. Agr. Food Chem.*, **2001**, *49*, 2552-2562.
12. Higami, M.; Ueno, S.; Segawa, T.; Iwanami, K.; Sato, K. *J. Am. Oil Chem. Soc.*, **2003**, *80*, 732-739.
13. Larsson K.; Quinn, P.; Sato, K. ; Tiberg, F. *Lipids : Structure, physical properties and functionality*, The Oily Press, Bridgwater, 2006, pp. 9-71.

Micro- and Nanoencapsulation for Food Applications

Chapter 12

Benefits of a Soy Lecithin Based Nanotechnology for the Animal and Human Food Industry

Scott E. Peters and Charles H. Brain

**Ingredient Innovations International, 146 South Bever Street,
Wooster, OH 44691**

The pharmaceutical industry has embraced nanotechnology to improve drug solubility and increase drug uptake. This nanotechnology can also be adapted to the animal and human food industry, delivering many of the same benefits. One such technology uses soy lecithin as the main structural ingredient in the formation of aqueous nanodispersions that carry high loads of water-insoluble actives. These actives include water-insoluble nutraceuticals, fat-soluble vitamins, and flavors. The encapsulated actives disperse easily into water-based products, showing improved stability and increased bioavailability. Recent analyses have shown that nanodispersions help protect actives against oxidation and pH extremes. Research with newly weaned calves has shown that nutrients encapsulated in nanodispersions reduce morbidity and delay the progression of respiratory disease. A separate study has shown a seven-fold increase in intestinal cell uptake of CoQ10 in nanodispersions versus traditional powder formulations. This soy lecithin based technology, benefits, and research will be discussed.

Introduction

Orally administered pharmaceutical drugs represent the easiest and most convenient form for delivery. However, oral drugs present a challenge to formulators and chemists. The drug's stability and absorption in the gastrointestinal (GI) tract is a major hurdle. The GI tract presents a variety of hurdles for a drug, from morphological barriers (microvilli and mucus layers) to stringent physiological factors (pH extremes and enzymatic activities), which conspire to limit intestinal absorption of the drug. For poorly water-soluble drugs, the problems are compounded by the fact that the drug's dissolution time in the GI tract may be longer than the drug's transit time in the GI system (1). Chemists have spent years developing systems to improve the absorption and delivery of these poorly water-soluble drugs.

Today, animal and human food chemists are taking the technologies that were developed for the pharmaceutical industry and adapting them to their markets. Water-insoluble nutrients and nutraceuticals are being encapsulated into systems that help improve absorption efficiencies and bioavailability. Most of these technologies are particulate delivery systems that are soluble or dispersible in an aqueous environment.

One of these technologies involves a soy lecithin based technology. The strategy of this system is to (a) provide the encapsulated nutrient with protection against degradation in the GI tract; (b) prolong the nutrient's transit time in the small intestine; and (c) be small enough to aid and facilitate translocation of the nutrient across epithelial barriers, thus improving bioavailability.

Small Intestinal Absorption

If the small intestine is viewed as a simple tube, its absorption surface area would be on the order of 0.5 m^2 . But in reality, the absorption surface area of the small intestine is roughly 250 m^2 (2). At first glance, the structure of the small intestine is similar to other regions of the digestive tube, but the small intestine incorporates three features which account for its huge absorptive surface area, as shown in Figure 1.

Mucosal folds, the inner surface of the small intestine, are not flat, but organized into circular folds, which not only increase surface area, but aid in mixing the ingesta by acting as baffles. Villi, multitudes of projections of the mucosa which protrude into the lumen, are covered with epithelial cells. Microvilli are located on the luminal plasma membrane of absorptive epithelial cells. The epithelial cell wall is studded with these densely-packed microvilli.

The transport of chemicals across the small intestinal membrane is a complex process involving several mechanisms (3). Hydrophilic molecules are absorbed through the paracellular route, a passive, diffusional transport pathway

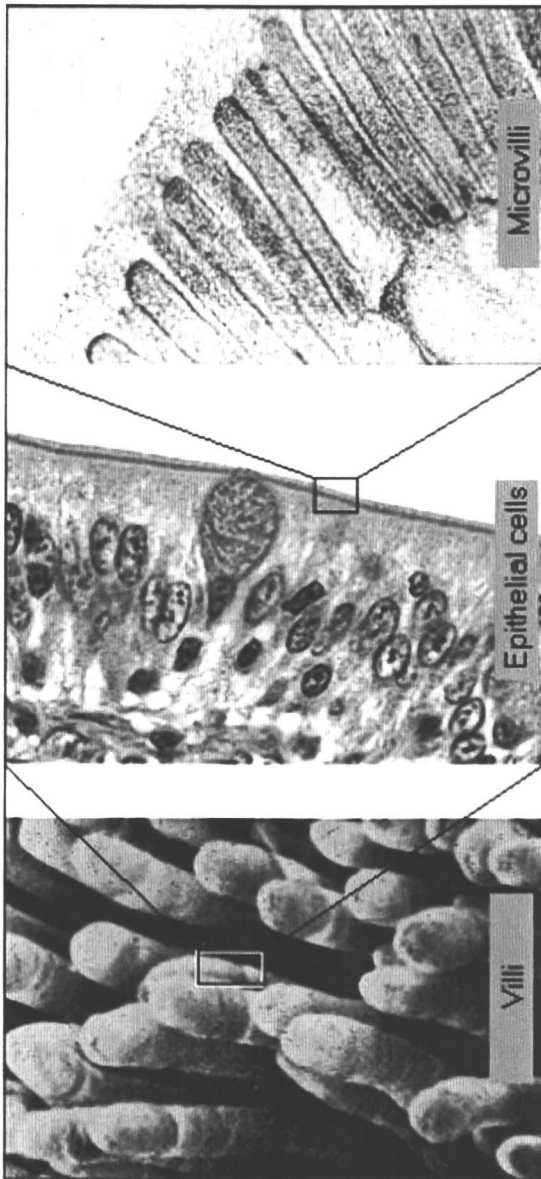


Figure 1. Three features of the small intestine's absorptive surface: villi, epithelial cells, and microvilli (2).

through the tight junction channels between adjacent epithelial cells. Hydrophobic, and lipophilic, molecules are absorbed through the lipid bilayer and the membrane-bound protein regions of the cell membrane located on the microvilli. The extent of uptake through the absorbing membrane varies considerably depending on the particle size, charge, and chemical composition/hydrophobicity.

The uptake of particles within the small intestine increases with decreasing particle size (4-6). Jani et al. (7,8) assessed the uptake of nanoparticles by rat intestines by monitoring the nanoparticles' appearance in the systemic circulation and distribution into different tissues. After administering equivalent doses, 33% of administered nanoparticles of 50-nm diameter and 26% of administered nanoparticles of 100-nm diameter were detected in the intestinal mucosa and gut-associated lymphoid tissues. Only 10% were found in the intestinal tissues for administered particles of 500-nm diameter. The uptake of particles administered with a diameter greater than 1 μm was marginal.

Studies also indicate that particles consisting of hydrophobic materials are more readily absorbed in the small intestines than hydrophilic particles (8). Additional studies examining the charge of these nanoparticles (7,10-12) concluded that neutral and positively charged nanoparticles have a higher affinity for intestinal epithelia than negatively charged nanoparticles. However, negatively charged nanoparticles were found to have bioadhesive properties, which may favor the transport process.

Technology for the Animal and Food Industries

The food and health markets have similar obstacles with regards to absorption of nutrients as the pharmaceutical market has with drugs. Many lipophilic nutrients are poorly absorbed by both animals and humans. The lessons learned in the pharmaceutical industry may be adapted to these markets with three real-world constraints.

First, the products produced must be made with ingredients that are accepted for use in the appropriate market. For example, FDA food grade ingredients must be used for anything entering the food market. Secondly, the product must be produced under conditions and at facilities acceptable for the market such as food GMP approved facilities. Finally, products must be produced in an economical manner.

Liposomes to Nanodispersions

Liposomes have been studied for years as drug carriers, for example to deliver insulin by oral administration (13). The food industry has also

investigated the use of liposomes as delivery systems for ingredients (14). Encapsulation of enzymes for accelerated cheese ripening, targeting of antimicrobial agents, and stabilization of vitamin C are some of the applications that have been tested and utilized in the food market. However, most of these applications refer to encapsulation of hydrophilic (water-soluble) materials. Liposomes have very little capacity to carry lipophilic (fat-soluble/water-insoluble) materials. The lipid bilayer of the liposome will only allow a payload of 1 to 2 percent lipophilic material.

We can adapt the liposome technology to allow for higher lipophilic loads. Additional ingredients can be added and ingredient ratios can be adjusted, resulting in nanoparticles that have interior lipophilic loads of 20 to 25 percent. Even though the lipid payload has increased dramatically, the outer chemical structure and physical properties of these nanoparticles are nearly identical to liposomes. For purposes of the remainder of this chapter, we will refer to these “adapted” liposomes as nanodispersions.

The main structural component of liposomes is the phospholipid. In the pharmaceutical industry, liposomes are produced using highly refined fractions of phosphatidylcholine, usually from an egg source. Nanodispersions also utilize phospholipids as the main structural component. Soy lecithin is usually the food grade source of these lipids, which consists of a mixture of phosphatidylcholine, phosphatidylethanolamine, phosphatidylinositol, phosphatidic acid, minor phospholipids, and various glycolipids. Food grade soy lecithins include standard soy lecithin, enzyme-modified soy lecithin, and hydroxylated soy lecithin.

In order to carry additional lipophilic loads, the nanodispersion formulation usually includes a co-surfactant. This co-surfactant aids in the emulsification and incorporation of the lipophilic material into the core of the nanodispersion. Examples of co-surfactants include polysorbates, polyglycerol fatty acid esters, copolymer condensates of ethylene oxide and propylene oxide, sucrose esters, and saponins.

These water-dispersible nanodispersions would normally be in aqueous solution at a neutral pH. However, at this pH, the fear of microbial contamination from bacteria, yeast, and molds is too great. Therefore, nanodispersion formulations frequently utilize an acidulant and antimicrobial agent to protect the product from microbial contamination. Acidulants, such as citric acid and ascorbic acid, are used to drop the solution pH to below 4.3, and antimicrobials like potassium sorbate and sodium benzoate may be added depending on the final acidity of the nanodispersion product.

Additional ingredients that may be utilized in the system include fat-soluble antioxidants, flavors, fats, and oils that may aid in the solubility of an active ingredient. A good example of a formula of a nanodispersion is the 10% Coenzyme Q10 Nanodispersion marketed by Tishcon Corporation, shown in Table I.

Table I. 10% Coenzyme Q10 Nanodisperion Formulation.^a

Ingredient	% in Formulation
Water	71.7%
Coenzyme Q10	10.0%
Medium Chain Triglycerides	10.0%
Soy Lecithin	4.0%
Polysorbate 80	2.5%
Citric Acid	0.4%
Potassium Sorbate	0.3%
Alpha-Tocopherol	0.1%

^a Tishcon Corporation's Liquid-Q® (Li-Q-Sorb®)

Even though the nanodispersions have a lipophilic payload of 20 to 25 percent, they still have very similar physical characteristics to liposomes. The outer structure of the nanodispersions still consists of phospholipid head groups, giving the particles a slight negative charge which aids in their charge repulsion of one another. This charge repulsion keeps the particles from agglomerating and results in an even dispersion throughout an aqueous medium. The mean particle size (mean diameter) of the nanodispersions, determined by laser diffraction particle analysis, is between 100 and 200 nm. This size also aids in the nanodispersion's dispersibility in aqueous medium via Brownian Motion. Because of the packing structure of the lecithin molecules in the outer shell of the nanodispersion, the nanodispersions have the advantage of being infinitely dilutable. Normal surfactant-based emulsions lose stability below their critical micelle concentrations.

Benefits of Nanodispersions

Increasingly more technologies promise benefits in the health and wellness market. It can be confusing to the formulation chemist whose job it is to utilize these technologies to formulate the best possible product for the consumer. Soy lecithin nanodispersions certainly do not solve all the formulation chemists' challenges. For some actives and final products, nanodispersions should not even be considered. Some of these may include products with high alcohol and propylene glycol concentrations, high surfactant content (as in shampoos), and pH ranges below three and above ten. However, for many applications, nanodispersions may provide benefits that help the formulation chemist achieve his or her goals of a new and improved product.

Ease of Dispersion

Nanodispersions can be easily added to any water-based consumer product. Because of their size and dispersibility, they are ideal for adding ingredients to beverages. There is no need for additional dispersing agents or weighting agents, and under almost every condition, the nanodispersions stay uniformly dispersed in the beverage for the shelf life of the product. Table II is a partial list of the actives that have been successfully encapsulated in nanodispersions.

Nanodispersions also give the product formulator an alternative to using solubilizing agents for some ingredients. For example, the most popular mouthwashes on the market today contain up to 27 percent alcohol. The alcohol is used to solubilize the flavors and antimicrobial agents that fight against “bad breath”. However, alcohol in mouthwashes is known to dry out the mouth and harden the enamel of the teeth. Alcohol mouthwashes are also not recommended for infants and young children. Encapsulating the mouthwash flavors and antimicrobial actives in nanodispersions gives the product formulator a non-alcohol solution.

Targeting

Nanodispersions can also be targeted to specific substrates to aid in delivery of actives to the intended site. Much of this technology was originally conceived and practiced in the pharmaceutical field. Drug delivery via liposomes can be targeted to a specific site utilizing “target” molecules that stick out of the liposome membrane and show binding affinity for a specific site in the body. Insulin delivery to the liver and chemotherapeutic drugs to cancerous tumors are two such examples of this technology.

In consumer products, this technology has been used extensively in the cosmetic field. Binding nanodispersions to the skin help in water resiliency for encapsulated sunscreens. Insect repellent actives, such as DEET, have been encapsulated in skin binding nanodispersions. The encapsulation not only keeps the active repellent on the skin longer, but decreases the deposition of the repellent into the skin. Thus the insect repellent is safer for subjects who may be harmed by excessive application of DEET-containing products.

The nanodispersions can also be modified to provide affinity to mucin-coated surfaces. Figure 2 demonstrates that nanodispersions modified by adding cetylpyridinium chloride (CPC) have a greater affinity for mucin (15). This specific experiment utilized mucin-coated sepharose beads. The CPC-modified nanodispersions have a greater affinity for the mucin-coated beads and remain associated to the beads even after a number of water washes.

Table II. Examples of Actives encapsulated in Nanodispersions.^a

Active Ingredient	% in Formulation
Astaxanthin	1%
Beta-Carotene	1%
Coenzyme Q10	10%
Essential Oils	20%
Fish Oils	20%
Flavor Oils	20%
Fragrance Oils	20%
Fruit Seed Oils	20%
Lutein Esters	1%
Lycopene	1%
Phosphatidylserine	1.5%
Phytosterol Esters	20%
Rose Hip Oil	20%
Sunscreen Actives	25%
Tocopherols	20%
Tocotrienols	20%
Vitamin A Palmitate	15%
Vitamin D	10%
Vitamin K	10%

^a Proprietary products produced by Ingredient Innovations Intl.

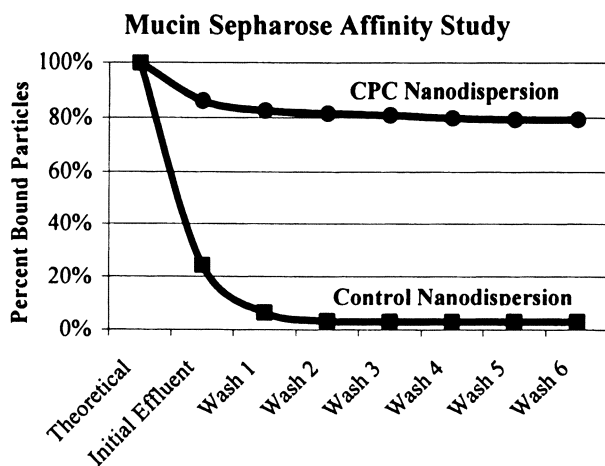


Figure 2. Affinity of targeted nanodispersions to mucin-coated sepharose (15).

Since the mouth and entire GI tract are mucin-coated, one could imagine numerous possibilities for this targeting technology. Mouthwash actives would have longer residence time in the mouth, so that flavor and antimicrobial actives would linger.

Controlled Release

Nanodispersions also control the release of their encapsulated actives. The mode of this release may vary depending on the conditions of the environment. For nutritional ingredients encapsulated and delivered orally, the mode of release from the nanodispersion is enzymatic degradation in the mouth from saliva and gastric acid degradation in the stomach. However, a large percentage of nanodispersions survive these conditions to reach the smaller intestines and aid in nutrient absorption.

Volatile components, such as flavors and fragrances, may also be encapsulated in nanodispersions. In the case of volatile compounds, the main mode of release for the nanodispersion is simple volatilization. When a flavor is encapsulated in a nanodispersion, the flavor will volatilize more slowly in the food product than it would if incorporated neat.

The release profile of fragrances can also be extended. A deodorant fragrance was encapsulated into a nanodispersion and formulated into an antiperspirant stick. The experimental antiperspirant was then compared to an antiperspirant that was formulated with neat fragrance at the same level. The test antiperspirants were applied to human subject's arms and compared by a standard sensory sniff test. Two benefits of the encapsulated fragrance can be seen from the data in Figure 3 (16).

Initially, the fragrance is stronger in the nanodispersion formulated antiperspirant. The higher initial fragrance in the nanodispersion product is due to the protection afforded to the fragrance during the antiperspirant production. Antiperspirant bases are prepared at temperatures of 60 to 75 °F. The fragrances are usually added as the bases are being cooled, but before the product becomes a solid. Some of the fragrance is inevitably flashed off during this process. The nanodispersions decrease the volatility of the fragrance and less fragrance is lost, resulting in a stronger fragrance initially.

After four hours, the decrease in fragrance perception is less for the antiperspirant formulated with the nanodispersions as compared with the fragrance incorporated neat. The fragrance is released more slowly from the nanodispersions, which increases the fragrance perception level for a longer period of time.

Similar results have been reported for flavors formulated into foods (17). Flavors have been retained better during heat processing and in baked goods, resulting in longer flavor perception in the mouth.

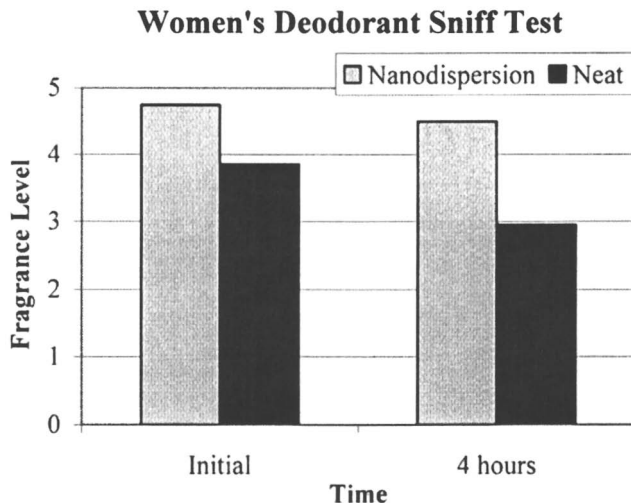


Figure 3. Fragrance sniff test of two antiperspirants (16).

Protection of Ingredients

Nanodispersions can protect a sensitive payload against the surrounding environment, such as pH extremes and other ingredient interactions that may take place. Oxidation of ingredients is always a concern, especially with flavors and unsaturated oils. For example, fish oil which has reported benefits for human health, is unstable. The beneficial, polyunsaturated fatty acids in the oil are very susceptible to oxidation, resulting in a “fishy” odor and flavor. Needless to say, this “fishy” flavor complicates food and beverage formulations.

Encapsulating the fish oil into a nanodispersion does increase the protection of the oil against oxidation, but by no means eliminates it. The oxidative stability of the fish oil can be increased further by adding antioxidants to the system. Ascorbic acid is a notable water-soluble oxygen scavenger. However, when a formulation chemist dilutes the nanodispersions into the final food or beverage, the ascorbic acid is also diluted and does not protect the product as well. Therefore, it is best to formulate lipophilic antioxidants into the nanodispersions rather than using water-soluble antioxidants. Encapsulation assures that the antioxidant activities remain intact even after dilution of the nanodispersions. Beverages with antioxidant rich, fish oil nanodispersions have shown a 10-fold increase in shelf life (until “fishy” odor appears) compared to other oil-in-water emulsion systems (18).

Another example of ingredient protection afforded by nanodispersions was shown through a study of newly received feedlot cattle at The Ohio State University’s Agricultural Research and Development Center (19). Stresses and

nutrient deficiencies associated with weaning beef calves and placing them in a feedlot increases susceptibility to respiratory disease. This is a \$500 million problem annually in the beef industry today.

The rumen environment has a major affect on nutrients available for absorption in cattle. The rumen is the first compartment of the ruminant stomach of cattle and is the site of bacterial fermentation of feeds. Bacterial fermentation and growth allow for fiber digestion and supply the host animal with energy, amino acids, and some vitamins. However, this fermentation environment also has some negative consequences, such as destruction of vitamins and alteration of mineral-containing compounds, which reduce their availability for absorption.

Nanodispersions were used to protect nutrients believed to improve health and enhance immune function. Nanodispersions were added to the feed of these cattle to protect the nutrients in the rumen and facilitate a quicker passage of nutrients to the small intestines where they could be absorbed. Through the first 16 days of treatment calves fed the nanodispersion-enriched diets were 5 times less likely to develop respiratory disease as those cattle receiving traditional nutrient-enriched feed. Serum levels of vitamin E were also shown to be higher in the nanodispersion feed group, providing evidence that nanodispersions conferred some ruminal protection of vitamin E.

Increased Bioavailability

Whereas the benefits discussed above are interesting and exciting, the potential for increased bioavailability of nutrients may be the most significant application of nanodispersions. As reviewed earlier in this chapter, nanodispersions have the physical characteristics to be superior carriers of nutrients and nutraceuticals. They can aid in protecting the payload against the environment of the GI tract and in promoting the final absorption of nutrients in the small intestine. Some evidence may infer that vitamin E absorption was enhanced in the small intestine in the above cattle study.

No better study can be given for the bioavailability enhancement provide by nanodispersions than a study done at The Ohio State University Department of Human Nutrition (20). Coenzyme Q10 has been shown to have many beneficial effects on the heart, brain, kidneys, and other human tissues. Coenzyme Q10 plays a key role in mitochondrial cell physiology and is known as a powerful systemic antioxidant. However, coenzyme Q10 is a crystalline material that is insoluble in water and has very limited solubility in oil. The absorption of CoQ10 when administered orally tends to be slow and ineffective. Only 5 to 10 percent of the administered dose of coenzyme Q10 is absorbed by the body and shows appreciable variability.

The investigational study conducted at The Ohio State University followed an experimental design such as the one shown in Figure 4 (21). The coenzyme

Q10 products were subjected to simulated gastric and small intestinal digestion by a slight modification of the method reported by Garret et al. (22,23). The digesta was added to wells containing differentiated monolayers of Caco-2 human intestinal cells. Following incubation, the cells were washed and cellular coenzyme Q10 content was determined by HPLC.

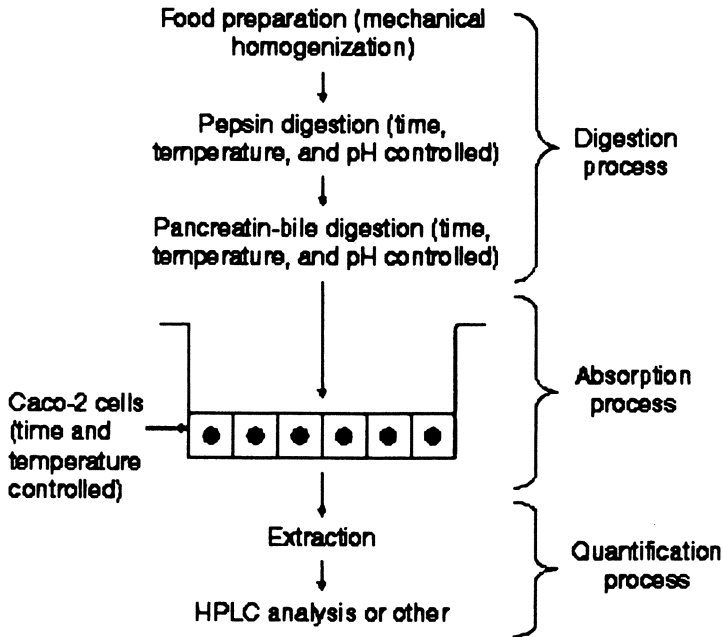


Figure 4. Diagram of an in vitro method to determine bioavailability using a Caco-2 cell culture (21).

The study examined the digestive stability and absorption of coenzyme Q10 from a variety of commercially available coenzyme Q10 products. The amount of coenzyme Q10 accumulated in the cells incubated with micelles generated during simulated digestion of the test products is shown in Table III. The percent uptake was relative to the reference product set to 100 percent.

The nanodispersions containing coenzyme Q10 shows a 7-fold uptake into Caco-2 cells compared to commercial dry tablet forms. The nanodispersions also show a 2-fold improvement in cell uptake over a commercial chewable tablet and a commercial softgel formulation. The Caco-2 human intestinal cell model tested for other essential nutrients has consistently provided results that are quantitatively comparable to bioavailability data from human studies (24,25),

Table III. CoQ10 uptake (%) by Caco-2 Cells (20).

Product	CoQ10 uptake ^a (pmol/mg protein)	% Uptake ^b
CoQ10 (USP)	35 ± 6	100
CoQ10 Tablet A	49 ± 4	141
CoQ10 Tablet B	34 ± 9	98
CoQ10 Tablet C	30 ± 7	86
Chew-Q® ^c Tablet	119 ± 33	342
Q-Gel® ^c Softgel	126 ± 26	362
Hydro-Q-Sorb® ^c powder	257 ± 5	739
Liquid-Q® ^d (Li-Q-Sorb® ^d)	241 ± 10	693

^a Values are mean ± SEM, n=6.

^b CoQ10 powder, reference product was assigned a value of 100%.

^c Tishcon Corporation.

^d Nanodispersion of CoenzymeQ10, Tishcon Corporation.

so it can be inferred that improved uptake for the nanodispersion encapsulated coenzyme Q10 would also occur in humans.

Production and Economic Considerations

Soy lecithin based nanodispersions offer human and animal food/health markets a broad range of benefits. Chemists, in labs everywhere, can produce nanodispersions and other delivery systems that supply certain benefits. First, your formulation must contain only food-approved ingredients. These ingredients must also be at levels that, when formulated into any final products, conform to FDA guidelines. However, producing nanodispersions at a large enough scale with economical feasibility to supply the human food market, requires taking nanodispersion technology a step further.

Production of nanodispersions can be done several ways in a lab environment, but only a few companies can provide the quantities suitable for economically feasible large-scale production. Ultra-high shear homogenizers and microfluidizers are available and can produce products at approximately 1000 pounds per hour. This ultra-high shear equipment must also be FDA approved for food products and be easily cleaned.

Even if one were fortunate enough to have equipment and food-grade formulations at the ready, the market still “drives the bus”. Companies, marketing the final food product, will make the final judgement regarding nanodispersions and weigh the benefits in their individual markets. Does the 7-

fold increase in bioavailability of coenzyme Q10 afforded through the use of nanotechnology justify the added cost to a beverage manufacturer looking for a “heart healthy” formula? Is increasing the cost of yogurt a penny per serving an acceptable charge, if it results in a perceptible extension of flavor for the customer? Is a vitamin formulation intended for cattle, with improved protection against ruminal degradation, a safer and more economical alternative to antibiotic usage?

Studies confirming the benefits of nanodispersion technology and the benefits provided to manufacturers and their customers are ongoing. The industry eagerly awaits the completion and distribution of these findings.

References

1. Horter, D.; Dressman, J. B. *Adv. Drug Delivery Rev.* **2001**, *46*, 75-87.
2. Bowen, R. Gross and Microscopic Anatomy of the Small Intestine. <http://www.vivo.colostate.edu/hbooks/pathphys/digestion/smallgut/anatomy.html> (accessed March 2007).
3. Francis, M. F.; Cristea, M. *Pure Appl. Chem.* **2004**, *76*, 1321-1335.
4. Florence, A. T.; Hussain, N. *Adv. Drug Delivery Rev.* **2001**, *50*, S69-S89.
5. Sass, W.; Dreyer, H. P.; Seifert, J. *Am. J. Gastroenterol.* **1990**, *85*, 255-260.
6. Jenkins, P. G.; Howard, K. A.; Blackball, N. W.; Thomas, N. W.; Davis, S. S.; O'Hagan, D. T. *J. Controlled Release* **1994**, *29*, 339-350.
7. Jani, P.; Halbert, G. W.; Langridge, J.; Florence, A. T. *J. Pharm. Pharmacol.* **1989**, *41*, 809-812.
8. Jani, P.; Halbert, G. W.; Langridge, J.; Florence, A. T. *J. Pharm. Pharmacol.* **1990**, *42*, 821-826.
9. Elridge, J. H.; Hammond, C. J.; Meulbroek, A.; Staas, J. K.; Gilley, R. M.; Tice, T. R. *J. Controlled Release* **1990**, *11*, 205-214.
10. Hillery, A. M.; Jani, P. U.; Florence, A. T. *J. Drug Target.* **1994**, *2*, 151-156.
11. Mathiowitz, E.; Jacob, J. S.; Jong, Y. S.; Carino, G. P.; Chickering, D.; Charturved, P.; Santos, C. A.; Vijayaraghavan, K.; Montgomery, S.; Bassett, M.; Morrell, C. *Nature* **1997**, *386*, 410-414.
12. Kriwet, B.; Walter, E.; Kissel, T. *J. Controlled Release* **1998**, *56*, 149-158.
13. Damge, C.; Michel, C.; Aprahamian, M.; Couvreur, P. *Diabetes* **1988**, *37*, 246-251.
14. Kirby, C. J. In *Liposome Technology, Entrapment of Drugs and Other Materials*; Gregoriadis, G., Ed.; 2nd ed., Vol. II; CRC Press; Boca Raton, FL, **1993**, 215-232.
15. Peters, S. E. Ingredient Innovations Int'l, Wooster, OH. Unpublished work, 2003.

16. Dente, S. Robertet Fragrances. Private communication, 2004.
17. Lengerich, B. V.; Haynes, L. C.; Levine, H.; Otterburn, M. S.; Mathewson, P.; Finley, J. Extrusion baking of cookies having liposome encapsulated ingredients. U.S. Patent 4,999,208, March 12, 1991.
18. Peters, S. E. Ingredient Innovations Int'l, Wooster, OH. Unpublished work, 2007.
19. Loerch, S.; Fluharty, F. *Liposome Protected Nutrients for Newly Received Feedlot Cattle*; Final Report; OARDC, The Ohio State University: Wooster, OH, May 2006.
20. Bhagavan, H.N.; Chopra, R.K.; Craft, N.E.; Chitchumroonchokchai, C.; Failla, M.L. *Int. J. of Pharm.* **2007**, *333*, 112-117.
21. Parada, J.; Aguilera, J. M. *J Food Sci.*, **2007**, *72*, R21-R32.
22. Garrett, D. A.; Failla, M. L.; Sarama, R. J. *J. Agric. Food Chem.* **1999**, *47*, 4301-4309.
23. Garrett, D. A.; Failla, M. L.; Sarama, R. J.; Craft, N. *J. Nutr. Biochem.* **1999**, *10*, 573-581.
24. Lau, Y. Y.; Chen, Y. H.; Liu, T. T.; Li, C.; Cui, X., White, R. E.; Cheng, R. C. *Drug Metab. Dispos.* **2004**, *32*, 937-942.
25. Chitchumroonchokchai, J.; Failla, M. L. *J. Nutr.* **2006**, *136*, 588-594.

Chapter 13

Enhancing Stability and Oral Bioavailability of Polyphenols Using Nanoemulsions

Xiaoyong Wang, Yu-Wen Wang, and Qingrong Huang^{*}

Department of Food Science, Rutgers, The State University of New Jersey,
65 Dudley Road, New Brunswick, NJ 08901

The health promotion properties of polyphenols have attracted a lot of attention in recent years because their biological and pharmacological effects including antioxidative, anticancer, and chronic disease prevention properties have been demonstrated in numerous animal, human, and *in vitro* studies. One of the major challenges of polyphenols is their poor stabilities and low oral bioavailabilities. Nanoemulsions are a class of extremely small emulsion droplets usually in the range of 50-200 nm, much smaller than the sizes (from 1 to 100 μm) of normal emulsions. Nanoemulsions offer advantages of excellent stability to encapsulate active compounds due to their small droplet sizes and high kinetic stability. High-pressure homogenized nanoemulsions formed by various amounts of water, oil, and emulsifiers were prepared, and their microstructure and size were measured using an inverted optical microscope and particle size analyzer, respectively. The pH and long-term stabilities of polyphenols including epigallocatechin gallate (EGCG) and curcumin encapsulated in nanoemulsions were evaluated by HPLC analysis and UV. The antiinflammation and antitumor functions of nanoemulsion-encapsulated polyphenols were tested in mice. The results suggest that nanoemulsions could improve stability and oral bioavailability of EGCG and curcumin.

Introduction

The functional food market is experiencing a rapid increase in recent years, driven by both increasing fortification with healthy food ingredients and consumer demand for novel food products. Polyphenols with health benefits have received much attention from the scientific community, consumers, and food manufacturers because polyphenols may be used to lower blood pressure, reduce cancer risk factors, regulate digestive tract system, strengthen immune systems, regulate growth, regulate sugar concentration in blood, lower cholesterol levels, serve as antioxidant agents and more (1, 2, 3). Although the use of polyphenols in capsules and tablets is abundant, their biological effects are frequently diminished or even lost since many of these polyphenols are not soluble in water, vegetable oils or other food-grade solvents. Furthermore, instability under conditions encountered in product processing (temperature, oxygen, light) or in gastro-intestinal tract (pH, enzymes, presence of other nutrients), insufficient gastric residence time, low permeability and solubility within the gut, as well as poor oral bioavailabilities limit the activity and potential health benefits of polyphenol molecules (4). Thus, the development of high quality, stable polyphenols with improved stability and oral bioavailability at the time of consumption, and deliver them to the physiological targets within the organisms represents a major potential impact on the functional food industry.

Tea Catechins

It was suggested that “as a warm or cold drink, perhaps tea should become a part of our dietary traditions to lower the incidence of major chronic disease, including cancer” (5). Tea is the second most popular beverage, next to water in the world in recent years, primarily because of their beneficial biological and pharmacological effects, including antioxidant, antimutagenic, anticarcinogenic, antiviral, antiinflammatory, and anticancer activities (6, 7). However, the most current suggestion offered by researchers is to drink more than ten cups of tea per day, which is obviously impractical for the general population. The problem is mainly from both low stability and poor oral bioavailability of tea polyphenols. In green tea, the polyphenol compounds are called tea catechins, including epigallocatechin gallate (EGCG), epigallocatechin (EGC), epicatechin gallate (ECG), and epicatechin (EC), as shown in Figure 1. EGCG is easily to be oxidized in neutral or basic pH (8, 9). The half-life of EGCG is less than 2 hours in solution of pH 7.4. The possible pathway for EGCG oxidization is believed that two hydroxy groups in phenyl B first convert into carbonyl groups, then they are oxidized into highly reactive quinone derivatives, which may be further oxidized into polymeric compounds like theaflavins, theasinensins, and thearubigins.

bigins (10), as shown in Figure 2. In *in vitro* cancer cell line studies (11, 12, 13), the applied EGCG concentration is usually higher than 10 μM , but consumption of green tea or pure EGCG by human subjects only resulted in plasma EGCG levels in low μM range, which was much lower than the concentration used in most *in vitro* studies. The effective EGCG levels in tissues and blood corresponded to 0.0003-0.45% of the ingested dose. Plus, tea catechins are also subjected to phase II metabolism of their methylated, glucuronidated, and sulfated metabolites. Particularly, most flavonoids exist in glucose-conjugated

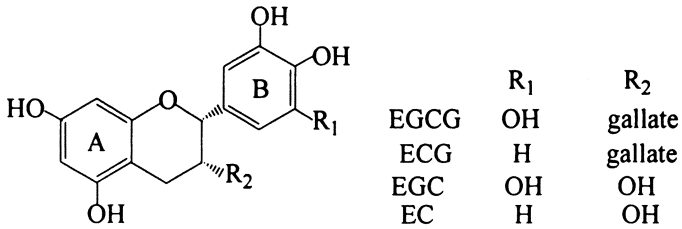


Figure 1. Chemical structures of tea catechins.

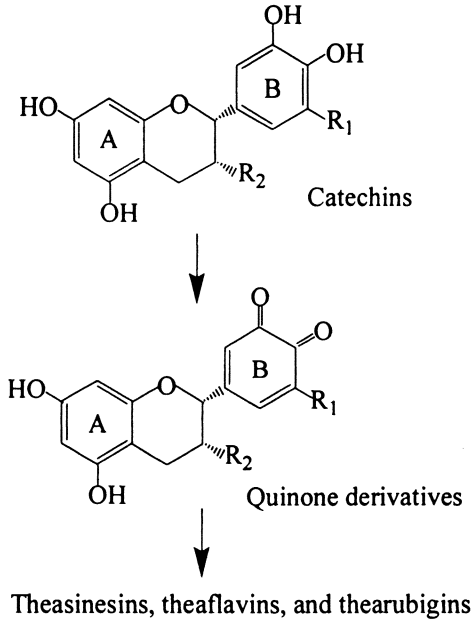


Figure 2. The possible pathway for EGCG oxidation.

form. They cannot be absorbed by the small intestine due to their high hydrophilicity.

Curcumin

Curcumin is a natural polyphenolic phytochemical extracted from the powdered rhizomes of turmeric (*Curcuma Longa*), and its chemical structure is shown in Figure 3. Curcumin is a FDA-approved food additive, and used widely as a preservative and yellow coloring agent for foods, drugs, and cosmetics. In addition to its effective antioxidant, antitumor, anti-inflammatory, antibacterial, antifungal, antiviral, anticoagulant, anticarcinogenic and free radical scavenger properties, it was reported that curcumin is a potent agent against many diseases including biliary disorders, anorexia, coughs, diabetes, hepatic disorders, rheumatism, sinusitis, cancer, and Alzheimer disease (14, 15). It was suggested that hydroxyl groups of the benzene rings, double bonds in the alkene part of the molecule, and the central β -diketone moiety may be responsible for its high biological activity (16). Despite its impressive array of beneficial bioactivities, orally administered curcumin is mostly excreted in the faeces and the urine, and little is detected in blood plasma (17). One reason is that curcumin has low solubility and does not disperse for absorption. Furthermore, the absorbed curcumin is rapidly metabolized in the intestine and liver to form several reduction products (di-, tetra-, and hexa-hydrocurcumin and hexahydrocurcuminol) and their glucuronide or sulfate conjugates (18). The poor absorption and fast metabolism may be responsible for the low bioavailability of curcumin. In addition, curcumin is also unstable in basic pH and very sensitive to light. Therefore, it is necessary to increase the stability and bioavailability of phytopolyphenols to expand their beneficial health potentials.

Encapsulation Techniques

Encapsulation of active ingredients, such as flavor, food color, and phytochemicals, is a very important component in food industry. To overcome instability and to enhance the bioavailability of these polyphenols, one option is to entrap these compounds of interest into a food matrix through encapsulation approach. Encapsulation can be used to protect active ingredients from moisture, heat, and oxidation, thus enhancing their stability and viability. Encapsulation can also be used to mask bad odors and bitter tastes of the compounds. Encapsulation is a technique by which one material or a mixture of materials are coated with or entrapped within another material or system (19). The coated

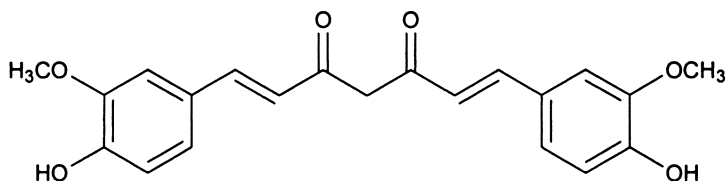


Figure 3. Chemical structure of curcumin.

material is called active or core material, and the coating material is called shell, wall material, carrier, or encapsulant. Many encapsulation techniques, such as spray drying, spray chilling and cooling, coacervation, fluidized bed coating, liposome entrapment, rotational suspension separation, extrusion and inclusion complexation, have been developed in the food and dietary supplement industries.

Emulsion

Emulsion is one common encapsulation technique for constructing an appropriate vehicle. An emulsion is a complex system made up of two immiscible fluids (usually oil and water), with one of the liquids dispersed as small spherical droplets in the other. A system that consists of oil droplets dispersed in an aqueous phase is called an oil-in-water or O/W emulsion, whereas water-in-oil or W/O emulsion means water droplets dispersed in an oil phase. HLB (hydrophile-lipophile balance) is useful in emulsifier selection. An emulsifier with low HLB value favors the formation of W/O emulsion, while higher HLB value favors the formation of O/W emulsion. In addition to the conventional O/W or W/O emulsions, there are various types of multiple emulsions, such as oil-in-water-in-oil (O/W/O) or water-in-oil-in-water (W/O/W) emulsions

One important problem associated with emulsion systems is their stability. The main mechanisms of instability leading to complete phase separation of emulsions include flocculation, coalescence, creaming, and sedimentation, as shown schematically in Figure 4. The original emulsions are usually heterogeneous, containing both small and big droplets. When two or more droplets come together to form an aggregate in which the droplets retain their individual integrity, this is called "flocculation", whereas coalescence is the process wherein two or more droplets merge together to form a single larger droplet. Creaming and sedimentation are both forms of gravitational separation. Creaming describes the upward movement of droplets due to the fact that they have a lower density than the surrounding liquid, whereas sedimentation

describes the downward movement of droplets due to the fact that they have a higher density than the surrounding liquid. Creaming in emulsions may be described by Stokes' equation as follows (20): $v_{\text{Stokes}} = -\frac{2gr^2(\rho_2 - \rho_1)}{9\eta_1}$, where

v_{Stokes} is the creaming rate of an isolated droplet in emulsion, r is the radius of the droplet, g is the acceleration due to gravity, ρ_1 and ρ_2 are the density of the continuous and dispersed phases, respectively. The sign of v_{Stokes} determines whether the droplet move upward (+) or downward (-). Stokes' law indicates that the velocity at which a droplet moves is proportional to the square of its radius. Therefore, one way to decrease the creaming velocity of a spherical emulsion droplet is to reduce its diameter.

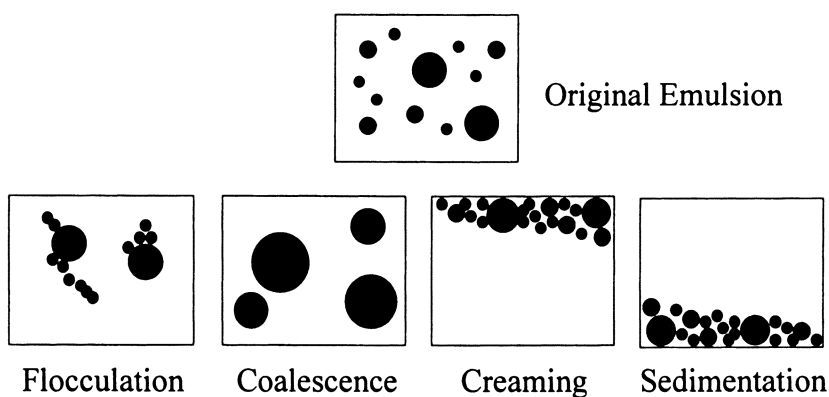


Figure 4. Various instable mechanisms for emulsions.

Nanoemulsion

The stability of emulsion could be significantly improved when the size of droplets in the emulsion is reduced to nano-scale, which may be called "nanoemulsions". Nanoemulsions are a class of extremely small droplet emulsions that appear to be transparent or translucent with a bluish coloration (21, 22). They are usually in the range 50-200 nm but much smaller than the range (from 1 to 100 μm) for conventional emulsions. Similar to the conventional emulsions, either oil-in-water (O/W) or water-in-oil (W/O) nanoemulsions could be prepared. Although nanoemulsions are usually thermodynamically unstable systems, due to their characteristic sizes, they may possess high kinetic stability against creaming or sedimentation. First, the very small droplet size causes a large reduction in the gravity force, and the Brownian

diffusion may prevent any creaming or sedimentation. Second, the steric stabilization prevents flocculation or coalescence of the droplets.

Nanoemulsion can be prepared by the so-called dispersion or high-energy emulsification methods (23), such as high-shear stirring, high-pressure homogenization, and ultrasonic homogenization. On the other hand, the condensation or low-energy emulsification methods (24), such as phase inversion temperature method, could produce nanoemulsion almost spontaneously. Although the preparation of nanoemulsions is more complex than that of conventional emulsions, an important advantage of nanoemulsions from a practical point of view is that they require lower amounts of stabilizers for their formation. Unlike conventional emulsions, which require a high concentration of emulsifiers for their preparation (usually in the range of 10-30 wt%), nanoemulsions can be prepared at moderate emulsifier concentration (in the range of 2-8 wt%).

High-pressure homogenizer is the most widely used emulsifying machine to prepare nanoemulsions in food industry, which leads to a better control of the droplet size and a large choice of compositions. Practically, high-pressure homogenizers are more effective at reducing the droplet sizes of pre-mixed emulsions than the simple mixtures of oil and water. Figure 5 shows the general process of constructing a nanoemulsion. First, water, oil, and emulsifier are mixed together at certain ratios under magnetic stirring. The mixtures then experience high-speed and high-pressure homogenization to finally obtain nanoemulsions. We vary the compositions of emulsions processed using high-speed and high-pressure homogenization, as shown in Table I. When the shear rate of high-speed homogenization is 24,000 rpm, stable emulsion can be obtained only when the emulsifier amount is higher than 10%. Otherwise, the emulsions are unstable and will separate within several hours. High-pressure homogenization at 1,000 bar can reduce the emulsifier amount to 2% to obtain stable emulsion. For the fixed emulsifier/oil/water ratio of 2/10/88, Figure 6 shows the optical microscope images of different emulsions measured by inverted optical microscope (Nikon TE2000, Nikon Corporation, Japan) (25). It is noted that the premixed emulsion has bigger droplets with diameters in the range of 10-20 μm , and this emulsion is very heterogeneous. There are some small droplets observed in high-speed homogenized emulsions, whereas we almost can not see any droplets in the high-pressure homogenized emulsions owing to much smaller sizes of emulsion droplets. Using dynamic light scattering (90 plus Particle Size Analyzer, Brookhaven Instrument Corporation, New York, NY), the average diameter of droplets in high-speed homogenized emulsion is about 618.6 nm, while the average diameters of droplets in high-pressure homogenized emulsion is 79.5 nm. Therefore, the higher homogenization pressure could result in both smaller droplets and more homogeneous size distribution in emulsions. Subsequently, we prepared EGCG and curcumin

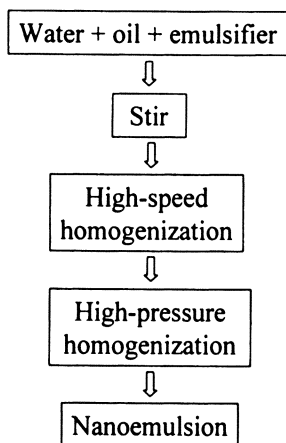


Figure 5. The general process to prepare nanoemulsions.

Table I. The emulsions with different formulations.

Emulsion	Stability				
HS ^a	stable	unstable	unstable	unstable	unstable
Oil	10%	10%	10%	10%	10%
Emulsifier	10%	6%	4%	2%	1%
Water	80%	84%	86%	88%	89%
HP ^b	stable	stable	stable	stable	stable
Oil	10%	10%	10%	10%	10%
Emulsifier	10%	8%	6%	4%	2%
Water	80%	82%	84%	86%	88%

^a High-speed homogenization at 24,000 rpm;

^b High-pressure homogenization at 1,000 bar.

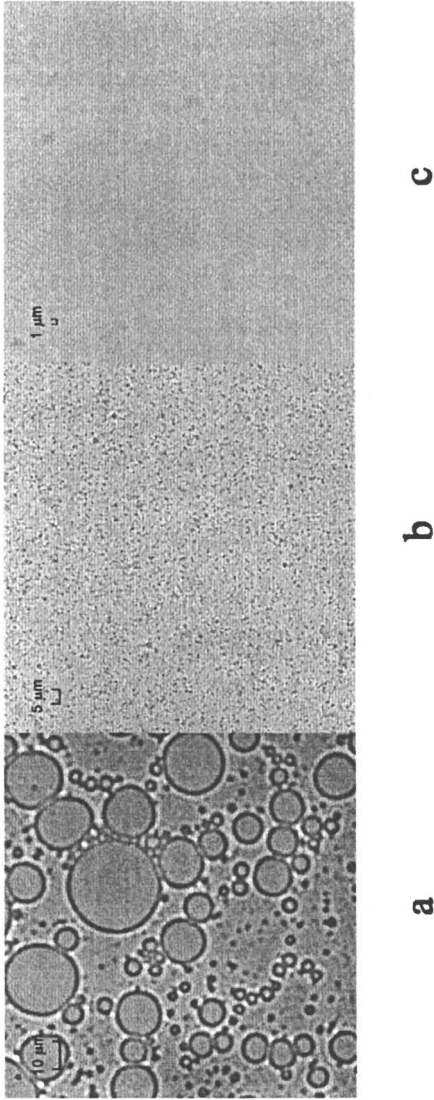


Figure 6. Optical Microscope images of emulsions. a: stir-only; b: high-speed homogenization at 24,000 rpm; c: high-pressure homogenization at 1,000 bar. (Reproduced with permission from reference 25. Copyright 2008.)

nanoemulsions with the pressure of high-pressure homogenization fixed at 1,000 bar.

Polyphenols Encapsulated in Nanoemulsions

Nanoemulsions have been proved to be appropriate vehicles for encapsulating and transporting phytochemicals due to their small droplet sizes and high kinetic stability (22, 26, 27). EGCG has been encapsulated in nanoemulsion at emulsifier/oil/water ratio of 2/10/88 prepared by high-pressure homogenization at 1,000 bar. After 11 days at pH 7.0, EGCG emulsion was measured by HPLC, and the result was compared with EGCG aqueous solution, as shown in Figure 7. EGCG peak in EGCG aqueous solution is found to be about half of that in EGCG nanoemulsion. There are two significant EGCG oxidation peaks in EGCG aqueous solution compared with one small EGCG oxidation peak in EGCG nanoemulsion. HPLC results in Figure 8 also suggest that more than 60% EGCG has been oxidized in EGCG solution compared to about 15% value in EGCG nanoemulsion. HPLC results clearly reveal that the nanoemulsion could improve pH stability of EGCG.

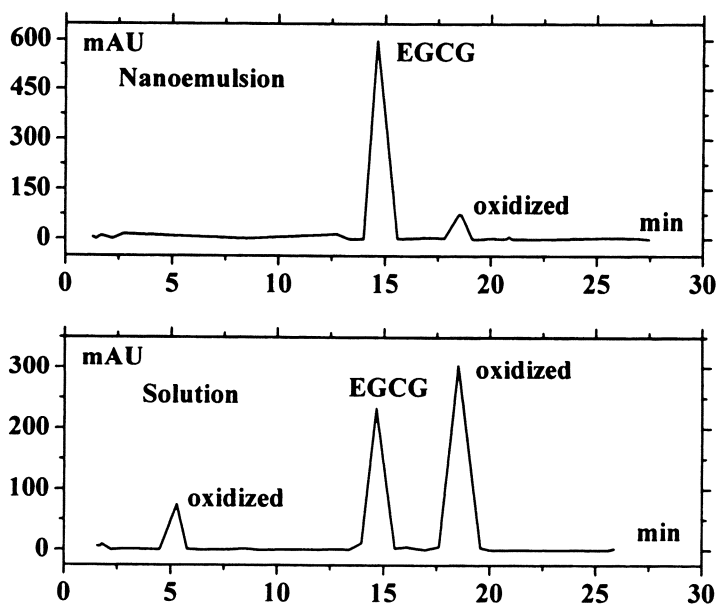


Figure 7. HPLC chromatograms of EGCG nanoemulsion (top) and EGCG aqueous solution (bottom).

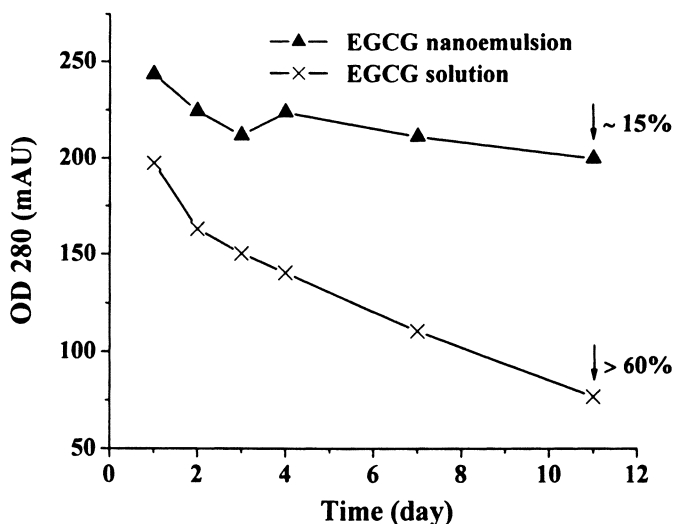


Figure 8. HPLC results of EGCG nanoemulsion and EGCG aqueous solution.

Nanoemulsions have been found to markedly enhance the solubility of curcumin to 1%, while curcumin is almost insoluble in water. Because of the π - π^* type excitation of the extended aromatic system, curcumin exhibits an intense, round-shaped absorption band in the visible region centered at 429 nm (28). UV-visible measurements were used to monitor the stability of curcumin encapsulated in O/W nanoemulsion. Figure 9 shows the UV-visible spectra of curcumin emulsion homogenized by high-pressure homogenization (HP 1500) during seven-day storage (25). The nearly-unchanged absorption peak of curcumin indicates that at a pH between 5.0 and 5.5, the stability of curcumin can be maintained in O/W nanoemulsions.

The preliminary tests of the anti-inflammation activity of nanoemulsified curcumin have been conducted *in vivo* using the mouse ear inflammation model, as shown in Figure 10. Topical application of 12-O-tetradecanoylphorbol-13-acetate (TPA) rapidly can induce edema of mouse ear in a dose- and time-dependent manner. Female CD-1 mice (6-7 weeks old; 5 mice per group) were orally administered with 1 ml vehicle or 1 ml curcumin solution or curcumin nanoemulsion by gavages at 30 min before topical application of 10 μ l acetone or TPA (1.5 nmol) in acetone. The mice were sacrificed by cervical dislocation. Ear punches (6-mm in diameter) were taken and weighed. Figure 11 shows the effects of oral administered curcumin nanoemulsions by gavages on TPA-induced edema of mouse ears. The oral administration of curcumin solution shows little or no effect of TPA-induced edema of mouse ears. However, our result indicates that the oral administration of high-pressure homogenized

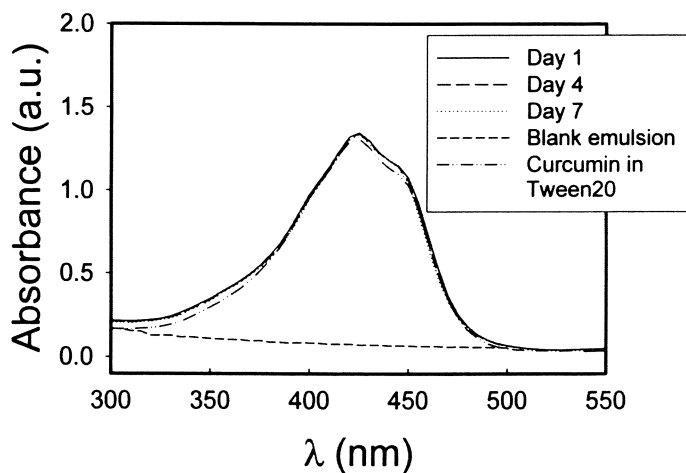


Figure 9. UV spectra of 1% curcumin nanoemulsion prepared by high-pressure homogenization at 1500 bar after 1, 4, 7 days, as well as the blank O/W emulsion and curcumin in 10% Tween 20 water solution. (Reproduced with permission from reference 25. Copyright 2008.)

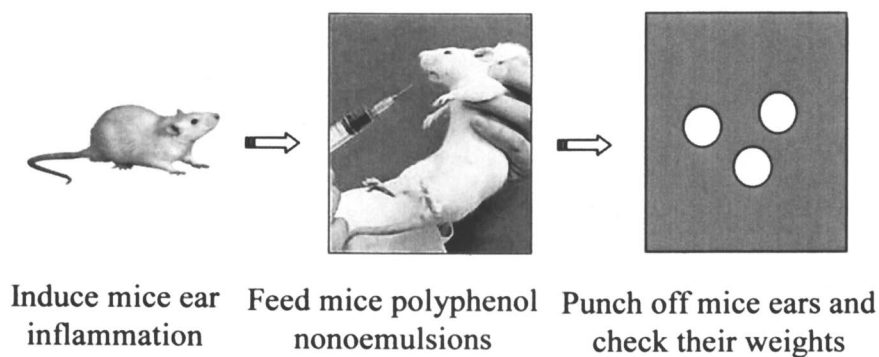


Figure 10. Mouse ear inflammation model for testing the anti-inflammation activity of nanoemulsified polyphenols.

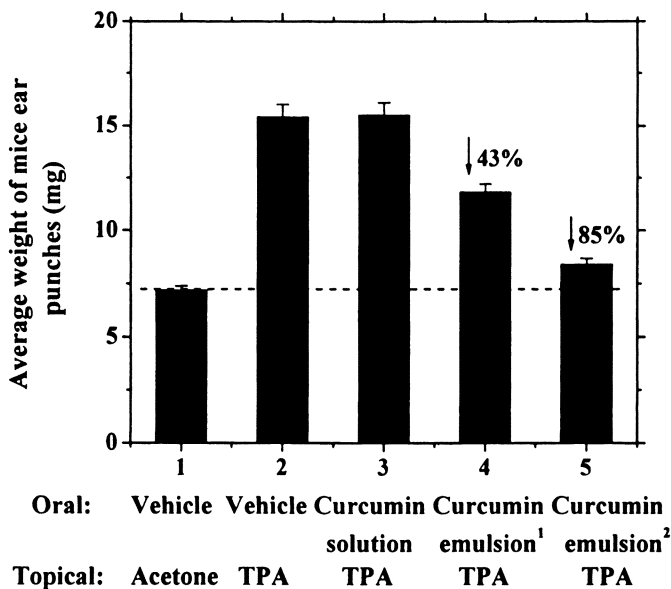


Figure 11. The effects of oral administered curcumin nanoemulsion on TPA-induced edema of mouse ears. The vehicle is the blank O/W emulsion without curcumin. ¹High-speed homogenization at 24,000 rpm; ²high-pressure homogenization at 1,500 bar. (Reproduced with permission from reference 25. Copyright 2008.)

curcumin nanoemulsions could markedly inhibited TPA-induced edema of mouse ears by 85%.

Another animal model is also used to demonstrate the effectiveness and improvement of nanoemulsified curcumin. We have studied the effects of oral administration of nanocurcumin emulsion on the growth of transplant human prostate cancer cell in male SCID mice. Eight male SCID mice (7-8 weeks old) were subcutaneously injected with human prostate cancer PC-3 cells (2×10^6 cells)/0.1 ml medium with metrigel on the back of each mouse, and then the mice were randomized into 2 groups (4 mice per group). Starting on the second day after tumor transplantation, the mice in the first group were given nanoemulsions without curcumin as the sole source of drinking fluid (vehicle control). The mice in the second group were given 0.3% curcumin nanoemulsions in vehicle as sole source of drinking fluid. Tumor appearance time, tumor sizes were measured and recorded during 5 weeks treatment. Table II shows that mice that drank 0.3% curcumin nanoemulsion as sole source of drinking fluid had less number of tumors per mouse, smaller tumor volumes and less tumor incidence in comparison to mice that drank the vehicle nanoemulsion control.

Table II. The effects of oral administration of nanocurcumin emulsions on the growth of transplant human prostate cancer cell in male SCID mice.

Tumor records	Vehicle control	Curcumin nanoemulsion	Inhibition
First tumor appear time	15 days after transplant	22 days after transplant	–
Total numbers of tumors	5	3	40%
Volume per tumor	212 ± 69 mm ³	83± 38 mm ³	61%
Total tumor volume	850 mm ³	333 mm ³	61%
Tumor incidence	100%	75%	25%

Conclusion

Due to the advantage of nanoscale size, nanoemulsions have provided excellent vehicles to encapsulate highly valuable polyphenols, such as tea catechins and curcumin, in order to increase their stability and bioavailability. High-pressure homogenizers give food industry a ready way to prepare large-scale nano-products encapsulated with highly valuable polyphenols. Nevertheless, when one encapsulation method is chosen, people have to consider various industrial constraints and requirements, including the properties of the active compounds, the degree of stability required during storage and processing, the specific release properties required, the maximum obtainable load, and the production cost.

References

1. *Phenolic compounds in food and their effects on health I: Analysis, Occurrence, and chemistry*; Ho, C. T.; Lee, C. Y.; Huang, M. T., Eds.; ACS Symp. Ser. 506; American Chemical Society: Washington, D.C., 1992.
2. Salah, N.; Miller, N. J.; Paganga, G.; Tijburg, L.; Bolwell, G. P.; Riceevans, C. *Arch. Biochem. Biophys.* **1995**, *322*, 339-346.
3. *Handbook of nutraceuticals and functional foods*; Wildman, R. E. C., Eds; CRC Press: Boca Roton, FL, 2001.
4. Bell, L. N. In *Handbook of nutraceuticals and functional foods*; Wildman, R. E. C., Eds.; CRC Press: New York, NY, 2001; pp. 501-516.
5. Weisburger J. H. *Cancer Res.* **1998**, *vol. 58, no. 18*, cover legend.
6. Havsteen, B. *Biochem. Pharmacol.* **1983**, *32*, 1141-1148.

7. Nakagawa, K.; Ninomiya, M.; Okubo, T.; Aoi, N.; Juneja, L. R.; Kim, M.; Yamanaka, K.; Miyazawa, T. *J. Agric Food Chem.* **1999**, *47*, 3967-3973.
8. Zhu, Q. Y.; Zhang, A.; Tsang, D.; Huang, Y.; Chen, Z.-Y. *J. Agric. Food Chem.* **1997**, *45*, 4624-4628.
9. Su, Y. L.; Leung, L. K.; Huang, Y.; Chen, Z.-Y. *Food Chem.* **2003**, *83*, 189-195.
10. Haslam, E. *Phytochem.* **2003**, *64*, 61-73.
11. Nakagawa, K.; Miyazawa, T. *J. Nutr. Sci. Vitaminol.* **1999**, *43*, 679-684.
12. Sukanuma, M.; Okabe, S.; Oniyama, M.; Tada, Y.; Ito, H.; Fujiki, H. *Carcinogenesis* **1998**, *19*, 1771-1776.
13. Yang, C. S.; Maliakal, P.; Meng, X. *Annu. Rev. Pharmacol. Toxicol.*, **2002**, *42*, 25-54.
14. Huang, M. T.; Smart, R. C.; Wong, C. Q.; Cooney, A. H. *Cancer Res.* **1988**, *48*, 5941-5946.
15. Huang, M. T.; Lou, Y. R.; Ma, W.; Newmark, H. L.; Reuhl, K. R.; Conney, A. H. *Cancer Res.* **1994**, *54*, 5841-5847
16. Osawa, T.; Sugiyama, Y.; Inayoshi, M.; Kawakishi, S. *Biosci., Biotechnol., Biochem.* **1995**, *59*, 1609-1612.
17. Pan, M. H.; Huang, T. M.; Lin, J. K. *Drug Metab. Disp.* **1999**, *27*, 486-494.
18. Ireson, C.; Orr, S.; Jones, D. J. L.; Verschoyle, R.; Lin, C. K.; Luo, J. L.; Howells, L.; Plummer, S.; Jukes, R.; Williams, M.; Steward, W. P.; Gescher, A. *Cancer Res.* **2001**, *61*, 1058-1064.
19. Madene, A., Jacquot, M., Scher, J., Desobry, S. *Int. J. Food Sci. Tech.* **2006**, *41*, 1-21.
20. *Food Emulsions: principles, practices, and techniques*; McClements, D. J., Eds.; CRC series in contemporary food science; CRC Press: Boca Roton, FL, 2004; pp 274-276.
21. Sonnevile-Aubrun, O.; Simonnet, J. T.; L'Alloret, F. *Adv. Colloid Interface Sci.* **2004**, *108-109*, 145-149.
22. Solans, C.; Izquierdo, P.; Nolla, J.; Azemar, N.; Garcia-Celma, M. J. *Curr. Op. Coll. Int. Sci.* **2005**, *10*, 102-110.
23. Walstra, P. In *Encyclopedia of Emulsion Technology*; Becher, P., Eds; Marcel Dekker: New York, NY, 1983; Vol 1. pp 57-127.
24. Rang, M. J., Miller, C. A. *J. Colloid Interface Sci.* **1999**, *209*, 179-192.
25. Wang, X. Y., Jiang, Y., Wang, Y.-W., Huang, M.-T., Ho, C.-T., Huang, Q. R. *Food Chem.*, **2008**, *108*, 419-424.
26. Garti, N., Aserin, A., Spermath, A., Amar, I. U.S. 20030232095.
27. Shefer, A., Shefer, S. D. U.S. 20030152629.
28. Zsila, F.; Bikádi, Z.; Simonyi, M. *Biochem. Biophys. Res. Commun.* **2003**, *301*, 776-782.

Chapter 14

Materials for Encapsulation of Food Ingredients: Understanding the Properties to Find Practical Solutions

**C. McCrae, S. Debon, B. Guthrie, J. Heigis, G. Mondro,
and W. Shieh**

Cargill R&D Centre Europe, Vilvoorde, Belgium

The food industry is continuously developing new materials and formulations for the efficient encapsulation of food ingredients to make them easier to handle and providing added functionality. The material(s) that can be used include carbohydrates, proteins, lipids, gums and cellulose, and the choice depends on factors such as the nature of the core material, the expected requirements, for instance, oxidation and process stability and controlled flavour release, the process of encapsulation, labeling concerns and economics. Each type of material has its own particular strengths and complex structural designs may be required for optimal functionality. To help in the selection of the optimum system, this paper examines the properties that make materials, particularly carbohydrates, applicable for encapsulation of food ingredients in terms of the basic underlying physico-chemical principles.

Introduction

Encapsulation is a technology for coating solids, liquids and gaseous materials into sealed capsules that preserve the substance in a finely divided state or as a whole ingredient and release their contents under certain conditions at specific rates. In the case of microencapsulation, the capsules may vary in size from several tenths of a micron to a few thousand micrometers. Nanocapsules and capsules produced by macrocoating are generally less than 2000 Å and greater than 5000 µm respectively (1). For each of these capsule classes, the technological challenges and type of coatings differ.

Numerous techniques have been evaluated for the encapsulation of food ingredients (including spray drying, extrusion, fluidized bed coating, spray cooling/ chilling, freeze drying, spinning disk and centrifugal coextrusion, coacervation, co-crystallisation, liposome entrapment and molecular inclusion (2-6). The selection of an appropriate technique depends on the type of capsule required, the physico/chemical properties of the core and coating material and economics. In the food industry, spray drying is the most widely used technique as it provides the most economical and flexible way to encapsulate hydrophobic ingredients such as fats, oils, flavours and vitamins. It involves the formation of an emulsion or suspension of core and coating material and nebulizing this feed solution in hot air. Moisture evaporates quickly on contact with the hot air rendering free-flowing powder particles with the active core material entrapped inside a coating matrix. During spray drying, the temperature of the core is much lower (<100 °C) than that of the hot air (3), enabling encapsulation of heat-sensitive food ingredients. However, loss of low boiling core compounds may occur. In addition, core material may adhere to the surface of the capsule and be prone to oxidation by direct contact to the air.

Not only the drying process but also the nature of the coating material, the distribution of particles in the feed solution, the viscosity of the feed solution and core loading affect the retention of core compounds. Extensively used coating materials in spray-dried encapsulation are hydrolyzed starches (7), because they are inexpensive, bland in flavour, easy to dissolve and exhibit low viscosity in solution, which is important in spray-drying applications. However, they lack emulsifying capacity and result in poor retention of organic compounds during drying (8). Therefore, in practice, they are combined with emulsifying polymers like gum arabic and whey protein or substituted with hydrophobic groups especially n-octenylsuccinic anhydride (n-OSA).

In spray-dried powders, the coating material acts as a barrier for the release of core compounds through volatilization and diffusion, and minimizes the penetration of moisture, oxygen and other components in the environment. The extent and nature of protection provided by the coating material both during drying and storage varies with the chemical composition and the physical state of

the coating material. Knowledge on how different characteristics of coating material affect the stability of core material both during drying and storage can help the food developer in selecting the optimal system. Therefore, the properties of coating material that control the coating's protective nature in the microencapsulation of organic compounds have been investigated.

Properties of the carrier

Molecular weight and viscosity

Hydrolysed starches are traditionally characterized by their dextrose equivalent (DE), which is a measure of their reducing power as compared to that of glucose (dextrose). An unhydrolysed starch has a DE value close to zero while glucose has a DE of 100. If the DE is less than 20, starch hydrolysates are called maltodextrins. Corn syrup solids have a DE of 20 or greater. Qi and Xu (9) showed the molecular distribution of starch hydrolysates with different DE values and confirmed the data from Kenyon & Anderson (10) that the DE is roughly proportional to the reciprocal of the average degree of polymerization (*i.e.* the average number of repeating glucose units in the carbohydrate molecules). However, by varying the type of hydrolyzing agent, it is possible to produce products with the same DE value but different carbohydrate profiles (11).

In agreement with earlier studies (12-14), Bangs & Reineccius (15) found that the DE of hydrolysed starch is inversely related to the retention of flavour compounds during spray drying at constant infeed solids content. This relation held true down to DE 15 for all of 12 combined aroma compounds and was most likely related to an increase in the rate at which an amorphous film was formed around droplets of the aroma compounds (16-18). Interestingly, Sheu & Rosenberg (19) found that this relation was of lesser importance in the presence of an emulsifier. Furthermore, Bangs & Reineccius (15) found that flavor retention decreased with DE values at $DE < 15$, but this decrease was not statistically significant, and for certain aroma compounds, this decrease could not be observed. The viscosity and solubility characteristics of hydrolysed starches vary with the average molecular weight (11). The higher the DE, the lower the viscosity and consequently, the higher the concentration of starch that can be dissolved prior to spray-drying. Various studies (15, 20 & 21) have shown that increasing the solids content of the infeed allowed better performance not only in terms of economics but also in retaining flavours during drying. Our studies confirm this finding. For example, at an oil load of 20%, an increase from 30 to 55% solids increased the retention of oil from ca. 93% to full recovery (Table 1). In addition, our studies show that the maximum level of oil

that could be retained at 55% solids was ca. 20% (Table 1). Increasing the oil load to levels above 20% led to losses of oil during drying.

Table I. Influence of infeed solids content and oil load on the retention of orange oil during spray drying.

Carrier	Orange oil load (%)	Infeed solids (%)	Oil retention (%)
Glucose syrup DE52/ n-OSA starch (3:1, w/w)	20	30	92.8
	20	55	98.4
	25	55	76.1

The importance of infeed solids content in retaining flavour during drying was related to an increase in the rate of film formation (22). Interestingly, Bangs & Reineccius (15) showed that the advantage of higher infeed solids content at higher DE values did not offset the improved film forming ability of higher molecular weight dextrans for flavours with a boiling point $>160^{\circ}\text{C}$. In agreement with later studies (21), infeed solids content influenced the more volatile components to a greater extent.

The effectiveness of the matrix film in holding and protecting the core material is strongly depended on the physical state of the matrix material. The contribution of the molecular weight of hydrolyzed starches to this aspect of encapsulation has been further discussed below.

Amorphous state of the carbohydrate matrix

The success of encapsulation depends to a large extent on the formation of a metastable amorphous structure, a glass, with a low permeability to organic compounds but will let water diffuse through (Karel & Langer, 1988). Starch hydrolysis products are particularly useful for the formation of such a structure with selected permeability. The faster the matrix material forms an amorphous film around the core material, the more organic compound will be retained and thus, the higher for the flavour retention (23 & 24).

Hydrophilic amorphous matrices are formed when a low water activity has been reached upon rapid evaporation from droplet surfaces. The sudden water reduction increases the glass transition temperature of the matrix material. As long as the storage temperature remains below the glass transition temperature, the resulting matrix is believed to be in the amorphous state, which is characterised by a very low mobility of the carrier molecules. Because of this low mobility, permeability to organic compounds is strongly retarded and core material is released primarily by diffusion through the pores in the matrix (25 &

26). Consequently, release or retention of core material depends on factors such as the chemical composition of the matrix, pore size, molecular size (or DE), wall thickness and contact surface area.

For the carbohydrate matrix to remain in the amorphous state, the glass transition temperature may not drop below the room temperature. Thus, processes reducing the glass transition temperature need to be controlled. For example, increased hydrolyses results in starches with a higher DE and consequently, a lower glass transition temperature (9 and 27). In addition, starches with a higher DE are usually more susceptible to hygroscopicity (10) and the increased uptake of moisture reduces the glass transition temperature. The relation between increased moisture uptake and glass transition temperature has been illustrated by the results in Figure 1 for a carrier comprising glucose syrup (DE 40) and modified starch (3:1, w/w). Initially, the glass transition temperature was in the range 60 to 70 °C. Increasing the relative humidity to 60% increased the moisture content to 7% and reduced the glass transition temperature to well below room temperature. Thus, storage at low humidity (<50%) was required to keep the wall material of the powder in the amorphous state.

The effectiveness of an amorphous carbohydrate matrix film to retain flavour and inhibit uptake of oxygen is directly related to DE. For example, Anandaraman & Reineccius (28) found improved oxygen-barrier properties in parallel with DE on encapsulation of orange peel oil. In addition, Whorton & Reineccius (29) observed increased volatile retention with an increase in DE when they examined encapsulated vegetable oils containing short chain aldehydes at increasing water activities. Our studies have also demonstrated the importance of DE on oxidation stability and flavour retention in the encapsulation of orange oil (Figure 2). After 25 days of storage, most of the flavour was still retained and practically no limonene, which is present as the major component in orange oil, was oxidized at DE 40. However, reducing the value of DE to 17 increased the production of limonene oxide substantially and at the same time, led to a rapid loss in flavour.

In accordance with observations made by Benczedi (26), it may be speculated that at a higher DE, the increased concentration of low-molecular weight plasticizer led to a densification of the polymer followed by a reduction in permeability. On the other hand, a potential improvement in the viscoelastic properties of wall material may have played a role in reducing permeability. Sheu & Rosenberg (19 & 30) observed less dent formation and less cracks in wall material when the DE increased. It has been suggested that surface dents result from uneven shrinkage of the drying droplets during the early stages of drying. Subsequent thermal expansion of air or water vapours inside the drying particles can smooth them out to varying extents depending on the drying rate and on the viscoelastic properties of the wall matrix. Thus, differences in the viscoelastic properties of the carrier with a change in DE probably affected dent formation and cracking.

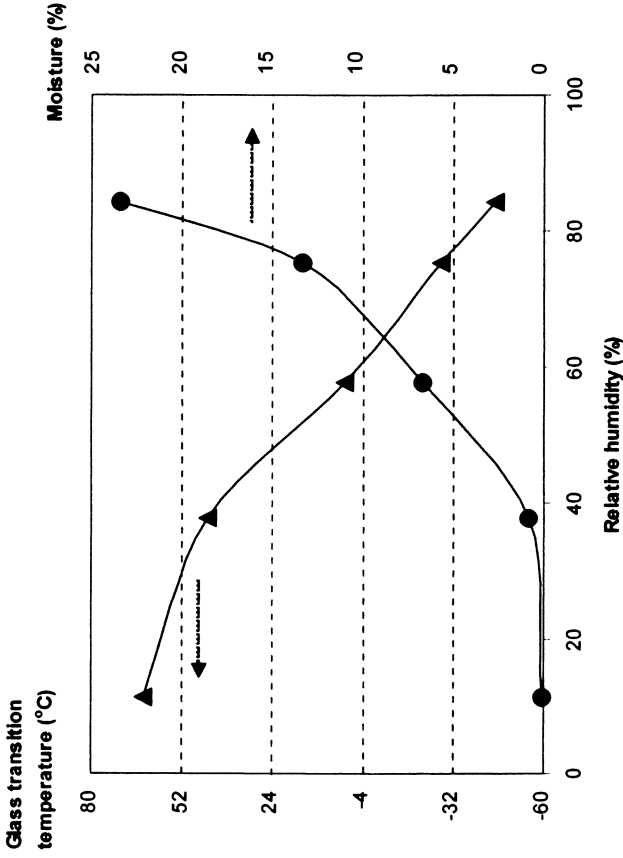


Figure 1. Influence of relative humidity on equilibrium moisture content (●) and glass transition (▲) of a carrier comprising glucose syrup DE 40 and n-OSA starch (3:1, w/w) in the encapsulation of orange oil (20%).

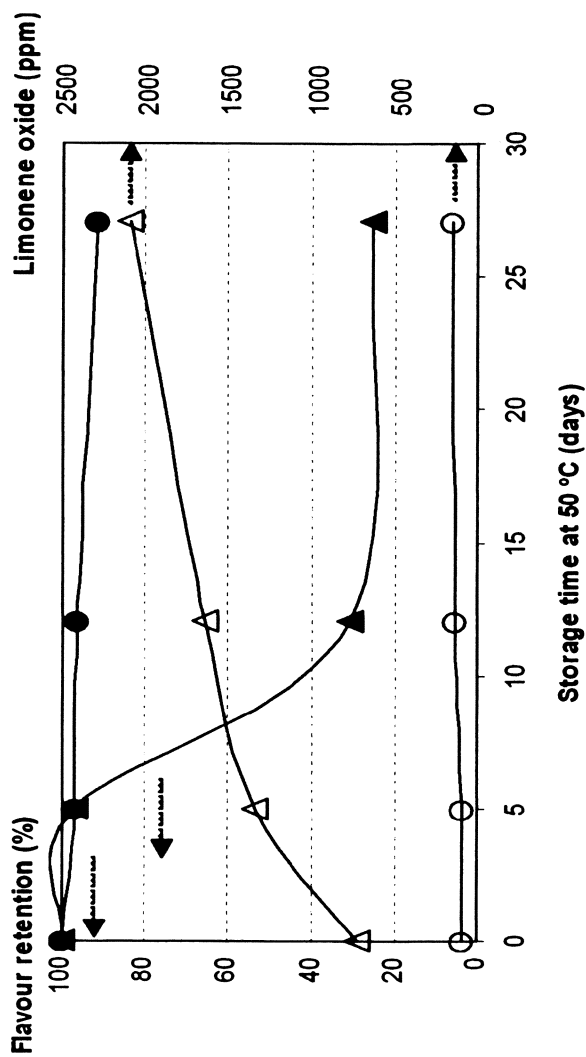


Figure 2. Shelf life stability (flavour retention: ●▲ and limonene oxide: ○△) at 50°C of orange oil (20%) encapsulated in a matrix containing glucose syrup of different DE and n-OSA starch (3:1). Properties of the coating: DE = 40 and Tg = 60-70°C (○●) and DE = 17 and Tg = 81-104°C (△▲).

Crystallisation of wall material ingredients

Hydrolysed starch products don't usually crystallise but loose flowability and eventually cake (10). This phenomenon can be attributed to the glass transition properties of the hydrolysed starches (9). When the glass transition temperature drops below the storage temperature with increasing moisture content, a transition takes place from solid glass to a liquid-like rubbery state. The hydrogen bonds responsible for the main structural forces in the amorphous matrix are weakened and consequently, molecular mobility and hence diffusion increase (25). When the moisture content continues to increase, the polymer matrix collapses resulting in caking (10). This caking, or collapse, is caused by the inability of the carrier to support itself against gravity as viscosity decreases. Holes in the particle wall reduce, the surface matrix shrinks thereby forcing some or all of the core material to the surface and diffusion is yet again retarded, effectively by 're-encapsulating' the remaining organic compound (29, 31 & 32). This ability to release and reseal core material could be used to impart a desired level of release depending upon the degree to which the collapse is allowed to progress.

Crystallization, like structural collapse, is promoted when the glass transition temperature drops below the storage temperature with increasing moisture content. It's a two-step process with the phase of initial nucleation and subsequent crystal growth. At a temperature above that of glass transition, particles have sufficient mobility to associate and form crystalline nucleus. Like collapse, crystallisation also leads to a reduction in pore size. As a result, core material is forced out from the crystallized matrix to the surface (27 & 31). Water may also be released from the crystallized areas into the amorphous regions, further plasticizing the wall material and decreasing the stability of the system (25).

Trehalose is an interesting molecule because it possesses a high glass transition temperature and, unlike hydrolysed starch, crystallises. In addition, it crystallises mainly as trehalose dihydrate thus immobilizing water and keeping the water activity at a low level. These interesting properties of trehalose have lead to a study on the use of trehalose as wall material in the encapsulation of orange oil. Table 2 lists the results obtained shortly after spray drying for the moisture content and the glass transition and melting characteristics of two powders, one encapsulated with glucose syrup and n-OSA starch and the other with trehalose and n-OSA starch. Differences between the powders in moisture content were insignificant. In the presence of glucose syrup (DE 38), the wall material was fully amorphous with a glass transition range in the region 78-95 °C. When trehalose replaced glucose syrup, the glass transition temperature was found to be slightly lower (70-82 °C) and a melting transition was observed. The extent of crystallinity was, derived from the melting transition, only ca 8%. Thus, both powders were fully or almost fully amorphous.

Table II. Moisture content and glass transition and melting characteristics of two spray-dried powders comprising orange oil (20%) and wall material of different compositions immediately after spray drying.

Parameter	Wall material	
	Glucose syrup DE 38/ n-OSA starch (3:1, w/w)	Trehalose/n-OSA starch (3:1, w/w)
Moisture (%) ^a	2.67	2.79
Glass transition temperature (°C) ^b		
onset	78.7 ± 0.4	70.7 ± 0.9
peak	87.4 ± 1.2	74.2 ± 1.1
end	95.0 ± 1.3	81.8 ± 1.1
Melting temperature (°C) ^b		
Onset	No melting	90.3 ± 0.7
Peak	No melting	98.1 ± 0.7
Crystallinity (%) ^c	Fully amorphous	Ca. 8

^aInfra-red moisture balance (130°C, 20 min); ^bDSC program: Equilibrated at 20°C and ramped from 20 to 130°C (scan rate 5°C/min). Average of 3 replicates; ^cCalculated with ΔH_m (trehalose dehydrate) = 86.2J/g ()

Table III. Influence of low molecular weight carbohydrates on the retention of orange oil during spray drying.

Carrier	Orange oil load (%)	Infeed solids (%)	Oil retention (%)
Glucose syrup DE 42/ n-OSA starch (3:1, w/w)	20	55	96.6
Trehalose/ n-OSA starch (3:1, w/w)	20	55	95.2
Trehalose/ n-OSA starch (3:1, w/w)	20	55	98.6
Erythritol/n-OSA starch (3:1, w/w)	20	55	35.4
Isomalt/n-OSA starch (3:1, w/w)	20	55	94.5

The extent of crystallinity in the orange oil powder encapsulated with trehalose was too small to affect the retention of orange oil during drying (Table 3). Similar results were obtained with isomalt (Table 3). However, erythritol resulted in a crystalline powder (extent of crystallinity was ca. 82%) with poor flavour oil retention (Table 3). Since no orange oil was lost with glucose syrup, trehalose or isomalt, these results suggest that for good flavour retention a matrix, which does not crystallise during processing, is required.

In the amorphous state, Drusch, *Serfert, van den Heuvel and Schwarz* (33) found that trehalose was a better ingredient for encapsulation of fish oil than glucose syrup (DE 38) due to its ability to provide better protection against oxidation. These results were obtained at a very low relative humidity. Figure 3 demonstrates the moisture sorption properties of similar carriers but for the encapsulation of orange oil under conditions of increasing relative humidity. The powder encapsulated in the presence of glucose syrup exhibited a continuous increase in the uptake of moisture as the relative humidity increased. In contrast, a plateau was observed for the powder encapsulated in the presence of trehalose at relative humidities in the region of 53.3 to 85.0%. This plateau corresponded to complete crystallisation of trehalose (Table 4). At complete crystallisation, there was no significant increase in the uptake of moisture (Figure 3) and consequently, the glass transition temperature did not significantly decrease (Table 4).

Collapse/caking was observed when the powder encapsulated with glucose syrup increased in relative humidity to 43% and at a relative humidity of 70%, this powder liquefied. Crystallisation of trehalose led to a hardening of the powder, limiting the range of applications to capsules requiring storage at low humidity. Drusch, *Serfert, van den Heuvel and Schwarz*. (33) came to the same conclusion based on the observation that rapid oxidation followed crystallisation of trehalose.

Emulsification capacity

The retention of oil during spray drying has been found to improve on addition of an emulsifier. For example, Trubiano & Lacourse (34) showed that even though maltodextrins matched the viscosity of gum Arabic, they didn't encapsulate as much oil possibly due to lack of emulsifying properties (Table 5). Gum Arabic is a complex mixture of macromolecules comprising predominantly carbohydrate and a small proportion (2%) of protein. Concentrations of 12% or higher are required to stabilize 20% (w/w) orange oil-in-water emulsions. Under these conditions, Randall, *Phillips and Williams* (35) showed that only 1-2% of gum Arabic bound effectively at the oil droplet surface and this adsorbed material contained a high proportion of protein. It has been proposed that the

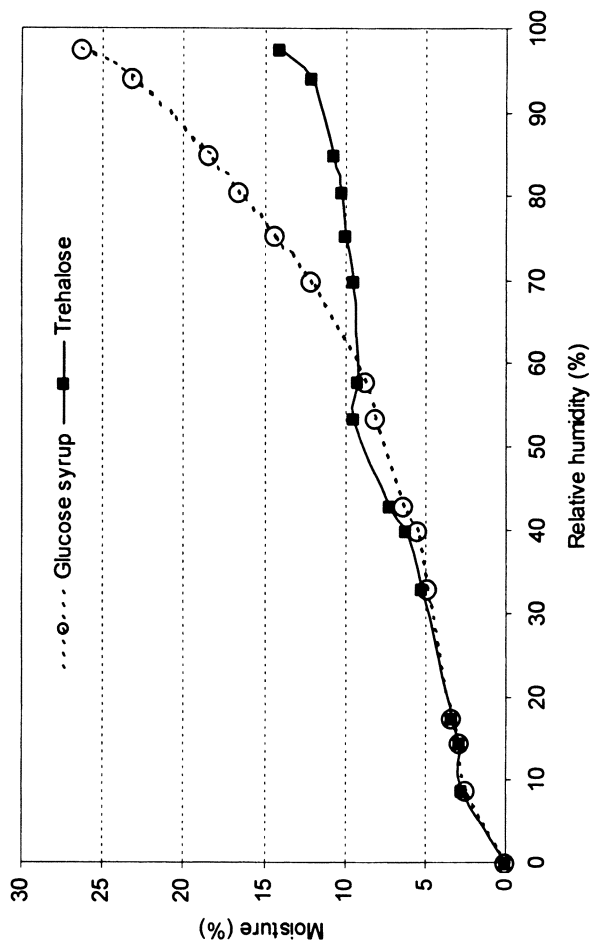


Figure 3. Moisture/sorption isotherms of two spray-dried powders comprising orange oil (20%) and wall material of different composition, i.e. (○) glucose syrup DE 42/n-OSA starch (3:1, w/w) and (■) trehalose/n-OSA starch (3:1, w/w).

Table IV. DSC Characteristics of two spray-dried powders comprising orange oil (20%) and wall material of different compositions at varying relative humidities

Parameters	Composition of wall material		
	Glucose syrup DE 38/ n-OSA starch (3:1, w/w)	Trehalose/n-OSA starch (3:1, w/w)	
Relative humidity (%)	43.0	58.0	80.5
Glass transition temperature (°C) ^a			
- onset	35.3	19.7	-31.7
- peak	44.1	30.1	-22.7
- end	52.5	39.8	-14.8
Crystallinity (%) ^b	Fully amorphous		7.7 ±0.2
			92.1 ±2.9
			5.9 12.1 18.4

^aDSC program: Equilibrated at 20°C and ramped from 20 to 130°C (scan rate 5°C/min). Average of 3 replicates; ^bCalculated with ΔH_m (trehalose dehydrate) = 86.2 J/g ()

protein component of gum Arabic embeds in the oil while the carbohydrate component extends into the water phase (36). The emulsifying properties inherent to gum Arabic are believed to be partially responsible for its ability to improve oil retention during drying. A stable emulsion of fine droplets of core material as infeed solution is critical to microencapsulation.

Risch & Reineccius (37) demonstrated the importance of particle size in the encapsulation of organic compounds. A smaller particle size led to a better retention of citrus oil during drying and yielded spray-dried powders, which contained less extractable surface oil. These findings are in agreement with the results obtained from various studies and listed in Table 5. Surface oil may be critical to powder stability because oil droplets on the surface of powder particles are not protected against atmospheric oxygen. However, a reduction in extractable surface oil with smaller particle size did not result in better shelf stability or resistance to oxidation. The fact that surface oil is not critical to shelf stability has been confirmed by various studies (32, 34 & 38), which suggests that other factors such as matrix porosity may be more significant in determining the rate of oxidation of encapsulated core materials.

As an alternative to gum Arabic, a chemically modified starch has been used successfully in the microencapsulation of organic compounds. The starch derivative is prepared by a standard esterification reaction using *n*-octenyl succinic anhydride (*n*-OSA). The substitution of a hydrophobic octenyl side chain is at a level of about 1 per 50-60 anhydrous glucose units, which corresponds to 3% *n*-OSA in weight, the maximum level approved for food use. To lower viscosity, *n*-OSA starches are hydrolyzed either by acid thinning, pyrodextrinization or enzyme hydrolyses. Enzymes that can be used are the α - and β -amylase or a combination of both. *n*-OSA Starches offer excellent emulsifying properties leading to good quality infeed solutions with average oil droplet sizes of less than one micron (Table 5: Cargill and 32). Compared to gum Arabic, *n*-OSA starch provides wall materials that have higher levels of retained core material and less extractable surface oil (Table 5:32 & 34). These improved properties result in a direct economic benefit to the manufacturer and user of the product. They did not, however, result in better oxidation stability. Both Trubiano & Lacourse (34) and Partanen, Yoshii, Kallio, Yang & Forssell (32) found that the oxidation resistance of wall material comprising *n*-OSA starch was similar, but not worse, to that of gum Arabic.

In our studies, excellent results were obtained at an oil load of 20% and an infeed solids concentration of 55%. Retention of oil during spray drying was high (Table 1 and 5) and due to the high DE of the coating material, the spray-dried powder displayed excellent stability against oxidation (Figure 2). In addition, Figure 4 illustrates that the spray-dried capsules had little surface indentations (Figure 4), which likely contributed to the excellent stability during storage.

Table V. Encapsulation performance of gum Arabic, dextrin and n-OSA starch.

Carrier	Core material (%)	Infeed solids (%)	Average diameter (μm)	Oil retention (%)	Surface oil (%)	Reference
Gum Arabic	30	30	<3	94.0	16.5	34
Dextrin	30	40	2-10	76.5	25.6	
n-OSA Starch	30	40	<2	99.7	1.0	
Syrup DE42 / n-OSA starch (3:1)	20	55	0.63	98.6	-	Cargill
n-OSA Starch (DE 32-37)	30	52	0.8	100	0.2	32
Dextrin DE18.5/ Gum arabic (1:7)	30	52	4.4	100	32.6	

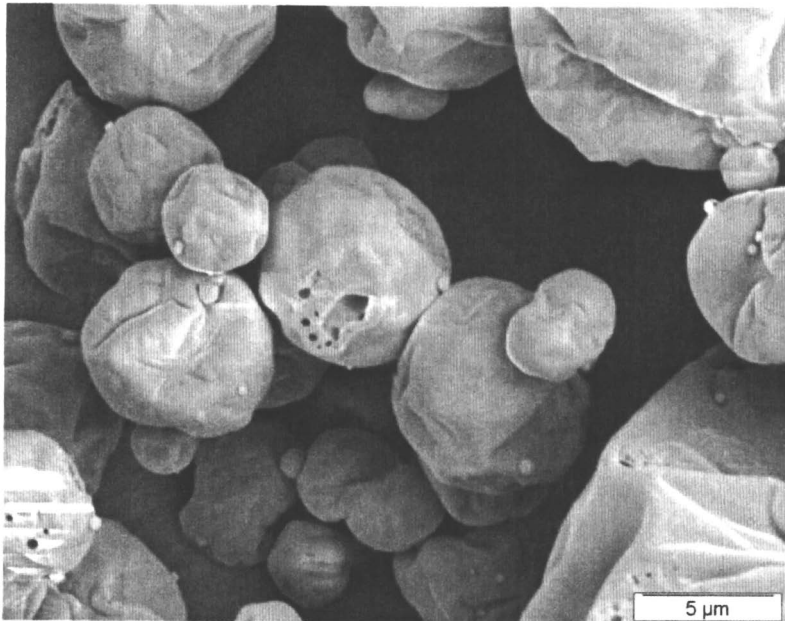


Figure 4. A SEM image of spray dried powders containing orange oil (20%) encapsulated with glucose syrup DE 42/n-OSA starch (3:1) at an average particle size of 25-55 μm

The emulsifying properties inherent to gum Arabic are due to the presence of proteins. Proteins in isolation can be good emulsifiers but under certain conditions, they can lose stability due to aggregation or precipitation. This instability is most pronounced at pH values close to the protein's isoelectric point. Ideally, proteins suitable for microencapsulation by spray drying should be soluble over a wide pH range, have good emulsifying properties and exhibit a low viscosity profile on dissolution in water. A promising group of proteins that fulfills these requirements are whey protein isolates. In combination with carbohydrates, Sheu & Rosenberg (19 & 30) showed that whey proteins provided good quality infeed solutions and improved the surface smoothness of carbohydrate-based microcapsules. Best results were obtained with blends of whey protein isolate and carbohydrates of high DE.

Conclusion

Successful microencapsulation is the result of a judicious choice of wall material composition for a given core material. The basic principles governing the function of starch hydrolysis products in the microencapsulation of organic compounds are quite well understood. For example, low molecular carbohydrates are effective in providing protection against oxidation, possibly by increasing the density and improving the viscoelasticity of the wall matrix, but they lack emulsifying properties. Lower DE value maltodextrins accelerate film formation and lead to improved retention of core material during drying. However, this effect could not be confirmed in the presence of an emulsifier. Emulsifiers like gum Arabic, modified starches and proteins are added to provide a good quality infeed solution with properly sized oil droplets (<1 micron). A stable emulsion of fine oil droplets as infeed solution is critical to microencapsulation.

In practice, the choice of wall material is determined by the requirements for optimal microencapsulation of a given core material in terms of (a) the infeed solids content, (b) particle size of the infeed solution, (c) DE, (d) ratio of emulsifier to low molecular weight carbohydrates and (e) hygroscopicity. Higher infeed solids content can be made with hydrolyzed starches of higher DE, hence lower viscosity. In the presence of less water, a film is formed faster around the core material leading to a better retention of core material and to less oil on the surface of the powder.

A smaller particle size increases the rate of film formation and results in a better retention of core material in the spray-dried powder. In addition, the product is more stable upon reconstitution in beverage applications where viscosity cannot be increased to help stabilize the core material.

In the amorphous state, the effectiveness of a carbohydrate matrix film to retain core material and inhibit the uptake of oxygen is directly related to DE. From this it can be concluded that the use of low molecular weight carbohydrates with a higher DE is preferred. However, hydrolysed starches with a higher DE have a lower glass transition temperature. The DE should be selected at a value, which is not too high as to remain below the glass transition temperature. In addition, hydrolysed starches with a higher DE are usually more susceptible to hygroscopicity. Increased moisture uptake leads to a reduction in the glass transition temperature and consequently, controlled storage conditions may be required.

Acknowledgement

The authors wish to express their sincere thanks to Daniele Karleskind and Pat Clarkin for their enthusiastic and invaluable support to this project, to Dirk Fonteyn, Annick van den Heuvel and Dounia Sahmaoui for their technical support and to Marline Moris and Myriam Marinoni for their contribution in searching the literature.

References

1. Jackson, L.S. & Lee, K. (1991). Microencapsulation in the food industry. *Lebensmittel-Wissenschaft und Technologie*, 24, 289-297.
2. Balassa, L.L. & Fanger, G.O. (1971). Microencapsulation in the food industry. *CRC Critical Reviews in Food Technology* 2 (2) 245-265.
3. Dziezak, J.D. (1988). Microencapsulation and encapsulated ingredients. *Food Technology*, 42, 136-151
4. Gibbs, B.F., Kermasha, S., Alli, I. & Mulligan, C.N. (1999) *international Journal of Food Sciences and Nutrition* 50, 213-224.
5. Gouin, S. (2004) Micro-encapsulation: Industrial appraisal of existing technologies and trends. *Trends in Food Science & Technology* 15, 330-347.
6. Desai, K.G.H. & Park, H.J. (2005) Recent developments in microencapsulation of food ingredients. *Drying Technology* 23 (7) 1361-1394.
7. Madene, A., Jacquot, M., Scher, J. & Desobry, S. (2006) Flavour encapsulation and controlled release – a review. *International Journal of Food Science and Technology* 41, 1-21.
8. Reineccius, G.A. (1991) Carbohydrates for flavor encapsulation. *Food Technology* March, 144-146.

9. Qi, A.H. & Xu, A. (1999) Starch-based ingredients for flavor encapsulation. *Cereal Foods World* 44 (7): 460-465.
10. Kenyon, M.M. & Anderson, R.J. (1988). Maltodextrins and low-dextrose-equivalence corn syrup solids: production and technology for the flavor industry. In: *Flavor Encapsulation* (edited by S.J. Risch & G.A. Reineccius). Pp. 7-12. Washington, DC: American Chemical Society
11. Kenyon, M.M. (1995) Modified starch, maltodextrin, and corn syrup solids as wall materials for food encapsulation. In: *Encapsulation and Controlled Release of Food Ingredients* (edited by S.J. Risch & G.A. Reineccius). Pp. 43-50. ACS Symposium Series 590. Washington, DC: American Chemical Society
12. Reineccius, G. A. & Coulter, S.T. (1969) Flavor retention during drying. *J. Dairy Sci.* 52 (8): 1219-1223.
13. Kerkhof, P.J.A.M. & Thijssen, H.A.C. (1975) *Aroma Research, Proceedings of the International Symposium*; Pudoc: Wageningen, The Netherlands. Pp 167-192.
14. Voilley, A. & Simatos, D. (1980) Retention of aroma during freeze and air drying. "Food Process Engineering". Vol. 1. Appl. Sci. Pub. Ltd., London.
15. Bangs, W.E. & Reineccius, G.A. (1981) Influence of dryer infeed matrices on retention of volatile flavor compounds during spray-drying. *Journal of Food Science*, 47, 254-259.
16. Karel, M & Langer, R. (1988) Controlled release of food ingredients. In: "Flavor encapsulation" (Reineccius, G.A. & Risch, S.J., eds). ACS Symposium Series No. 370. American Chemical Society, Washington, D.C., 177-190.
17. Bangs, W.E. & Reineccius, G.A. (1990) Characterization of selected materials for lemon oil encapsulation by spray drying. *J. Food Sci.* 55: 1356-1358
18. Goubet, I., Le Quere, J.L. & Voilley, A. (1998) Retention of aroma compounds by carbohydrates: influence of their physicochemical characteristics and of their physical state. *Journal of Agricultural and Food Chemistry*, 48, 1981-1990.
19. Sheu, T.Y. & Rosenberg, M. (1995). Microencapsulation by spray-drying ethyl caprylate in whey protein and carbohydrate wall systems. *Journal of Food Science*, 60, 98-103.
20. Leahy, M.M., Anandaraman, S., Bangs, W.E. & Reineccius, G.A. (1983) Spray drying of food flavors II. A comparison of encapsulating agents for the drying of artificial flavors. *Perfumer & Flavorist* 8: 49-56
21. Reineccius, G.A. & Bangs (1985) Spray drying of food flavors. III. Optimum infeed concentrations for the retention of artificial flavors. *Perfumer & Flavorist* 9: 27-29.

22. Menting, L.C. & Hoogstad, B. J. (1967) Volatiles retention during the drying of aqueous carbohydrate solutions. *Journal of Food Science* 32: 87-90.
23. Reineccius, G.A. (1988) Spray drying of food flavors. In: *Flavor Encapsulation* (edited by S.J. Risch & G.A. Reineccius). Pp. 55-64. Washington, DC: American Chemical Society.
24. Rosenberg, M, Kopelman, I.J. & Talmon, Y. (1990) Factors affecting retention in spray drying microencapsulation of volatiles materials. *J. Agric. Food Chem*, 38: 1288-1294.
25. Whorton, C, (1995) Factors influencing volatile release from encapsulation matrices. In: "Encapsulation and controlled release of food ingredients" (edited by S.J. Risch & G.A. Reineccius). Pp. 134-139.. Washington, DC: American Chemical Society
26. Benczedi, D. (2002) Flavour encapsulation using polymer-based delivery systems. In: "Food Flavour Technology" (edited by A.J. Taylor). Pp153-166. Sheffield Academic Press Ltd., UK.
27. Roos, Y. & Karel, M. (1991). Water and molecular weight effects on glass transitions in amorphous carbohydrates and carbohydrate solutions. *Journal of Food Science* 56 (6) 1676-1681
28. Anandaraman, s. & Reineccius, G.A. (1986) Stability of encapsulated orange peel oil. *Food Technology* 40, 88-93.
29. Whorton, C. & Reineccius, G.A. (1995) Evaluation of the mechanisms associated with the release of encapsulated flavor materials from maltodextrin matrices. In: "Encapsulation and controlled release of food ingredients" (edited by S.J. Risch & G.A. Reineccius). Pp. 143-159. Washington, DC: American Chemical Society
30. Sheu, T.Y. & Rosenberg, M. (1998). Microstructure of microcapsules consisting of whey proteins and carbohydrates. *Journal of Food Science*, 63, 491-494.
31. Labrousse, S., Roos, Y. & Karel, M. (1992) Collapse and crystallization in amorphous matrixes with encapsulated compounds. *Sci. Aliments* 12: 757-769
32. Partanen, R., Yoshii, H., Kallio, H., Yang, B. & Forssell, P. (2002) Encapsulation of sea buckthorn kernel oil in modified starches. *Journal of the American Oil Chemists Society*, 79 (3) 219-223
33. Drush, S., Serfert, Y., Heuvel van den, A. & Schwarz, K. (2006) Physicochemical characterization and oxidative stability of fish oil encapsulated in an amorphous matrix containing trehalose. *Food Research International* 39, 807-815.
34. Trubiano, P.C. & Lacourse, N.L. (1988) Emulsion-stabilized starches. In: *Flavor Encapsulation* (edited by S.J. Risch & G.A. Reineccius). Pp. 55-64. Washington, DC: American Chemical Society.

35. Randall, R.C., Phillips, G.O. & Williams, P.A. (1988) The role of the proteinaceous component on the emulsifying properties of gum arabic. *Food Hydrocolloids*, 2: 131-140.
36. Gardi, N. (1999). Hydrocolloids as emulsifying agents for oil-in-water emulsions. *Journal of Dispersion Science and Technology*, 20: 327-355.
37. Risch, S.J. & Reineccius, G.A. (1988) Spray-dried orange oil. Effect of emulsion size on flavor retention and shelf stability. In: *Flavor Encapsulation* (edited by S.J. Risch & G.A. Reineccius). Pp. 67-77. Washington, DC: American Chemical Society.
38. Buffo, R. & Reineccius, G. (2000). Optimization of gum acacia/modified starch/maltodextrin blends for the spray drying of flavors. *Performer and Flavorist*, 25, 37-51.

Chapter 15

Approaches to Encapsulation of Active Food Ingredients in Spray-Drying

Anna Millqvist-Fureby

**YKI Institute for Surface Chemistry, Box 5607, SE 114 86,
Stockholm, Sweden**

Microencapsulation can be used to improve the stability and control the release of dried active food ingredients such as flavors, enzymes, probiotics and oxidation sensitive oils. Spray-drying can be used for encapsulation and powder generation in one step by utilizing different phenomena that occur during drying. Dry emulsion is a classic way to supply encapsulated flavors and protect oxidation sensitive oils. By controlling the formulation and processing, improved flavor stability and releasing profiles can be obtained. A recently developed concept is the application of two-phase aqueous systems for encapsulation of water-soluble materials and probiotic bacteria. During spray-drying, surface-active components interact with the droplet surface, and will coat the powder surface according to their adsorption efficiency. Through understanding of these events, formulation and drying conditions can be designed for optimum coating and encapsulation.

Introduction

Microencapsulation of ingredients for food manufacture has received attention for a long time, such as flavor and vitamin encapsulation to improve storage stability and delivery in use, separation of incompatible ingredients, and conversion of liquid ingredients to easy-to-handle dry powders. The most common techniques for encapsulation of food ingredients in dry formulations include coacervation, spray granulation, spray chilling and spray drying. Wet capsules can also be obtained by a variety of techniques, such as coextrusion and entrapment in alginate beads, but a liquid dispersion is more difficult to handle than a dry product. Spray drying has emerged as a versatile and economic technique to obtain dry encapsulated food ingredients from a large variety of feed stocks, including solutions, dispersions, and emulsions. Typically, a matrix type encapsulation, rather than a pure core-shell type particle is obtained, where a multitude of small flavor droplets are dispersed in a continuous wall material. The efficiency of the encapsulation is determined by the level of surface oil, for dried emulsions, and by the storage stability. Certain factors are known to influence the storage stability, such as emulsion droplet size, particle size, and residual water content. By improving the understanding of how particles are generated in the spray-drying process, and combining this with material science of food materials, improved dry food ingredients may be achieved.

Surface formation in spray-drying

In the spray-drying process, small droplets are created by the nozzle. These droplets are contacted with warm air, and water starts to evaporate from the droplet surface. The water evaporation rate is soon limited due to a crust or film forming at the surface. The time to reach this stage is very short – typically 5-20 ms, depending on droplet size, and thus it could be imagined that the components with low solubility will precipitate first and dominate the particle surface (Masters, 1991). However, there are other processes occurring in the droplet during this first period, such as convection and diffusion of species, and changes in interactions between molecules due to increased concentration. In addition, any surface active components will adsorb to the air/liquid interface. The extent of this can be anticipated to be related to the transport rate and the adsorption kinetics.

In order to analyze the surface composition only few techniques are available that provide quantitative analysis of a thin surface layer. X-ray photoelectron spectroscopy (XPS) and time-of-flight secondary ion mass spectrometry (ToF-SIMS) are two methods available that can provide this, with different surface sensitivity (5-10 nm and 1-2 nm, respectively). We have used XPS exten-

sively to study the surface composition of powders and how this relates to composition and processing. The principle of XPS is that the sample, placed under high vacuum, is irradiated by monochromatic X-rays, which excite electrons in the different orbitals, and these emit photoelectrons with different kinetic energy. Photoelectrons will be emitted from the entire sample, but due to energy dissipation during passage through the solid material, only the photoelectrons originating from the surface layer can escape and be detected. The kinetic energy of the photoelectrons is analyzed, and by knowing the energy of the X-ray radiation, the binding energy of the emitted electrons can be calculated, thus providing the atomic surface composition. When this is measured for samples and the pure molecular components in the sample, the surface composition of the sample can be estimated in terms of molecular components, rather than atomic surface composition, by use of different calculation methods (Fäldt et al, 1993; Millqvist-Fureby & Smith, 2007; Ernstsson et al, 1999).

The application of XPS for surface composition analysis, on spray-dried powders of different composition has shown that the surface is dominated by the surface active species in the feed for different powders (emulsions, protein solutions) (e.g., Fäldt & Bergenståhl, 1994, Adler et al, 2000; Millqvist-Fureby et al, 1999a; Elversson & Millqvist-Fureby, 2006). This is illustrated in Figure 1, where the enrichment of protein (casein micelles) at the perimeter of the cross-sectioned particle is obvious. Considering the droplet life-time and the diffusion process for a typical protein ($D=5 \cdot 10^{-11} \text{ m}^2/\text{s}$), it is unlikely that diffusion is the only transport mechanism at play.

Spray-dried emulsions

Spray-dried milk-like emulsions have been used as model system for spray-dried milk, and several studies have been conducted on this system. These studies have led to the conclusion that the surface of such spray-dried emulsions consists of protein and lactose, with patches of fat that have spread from disrupted fat droplets (Millqvist-Fureby & Elofsson, 2004). The extent of protein and fat coverage of the surface depends upon the nature of the protein component (Millqvist-Fureby et al, 1999c), the fat type (Fäldt & Bergenståhl, 1995; Millqvist-Fureby, 2002), and the degree of homogenization. Figure 2a shows how the surface composition varies according to protein component. The fat encapsulation improves in the order whey protein concentrate (WPC) < sodium caseinate (NaCas) < calcium caseinate (CaCas) < skim milk protein (SMP) < casein micelles (CasMic), i.e. the order corresponding well with the size of these protein components.

The degree of homogenization also influences the surface composition for a given protein component, as shown in Figure 2b. Note that the data for surface composition fall on a straight line, which when extrapolated to zero fat content

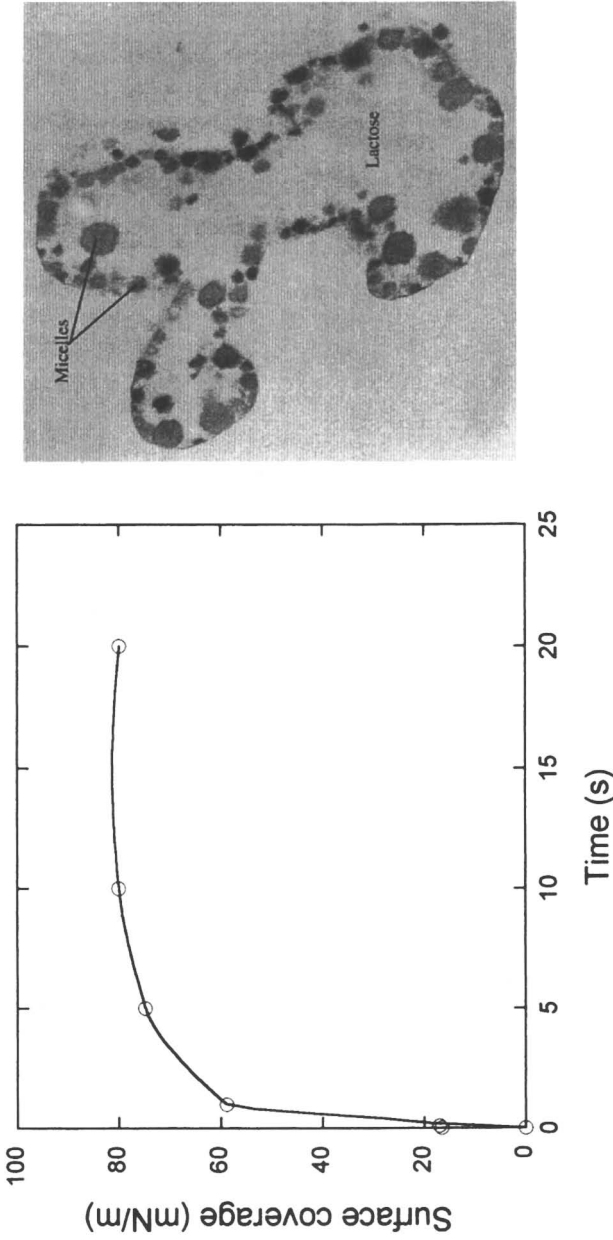


Figure 1. (a) Surface composition of spray-dried powders composed of casein micelles and lactose. (b) TEM micrograph of a particle containing 20% casein micelles and 80% lactose. Casein micelles are stained with osmium tetroxide.

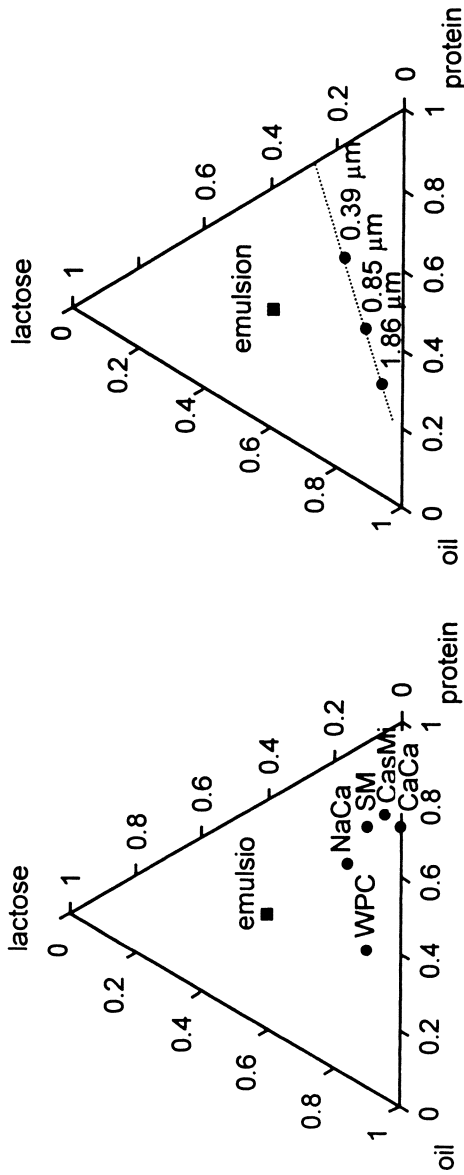


Figure 2. (a) Surface composition of spray-dried protein/rapeseed oil/lactose emulsions. (b) Surface composition of spray-dried sodium caseinate/rapeseed oil/lactose emulsion produced with different homogenization pressures, resulting in different droplet sizes. The median droplet sizes are indicated.

coincides with the surface composition obtained for a spray-dried powder composed of sodium caseinate and lactose in the same proportions (Fäldt & Bergenståhl, 1994).

In-situ coating of powders

Coatings are applied to powders for a variety of reasons, such as encapsulation of ingredients, controlled release, taste masking, prevention of oxidation, powder handling properties, etc. The most common ways to do this include spray-coating in a fluidized bed system. In this technique the coating becomes relatively thick, and the material may not be coated completely. In addition, agglomeration may occur simultaneously with coating. A new approach to this problem is to use the behavior of surface-active materials in spray-drying described above, and employ the non-equilibrium state in the spray droplets: Surface-active materials in the liquid will adsorb to the air/liquid interface, and in a competitive situation the component that adsorbs fastest and most efficiently will tend to dominate at the surface. This approach has been studied for spray-drying of protein in carbohydrate matrices using low-molecular weight surfactants (e.g., Millqvist-Fureby et al, 1999a, Adler et al, 2000) and surface-active polymers (Elversson & Millqvist-Fureby, 2006). The addition of the non-ionic surfactant polysorbate to trypsin-lactose mixture improved the retention of enzyme activity and decreased the surface coverage of protein, which can be explained by the large difference in diffusion coefficient between polysorbate and trypsin (Millqvist-Fureby et al, 1999a).

When surface-active polymers are used as coating substances, the transport of the coating polymer and a protein to the interface can be expected to occur at similar rates. The outcome of this competition for the interface will be determined by the relative adsorption rates for these polymers, since an equilibrium situation cannot be expected. This can be studied by dynamic surface tension analysis, see figure 4a. Although the protein may give a lower equilibrium surface tension (comparing e.g. insulin and poly(vinyl alcohol) (PVA)), the polymer reduces the surface tension more rapidly, and in a mixture of protein and polymer, the final surface tension is determined by the polymer rather than the protein. This indicates that the replacement of an adsorbed polymer by the more surface active protein is a very slow process. The behavior during dynamic surface tension measurements can be correlated with the surface composition of corresponding spray-dried samples, see figure 4b. The structure of bovine serum albumin (BSA) in formulations with and without coating polymers was investigated, and it was found that in this case, the coating did not influence the protein structure. However, the powder properties were affected: the dissolution rate was decreased by the polymer coating, and flow properties of coated powders were improved in some cases. This provides an opportunity to direct the powder prop-

erties, as well as influencing the release rate. Possible uses include coating of particles for protection in oral delivery for release in the intestine, and release of active components in liquid foods or after rehydration of powdered foods. This may also be used as a means of sustained release, providing the coating material swells and acts as a permeable release barrier.

The same approach can also be used to provide a functional coating composed of surface active smaller molecules such phospholipids. This has been described for dairy ingredients in chocolate application (Millqvist-Fureby & Smith, 2007). Phospholipids were added to lactose or dairy protein solutions, and after spray-drying the surface was dominated by phospholipids in the case of lactose and skim milk powder, but not in the case of whey protein concentrate due to the binding of phospholipid molecules to whey proteins. The phospholipid coated particles showed more rapid settling when mixed with cocoa butter than uncoated powders or when phospholipids were added in the fat phase. The settling rate reflects the rheological behavior of the system, and it can be anticipated that the transient rheological behavior would be improved when using pre-coated dairy particles. The overall addition of phospholipids in the product could be expected to be reduced.

Encapsulation in aqueous two-phase systems

When two neutral polymers are mixed in a common solvent, phase separation will occur spontaneously due the unfavorable entropy of mixing combined with an enthalpic contribution. When water is the solvent, these systems are called aqueous two-phase systems (ATPS), and the most extensively studied examples is probably poly(ethylene glycol) (PEG)/dextran that has been applied for separation of proteins, cell organelles and whole cells. Such systems can also be formed by, for example PEG/phosphate (Albertsson, 1960) or protein/polysaccharide under appropriate conditions (Grinberg & Tolstoguzov, 1997). The interfacial tension in ATPS is very low, and thus sensitive biological structures are generally not negatively influenced by the interface. Each phase will be enriched in one of the polymers and contains only a small amount of the other polymer, which can be illustrated in a phase diagram.

When stirring is applied to an ATPS, a water-in-water emulsions is easily obtained, which can be used to encapsulate the dispersed phase in the continuous phase through spray-drying, as illustrated in Figure 5. The phase separation persists after drying, and thus results in double encapsulation of the materials that partition to the dispersed phase. The phase that is to become dispersed is primarily determined by the phase volume ratio.

For an optimal ATPS for encapsulation several requirements need to be fulfilled:

- The selected polymers form a two-phase system

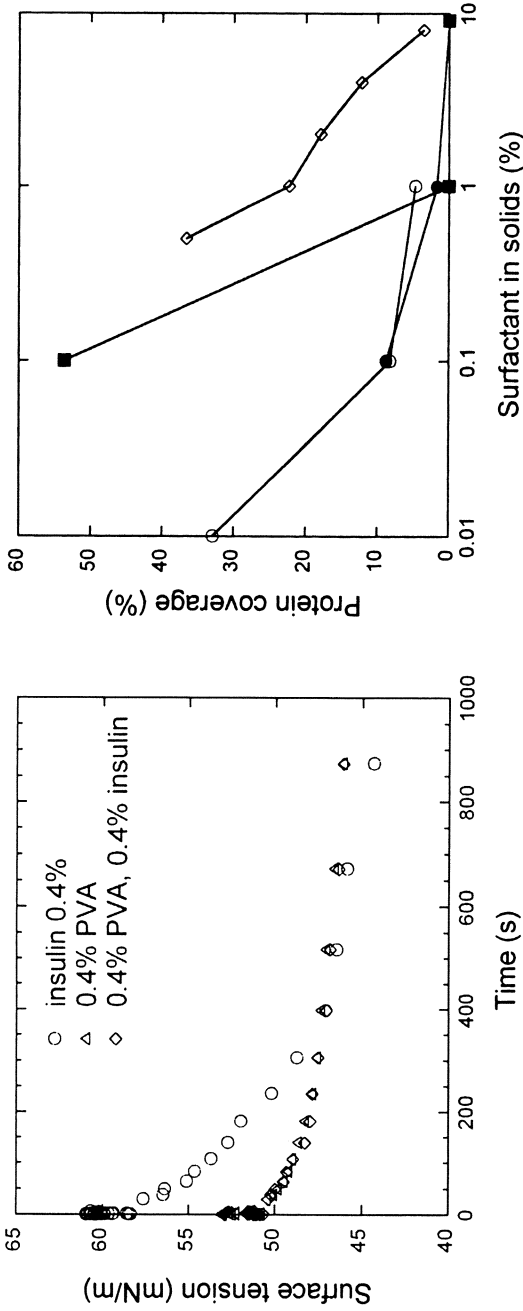


Figure 4. (a) Dynamic surface tension analyses of PVA, insulin and mixed PVA and insulin. (b) The efficiency of different surface-active polymers in removing BSA from the powder surface (O) insulin/Poloxamer 188, (●) BSA/Poloxamer 188, (■) BSA/HPMC, and (◇) BSA/PVA. The surface coverage of insulin and BSA in the absence of surface-active additives was 59% and 57%, respectively.

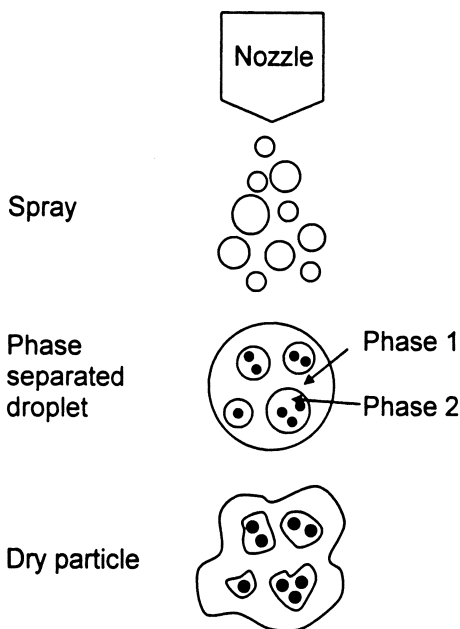


Figure 5. Schematic illustrating encapsulation in ATPS in spray drying. The active component (indicated as black dots) is distributed to phase 2, and becomes encapsulated when phase 2 is dispersed in phase 1. The phase separation persists in the dried material.

- The active component partitions strongly to one of the phases
- The viscosity of the ATPS must be suitable for spray-drying, i.e. not too high and no substantial extensional viscosity
- The polymers must not interact negatively with the active component.
- The polymers must comply with the regulations for the area of application, e.g. food, feed, or pharmaceuticals.

The system PVA/dextran has been studied in some detail by Elversson & Millqvist-Fureby (2005) for encapsulation of BSA. BSA partitions strongly to the dextran-rich phase to be a useful model protein. It was found that the two-phase system persists in the dried state, manifested as two separate glass transitions, corresponding to PVA and dextran, respectively. The surface composition did not reflect the phase separation, since the PVA in the dextran continuous phase at low PVA content was sufficient to coat the surface in competition with BSA. This was also manifested in the dissolution properties, the dissolution time ranges from 10 minutes for dextran as the sole polymer up to 60 minutes for

PVA as the only polymer. Pycnometry measurements indicated that the gas permeability of the surface layer is reduced when the PVA content is increased, since the apparent density was reduced from 1.2 g/cm³ to 0.4 g/cm³ for dextran and PVA respectively. This indicates that such systems could be applied to encapsulation of air sensitive materials.

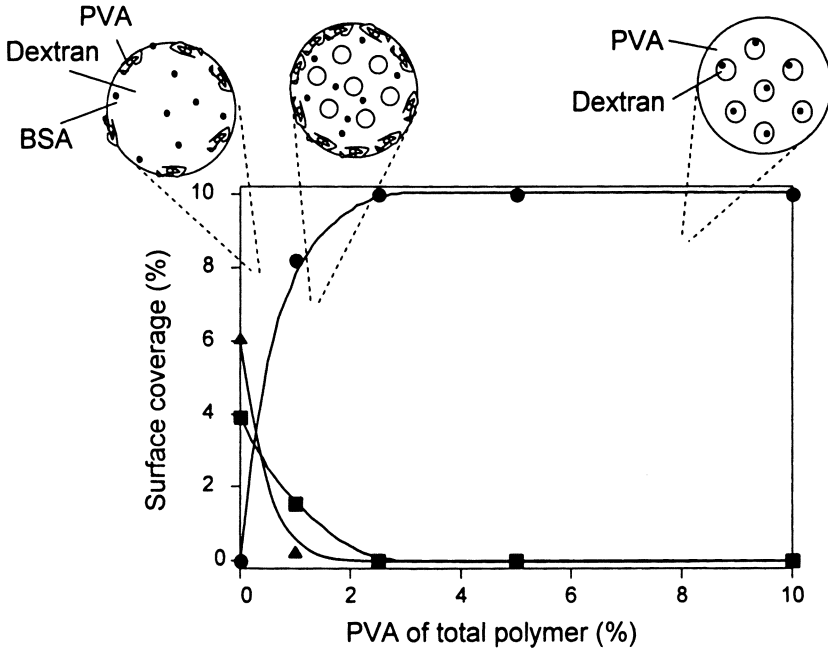


Figure 6. The surface composition as estimated from XPS data for spray-dried PVA/dextran with encapsulated BSA, and schematic illustrations of the internal particle structure. (●) PVA, (■) dextran and (▲) BSA.

The ATPS concept for encapsulation of biologicals has also been investigated for live probiotics (Millqvist-Fureby et al, 2000; Millqvist-Fureby & Elofsson, 2001). Currently, most probiotic products are sold as fresh, liquid foods, such as yoghurts and fruit drinks. The dried products (capsules, tablets, straws for drinks, etc) presently marketed are mainly freeze-dried. The drawback of freeze-drying is the expense and the long processing time. Cheaper dry preparations of live probiotics would increase their applicability in food and feed, as well as enable new types of products.

We have investigated the encapsulation of a number of probiotic strains in a variety of ATPS. Figure 7 illustrated the survival rate of *Lactobacillus*

plantarum in methyl cellulose/dextran, where the cells partition virtually exclusively to the dextran-rich phase. It can be observed that the two-phase systems are superior in terms of survival rate both in fresh and stored powders. The low survival rate at 75% MeC/25% dextran is presumably due to the small dextran-rich phase, so that the cell density effectively becomes very high. The survival rates could be improved by adding various saccharides, which are known lyoprotectants for freeze-drying of proteins. These act as 'water replacers' and take part in hydrogen bonds with the biological material in the dry state, thereby increasing the retention of native structures. The superior efficiency of trehalose compared to lactose and sucrose cannot be explained. It is known that trehalose is the main carbohydrate produced in yeast when it is exposed to dehydration.

Concluding remarks

Spray-drying is a versatile tool to produce structured particles with controlled surface properties. The underlying principle is the adsorption of surface-active components to the air/liquid interface of the spray droplets. By choosing suitable materials, e.g. surface-active polymers, a coating effect can be achieved, that will influence stability of coated proteins, particle shape and dissolution properties.

Coating of materials can also be achieved by applying ATPS for partitioning of the active ingredient. In such systems, the polymers must be carefully selected to provide the desired performance and have appropriate processing performance. These formulations also provide enhanced encapsulation, prolonged stability, and have effects on particle morphology and release properties.

References

- Adler, M.; Unger, M.; Lee, G. *Pharm Res*, **2000**, *17*, 863-870.
- Albertsson, P.Å. *Partition of cell particles and macromolecules*, Almqvist & Wiksell: Stockholm, 1960.
- Elofsson, U.; Millqvist-Fureby, A. *Minerva Biotechnologia*, **2001**, 279-286
- Elofsson, U.; Millqvist-Fureby, A. *Food colloids, biopolymers and materials*; Bos, M.; van't Vliet, T., Eds.; The Royal Society of Chemistry: Cambridge
- Elversson, J.; Millqvist-Fureby, A. *Int J Pharm.* **2006**, *323*, 52-63.
- Elversson, J.; Millqvist-Fureby, A. *Int J Pharm.* **2005**, *294*, 73-87.
- Ernstsson, M.; Claesson, P.M.; Shao, S.Y. *Surface Interface Analysis.* **1999**, *27*, 915-929.

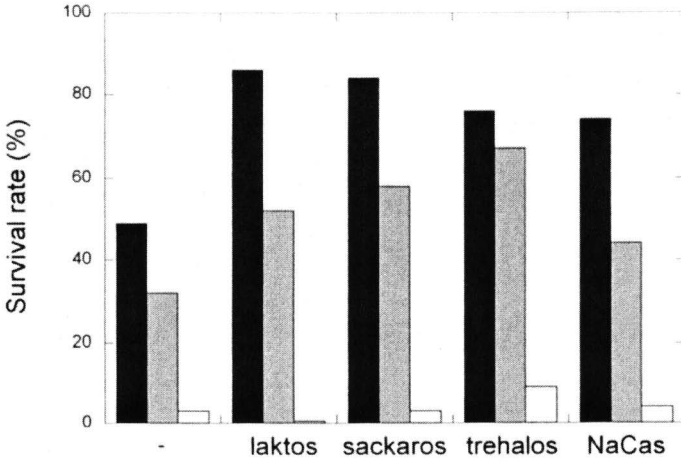
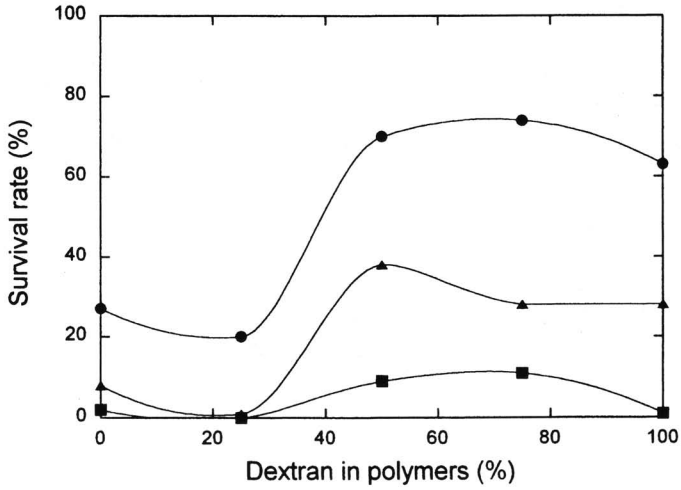


Figure 7. (a) Survival rate of *L. plantarum* in spray-dried ATPS composed of MeC/dextran, (●) in fresh powder, (■) after 5 weeks at room temperature, and (▲) 5 weeks at 4°C. (b) The survival rate in MeC/dextran with various additions in fresh powders (black bars) and powders stored 5 weeks at 4°C (grey bars).

- Fäldt, P.; Bergenståhl, B. *Coll. Surf. A: Physicochemical and Engineering Aspects*. **1994**, *90*, 183-190.
- Fäldt, P.; Bergenståhl, B. *JAOCS*. **1995**, *72*, 171-176
- Fäldt, P.; Bergenståhl, B.; Carlsson, G. *Food Structure*. **1993**, *12*, 225-234.
- Grinberg, V.Y.; Tolstoguzov, V.B. *Food Hydrocolloids*, **1997**, *11*, 145-158.
- Landström, K.; Alsins, J.; Bergenståhl, B. *Food Hydrocolloids*. **2000**, *14*, 75-82.
- Masters, K. *Spray Drying Handbook*; 5th ed; Longman Scientific & Technical: Essex, 1991.
- Millqvist-Fureby, A.; Smith, P. *Food Hydrocolloids*. **2007**, *21*, 920-927.
- Millqvist-Fureby, A. *Colloids Surf B*. **2003**, *31*, 65-79
- Millqvist-Fureby, A.; Malmsten, M.; Bergenståhl, B. *Int J Pharm*. **1999a**, *188*, 243-253.
- Millqvist-Fureby, A.; Malmsten, M.; Bergenståhl, B. *Int J Pharm*. **1999b**, *191*, 103-114.
- Millqvist-Fureby, A.; Malmsten, M.; Bergenståhl, B. *J Colloid Interface Sci*. **2000**, *225*, 54-61.
- Millqvist-Fureby, A.; Burns, N.; Landström, K.; Fäldt, P.; Bergenståhl, B. *Food Emulsions and Foams*. Dickinson, E.; Rodriguez Patino, J.M., Eds.; The Royal Society of Chemistry: Cambridge, 1999c; pp 236-245.

Chapter 16

Aroma Release at the Nano- and Microscale: Molecules to Droplets

A. J. Taylor, K. Pearson, T. A. Hollowood, and R. S. T. Linforth

**Division of Food Sciences, University of Nottingham, Sutton Bonington
Campus, Loughborough LE12 5RD, United Kingdom**

Aroma release is governed by physico-chemical factors like partition coefficients which regulate the relative amounts of an aroma in the gas and food phases. While this relationship holds good for many liquid and semi-solid foods, it only applies to systems where aroma is homogeneously distributed and where aroma is present in solution. The effect of length scale on aroma release *in vivo* and *in vitro* has been studied to better understand release from encapsulated systems. When aroma was incorporated into foods in alternate aromatized and un-aromatized layers, overall release was not affected due to mixing by mastication, which negated the aroma separation. In the presence of co-solutes (propylene glycol, triacetin, ethanol) aroma release from high solids gel systems was affected. The physical state of the aroma (solubilized or microdroplet) also has significant effects and may explain the aroma burst observed from encapsulated flavors.

Introduction

In order for consumers to sense the aroma of a food product, volatile compounds must be released from the food and transported to the olfactory receptors located high in the nose. Flavor scientists recognize two routes for aroma transport. The first route typically occurs before eating when we sniff the food and take in the volatile compounds through the orthonasal route. The second route occurs during eating, when aroma is transported from the mouth to the receptors in the nose (the retronasal route) either by chewing actions, which pump small volumes of air into the throat, or by swallowing, when air is transferred from the mouth to the throat and then exhaled via the nose. Methodologies for measuring the aroma profiles above foods have been developed using *in vitro* and *in vivo* techniques. Orthonasal aroma profiles are often mimicked using Dynamic Headspace Dilution Analysis, in which a solution of aroma compound is first equilibrated with a fixed volume of air (the headspace) and then diluted by a known flow rate of air. The concentration in the headspace is monitored with time and a typical exponential decay is seen until the system reaches a steady state where removal of aroma is balanced by release from the solution. This type of analysis has been applied to study the changes in tea headspace aroma (1) or the effects of emulsion composition on aroma release in model systems (2) or in real food (3). To study aroma release during eating, direct monitoring of volatile compounds using mass spectrometric techniques have been used to measure the aroma profile in exhaled air from the nose (4, 5). Other workers have developed model mouths, which reduce the variability found *in vivo*, but it is difficult to reproduce the complex actions of saliva, tidal air flow and mastication and few systems have been validated by comparison against release *in vivo* (6).

Some theoretical physical principles surrounding aroma release (7) have limitations when applied to food systems but partition has been shown to have relevance both under static equilibrium conditions as well as dynamic release conditions. In the latter situation, partition still defines release at the interface but other factors (surface area, gas flow rate, diffusion) also make significant contributions to the overall release process (8). In encapsulated systems, there are other aspects to consider when predicting release behavior. The length scale of release (nano or micro) has potential effects as has the form of the flavor (solublized in water or present as droplets) not to mention the nature of the encapsulating material. The purpose of this paper was to study aroma release from liquid and gel systems containing co-solvents (e.g. propylene glycol), containing non-homogenous distribution of flavor or non-solublized micro droplets of aroma to determine which factors were significant and to provide an understanding of how aroma can be delivered from encapsulated systems in a controlled manner.

Materials and Methods

Aroma solutions (limonene and hexanol; Sigma-Aldrich) were prepared in HPLC grade water by mechanical shaking (2 h) in stoppered, all glass flasks. When co-solvents were used, the aroma compound was first dissolved in the co-solvent and this solution added to water to obtain the same final concentration and shaken for 2 h. Xanthan solution (0.8 %; Red Carnation Gums) was prepared by dispersing xanthan in water at room temperature and stirring for 2 h to ensure complete hydration and solution.

Gelatin-sucrose gels were prepared using 30 g of pre-soaked gelatin (Gelatin Weishardts, Type A, 225 Bloom) in 100 mL of distilled water, a sucrose syrup (150g in 75 mL water) and 200 g of glucose syrup (Cargill Sweeteners, 42DE). The syrup was heated to 112 °C and stirred to ensure complete dissolution; it was then cooled to 75 °C and the gelatin solution was added and stirred in along with 5 g of citric acid in 20 mL of water and aroma solutions (125 mg/kg). After cooling, 20mm gel cubes were produced. The product formed was a relatively hard gel with a texture similar to that found in Gummi-bear or wine-gum confectionery. Layered gels (4 layers) were prepared by casting a flavored layer and then adding an unflavored layer and allowing it to cool.

Layered chewing gum samples were prepared at Firmenich SA, Geneva by incorporating aroma into a portion of the gum base and rolling to make 2-8 layers of alternate, flavored and unflavored gum.

Droplets of aroma compounds were colored with β -carotene (20 mg) dissolved in pure aroma compound (2 mL) to visualize them. Aroma release from droplets in water was achieved by expelling a 1 μ L droplet from a syringe beneath the surface of the water and videoing the interface from above to show the release behavior. Later, carbon black was shaken onto the air-water interface prior to the droplet being released and the interface videoed. Quantitative data were obtained by monitoring release of aroma compounds into the headspace using APCI-MS.

Aroma release with time was monitored using Atmospheric Pressure Chemical Ionization-Mass Spectrometry (9). For the gels and chewing gum, all combinations of flavored and non-flavored layers were prepared for 1, 2, 4 and 8 layered samples and eaten by a panel of four people in triplicate. Aroma release was recorded using APCI-MS and the time to maximum intensity (T_{max}) and the maximum intensity (I_{max}) values recorded and averaged across panelists and replicates.

Sensory analysis of aroma release from droplet systems was carried out with a panel of 14 panelists trained in Time Intensity analysis. They underwent a training session to familiarize themselves with the samples and their maximum and minimum flavor intensities and then, in a single session, assessed each sample in triplicate, in a balanced presentation order. From the TI curves, the

maximum sensory intensity (I_{max}) and the Time to Maximum Intensity (T_{max}) were averaged using the Fizz software (Biosystemes) and compared statistically using Analysis of Variance and Tukeys HSD multiple comparison test at a 5% level of significance

Results

Effect of non-homogenous distribution – millimeter scale layers

Statistical analysis of *in vivo* aroma release by comparing the T_{max} and I_{max} values for the sucrose-gelatin and chewing gum samples showed no significant differences. This demonstrated that the location of the flavor in the layers had no effect on aroma release because mastication effectively mixed the layers forming a saliva phase with the same, homogenous aroma content from which the same release into the gas phase occurred. Data from Prinz (10) showed that chewing of layered chewing gum resulted in mixing of the colored layers after a period of minutes, which supports the hypothesis above.

Effect of co-solvent - molecular scale level

Aroma compounds are often delivered using mixtures of water with co-solvents like ethanol, propylene glycol or triacetin to overcome the difficulty of solubilizing directly in water. The effects of these solvents in aqueous-based systems has been reported (11, 12) but, in systems where water is limiting (as in the gelatin-sucrose gel formulation used here) it is difficult to define the physical state and location of the aromas. Water is likely to be attracted to the more hydrophilic gelatin and sucrose components, suggesting that there may be some phase separation and that the aroma may exist in a co-solvent rich phase, rather than an aqueous solution. The effect of this molecular scale effect was studied by preparing the gelatin-sucrose gels with two volatile compounds with different hydrophobicities, expressed by their different log P values (limonene, 4.83 and hexanol 1.74).

The aroma release during consumption of gels containing the two compounds is shown in Figure 1a and b. There is a clear effect of co-solvent on limonene release and this sparingly soluble terpene has been reported to form microemulsions with ethanol and propylene glycol (13). Similar effects of co-solvents have also been seen in aroma release from hard candies (14) and the low water environment of hard candies also leads to aroma-aroma interactions which affects release (15). Thus, in some situations, the presence of co-solvents can change aroma release both *in vivo* and *in vitro* and this is probably due to a change in microstructure.

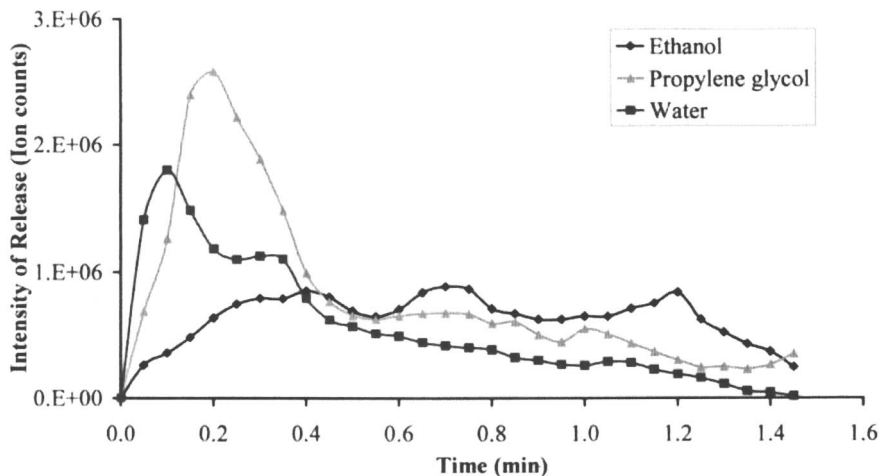


Figure 1a. In vivo release of limonene from gels containing 2% of water or a co-solvent. Values are the mean of 9 determinations.

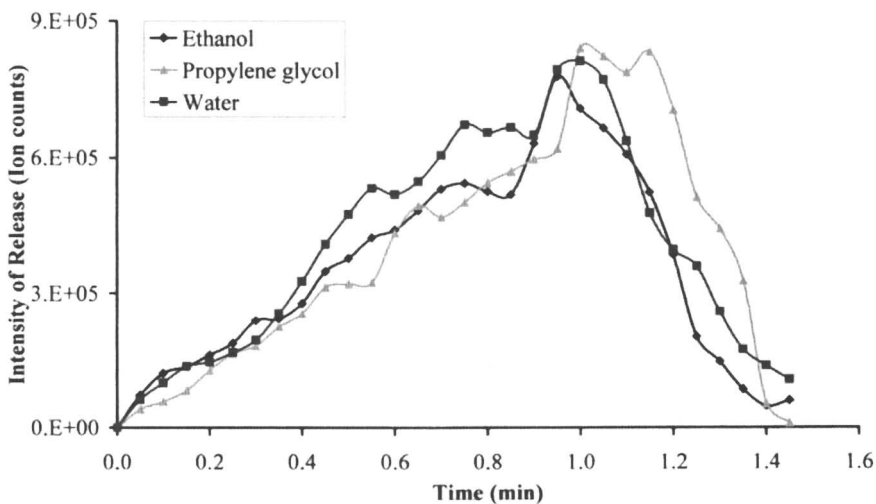


Figure 1b. In vivo release of hexanol from gels containing 2% of water or a co-solvent. Values are the mean of 9 determinations.

Effect of non-solubilized droplets in vitro – millimeter scale

The previous sections described how aroma is released when it is solubilized in the test system. In commercial encapsulated systems, the manufacturing process results in small droplets of aromas coated with a barrier to prevent volatilization and oxidation during storage. Release occurs when the coating breaks down on hydration but whether the aroma compounds dissolve in the aqueous phase or are released by some other mechanism is not always clear. To study the phenomenon of droplet release from water, 1 μ L droplets of ethyl butyrate were colored with β -carotene and released from a syringe held at a depth of 30 mm below the air-water interface. The interfacial region was monitored with a video camera mounted above the interface and Figure 2 shows still frames taken from the video at certain points after droplet release. Exact times are not given as the time taken for the droplet to leave the syringe and reach the surface varied due to the difficulty of releasing droplets from the tip of the syringe in a consistent way. Figure 2 shows a typical sequence of events. Initially the droplet moves from the point of release to the surface where it forms a ring of aroma compound at the interface with the main bulk of the droplet still intact. As more of the droplet reaches the interface, the ring of released aroma compound broadens and travels outwards from the initial point. When all the aroma compound has been released to the interface, there are signs of motion as the interface oscillates as if “mini waves” were present.

To ensure that the effect was not unique to ethyl butyrate, a range of other compounds were tested (ethyl decanoate, carvone, α -damascenone, limonene, linalool, heptanol, heptanone, anethole) and all showed the same behavior when released as pure compounds or as mixtures. To confirm that the droplet was reaching the interface, the experiments were repeated with a layer of carbon black sprinkled onto the air-water interface before the droplet was released. For all compounds, release of the droplet caused the carbon black to be pushed away from the area where release was occurring, which could be easily located by observing the colored aroma compound. Experiments where commercially encapsulated aromas (Flexarome, Firmenich) were placed in a beaker, covered with water and the surface covered with carbon black also showed the same behavior with the released aroma compounds pushing back the carbon black. These observations suggested that release from some commercial systems was also via the droplet route.

It was postulated that, in the case of droplets, aroma release occurred because the droplets were buoyant in the water phase and rapidly moved to the hydrophobic air-water interface where release occurred by volatilization. These observations were made in vitro using carefully controlled conditions and the next stage was to determine whether these effects would be seen in vivo or whether mastication would negate them.



Figure 2. Frames from video monitoring of the interface as a 1 μ L droplet of ethyl butyrate, dyed yellow with β -carotene is released from 30 mm under the surface. Left to right: i) the droplet can be seen just under the surface with a ring of released material around it; ii) traces of the droplet can be seen within the ring which is now larger; iii) the interface shimmers in this frame as a result of motion at the interface.

Effect of droplets *in vivo* – millimeter scale

The results above show that droplet release *in vivo* can have major effects on aroma release in a model system. The next task was to study whether these effects were significant *in vivo*, where the volume of saliva is smaller and the possibilities of mixing and interaction with other food or mouth constituents (e.g. salivary proteins) may lessen the effect.

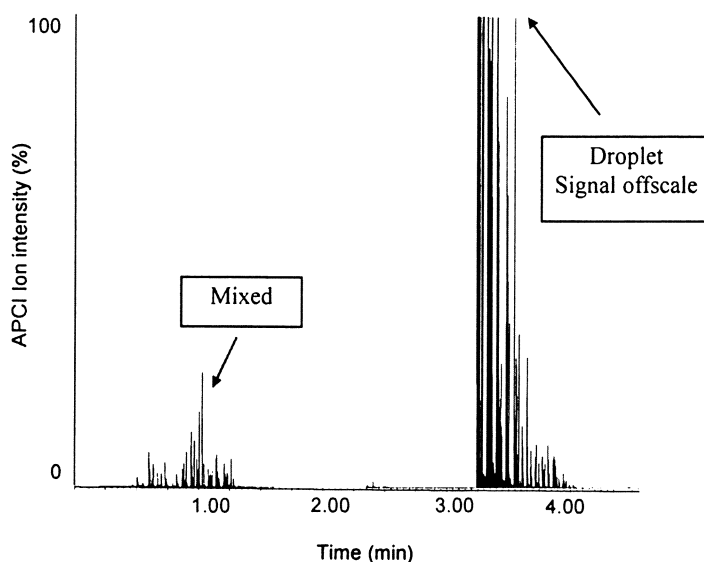


Figure 3. In vivo release of ethyl butyrate from xanthan solutions containing 1 μ L of aroma. Samples were either mixed for 10 s (Mixed) and then consumed or consumed unmixed as a single droplet (droplet) while the concentration of ethyl butyrate in exhaled air from the nose was monitored by APCI-MS (relative units) against time (X axis seconds).

To deliver droplets for *in vivo* consumption, it was necessary to place the droplet in the centre of a thickened solution of 0.8 % xanthan (15 mL), which held the droplet in place in a small tube. Human panelists consumed the samples either in the single droplet form or by vigorously mixing the droplet and xanthan solution by shaking for 10 s and then consuming the whole sample. The release of aroma was measured in nose using APCI-MS and Figure 4 shows the typical pattern of aroma release observed. Release from the single droplet was always higher than the mixed droplets demonstrating that there is an effect of length scale on particle size which presumably controls the way the droplets can move

to the interface. This aspect needs more rigorous research to determine the effect of particle size, density, surface tension etc. on aroma release.

The xanthan system represented a liquid food where the droplets could move through the liquid phase and be brought to the surface by mastication and mouth movements. Would release also occur in a gel system containing a single suspended droplet where mastication was needed to fracture the gel and where mixing might cause some solubilization? Gelatin-sucrose gels were made with 1 μL of aroma either dissolved in the gel during production or added as a droplet to the gel as it cooled so that both samples contained the same amount of aroma. Samples were eaten and release measured by APCI-MS analysis of the exhaled air (Table 1).

Table 1. In vivo release of aroma compounds from gelatin-sucrose gels containing either a 1 μL droplet or 1 μL dissolved in the gel during production. Ratios are the average from one subject eating 4 replicate gels

<i>Compound</i>	<i>Log P^a</i>	<i>Log vapor pressure^a</i>	<i>Imax Ratio Droplet/Dissolved</i>
2-Butanone	0.26	1.99	4.2
Methyl acetate	0.37	1.72	4.3
Ethyl acetate	0.86	1.99	14.3
Hexanal	1.80	0.98	83.7
Ethyl butyrate	1.85	1.16	666
2,3-Diethyl pyrazine	2.02	-0.11	12.5
Octanone	2.22	0.37	421
Amyl acetate	2.26	0.62	1793
Octanol	2.73	-0.62	6.6
Ethyl hexanoate	2.83	0.26	2432
Carvone	3.07	-0.89	7.6
Linalool	3.38	-0.80	388
Citral	3.45	-1.04	9.9
Ethyl octanoate	3.81	-0.63	764
Menthofuran	4.29	-1.09	88.0
Limonene	4.83	0.16	11.3

^a values obtained from EPI Suite, US Environmental Protection Agency and Syracuse Research Corporation

Differences were compound dependent but ranged from a factor of 2400 to a factor of 3, depending on the compound's log P and vapor pressure values (data not shown). When the data from Table 1 were plotted (data not shown), there was a parabolic relationship between release and log vapor pressure and log P with an optimum around log VP of 0.25 and log P of 3.2.

While APCI-MS measurements in nose show that the aroma compounds were released differently from gels, it did not necessarily mean that there was a sensory effect, so experiments were carried out to test for, and quantify, any sensory differences, using Time Intensity sensory analysis. Figure 4 shows the average time intensity traces from 14 panelists who consumed the two samples in triplicate. The differences in the maximum perceived fruity flavor and the time to this maximum were significantly different (Table 2) and the sensory effects showed a degree of “smoothing” of the aroma signal (Figure 4).

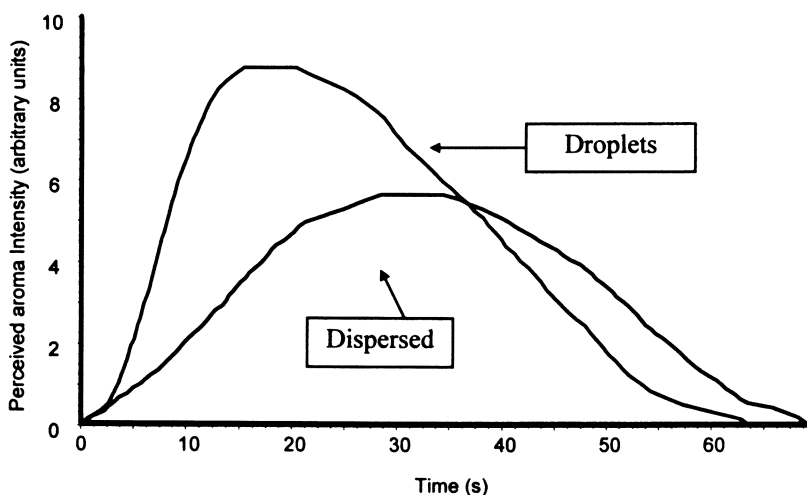


Figure 4. Average time intensity traces from 14 panelists who consumed gels containing a single droplet (1 μ L) of ethyl butyrate or a gel containing the same amount of ethyl butyrate dispersed in the gel during manufacture.

The significance values in Table 2 show that clear differences in sensory perception were observed across all 14 panelists. T_{max} and I_{max} have already been explained and slope refers to a linear estimation of the initial rate of aroma release which has been related to sensory perception in gels (16). Area is considered as a measure for the total aroma released during the consumption event and the values are significantly different but at the 5% level of confidence.

In conclusion, the results show that, while much attention has been focused on the process of aroma encapsulation and the stability of the micro/nano scale structures formed, the way the structures break down and release the aroma compounds is also important. Those familiar with aroma encapsulation will realize there is a potential conflict in making small droplets during the emulsification stage of encapsulation (so that each droplet is coated with its

Table 2. Statistical analysis of sensory time intensity parameters derived from Figure 4 for the 14 panelists

<i>Parameter</i>	<i>Dispersed</i>	<i>Droplets</i>	<i>Significance</i>
Tmax	28.5	15.4	P<0.001
Imax	5.7	8.8	P<0.001
Slope	0.4	1.1	P<0.001
Area	222	290	P<0.05

protective barrier to ensure minimal degradation on storage) and optimizing droplet size for aroma release under the conditions described above (17, 18). This is another aspect that needs further investigation. The direct release of aroma compounds to the air-water interface, and their subsequent volatilization, requires more study to understand what physico-chemical principles govern release under these conditions and how they might be applied to give suitable bursts of flavor in foods.

Acknowledgements

This work was supported through an EPSRC CASE studentship allocated to the Food Processing Faraday (FPF) and supported by Firmenich, UK. Thanks are due to the FPF and EPSRC for the scholarship; the financial and technical contributions of Firmenich are acknowledged.

References

1. Wright, J.; Wulfert, F.; Hort, J.; Taylor, A. J., Effect of preparation conditions on release of selected volatiles in tea headspace. *J. Agric. Food Chem.* **2007**.
2. Desamparados, S.; Bakker, J.; Langley, K. R.; Potjewijd, R.; Martin, A.; Elmore, S., Flavour release of diacetyl from water-sunflower oil and emulsions in model systems. *Food Qual. Pref.* **1994**, *5*, 103-107.
3. Charles, M.; Rosselin, V.; Beck, L.; Sauvageot, F.; Guichard, E., Flavor release from salad dressings: Sensory and physicochemical approaches in relation with the structure. *J. Agric. Food Chem.* **2000**, *48*, 1810-1816.
4. Linforth, R. S. T.; Martin, F.; Carey, M.; Davidson, J. M.; Taylor, A. J., Retronasal transport of aroma compounds. *J. Agric. Food Chem.* **2002**, *50*, 1111-1117.

5. Linforth, R. S. T.; Taylor, A. J., Direct mass spectrometry of complex volatile and non-volatile flavour mixtures. *Int. J. Mass Spec.* **2003**, 223-224, 179-191.
6. Deibler, K. D.; Lavin, E. H.; Linforth, R. S. T.; Taylor, A. J.; Acree, T. E., Verification of a mouth simulator by in vivo measurements. *J. Agric. Food Chem.* **2001**, 49, 1388-1393.
7. Taylor, A. J., Physical chemistry of flavour. *Int. J. Food Sci. Tech.* **1998**, 33, 53-62.
8. deRoos, K. B., Physicochemical models of flavor release from foods. In *Flavor release*, Roberts, D. D.; Taylor, A. J., Eds. American Chemical Society: Washington D.C., 2000; Vol. 763, pp 126-141.
9. Taylor, A. J.; Linforth, R. S. T.; Harvey, B. A.; Blake, A., Atmospheric pressure chemical ionisation for monitoring of volatile flavour release in vivo. *Food Chem.* **2000**, 71, 327-338.
10. Prinz, J. F.; De Wijk, R. A., The role of oral processing in flavour perception. In *Flavour perception*, Taylor, A. J.; Roberts, D. D., Eds. Blackwells: Oxford, 2004; pp 39-56.
11. Boelrijk, A. E. M.; Basten, W.; Burgering, M.; Gruppen, H.; Voragen, F.; Smit, G., The effect of cosolvent on the release of key flavours in alcoholic beverages: Comparing in vivo with artificial mouth-MS nose measurements. In *Flavour research at the dawn of the twenty first century*, LeQuere, J.-L.; Etievant, P. X., Eds. Intercept: Paris, 2003; pp 204-207.
12. Millard, J. W.; Alvarez-Nunez, F. A.; Yalkowsky, S. H., Solubilization by cosolvents - establishing useful constants for the log-linear model. *International Journal of Pharmaceutics* **2002**, 245, 153-166.
13. Yaghmur, A.; Aserin, A.; Garti, N., Phase behavior of microemulsions based on food-grade nonionic surfactants: Effect of polyols and short-chain alcohols *Colloids and Surfaces A-Physicochemical and Engineering Aspects* **2002**, 209, 71-81.
14. Schober, A. L.; Peterson, D. G., Flavor release and perception in hard candy: Influence of flavor compound-flavor solvent interactions. *J. Agric. Food Chem.* **2004**, 52, 2628-2631.
15. Schober, A. L.; Peterson, D. G., Flavor release and perception in hard candy: Influence of flavor compound-compound interactions. *J. Agric. Food Chem.* **2004**, 52, 2623-2627.
16. Baek, I.; Linforth, R. S. T.; Blake, A.; Taylor, A. J., Sensory perception is related to the rate of change of volatile concentration in-nose during eating of model gels. *Chem. Senses* **1999**, 24, 155-160.
17. Gunning, Y. M.; Gunning, P. A.; Kemsley, E. K.; Parker, R.; Ring, S. G.; Wilson, R. H.; Blake, A., Factors affecting the release of flavor

- encapsulated in carbohydrate matrixes. *J. Agric. Food Chem.* **1999**, *47*, 5198-5205.
18. Whorton, C., Factors influencing volatile release from encapsulation matrices. In *Encapsulation and controlled release of food ingredients*, Risch, S. J.; Reineccius, G. A., Eds. American Chemical Society: Washington D.C., 1995; Vol. 590, pp 134-142.

Chapter 17

Flavor Delivery via Lipid Encapsulation: Flavor Retention in Cake and Loaf Volume in Bread

John Finney and Gary Reineccius

Department of Food Science and Nutrition, University of Minnesota,
St. Paul, MN 55108

The ability of lipids to deliver flavorings in cake and bread applications was studied. A model flavoring (esters or garlic oil) was added to molten lipids (varying in melting point), the lipid allowed to solidify, and then it was cryo-ground to the desired particle size. This flavored lipid powder was then added to cake batter (esters) or bread dough (garlic oil) and the products prepared, baked and analyzed (cakes for ester retention and bread for loaf volume). For comparison, the model ester flavorings were prepared in liquid form and by spray drying. There was no benefit of incorporating esters in either lipid or spray dried form on ester retention during baking: losses ranged from 3-99% increasing with volatility of the ester. There was no benefit of incorporating garlic oil in a lipid capsule on bread loaf volume Vs. adding it in liquid or spray dried form.

Introduction

The flavor losses associated with high temperature processing and cooling (i.e. baking) are well known (1, 2). In some cases, these losses can be compensated for by adding more flavor (3, 4). However, losses are not uniform across a flavor: the most volatile compounds are preferentially lost thereby altering the flavor profile of the product (1). Thus, the addition of more flavor does not necessarily solve the problem. While flavor loss during heating and cooling are problematic, flavor losses during mixing/hydration and through interactions with major ingredients also contribute to changes in flavor profile (5, 6, 7, 8).

The food / flavor industry has employed a variety of means in order to encapsulate flavor compounds in order to minimize flavor loss while maintaining the release properties necessary to deliver an acceptable level of flavor to the consumer (9, 10, 11, 12, 13). Most flavorings are encapsulated in water soluble polymers and thus, the flavors are released on the addition of water to a formulated mix/dough. Encapsulating a flavor in a lipid would slow release and may thereby offer some protection to a flavoring.

A second consideration is that some essential oils/flavorings have antimicrobial activity. This activity can slow yeast growth thereby increasing proofing time and decreasing loaf volume (bread) (14, 15). Sequestering essential oils in a lipid capsule may again slow release and minimize the antimicrobial activity of an oil such as garlic. This study was conducted to determine if there is any benefit of putting flavorings into a lipid capsule on both flavor retention (flavored cake mix) and antimicrobial activity of garlic oil (yeast leavened bread).

Materials and Methods

Materials:

Study 1 – Bread loaf volume

Bread ingredients include bread flour (Pillsbury, Minneapolis MN), granulated white sugar (American Crystal Sugar Company, Moorhead, MN), Salt (Morton Salt, Chicago, IL), Shortening (Crisco, J.M. Smucker Co., Orrville, OH), and yeast (Red Star Dry, Milwaukee, WI). Drix C (ACH Foods, Memphis TN) and Chinese garlic oil (Aldrich Chemical Company, Milwaukee, WI) served as a flavor carrier and flavor, respectively.

Study 2 – Ester loss from cakes

The cake ingredients included cake flour (Gold Medal SoftaSilk, General Mills, Minneapolis, MN), granulated white sugar (American Crystal Sugar Company, Moorhead, MN), non-fat dry milk (SuperInstant, Plainview Milk Products, Plainview, MN), dried egg whites (DEB-EL Just Whites, Elizabeth, NJ), double acting baking powder (Calumet), and salt (Morton Salt, Chicago, IL). The flavor system consisted of ethyl acetate, ethyl butyrate, ethyl hexanoate, and ethyl octanoate (Aldrich Chemical, Milwaukee, WI).

Sample preparation:

Study 1 – Bread loaf volume

Garlic flavor incorporation into lipid capsule: A 10% (w/w) garlic oil load lipid was prepared by blending 5.0 g of commercial garlic oil into 45.0 g of molten Dritex C. In order to reduce flavor loss, aluminum foil was used to close the vessel immediately after garlic oil addition. The beaker was placed on a stir plate and the garlic oil + lipid solution was allowed to stir for 2-3 min before being allowed to cool and solidify.

The solid garlic oil + lipid was broken into chunks of approximately 3-6 cm in order to simplify feeding it into a hammer mill (Homiloid model, Fitzpatrick company, Elmhurst, IL) which was fitted with a 1.57 mm screen. Due heat generation in hammer milling, approximately 2.3 kg of dry ice was milled before the sample to pre-cool the equipment. Furthermore, the lipid chunks were also cooled in dry ice prior to hammer milling. The hammer milled samples were collected in plastic bags and then transferred to amber glass screw top containers and immediately placed in a freezer until use.

Bread preparation: Loaves of bread were initially formulated based on AACC Method 10-09 (Basic straight dough bread baking method – long fermentation). After several trials baking full size loaves, it was determined that AACC Method 10-10B (Optimized straight dough bread making method) better suited the needs of this research project. Unlike the former method, the latter method allows for fermentation times ranging from 60 to 180 min and proof times of 24 to 60 min, depending on the quantity of yeast used.

The AACC bread making methods are designed to evaluate the quality of wheat flour and provide details of formula and methodology that cannot be found in a cookbook type of publication. Also, AACC publications are based on scientific research and are used as standards in the grain industry. In order to simplify the formula, the optional ingredients, malt flour, ascorbic acid, potassium bromate, soy flour, dough improvers or surfactants, and maturing agents, were excluded.

One hundred g of Pillsbury bread flour, 6.0 g sugar, 1.5 g salt, and 3.0 g of shortening were added to each of 20 Styrofoam cups. Each cup was covered with a plastic lid. The flour was weighed to ± 0.5 g, all other dry ingredients were within ± 0.1 g. The liquid addition for the control loaves, Drixex C garlic encapsulated loaves, and Drixex C blank loaves were prepared by weighing 60 g of distilled water (± 0.1 g) into 120 mL plastic containers (Corning Snap-Seal). Previous mixograph experiments had determined that 60 g of water per/100 g of flour would provide an acceptable level of hydration for this particular flour. The loaves to be flavored with free garlic oil had the flavor incorporated directly into the water. Pure garlic oil (or aqueous garlic oil dilutions) were weighed into the containers to within 0.005 g in order to achieve the desired ppm garlic oil level (20, 125, 250, 500, 1000, and 5000 ppm flour basis). Distilled water was then added to attain a total of 60.0 g (± 0.1 g) of solution.

The AACC 10-10B method was further simplified by replacing the sugar-salt solution and yeast suspension with dry active yeast. Finney and Bruinsma (16) reported that 0.76 g of dry yeast corresponds to 2.0 g of fresh compressed yeast. Following these modifications, several trials were made using 2.0 g of dry yeast rather than the 5.3 g of compressed yeast as specified by AACC 10-10B. These trials established that 2.0 g of dry yeast resulted in over leavened loaves. Consequently it was determined that 1.0 g of dry yeast provided an acceptable loaf volume. Therefore, 1 g of dry yeast (± 0.05) was weighed into each of 20 – 4 oz. plastic cups and sealed until needed. It is reasonable to assume that the Red Star dry yeast used in this experiment may be significantly different from the yeast used by Finney and Bruinsma (16). Therefore, the discrepancy regarding the yeast quantity is not surprising.

Mixing was done using a dough mixer/kneader with a 100 g bowl (National Mfg. Co, Lincoln, NE). The dry mix, yeast, and water (water + garlic oil solution where applicable) were poured into the 100 g mixing bowl. Flavored or non-flavored hammer milled Drixex C was weighed on a four place scale (Fisher-Scientific A-250) at the time of addition. All mixing times were based on previously collected Mixograph data. Immediately following mixing, each sample of dough was placed into a greased stainless steel bowl. Each bowl was then placed in a proofing oven (National Mfg. Co, Lincoln, NE; 30 C (± 1 C); relative humidity of 85%). After 52 min (± 1 min), a first punch was accomplished by feeding the dough between three-inch wide rollers spaced 4.76 mm (3/16 inches) apart as per AACC method 10-10B. Second punch was completed in a similar manner 25 min later (± 1 min). Thirteen min (± 1 min) after second punch, molding was done by deflating the dough between a pair of rollers spaced 4.76 mm apart. Deflation was immediately followed by feeding the dough into the panning rollers and placing the now formed loaf into a greased 100 g pup-loaf pan. Each loaf was allowed to proof for 33 min (\pm

1 min) preceding baking at 215°C (419°F) for 13 min (+/- 1 min) in a rotary oven (Despatch, Minneapolis, MN). Following baking the loaves were allowed to cool for several min before being removed from the pans and placed on a wire cooling rack. Loaf volume measurements were taken approximately 1 hr later.

Study 2 – Ester loss from cakes

Cake flavor system

The model flavor system was prepared by blending 15.0 g ethyl acetate, 6.0 g ethyl butyrate, 3.0 g ethyl hexanoate, 30.0 g ethyl octanoate and 30 g ethyl decanoate. This provided a ratio of 5:2:1:10:10 for the five respective flavor compounds. A 10% flavor load (w/w) in lipid was made by first weighing 135 g (+/-1.0 g) of Drixex into an aluminum foil lined 600 mL beaker, melting the lipid in a double boiler, and adding the desired amount of model flavor. The flavoring was added in a manner that minimized losses due to evaporation. Briefly, a cardboard tube matching the inside diameter of the 400 mL beaker containing the molten lipid) had been fashioned which was covered on one end with aluminum foil. The foiled-covered end of the tube was inserted into the 400 mL beaker until the foil reached the surface of the melt. As the molten lipid was stirred, the needle of a 50 mL glass syringe was inserted through the aluminum foil and into the melt. The blended flavor was poured from a 50 mL beaker into the barrel of the syringe and the plunger was immediately inserted and pushed. At a previous time the masses of a 50 mL beaker and stopper in addition to the empty needle, barrel, and plunger were recorded. This allowed for the accurate calculation of the actual flavor addition to the melt.

It was apparent that highly volatile flavors such as ethyl acetate are likely to flash off from the molten lipid if added to a hot open system. The tube and aluminum foil apparatus provided a seal that minimized flavor loss during the flavor addition/blending process. After several min of mixing, the flavor-lipid solution was allowed to cool and solidify at room temperature. The aluminum foil used to cover the 400 mL beaker provided an easy means to remove the solid mass. Shurset 125 at a 10% (w/w) load was produced using an identical method.

Lipids with flavor concentrations of 15% (w/w) were produced using the same methodology with the exception of the flavor and lipid weights of 22.5 g and 127.5 g, respectively. Following complete cooling, all samples were double wrapped with aluminum foil, labeled, and placed in a sealed plastic bag and were kept frozen at -20°C.

Size reduction of lipid block

The flavored block of lipid was ground as noted above for the bread study except that three particle sizes were obtained, 1.016, 1.575, and 3.25mm, labeled as small, medium, and large, respectively.

Flavor delivery in spray dried form

An emulsion for spray drying was prepared by slowly adding 800 g of N-Lok (National Starch Corp., Bridgewater, NJ) into 1500g of warm water using a high sheer mixer (Greerco, model 1L.81). Immediately prior to spray drying, 200 g of the same ester blend as prepared above was added under high sheer. The resulting emulsion was 40% TS (including flavor) and ca. 20% flavor load (w/w) on a dry basis.

A Niro spray dryer was used to produce the dry flavor. This dryer uses a centrifugal wheel atomizer (24.5 cm diameter rotary vane wheel rotating at 24,400 rpm), is gas-heated, has a mass air flow of about 360 kg/h; drying chamber of 1.2 m diameter, 0.75 m cylindrical height, cone angle 60°; cyclone collector 0.3 m in diameter; and powder collection container of 20 L capacity. The dryer air temperatures were 200°C inlet and 100°C exit air. The feed rate was ~330 mL/min (varied in order to maintain outlet temperature).

A total of 761g of powder was collected. This flavored, free-flowing powder was added to the cake as one of the three flavor systems included in this study.

Cake formula and baking

AACC method 10-90 was used to prepare and bake cakes. Baking powder was calculated for 305 m MSL altitude (barometric pressure of 772.2- 764.0 mm Hg). Calculations for water were based on 135% absorption. In order to reduce variability, a single homogenous batch of batter was prepared in a commercial mixer (Hobart model A-200). The basal formula listed in AACC method 10-90 was multiplied by four in order to provide enough material for the fifteen cakes required for each batch. A total of two batches were prepared and baked.

Cake flour, granulated white sugar, non-fat dry milk, dried egg whites, double acting baking powder, and salt were combined and sifted three times. Room temperature shortening and approximately 60% of the water were added to the dry ingredients. All ingredients were weighed to +/- 1.0 g. Subsequent mixing and water additions were done in accordance with AACC method 10-90.

From the above batch, 217 g (+/- 1.0 g) of batter was measured into a 3.7 L stainless steel mixing bowl and the liquid, lipid, or sprayed dried flavor system was added (no flavor was added to the control cakes). A Kitchen Aid mixer

(Model K-45) with a paddle attachment was used to blend the flavor into the batter for 1 min. A greased round 15.24 cm cake pan was placed on a tarred scale and the flavored batter was then poured into the pan. This permitted an accurate record of actual batter weight. Each cake was baked at 191°C (375°F) for 25 min in a rotary oven (Despatch, Minneapolis, MN). After removal from the oven, each cake was cooled 5 min before de-panning, and then cooled to room temperature on a wire rack before being weighed with their respective pans. All cakes were wrapped with two layers of aluminum foil and stored in a blast freezer at -20°C until needed for analysis.

Analytical methods:

Study 1 – Bread loaf volume

Duplicate volume measurements of each loaf were taken via the rapeseed displacement method (17). Each of the three trials of twenty loaves was baked during a single session to reduce day-to-day variability.

Study 2 – Ester loss in cake

Cake – Flavor analysis: Initially a number of experiments were conducted to optimize cake sample preparation and analysis. In order to prepare the cake samples for analysis, the cakes were frozen, cut in half and a cheese grater was used to sample a cross section of the cakes after removal of the crust. Two g of grated cake was placed into a 20 mL HS (headspace) vial. Experimentation with several additions of water followed by 10s of high-speed Vortexing showed that approximately 4.0 g of water resulted in an acceptable slurry that was similar to heavy cream.

Headspace GC analysis was used to quantify the esters remaining in the baked cakes. An Hewlett Packard Model 1935A automated headspace analyzer was coupled to an HP 6890 GC for analysis. The autosampler was operated at a bath temperature of 60°C and a loop temperature of 75°C.

Dilutions of each flavor compound were prepared and analyzed in order to determine elution times under the following conditions: Injection port temperature 200°C; detector temperature (FID) 230°C; initial oven temperature 40°C; ramp 25°C/min to 200°C with a 6 min hold. A split injection (20 mL/min split flow) was used. The column was a DB5 (30m x 0.320mm x 1µm (J & W Scientific Inc.). The autosampler was operated using the following parameters: Bath temperature 60°C; loop temperature 75°C; vent time 5s; inject time 10s; and pressurization time 10s.

Quantification of esters: Four cakes were baked without flavor and containing Drixet C or Shurset 125. Each of the lipids was incorporated into each cake at 3.75 g or 5.60 g, respectively. This provided a representative cake-flavor carrier system blank that was used to develop a standard curve on flavor addition. In addition, a cake containing no lipid (i.e. Drixet C or Shurset 125) was baked. After freezing, all cakes were cut in half, the crust was removed, and the crumb was grated. Two g of the crumb material was placed into several 20 mL screw top HS vials. An identical ester model flavor system as previously described was prepared in ethanol. Dilutions were prepared in order to provide the model flavor at levels of 100, 40, 20, 10, and 5 of that added to the experimental cakes. The various dilutions were added (0.1g) to each blank cake sample and allowed to equilibrate at ambient conditions for 24 hrs. The next day 4.0 mL of the internal standard solution was added to each vial. The vial was Vortexed at high speed for 10s and then placed in the GC autosampler and allowed to equilibrate for 2 hrs before proceeding with analysis (as previously described). All samples were prepared and analyzed in triplicate.

Data analysis:

Study 1 – Bread loaf volume

MacAnova software was used to analyze bread loaf volume data. In addition to the loaf volume data, the treatment type, level of flavor, and block information were included in the analysis. An ANOVA analysis was followed by plotting standardized residuals Vs. fitted values, and standardized residuals Vs. normal scores. Both of these plots indicated that the data were normal and acceptable. All groups were combined in a pairwise comparison using a p value of 0.05. In addition, an interaction plot was created in order to illustrate any relationships between the levels of flavor and type of addition.

Study 2 - Analysis of flavor levels in cake

All statistical analysis was performed using MacAnova software. Data were analyzed in order to investigate any effect of lipid melting point, or particle size on ester retention during baking. Additional analysis included data from cakes using the spray dried flavor and flavor added as a liquid. The cake data were analyzed in two groups; (1) flavor in lipid (Drixet C or Sureset 125, each at three particle sizes) and (2) all treatment groups (i.e. flavor in lipid, spray dried, and liquid form). The former investigated any differences between the flavor level of

the lipid groups, while the latter examined the flavor levels for the groups which incorporated the flavor in the form of liquid, spray dried, and lipid encapsulated.

Results and Discussion

The first study being discussed is focused on reducing flavor losses from thermally processed baked goods (cake) though the use of lipid encapsulated flavorings. The second study involves the use of lipid capsules to protect yeast from flavorings that typically exhibit antimicrobial activities (i.e. garlic oil). In these studies, lipid encapsulated flavorings were not prepared via the traditional process of atomization of a molten lipid and solidification in a chamber (spray chilling or prilled flavoring) but by adding the flavoring to molten fat, allowing it to solidify and then grinding to the desired particle size in a hammer mill. While we might expect some differences in the retention of flavorings through the particle forming process, we do not expect that the change in processing would influence performance in the final applications studied.

The influence of lipid-based flavor delivery systems on ester retention in baked cake

As noted in the Materials and Methods section of this paper, one of the objectives was to determine if incorporating a model flavoring in a lipid form would result in improved retention during the baking of cakes. Thus, we put a series of esters into ethanol, lipid encapsulated and spray dried forms to determine if there was any benefit of flavor delivery form on ester retention. The results of this study are reported below.

The losses of ethyl acetate (EA) and ethyl butyrate (EB) during the baking of cake were greater than 99% irrespective of the flavor delivery system. Although the EA and EB were added to the batter at levels of 500 and 200 ppm, respectively, both were found at levels below 5 ppm in all of the baked samples (approximate detection thresholds). For ethyl hexanoate (EH), even though the flavor losses were considerable, it was retained at a mean level of 57 ppm for all flavor delivery systems. There were no statistically significant differences in the levels of EH retained in the cakes for the lipid encapsulated, liquid (ethanol solvent), or spray dried flavor delivery systems. Nearly all of the ethyl octanoate (EO) was retained in the baked cakes irrespective of the delivery system (ca. 97%). Unfortunately, an error was made in the level of EO added to the liquid flavored samples so no data are presented for this flavor system.

Despite using subambient temperatures in milling, a large portion of the EA was lost during the process of size reduction. Nearly 87% of the EA originally present in the prilled flavor system was lost after size reduction via hammer milling. The losses of EB, and EH due to hammer milling were 23.5, and 10.2%, respectively.

As a part of this work, we chose to determine if the particle size of the prilled flavoring would influence ester losses. One might hypothesize that larger lipid particles would result in improved retention during baking if diffusion into the cake batter was slowed by the greater diffusion distances (larger particle diameters). However, the mean particle size did not influence the retention of the model esters during the baking of cakes.

We also investigated the influence of melting point of the fat used as a flavor carrier for lipid encapsulation. One might hypothesize that a higher melting fat may offer greater protection to the loss of volatiles during baking since the particle would not melt until later in the baking process. However, the influence of melting point of the fat (Dritex C melting point 67°C Vs. SureSet 125 melting point 52°C) did not influence the retention of the model esters. This observation suggests that diffusional losses from the fat particles into the cake batter were unchanged by fat melting point.

In summary, there were no significant differences in retention of the ester model system between the lipid encapsulated, liquid, or spray dried flavor delivery systems after baking in cakes. Also, there was no benefit of using a larger lipid particle or higher melting point lipid for this application. Furthermore, as noted earlier, losses associated with the hammer milling process for volatiles such as EA approached 87%. Thus, volatile losses during hammer milling were very large and makes this approach undesirable for delivering very volatile flavorings for baked applications. Losses may be less if the particles were produced by a true spray chilling operation as opposed to hammer milling of a solidified fat.

The influence of a lipid delivery system for garlic oil on bread loaf volume

As discussed earlier, there is information in the literature that the addition of some flavorings to yeast leavened products will retard yeast metabolism thereby reducing product leavening (expressed as loaf volume). Thus, a series of experiments were carried out to determine if putting a flavoring (garlic oil in this study) into a fat carrier would slow its release into the dough thereby protecting the yeast and allowing higher loaf volumes.

An honest significant difference (HSD) pairwise comparison ($p=0.05$) found that the loaf volume of breads made with 5,000 ppm liquid garlic oil, 5,000 ppm garlic oil in Dritex C, or 1,000 ppm garlic oil in Dritex C were significantly lower

**Table I. HSD pairwise comparison of loaf volumes of bread baked using different levels of garlic oil and means of its incorporation.
HSD pairwise comparison of all groups (p=.05)**

Stat. Diff. ¹	Sample	Garlic oil (ppm ²)	Difference in loaf volume from mean (mL ³)
a	Oil	5,000	-97.1
a	Dritex+oil	5,000	-93.7
a	Oil	1,000	-87.1
ab	Dritex+oil	1,000	-72.1
abc	Oil	250	-32.1
abcd	Dritex+oil	500	-25.4
abcd	Oil	500	-13.7
abcd	Dritex+oil	250	-12.1
abcd	Dritex+oil	125	-8.73
bcd	Oil	20	12.9
cd	Dritex blank	1,000	27.9
cd	Dritex blank	500	36.3
cd	Dritex+oil	20	41.3
cd	Dritex blank	125	42.9
cd	Oil	125	44.6
cd	Dritex blank	250	52.9
cd	Dritex blank	5,000	54.6
d	Control	0	58.8
d	Dritex blank	20	69.6

¹ Samples with different letters are significantly different

² ppm (w/w flour)

³ Grand mean = 439 ml

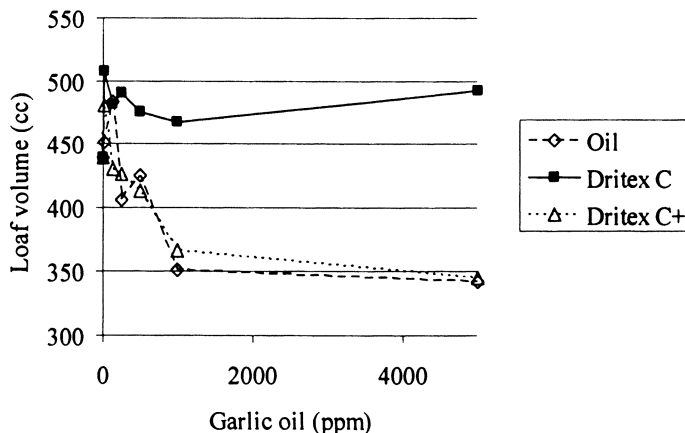


Figure 1. The effect of garlic oil concentration on bread loaf volume when added in different forms (Dritex C plus garlic oil [C+], liquid garlic oil [Oil] and Dritex C alone [Dritex C]).

than the loaf volumes of the control (no additions) or breads made with Dritex C 20ppm group. There was no evidence of significant differences between any of the other groups (Table I).

A plot of the data illustrates a reduction in loaf volume as the level of garlic oil is increased up to 1,000 ppm in both the liquid garlic oil, and garlic oil in Dritex C systems (Figure 1). There is no change in loaf volume when increasing the garlic oil from 1,000 to 5,000 ppm. It is also clear that there is no difference in loaf volumes when adding the garlic oil as a pure liquid oil Vs. encapsulating it in lipid: these two lines are nearly identical. Moreover, the level of non-flavored Dritex C appears to have little effect on loaf volume so the reduction in loaf volume is due to the presence of the garlic oil as opposed to additional fat. Essentially, there is no benefit of adding essential oils (e.g. garlic oil) in a lipid capsule for protecting yeast from inhibition by the oil.

Conclusions

We did not find any benefit to incorporating our model flavor system into a spray dried form or lipid capsule in retaining volatile flavorings during the baking of cakes. While one might hypothesize that putting the flavoring into a lipid capsule might slow release of the flavoring into the cake system thereby offering some protection against evaporative losses, no benefit as found. Nor did

we find any benefit of using a higher melt-point fat or using a larger lipid particle on volatile retention. It appears that our model flavor mixture readily moved from our capsules into the cake batter and was lost irrespective of being in fat, or the melt point or particle size of the fat capsules.

Based on the data on volatile losses from cakes, it is not surprising that we found no benefit of putting garlic oil into lipid capsules to help maintain loaf volumes. Irrespective of whether the garlic oil was added to the bread dough as a pure oil or encapsulated in lipid, the yeast was inhibited to the same extent (loaf volume decreased).

References

1. De Roos, K.; Mansecal, R. In: *Flavour Research at the Dawn of the Twenty First Century*. J.L. LeQuere ; P.X. Etievant, eds. Lavoisier: Cachan, 2003. pg. 27-32.
2. Brauss, M.; B., B.; R., L.; Avison, S.; Taylor, A. *Flavour Fragr. J.* 1999, 14, 351-357.
3. Jackel, S.S. *Cereal Foods World.* 1992, 37, 835-836.
4. Varadachari, S. *Cereal Food World.* 2002, 47, 84-86.
5. Reineccius, G.A.; Whorton, B.C. In: *The Maillard Reaction in Food Processing, Human Nutrition and Physiology*. P.A. Finot, H.O. Aeschbacher, R.F. Hurrell; R. Liardon, eds., Birkhauser Publ., Basel, 1990. pg. 197-208.
6. Guichard, E. *Food Rev. Int.* 2002, 18, 49-70.
7. Whorton, C.; Reineccius, G. In *Thermal Generation of Aroma*. T.H. Parliament, R. McGorin, C-T Ho, eds.; ACS Symposium series; Washington, D.C., 1989; pp.526-532.
8. Clawson, A.R.; Linforth, R.S.T.; Ingham, K.E.; Taylor, A.J. *Lebensm. Wiss. Technol.* 1996, 29, 158-162.
9. Bertolini, A.C.; Siani, A.C.; Grosso, C.R. *J. Agric. Food Chem.* 2001, 49, 780-785.
10. Reineccius, T.A.; Reineccius, G.A.; Peppard, T.L. *J. Food Sci.* 2002, 67(9). 3271-3279.
11. Sheu, T.Y.; Rosenberg, M. *J. Food Sci.* 1995, 60, 98-103.
12. Goubert, I.; Le Quere, J.L.; Voilley, A.J. *J. Agric. Food Chem.* 1998, 46, 1981-1990.
13. Wampler, D.J. *Cereal Foods World.* 1992, 37, 817-819.
14. Conner, D.E.; Beuchat, L.R. *J. Food Sci.* 1984, 49, 429-434.
15. Kim, J.W.; Kim, Y.S.; Kyung, K.H. *J. Food Protection.* 2004, 67, 499-504.
16. Bruinsma, B.L.; Finney, K.F. *Cereal Chem.* 1981, 58, 477-480.
17. Murano, P.S.; Johnson, J.M. *J. Food Sci.* 1998, 63, 1088-1092.

Chapter 18

Shelf Life and Flavor Release of Coacervated Orange Oil

Debbie Paetznick and Gary Reineccius

Department of Food Science and Nutrition, University of Minnesota,
St. Paul, MN 55108

Coacervated orange oil (gelatin/gum acacia or gelatin/polyphosphate wall systems) was found to have poor shelf-life (less than 2 weeks at 45°C). Stability was dependent upon storage RH, crosslinking and coacervate wall system. Non crosslinked samples were most stable at higher RHs (53%). The effect of RH in crosslinked samples was less clear. Of the coacervate systems, the gelatin/gum acacia system offered better protection against oxidation than the gelatin/polyphosphate system. There was no effect of crosslinking on flavor release. However, when looking at the matrix effects, the gelatin/gum acacia sample released limonene the fastest and attained the highest concentration of freed limonene. The observation that this system released the most limonene is proposed to be due to less binding with the matrix.

Introduction

Coacervation is an encapsulation technique used for flavor delivery in dry and liquid food systems. Coacervation offers a unique means of flavor release, which can be by diffusion and/or rupture. The basic process of making coacervates has been known since the 1930's and has been the subject of many patents, including those in the carbon-less paper, agrochemical, pharmaceutical and more recently, food areas (1 -11).

Coacervation can be simple or complex. Simple coacervation uses a single colloid while complex coacervation deals with two oppositely charged colloids. In food applications, complex coacervation is the preferred method. However, there is little information in the public domain on the formation of flavor coacervates other than the patent literature. This literature has largely focused on either processes or wall materials used in coacervate formation. In some cases the wall material was varied to satisfy Kosher requirements (8) and in others to avoid cross-linking with glutaraldehyde. For example, Subramaniam and Reilly (4) use a plant extract comprised of unsubstituted or substituted phenolic compounds for crosslinking, rather than glutaraldehyde; which has safety issues, but is approved specifically for use in complex coacervation. Soper and Thomas (7) use an enzyme to accomplish cross-linking. In terms of processes, Soper et al. (6) offer a novel means to load capsules after formation. The patent literature gives very little information on shelf-life stability or release from such capsules. In terms of published articles, none were found reporting on flavor stability (protection afforded against oxidation) and only two were found considering flavor release. These papers will be discussed later in the Results and Discussion section of this paper.

Our first objective was to evaluate the ability of coacervates to protect orange oil against oxidation during storage. We evaluated three coacervated capsules and one spray dried sample (prepared using a chemically modified starch), for comparison. Our experimental design for this study included three complex coacervate systems (gelatin/polyphosphate [with and without antioxidant added], gelatin/gum acacia [with and without antioxidant added], a gelatin/polyphosphate not crosslinked, and a chemically modified starch spray dried). In this part of the work, we monitored the rate of oxidation of a single fold orange peel oil. The second objective was to determine the influence of coacervate formulation variables (wall material and crosslinking) on flavor release of orange oil compared to the spray dried sample.

Materials and Methods

Flavoring

Midseason cold pressed orange oil was obtained from Treat USA (Lakeland, FL). This orange oil was used as the flavoring in all coacervate and spray dried microcapsules.

Encapsulation materials and their formation

Coacervate samples were obtained from Thies Technologies, Inc., (Henderson NE). Samples included a gelatin/polyphosphate (ca. 80% load), with and without antioxidant added, and a gelatin/gum acacia (ca. 94% load) again with and without antioxidant added. The antioxidant used was Kosher Grindox 497™ (water dispersible tocopherol). The next sample was a gelatin polyphosphate sample that had antioxidant added but was not crosslinked. Finally we spray dried orange oil in a chemically modified starch (Capsul™, National Starch Corp., Bridgewater, NJ) (see Table 1 below) to use as a comparison in observing protection of coacervated microcapsules (20% load).

Table 1. Samples used in study

<i>Code</i>	<i>Colloids</i>	<i>Crosslinked</i>	<i>Antioxidant added</i>
GP-C	Gelatin/Polyphosphate	Yes	No
GGA-C	Gelatin/Gum acacia	Yes	No
GP-A-C	Gelatin/Polyphosphate	Yes	Yes
GGA-A-C	Gelatin/Gum Acacia	Yes	Yes
GP-A	Gelatin/Polyphosphate	No	Yes
Capsul™	Chemically modified starch	No	No

The spray dried sample was prepared at the University of Minnesota. This was done by initially hydrating the carrier (Capsul™) overnight at 40% solids in water to allow complete dissolution. Orange oil (25% w/w carrier) was emulsified into the hydrated carrier immediately before spray drying using a bench-top high-speed mixer (Grifford-Wood Mixer, Greerco Corporation, Hudson, NH). This emulsion was then spray-dried using a Niro Atomizer Utility model drier (Ramsey, NJ); inlet and exit air temperatures 200°C and 100°C, respectively. Powders were stored at 4°C until analysis. Moisture content of carriers was taken into consideration to prepare the carrier solutions so to get an accurate concentration.

Sample storage - oxidation study

Samples were put into 1 cm-deep Lexan™ trays which were then placed into glass chambers (10-gallon fish tanks), and sealed using a high vacuum grease. Samples were all stored at 45 °C in a walk-in incubator with relative

humidities of 11% (LiCl), 33% (MgCl₂) and 52% (NaBr) (using saturated salt solutions in the fish tanks to obtain these RH's). A control sample of each powder was stored in a freezer for comparison. Samples were collected weekly and analyzed for limonene oxide by gas chromatography.

Analysis - Flavor release

The same capsule formulations as used in the oxidation study were analyzed by gas chromatography for flavor release. While several approaches were tried to measure release, only one will be reported here. In this analysis, limonene release was monitored using GC (described below).

Headspace analysis

Sample (0.25 g) and 5 mL of D.I. water were added to a GC headspace vial. The vial was capped, sealed and placed immediately in a 50°C headspace autosampler attached to a GC (see GC section below for details). The Capsul™ samples were shaken to solubilize the material before placing into the autosampler. This was not necessary for the coacervate samples; however they were simply swirled before placing into the autosampler. The GC analyzed the sample headspace for limonene release.

Gas Chromatographic analysis

Sample preparation

An acetone extraction method was used to monitor samples for oxidation (6). Briefly, encapsulates were hydrated at 10% solids in distilled water. One mL of this solution was pipetted into to a 10 mL vial and 4 mL of acetone were added slowly with constant mixing (internal standard, 2-heptanone at 0.05 mg/mL). The acetone layer was injected in to the GC (see GC section below for details). The ratio between limonene oxide and limonene was calculated. Samples were analyzed weekly in duplicate and the two runs averaged for reporting.

GC analysis

The acetone extracts obtained as described above were analyzed using an Hewlett-Packard Series II gas chromatograph equipped with a flame ionization

detector. An HP-5 fused silica capillary column (30 m x 0.32 mm x 0.25 μ m) was used in all analyses. The GC operating parameters were as follows: Carrier Gas: helium; Head Pressure: 15 psig; Split 1:12; Injection Port Temperature: 225°C; Detector Temperature: 250°C; Injection Volume: 1 μ L; Initial temperature: 100°C; Initial Time: 0 min; Ramp Rate: 20°C/min; Final Temperature: 200°C; Final Time: 5 min.

Quantitation of volatiles using Headspace Analysis. Headspace samples were analyzed using an Hewlett-Packard static headspace unit (model 19395A, Hewlett-Packard, Avondale, PA) in conjunction with a Hewlett-Packard 5890 gas chromatograph interfaced with a mass spectrometer (MS) (model HP-5972). All samples were equilibrated for 30 min at 50°C in the autosampler prior to injection into the GC/MS. A bonded phase DB-5 fused silica capillary column (30 m x 0.25 mm x 0.25 μ m) was used in all analyses. Operating parameters were as follows: Column head pressure: 12 psig; Split-less mode; Headspace sample loop: 3 mL; Initial Temperature: 40°C; Initial Time: 1 min; Temperature Program Rate: 20 °C/min; Final Temperature: 210 °C. All samples were run in duplicate and results were averaged for data presentation.

Results and Discussion

Oxidation

Figure 1 presents a comparison of limonene oxidation in samples prepared with gum acacia:polyphosphate (GP) wall materials, with and without glutaraldehyde crosslinking when stored at 11% relative humidity (RH). Our data show that the crosslinked GP sample oxidized at a slower rate when compared to the non-crosslinked sample. We have to note that samples are generally considered to be off flavored when the limonene oxide concentration exceeds 2 mg / g of limonene (this value is somewhat sample dependent). Using this criterion, both samples failed within the first week of storage at this storage temperature even though they contained antioxidant. Very poor protection against oxidation was afforded by this wall system.

When we compared the effects of crosslinking in samples stored at higher RH (32 and 53% ; Figure 2), we found that we had the opposite effect compared to the 11% RH samples. Here the crosslinked samples oxidized at a faster rate irrespective of crosslinked or not. Crosslinking has the potential to reduce the porosity and mobility of the matrix. At low water activities, decreased porosity may be important in limiting oxygen migration into the capsule. At higher water activities there may be adequate porosity and mobility to the matrix that crosslinking is less important. However, we cannot explain the fact that the

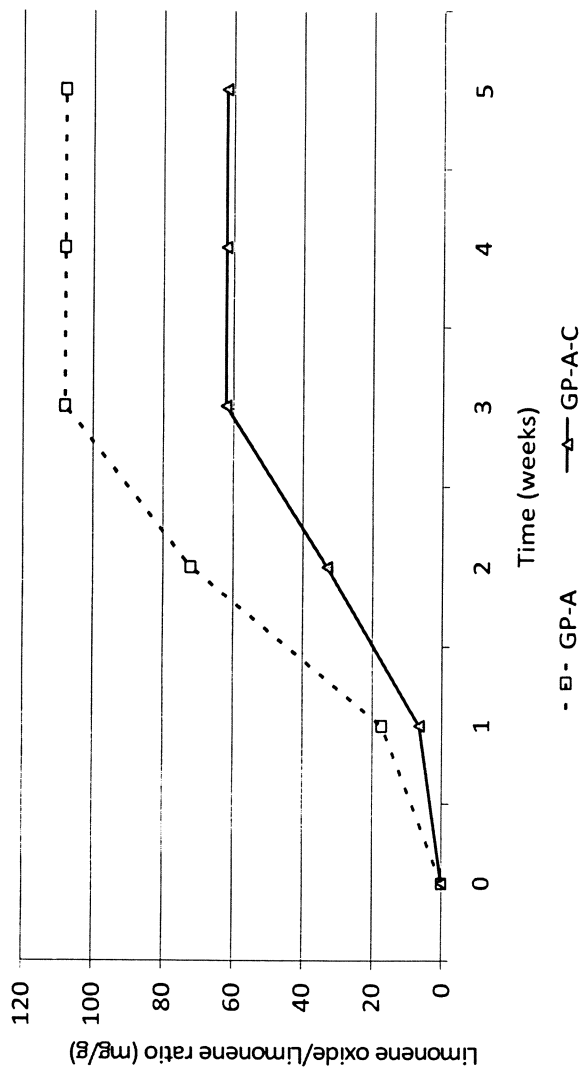


Figure 1. Effects of crosslinking on oxidation of orange oil during storage (45°C; RH 11%)

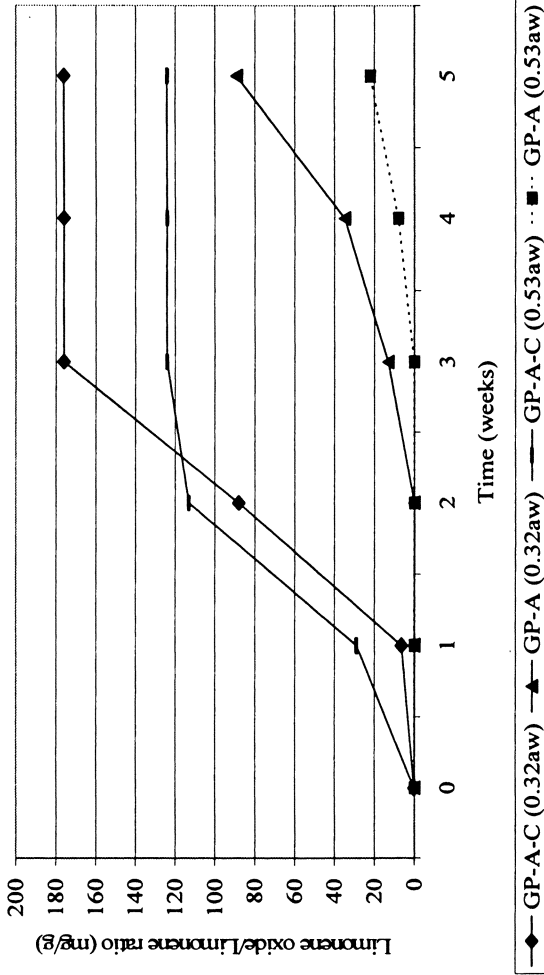


Figure 2. Effects of crosslinking on oxidation of orange oil during storage (45°C; RH 32 and 53%)

crosslinked samples oxidized more quickly. One may question the role of glutaraldehyde itself on limonene oxidation.

The effect of type of wall material used in coacervation on oxidative stability is illustrated in Figure 3. A plot of limonene oxidation in a spray dried product is also shown for reference. If we are to use a cut off of 2 mg limonene oxide / g of limonene as an end of shelf-life, the two coacervated products would be considered "spoiled" before the 1st week of storage testing. In this case, neither wall material, gelatin:polyphosphate nor gelatin:gum acacia, offered significant stability to the orange oil. While the orange oil oxidized more slowly over the entire storage period (4 weeks) when coacervated using the gelatin:gum acacia matrix, the orange oil would have been considered spoiled so early that, the long term behavior is of no relevance. For reference purposes, we chose to spray dry the orange oil in a chemically modified starch (Capsul™). We note that the orange oil was more stable when spray dried in this matrix than either of the coacervated samples.

The effect of antioxidant on orange oil oxidation is presented below in Figure 4. As expected, the addition of antioxidant resulted in reduced oxidation at both water activities. The samples oxidized more slowly when stored at a RH of 11% than at 53%. In essence, the rate of oxidation tended to increase at higher RHs for the GP samples.

The influence of water activity on stability is seen by comparing data on in Figures 1, 2 and 4. Stability is dependent upon whether the sample was crosslinked. The GP-A samples increased in stability with increasing a_w ($0.11 < 0.32 < 0.53$). The samples based on GP-A-C increased in stability in the order of 0.32, 0.53 and 0.11 a_w . Thus, there was no consistent influence of a_w on stability for coacervated based on gelatin and polyphosphates.

Flavor Release

Accurately measuring the release of orange oil from coacervates was problematic. After trying several approaches, we chose a headspace method. While headspace analysis was found to be reproducible, it gave a slow response to flavor migration from the capsules.

In the case of coacervates, the particle does not dissolve when placed in water: any release of the capsule contents is due to diffusion through the particle wall. One might expect the capsule wall to be less porous (or subject to swelling) when it is crosslinked thus, giving slower release. Our data do not show any effect of crosslinking on the release of limonene: the GC headspace profiles (Figure 5) are very similar (within data variability). It appears that crosslinking does not affect limonene release. Yeo et al. (13), reported on flavor release from complex coacervated microcapsules as influenced by polyion concentrations, degree of homogenization and temperature (frozen to 100°C).

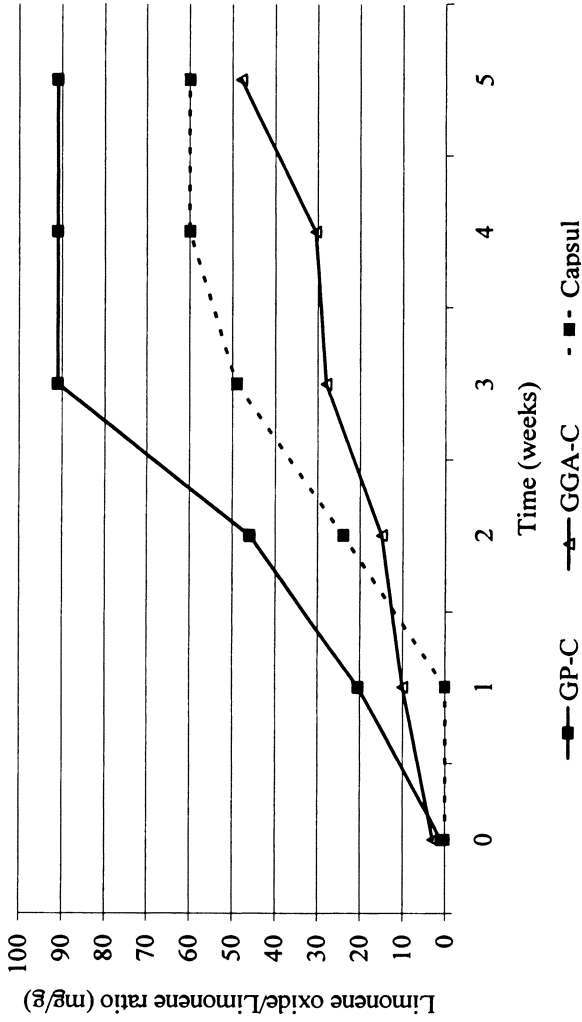


Figure 3. Matrix effects of samples on oxidation of orange oil during Storage (45°C; RH 11%)

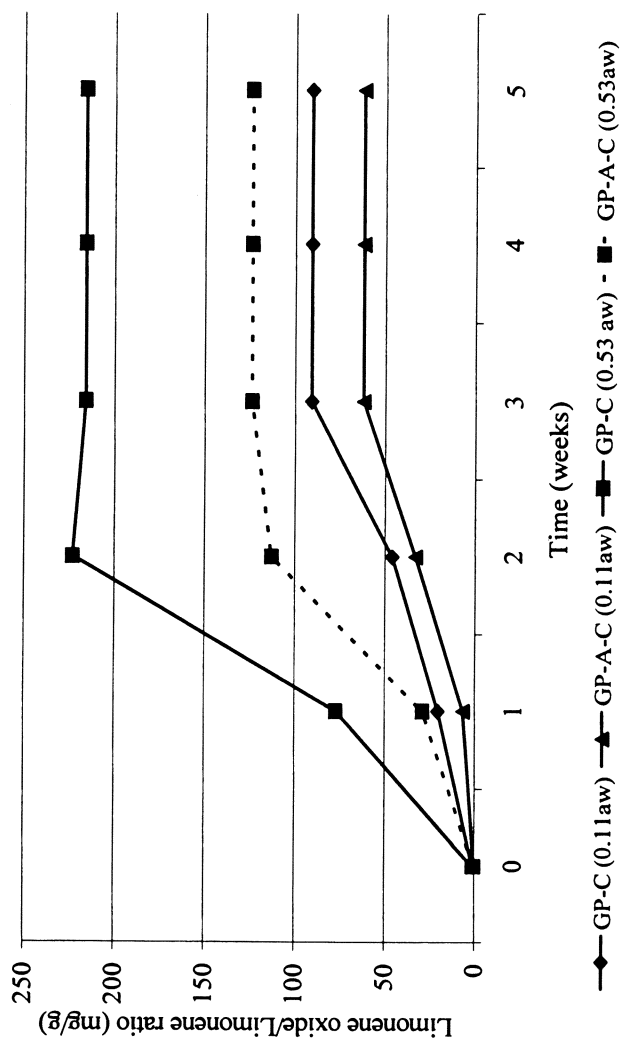


Figure 4. Effects of antioxidant and RH on oxidation of orange oil during storage (45°C; 11 and 53% RH)

They reported nearly complete release when samples with low homogenization were placed in 100°C water but less release when the samples were well homogenized. Placing the samples in solutions containing polyions resulted in rapid release. The coacervates were quite stable to low temperatures. Due to differences in coacervate systems and methodology, our data cannot be compared to theirs.

Weinbreck et al. (8) also reported on flavor release from whey protein and gum acacia coacervates. Contrary to our observations, they found that crosslinking hindered the release of flavor from the microcapsules. Also, that larger capsules gave a stronger release, which they contributed to a tough, dense biopolymer wall that was difficult to break by chewing. The differences in results likely are due to differences in methodologies and coacervate systems studied. Different from our study, they used a MS nose (mass spectrometry) for their analysis and the study was conducted in “real-time” as opposed to our study over a longer time period.

The effect of wall matrix components on flavor release is presented in Figure 6. We find that the spray dried sample released the volatile components (limonene) the quickest of the samples (note the higher headspace concentration at time = 0). In this plot, time 0 is actually after 30 min of equilibration in the autosampler. Since the spray dried sample is water soluble, the capsule contents would be immediately released and high levels of limonene would quickly be found in the sample headspace. The spray dried sample never reached as high headspace concentrations as the coacervates since it only contained about a 20% loading while the coacervates > 80% loading.

Of the coacervate samples, the GGA (crosslinked) sample released the fastest and the highest concentration of limonene. While this sample contains the highest flavor load, the magnitude of difference in flavor release appears to be much greater than one would expect based on the difference in flavor load: we found nearly a 2 fold difference in maximum headspace concentration between samples while only a 15% difference in sample loading. The fact that this discrepancy exists at equilibrium suggests flavor binding by the GP system as opposed to limited diffusion. If one looks at the rate of change in headspace concentration over time, the GGA system reaches a maximum headspace concentration much more slowly (questionable if it reached maximum in the 330 min of testing) while the GP system reached a maximum more quickly (90-120 min). These data suggest that diffusion is slowing release from the GGA system.

Conclusions

A primary finding of this study is that coacervation did not afford significant protection to encapsulated orange oil against oxidation: shelf-life was less than the equivalent orange oil spray dried in a chemically modified starch (which is

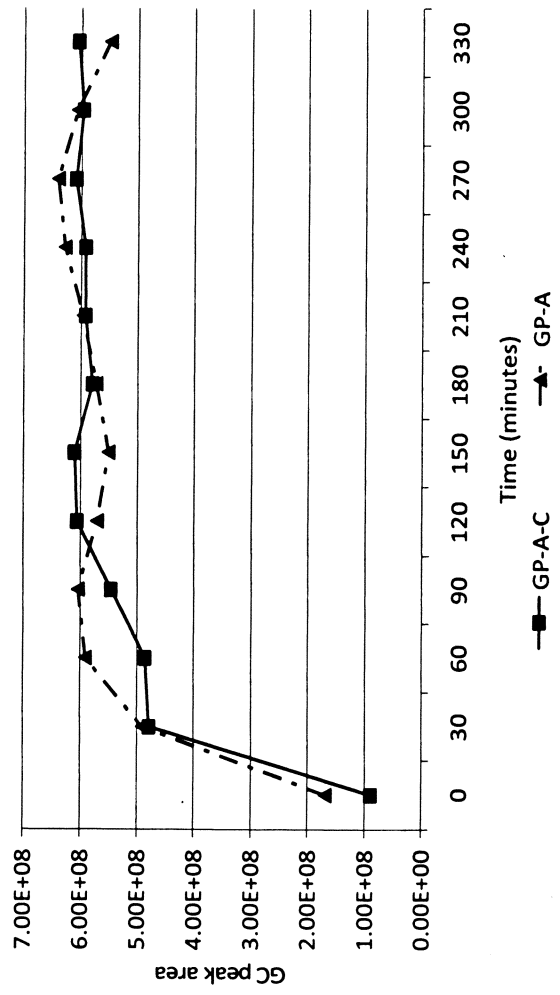


Figure 5. Flavor release – Comparison of crosslinkingcoacervates on the release of limonene

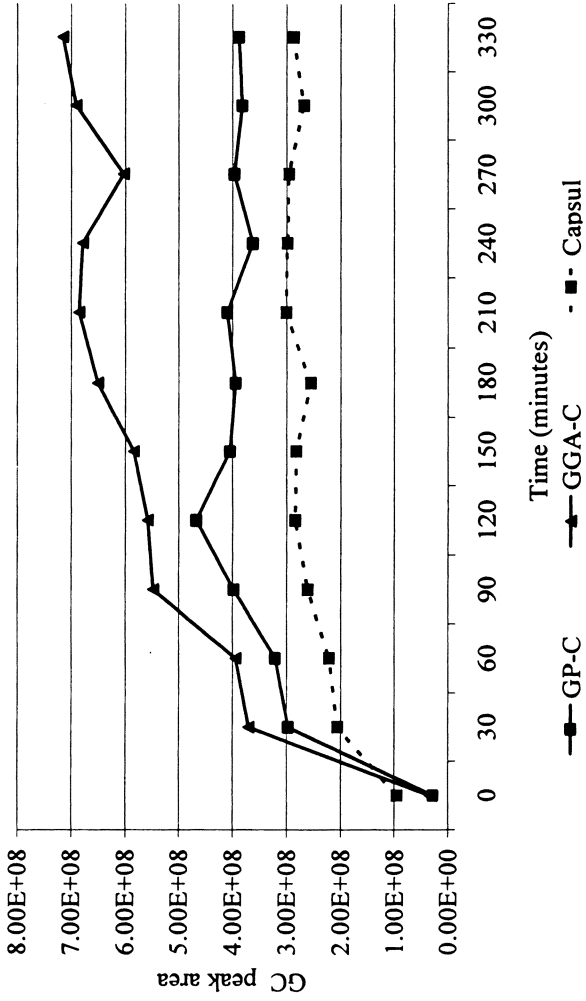


Figure 6. Headspace comparison of flavor release due to matrix effects

not well known for its protection properties). Crosslinking the coacervates had a beneficial effect (i.e. reduced oxidation) when stored dry (RH 11%) but a negative effect when stored at higher RHs (33 and 53%). The effect of RH on stability was dependent upon whether the sample was crosslinked. The GP-A samples increased in stability with increasing a_w ($0.11 < 0.32 < 0.53$). The samples based on GP-A-C increased in stability in the order of 0.32, 0.53 and 0.11 a_w . Of the coacervate systems, the GGA system offered better protection against oxidation than the GP system.

When considering the flavor release data, we find that crosslinking the coacervates has no effect on flavor release (i.e. limonene). However, when looking at the matrix effects of the coacervated samples, the GGA sample released limonene the fastest and attained the highest concentration of freed limonene. The observation that this system released the most limonene is proposed to be due to less binding with the matrix.

References

1. Arshady, R. "Microspheres and Microcapsules, a Survey of Manufacturing Techniques Part 11: Coacervation". *J. Polymer Engineering and Science*, **1990**, 30(15), 905-914.
2. Rozenblat, J., Magdassi, S., and Garti, N. "Effect of electrolytes, stirring and surfactants in the coacervation and Microencapsulation processes in presence of gelatin". *J. Microencapsulation*, **1989**, 6(4), 515-526.
3. B.K. Green and L. Schleicher, U.S. Patents 2,730,456, (1956) and 2,730,457 (1956).
4. Subramaniam; A.; Reilly, A. Process for the preparation of flavor or fragrance microcapsules U.S. Pat. Appl. Publ. 20,050,123,757 (2005).
5. Graf, E.; Soper, J.C. Flavored flour containing allium oil capsules and method of making flavored flour dough product. Tastemaker. U.S. Patent 5,536,513 (1996).
6. Soper, J.C.; Yang, X.; Josephson, D.B. Encapsulation of flavors and fragrances by aqueous diffusion into microcapsules. Givaudan Roure U.S. 6106875 (2000)
7. Soper; J.C.; Thomas, M.T. Enzymatically protein-encapsulating oil particles by complex *coacervation*. Givaudan Roure Flavors Corporation. US Pats. 6,325,951 (2001) and 6,039,901 (2000).
8. Soper, J.C. Method of encapsulating food or flavor particles using warm water fish gelatin, and capsules produced from them. Tastemaker WO 9620612 (1996).
9. Soper, J.C. 1995. Utilization of coacervated flavors. In: *Encapsulation and Controlled Release of Food Ingredients*. S.J. Risch; G.A. Reineccius, eds. American Chemical Society, Washington DC. Pg. 104-112.

10. Subramaniam, A.; Reilly, A. Flavor microcapsules obtained by coacervation with gelatin. Firmenich. U.S. Pat. Appl. Publ. US 2004041306 (2004)
11. Subramaniam, A; Reilly, A. Process for the preparation of flavor or fragrance microcapsules. U.S. Pat. Appl. 2004032036 (2004)
12. Anandaraman, S. and Reineccius, G.A. Stability of encapsulated orange peel oil. *Food Technol.* **1986**, *40*(11), 88-93.
13. Yeo Y., Bellas E., Firestone W., Langer R., and Kohane D. "Complex Coacervates for Thermally Sensitive Controlled Release of Flavor Compounds". *J. Agric. Food Chem.*, **2005**, *53*(19), 7518-7525.
14. Weinbreck, F., Minor, M., and De Kruif, C.G. "Microencapsulation of oils using whey protein/gum Arabic coacervates". *J. Microencapsulation*, **2004**, *21*(6), 667-679.

Author Index

- Akinshina, Anna, 46
Alexander, M., 157
Brain, Charles H., 183
Chen, Lingyun, 98
Corredig, M., 157
Debon, S., 213
Dickinson, Eric, 46
Duta, D., 35
Ettelaie, Rammile, 46
Faulks, Richard M., 67
Finney, John, 259
Given, Peter, xi
Guthrie, B., 213
Hasuo, N., 169
Heigis, J., 213
Hollowood, T. A., 246
Huang, Qingrong, 198
Linthorpe, R. S. T., 246
Liu, J., 157
Mackie, Alan R., 67
McClements, David Julian, 3
McCrae, C., 213
Millqvist-Fureby, Anna, 233
Moffat, J., 35
Mondro, G., 213
Naouli, Nabil, 116
Noel, T. R., 35
Padua, Graciela W., 143
Paetznick, Debbie, 272
Parker, R., 35
Pearson, K., 246
Peters, Scott E., 183
Plunkett, Mark, 89
Qian, Michael, xi
Reineccius, Gary, 259, 272
Remondetto, Gabriel E., 98
Ridout, Michael J., 67
Ring, S. G., 35
Rosano, Henri L., 116
Sato, K., 169
Shieh, W., 213
Singh, Harjinder, 131
Smith, Paul, 89
Sonoda, T., 169
Subirade, Muriel, 98
Taylor, A. J., 246
Thompson, Abby, 131
Ueno, S., 169
Wang, Qin, 143
Wang, Xiaoyong, 198
Wang, Yu-Wen, 198
Wickham, Martin S. J., 67
Wilde, Peter J., 67
Ye, Aiqain, 131

Subject Index

A

Active ingredients

- encapsulated in nanodispersions, 190*t*
- mechanisms for release from foods, 43

See also Biopolyelectrolyte multilayers

Adsorption

- zein, kinetics, 149*f*
- zein, to carboxylic and methylated surfaces, 150*f*
- zein, to hydrophobic and hydrophilic surfaces, 146–147

Animal fats, lipids, 5, 7*t*

Anionic polysaccharides, biopolymers, 7, 7*t*

Anionic surfactants, building blocks, 5–6, 7*t*

Antiperspirants, fragrance sniff test of two, 191, 192*f*

Appetite scores, emulsions and satiety, 81

Aqueous two-phase systems (ATPS)

- encapsulation in, 239, 241–242, 244
- encapsulation of biologicals, 242, 243*f*, 244
- poly(vinyl alcohol)/dextran system, 241–242
- requirements for optimal, 239, 241
- schematic illustrating encapsulation, 241*f*
- survival rate of *Lactobacillus plantarum* in methyl cellulose/dextran, 242, 243*f*, 244

Aroma release

- atmospheric pressure chemical ionization–mass spectrometry (APCI–MS), 248
- average time intensity traces from panelists, 255*f*
- co-solvent effect at molecular scale, 249, 250*f*
- effect of droplets *in vivo* – millimeter scale, 253–256
- effect of non-homogeneous distribution – millimeter scale layers, 249
- effect of non-solubilized droplets *in vitro* – millimeter scale, 251
- gelatin-sucrose gel preparation, 248
- in vivo* release from gelatin-sucrose gels as droplet or dissolved in gel during production, 254*t*
- in vivo* release of ethyl butyrate from xanthan solutions mixed vs. single droplet, 253–254
- in vivo* release of hexanol from gels, 250*f*
- in vivo* release of limonene from gels, 250*f*
- materials and methods, 248–249
- sensory analysis, 248–249
- statistical analysis of sensory time intensity parameters, 256*t*
- theoretical physical principles, 247
- typical pattern by APCI–MS, 253*f*
- video monitoring of droplet release, 252*f*
- volatiles from food, 247

Assembly

- directed, 10
- See also* Self-assembly
- Astaxanthin, encapsulation in nanodispersions, 190*t*

B

Barrier, coating material as, for core compounds, 214–215

Beads

soy protein, 101–102, 103*f*
 Young's modulus and rupture force of, with alginate and soy protein isolate, 102, 103*f*

See also Soy protein

Beef industry, ingredient protection example, 192–193

Beta-carotene, encapsulation in nanodispersions, 190*t*

Bile salts

fat digestion, 78–79
 stripping adsorbed components from surface, 83–84
 surface dilatational modulus vs. surface pressure, 83, 84*f*

Bioactive compounds, milk components for nanoparticles to encapsulate and deliver, 132

Bioavailability, nutrients in nanodispersions, 193–195

Biologicals, survival in aqueous two-phase systems (ATPS), 242, 243*f*, 244

Biopolyelectrolyte multilayers approaches, 36

disassembly of multilayers, 36, 38

food biopolymer multilayers, 42

Fourier Transform infrared–attenuated total reflection (FTIR–ATR) spectroscopy method, 37

infrared amide I peak absorbance vs. pH for 8-layer pectin/BLG multilayer, 39, 40*f*

infrared spectra of 10 layer pectin/poly-L-lysine hydrobromide (PLL) multilayer at various pD, 40, 41*f*
 materials and methods, 36–38

mechanisms for release of active ingredients from foods, 43

microelectrophoresis, 38

multilayer-coated emulsion preparation, 37

pH decreasing with shrinkage of multilayer, 40

pH titration on 8-layer pectin/ β -lactoglobulin (BLG) multilayer, 38, 39*f*

positively charged biopolymer in assembly of multilayers, 39

quartz crystal microbalance with dissipation monitoring (QCMD), 37–38

response of changing pH using QCMD and FTIR–ATR, 40

spectra for multilayer rinsed with buffers of increasing pH, 38–39

spectrum of multilayer in frequency range 1500–1800 cm^{-1} , 38

swelling ratio vs. pH for 10-layer pectin/PLL multilayer, 40, 41*f*

zeta potential of emulsion droplets at pH 5.6 vs. layer number, 42, 42*f*

Biopolymer combinations, primary and secondary emulsions, 22

Biopolymer films

density profiles at interface, 63–64

See also Mixed interfacial biopolymer films

Biopolymers, building blocks, 7, 7*t*

Bovine serum albumin (BSA)

encapsulation in poly(vinyl alcohol)/dextran, 241–242

formulations with and without coating, 238, 240*f*

potential nano-encapsulation systems, 133, 135

Bread

data analysis, 266

effect of garlic oil concentration and method of addition on loaf volume, 270*f*

- garlic flavor incorporation into lipid capsule, 261
 - honest significant difference (HSD) pairwise comparison at different garlic levels and addition method, 269*t*
 - influence of lipid delivery system for garlic oil on loaf volume, 268, 270
 - ingredients, 260
 - loaf volume, 260, 261–263, 265, 266
 - preparation, 261–263
 - See also* Flavor delivery via lipid encapsulation
- C**
- Cake**
- analysis of flavor levels in, 266–267
 - ester retention in, and lipid-based flavor delivery, 267–268
 - flavor analysis, 265
 - flavor delivery in spray dried form, 264
 - flavor system, 263
 - formula and baking, 264–265
 - ingredients, 261
 - quantification of esters, 266
 - size reduction of lipid block, 264
 - See also* Flavor delivery via lipid encapsulation
- Calcium**
- crosslinking soy protein to hydrogels, 100–101
 - soy protein beads, 101–102, 103*f*
 - soy protein microspheres, 102, 104, 105*f*
- Calcium chloride, nanoparticle**
- dispersion of caseinate/gum arabic, 136–137, 139*f*
- Carbon-13 labeled fatty acid, emulsions and satiety, 81**
- Cardiovascular disease (CVD), obesity, 68**
- Carrier properties**
- amorphous state of carbohydrate matrix, 216–217, 220
 - collapse/caking, 222
 - crystallization of trehalose, 220, 222
 - crystallization of wall material ingredients, 220, 222
 - dextrose equivalent (DE) and effectiveness of carbohydrate matrix film, 229
 - DSC characteristics of two spray-dried powders with orange oil and different wall materials, 224*t*
 - emulsification capacity, 222, 225, 228
 - encapsulation performance of gum arabic, dextrin and n-octenyl succinic anhydride (n-OSA) starch, 226*t*
 - esterification using n-OSA for starch derivative, 225
 - infeed solids content and oil load influencing retention of orange oil during spray drying, 216*t*
 - low molecular weight carbohydrates and orange oil retention during spray drying, 221*t*
 - moisture content and glass transition and melting characteristics of powders immediately after spray drying, 221*t*
 - moisture/sorption isotherms of two spray-dried powders with orange oil and different wall materials, 223*f*
 - molecular weight and viscosity, 215–216
 - particle size and film formation rate, 228

- proteins as emulsifiers, 228
- relative humidity affecting
 - moisture content and glass transition temperature, 218*f*
- scanning electron microscopy (SEM) of spray-dried powders with orange oil encapsulated with glucose syrup/n-OSA starch, 227*f*
- shelf life stability of orange oil encapsulated in glucose syrup/n-OSA matrix, 219*f*
- starch derivative as alternative to gum arabic, 225
- trehalose and fish oil encapsulation, 222
- trehalose replacing glucose syrup, 220
- wall material choice and success of microencapsulation, 228
- Caseins
 - nanoparticles to encapsulate and deliver nutrients, 132
 - potential nano-encapsulation systems, 132–133, 134*f*
 - unique physio-chemical properties, 133
- Catechins
 - tea, 199–201
 - See also* Polyphenols
- Cationic polysaccharides, biopolymers, 7, 7*t*
- Cationic surfactants, building blocks, 5–6, 7*t*
- Charged polysaccharides
 - controlling bulk properties of protein-stabilized emulsions, 158–159
 - high methoxyl pectin (HMP) and soy soluble polysaccharide (SSPS), 159
 - See also* Oil-in-water (O/W) emulsions
- Chronic diseases, nutraceuticals, 99
- Coacervation
 - analysis of flavor release, 275
 - antioxidant and relative humidity (RH) on oxidation of orange oil during storage, 279, 281*f*
 - comparing crosslinking coacervates on limonene release, 283*f*
 - crosslinking and oxidation of orange oil during storage, 276, 278*f*, 279
 - encapsulation materials and formation, 274
 - encapsulation technique, 272–273
 - flavoring, 273
 - flavor release, 279, 282, 283*f*
 - gas chromatographic (GC) analysis, 275–276
 - headspace analysis, 275
 - headspace comparison of flavor release due to matrix effects, 282, 284*f*
 - influence of water activity on stability, 279
 - limonene oxidation with and without glutaraldehyde crosslinking, 276, 277*f*
 - materials and methods, 273–276
 - matrix effects of samples on oxidation of orange oil during storage, 279, 280*f*
 - quantitation of volatiles using headspace analysis, 276
 - sample storage – oxidation study, 274–275
 - samples used in study, 274*t*
- Coating material
 - barrier for release of core compounds, 214–215
 - nature of, for encapsulation, 214
 - See also* Carrier properties
- Coenzyme Q10
 - beneficial effects, 193
 - encapsulation in nanodispersions, 190*t*

- experimental design of
 - nanodispersion with, 194–195
 - uptake by Caco-2 human intestinal cells, 195*t*
 - Colloidal interactions, mixed adsorbed films, 59–60, 61*f*
 - Composite systems
 - milk proteins-polysaccharide, 135–137
 - See also* Milk proteins-polysaccharide
 - Contact angle
 - hydrophobin in water, 92, 95*f*
 - measurements, 92
 - Contact emulsion
 - charge and size of droplets, 26, 29, 30*f*
 - laminated coatings, 26, 28*f*, 29
 - Controlled release, nanodispersions, 191
 - Conventional emulsions, structured delivery systems, 10, 11*f*
 - Co-solvent, molecular scale effect, 249, 259*f*
 - Co-surfactant, nanodispersion formulation, 187
 - Crossflow membrane emulsification (XME)
 - emulsions using food grade ingredients, 77
 - schematic, 76*f*
 - techniques, 75–76
 - See also* Emulsions
 - Crosslinking. *See* Coacervation
 - Crystallization
 - differential scanning calorimetry (DSC) cooling thermopeaks of, of lauric acid (LA) solubilized in bulk oil and in emulsion, 176*f*
 - emulsions retarding, 178
 - trehalose, 220, 222
 - wall material ingredients, 220, 222
 - x-ray diffraction patterns of bulk LA and emulsion with solubilized LA, 176–177
 - See also* Long-chain fatty acids
 - Curcumin
 - application of, nanoemulsion on 12-O-tetradecanoylphorbol-13-acetate (TPA)-induced edema of mouse ears, 208, 210*f*
 - chemical structure, 202*f*
 - encapsulation in nanoemulsions, 208, 210
 - nanocurcumin emulsions on growth of transport human prostate cancer cell in mice, 210, 211*t*
 - UV spectra of, nanoemulsion, 209*f*
 - See also* Polyphenols
- D**
- Daily diet, proteins, 99
 - Delivery systems
 - attributes of edible, 4
 - building blocks, 5–6, 7*t*
 - conventional emulsions, 10
 - emulsion-based, 11*f*
 - filled hydrogel particles, 12
 - liposomes as drug carriers, 186–187
 - multilayer emulsion-based, 12–22
 - multilayer emulsions, 10, 12
 - multiple emulsions, 10
 - oil-in-water (O/W) emulsion and microemulsion, 170
 - solid lipid nanoparticles, 12
 - See also* Multilayer emulsion-based delivery systems; Soy protein
 - Delivery vehicles. *See* Hydrophobins
 - Deodorant fragrance, release profile, 191, 192*f*
 - Deposition emulsion, laminated coatings, 26, 28*f*, 29
 - Dextrin, encapsulation performance, 226*t*
 - Diet, human health, 132, 144
 - Dietary fat
 - United Kingdom, 68

See also Fat

- Dietary strategies, reducing fat or energy intake, 80
- Digalacto diacylglycerols, surface elastic modulus vs. interfacial tension of mixtures of phosphatidyl choline and, 82–83
- Digestion, fat, 78–79
- Directed assembly, structural design principle, 10
- Directed self-assembly, structural design principle, 9–10
- Droplets. *See* Aroma release

E

- Echo planar imaging (EPI), emulsions and satiety, 81
- Economics, soy lecithin based nanodispersions, 195–196
- Edible coatings
 - applications of laminated, 22–23
 - example of possible multilayered edible film, 26, 27*f*
 - formation of laminated, 23, 24*f*, 26
 - possible components for assembling, 23, 25*f*
 - preliminary studies, 29
- Edible delivery system, attributes, 4
- Electrostatic deposition, layer-by-layer (LbL), 13, 14*f*, 23
- Electrostatic interactions, force between food components, 8
- Emulsification–gelation, soy protein microspheres, 104–105
- Emulsifiers
 - effectiveness of food, 12–13
 - proteins, 228
- Emulsions
 - crossflow membrane emulsification (XME), 75–76
 - encapsulation technique, 202–203
 - influence of stabilizing layer, 72–73
 - instability mechanisms, 203*f*
 - interfacial structure of simple, 73–74, 75*f*
 - microemulsions vs. macroemulsions, 117
 - multiple, 74–78
 - optical microscope images, 206*f*
 - physical properties, 71–72
 - rheology of, stabilized by protein, 72
 - satiety and, 81–84
 - spray-dried, 235, 238
 - structured delivery systems, 10–12
 - visual appearance, 117
- See also* Microemulsions; Oil-in-water (O/W) emulsions
- Encapsulation
 - aqueous two-phase systems (ATPS), 239, 241–242, 244
 - coacervation of orange oil, 272–273
 - emulsion, 202–203
 - food ingredients, 214, 234
 - nanoemulsion, 203–204, 207
 - poly(lactic-co-glycolic acid) (PLGA), 144
 - techniques, 201–202
 - wall material choice for success, 228
- See also* Aqueous two-phase systems (ATPS); Coacervation; Flavor delivery via lipid encapsulation; Polyphenols; Soy protein; Zein
- Energy intake, dietary strategies, 80
- Entero-endocrine feedback, fat digestion, 79–80
- Epigallocatechin gallate (EGCG)
 - chemical structure, 200*f*
 - encapsulation in nanoemulsions, 207–208
 - oxidation, 199–200
 - tea catechin, 199
- See also* Polyphenols

- Epithelial cells, small intestine's absorptive surface, 185*f*
- Essential oils, encapsulation in nanodispersions, 190*t*
- Esters. *See* Cake
- Ethyl butyrate
 average time intensity traces from panelists with droplet or gel containing, 255*f*
in vivo release from xanthan mixed or as single droplet, 253–254
 statistical analysis of sensory time intensity parameters from panelists, 256*t*
 video monitoring of droplet release, 251, 252*f*
- Experimental design, nanodispersions with coenzyme Q10, 194–195
- Extrusion
 soy microspheres by, 102, 104, 105*f*
 soy protein beads, 101–102, 103*f*
- F**
- Fat
 bile salts, 83, 84*f*
 caloric intake, 68
 designing structures enabling delivery, 84–85
 dietary strategies to reduce, 80
 digestion, 78–79
 emulsions and satiety, 81–84
 factors controlling intake, 68–69
 glycolipids, 81–84
 role of, at interface in emulsions, 70–74
 role of gastrointestinal (GI) tract and GI-endocrine feedback, 79–80
 sensory perception, 69–70
 sensory scores of perceived, content, 75*f*
 surface elastic modulus vs. interfacial tension at olive oil-aqueous phase interface, 83*f*
See also Lipid delivery
- Fatty acid
 zein-fatty acid organization, 151, 154–155
See also Long-chain fatty acids
- Filled hydrogel particles, structured delivery systems, 11*f*, 12
- Films. *See* Zein
- Fish oils
 encapsulation in nanodispersions, 190*t*, 192
 lipids, 5, 7*t*
 trehalose for encapsulation, 222
- Flavor delivery via lipid encapsulation
 analysis of flavor levels in cake, 266–267
 bread loaf volume, 260, 261–263, 265, 266
 bread preparation, 261–263
 cake flavor system, 263
 cake formula and baking, 264–265
 data analysis, 266–267
 ester loss from cakes, 261, 263–265, 265–266
 ester retention and lipid-based delivery systems, 267–268
 flavor analysis, 265
 food industry, 260
 garlic flavor incorporation into lipid capsule, 261
 garlic oil concentration and form affecting bread loaf volume, 270*f*
 garlic oil delivery system and bread loaf volume, 268, 270
 honest significant difference (HSD) pairwise comparison of loaf volumes by garlic oil and incorporation method, 268, 269*t*
 materials, 260–261
 quantification of esters, 266

- size reduction of lipid block, 264
 - spray dried delivery, 264
 - Flavor oils
 - encapsulation in nanodispersions, 190*t*
 - lipids, 5, 7*t*
 - Flavors, volatile components, 191, 247
 - Flexible proteins, biopolymers, 7, 7*t*
 - Flory–Huggins interaction parameters, monomer types, 56*t*
 - Foams
 - hydrophobins, 92
 - stability measurement, 92
 - See also* Hydrophobins
 - Food colloid formulations, proteins and polysaccharides, 47
 - Food emulsifiers, effectiveness, 12–13
 - Food emulsions
 - oil-in-water type, 158
 - See also* Lipid delivery; Oil-in-water (O/W) emulsions
 - Food industry
 - encapsulation of ingredients, 214, 234
 - lipophilic components, 4
 - See also* Carrier properties; Structural design principles
 - Food protein-based matrices, controlled release of functional components, 99
 - Foods, structure and composition affecting release, 36
 - Food systems, interactions between proteins and polysaccharides, 47
 - Formulated foods, proteins, 99
 - Fragrance oils, encapsulation in nanodispersions, 190*t*
 - Freeze drying, influence on emulsion stability, 21–22
 - Freeze-thaw cycling, influence on emulsion stability, 19, 21
 - Fruit seed oils, encapsulation in nanodispersions, 190*t*
 - Functional foods
 - controlled release, 99
 - market growth, 199
 - See also* Polyphenols
 - Functional ingredients in foods, proteins and polysaccharides, 47
 - Fungi, hydrophobins, 90
- ## G
- Galactolipids, plants, 82
 - Garlic. *See* Bread; Flavor delivery via lipid encapsulation
 - Gastrointestinal (GI) tract
 - drug's stability and absorption in, 184
 - hydrophilic nutrients, 106–107, 108*f*
 - hydrophobic nutrients, 107, 109, 112*f*
 - nutrient encapsulation and release, 105–109
 - riboflavin, 106–107, 108*f*, 111*f*
 - role in fat digestion, 79–80
 - TNO intestinal model, 106, 107, 110*f*
 - See also* Soy lecithin based nanotechnology
 - Gelatin samples, coacervation of orange oil, 274
 - Globular proteins, biopolymers, 7, 7*t*
 - Glucose syrup
 - collapse/caking, 222
 - dextrose equivalent (DE), 215
 - differential scanning calorimetry (DSC) characteristics of spray-dried powders with orange oil and different wall materials, 224*t*
 - infeed solids and oil load
 - influencing orange oil retention during spray drying, 216*t*
 - moisture/sorption isotherms of two spray-dried powders with orange oil and different wall material, 223*f*

- relative humidity influencing moisture content and glass transition of carrier with, and modified starch, 217, 218*f*
- scanning electron microscopy (SEM) of spray-dried powders with orange oil encapsulated with, and modified starch, 227*f*
- shelf life stability of orange oil encapsulated in matrix with, and modified starch, 217, 219*f*
- trehalose replacing, 220, 221*t*
- See also* Carrier properties
- Glycolipids, surfactants, 81–84
- Gum arabic
- encapsulation performance, 226*t*
 - starch derivative as alternative, 225
- Gut hormones, role in fat digestion, 79–80
- H**
- Health concerns, obesity, 68
- Hexanol, *in vivo* release from gels, 249, 250*f*
- High density lipoproteins (HDL), fat intake, 68
- High methoxyl pectin (HMP)
- charged polysaccharide, 159
 - diameter vs. pH during acidification of emulsions with, 164*f*
 - diameter vs. polysaccharide to sodium caseinate emulsions, 161, 162*f*
 - interaction with charged casein patches, 165
 - values of $1/($ photon transport mean free path) $[1/l^*]$ vs. HMP concentration, 163*f*
 - values of $1/l^*$ of control emulsions and emulsions with, 165, 166*f*
- See also* Oil-in-water (O/W) emulsions
- Human health, diet, 132, 144
- Human prostate cancer cell in mice, nanocurcumin emulsion, 210, 211*t*
- Hydrogels
- calcium ions crosslinking soy protein, 100–101
 - See also* Soy protein hydrogels
- Hydrogen bonding, force between food components, 8
- Hydrolyzed starches
- amorphous state of carbohydrate matrix, 216–217, 220
 - dextrose equivalent (DE), 215
 - encapsulation performance, 226*t*
 - moisture/sorption isotherms of spray-dried powders with orange oil and different wall materials, 223*f*
 - molecular weight and viscosity, 215–216
 - relative humidity influencing moisture content and glass transition of carrier of glucose syrup and n-octenyl succinic anhydride (n-OSA) starch, 218*f*
 - shelf life stability of orange oil encapsulated in matrix of glucose syrup and n-OSA starch, 219*f*
 - starch derivative as alternative to gum arabic, 225
 - See also* Carrier properties
- Hydrophilic surfaces, zein adsorption to, 146–147, 150*f*
- Hydrophobic interactions, force between food components, 8
- Hydrophobic surfaces, zein adsorption to, 146–147, 152*f*
- Hydrophobins
- 3D structure, 90, 91*f*
 - amphiphilic molecule, 90
 - discovery, 90
 - effect of increasing content on contact angle between water and air, 92, 95*f*

- experimental, 90, 92
 foam building ability, 92
 fungi's life, 90
 particle sizing distribution, 92, 93*f*,
 94*f*
 surface rheology data for, gels, 92,
 96*f*
See also Proteins
- I**
- Immunoglobulins, potential nano-
 encapsulation systems, 133, 135
 Ingredient production,
 nanodispersions, 192–193
 Insulin, surface-active polymers, 238,
 240*f*
 Interfacial films. *See* Mixed interfacial
 biopolymer films
- K**
- Kinetic trapping, distinguishing
 between two different structure
 types, 47
- L**
- α -Lactalbumin, potential nano-
 encapsulation systems, 133, 135
Lactobacillus plantarum, survival in
 aqueous two-phase systems
 (ATPS), 242, 243*f*, 244
 β -Lactoglobulin (BLG)
 infrared amide I peak absorbance
 vs. pH for 8-layer pectin/BLG
 multilayer, 38–39, 40*f*
 infrared spectra of 8-layer
 pectin/BLG multilayer, 38,
 39*f*
 potential nano-encapsulation
 systems, 133, 135
See also Biopolyelectrolyte
 multilayers
 Laminated edible coatings
 applications of, 22–23
 formation, 23, 24*f*, 26
 preliminary studies, 26, 29
 Lauric acid (LA)
 differential scanning calorimetry
 (DSC) cooling thermopeaks of
 LA in bulk oil and in emulsion,
 176*f*
 material, 171
 solubilized quantities in emulsion
 vs. bulk oil, 173, 176
 solubilized quantity in emulsion,
 bulk oil, and aqueous micelle
 solution, 173, 175*t*
 solubilized quantity of, with
 varying oil concentration in
 emulsion, 172, 173*f*
 synchrotron radiation x-ray
 diffraction (SR–XRD) patterns
 of bulk LA and emulsion with
 solubilized LA during cooling
 and heating, 176–177
 time variation of solubilized
 quantity in emulsion, 172–173,
 174*f*
See also Long-chain fatty acids
 Layer-by-layer (LbL), electrostatic
 deposition, 13, 14*f*, 23
 Limonene, *in vivo* release from gels,
 249, 250*f*
 Lipase, fat digestion, 78–79
 Lipid delivery
 bulk storage/loss modulus for
 emulsions stabilized by whey
 protein isolate and surfactants,
 74*f*
 challenge to design rules for
 optimizing physical structure,
 77–78
 cross flow membrane
 emulsification (XME) method,
 75, 76*f*

- dispersed phase volume of cream
 - layer in oil-in-water emulsions vs. time, 73*f*
- fat digestion, 78–79
- interfacial composition of model emulsions, 74, 75*f*
- measuring rheology of cream layer in situ, 72, 73
- membrane emulsification
 - development, 76
- modulating fat digestion, 78–84
- multiple emulsions, 74–78
- optical micrograph of water-oil-water (WOW) multiple emulsion, 77*f*
- physical properties of emulsions, 71–72
- reduced fat, 69–78
- rheology of emulsions, 72
- role of interface, 70–74
- sensory perception of "creaminess" for stabilized emulsions, 73–74, 75*f*
- sensory perception of fat, 69–70
- sensory scores of perceived fat content of model emulsions vs. fat content of stabilized emulsions, 75*f*
- surfactants, 72
- typical interfacial shear elastic behavior of protein, 71*f*
- XME method, 76
- See also* Fat; Flavor delivery via lipid encapsulation
- Lipid droplets, adsorbing substance for layers, 26
- Lipid oxidation, primary and secondary emulsions, 22
- Lipids
 - adsorbing substance for layers, 26
 - building blocks, 5, 7*t*
 - model of, solubilization into emulsion droplets, 177*f*, 178
 - See also* Long-chain fatty acids
- Lipolysis, pancreatic lipase, 79
- Lipophilic active components
 - delivery system types, 4–5
 - food industry, 4
- Liposomes
 - drug carriers, 186–187
 - formation from milk fat globule membrane (MFGM)-phospholipids, 140–141
 - phospholipid, 187
- Live probiotics, survival in aqueous two-phase systems (ATPS), 242
- Long-chain fatty acids
 - concentration of lauric acid (LA) in emulsion on solubilization quantity, 172, 173*f*
 - crystallization measurement, 172
 - crystallization rate retardation, 178
 - differential scanning calorimetry (DSC) cooling thermopeaks of crystallization of LA in bulk oil and in emulsion, 176*f*
 - increasing solubility in emulsion droplets, 178
 - LA, myristic acid (MA) and palmitic acid (PA), 170
 - materials and methods, 171–172
 - model of solubilization of lipid into emulsion droplets, 177*f*
 - solubilization experiments, 171–172
 - solubilization in emulsion droplets, 170
 - solubilization mechanisms, 178
 - solubilized quantities in emulsion vs. bulk oil, 173, 176
 - solubilized quantity of, in emulsion, bulk oil and aqueous micelle solution, 173, 175*t*
 - synchrotron radiation x-ray diffraction (SR-XRD) patterns of bulk LA and solubilized in emulsion during cooling and heating, 176–177

time variation of solubilization
quantity of LA, MA, and PA,
174*f*, 175*f*

Low density lipoproteins (LDL), fat
intake, 68

Lutein esters, encapsulation in
nanodispersions, 190*t*

Lycopene, encapsulation in
nanodispersions, 190*t*

M

Microemulsions

applying titration method, 123
calculation of minimum amount of
primary surfactant needed, 119,
122

determination of surfactant molar
composition at oil-in-water
(O/W) interface, 123–125

effect of oil penetration on,
formation, 127, 128*f*

equation for average number of
ethylene oxides (EO) per
molecule at interface, 124

equation for molar ratio of
cosurfactant at interface, 124

equation for total interfacial area,
119

equation for volume of dispersed
phase, 119

O/W and water-in-oil (W/O), 117–
118

role of surfactant solubility at O/W
interface, 126, 127*f*

structure and HLB of nonylphenol
ethylene oxide (NP(EO)_n)
surfactants, 118*f*

terms, 117

titration method, 118, 119, 122–
125

typical graph of, titration, 126*f*
W/O and O/W, with NP(EO)_n
surfactants, 120*t*, 121*t*

See also Emulsions

Microencapsulation, applications, 132

Microscale. *See* Aroma release

Microspheres

emulsification-gelation, 104–105

fluorescence photomicrographs,
105*f*

soy protein, 102, 104–105

See also Soy protein

Microvilli, small intestine's absorptive
surface, 185*f*

Milk, nanoparticles for encapsulation
and delivery of bioactive
compounds, 132

Milk fat globule membrane- phospholipids

formation of liposomes from, 140–
141

microfluidization, 140, 141*f*

milk, 137, 140

stability of liposome dispersions,
141

Milk phospholipids, potential
nanoencapsulation systems, 137,
140–141

Milk proteins

potential nano-encapsulation
systems, 132–135

proteins-polysaccharide composite
systems, 135–137

Milk proteins-polysaccharide

absorbance vs. pH of sodium
caseinate and mixture with gum
arabic, 136, 138*f*

composite systems, 135–137

effect of NaCl and CaCl₂ on
properties of nanoparticles, 136,
136–137, 139*f*

mechanism of nanoparticle
formation, 136

particle sizes of stable dispersions
in pH range 5.4 to 3.0, 136

Millimeter scale

droplets *in vivo*, 253–256

non-homogeneous distribution, 249

- non-solubilized droplets *in vitro*, 251, 252*f*
- Mixed interfacial biopolymer films
 - adsorption behavior of polysaccharides onto protein at interface, 63
 - calculated density profiles for biopolymers for two salt volume fractions, 56, 57*f*, 58
 - calculated density profile variation of polyelectrolyte in interfacial region, 58, 59*f*
 - charged segments per chain, 60–61
 - colloidal interactions mediated by mixed adsorbed films, 59–61
 - density profile for hydrophilic chains showing emerging secondary layer, 54, 55*f*
 - density profile of biopolymer at interface, 63–64
 - density profile variation of hydrophilic and amphiphilic chains vs. distance from solid surface, 52, 53*f*, 54
 - effect of varying charge of polyelectrolyte, 58–59
 - excess hydrophilic polymer in interface vs. strength of interaction, 53*f*
 - excess polyelectrolyte at interface vs. number of charge groups on chains, 59, 60*f*
 - excess polyelectrolyte at interface vs. pH, 62, 62*f*
 - extent of adsorption of polyelectrolyte chains varying with degree of charging, 64
 - flexibility assumption in model, 64
 - Flory–Huggins interaction parameters between monomer types and pKa values for charged amino acids, 55, 56*t*
 - influence of pH and background electrolyte, 61–63
 - interactions between two flat surfaces using SCF theory, 59–60, 61*f*
 - mixed layers of α s1-casein and polyelectrolyte, 54–56, 58
 - possibility of binding polyelectrolyte to protein layers at pH above iso-electric point, 63
 - SCF (self consistent field) calculations and methodology, 49–51
 - simple model for short range interactions, 51–52, 54
 - thermodynamic similarity of homopolymer chains adsorbing onto primary polymer layer, 52, 54
- Mixed structures, surface interfaces, 48
- Molecular interactions, forces between food components, 6, 8
- Mouse ear inflammation model nanoemulsified polyphenols, 208, 209*f*
See also Polyphenols
- Mucin-coated sepharose, affinity of targeted nanodispersions to, 189, 190*f*
- Mucosal folds, small intestine, 184, 185*f*
- Multilayer emulsion-based delivery systems
 - emulsifier and biopolymer combinations, 22
 - emulsifiers, 12–13
 - formation of stable multilayer emulsions, 15, 16*f*
 - freeze drying, 21–22
 - freeze-thaw cycling, 19, 21
 - improving emulsion stability and performance, 13
 - improving stability to environmental stresses, 17–22

- layer-by-layer (LbL) electrostatic deposition, 13, 14*f*
 - lipid oxidation, 22
 - monitoring using ζ -potential measurements, 15, 16*f*
 - pH-dependence of ζ -potential, mean particle diameter and creaming stability of primary and secondary emulsions, 15, 17, 18*f*
 - preparation of multilayered emulsions, 15
 - primary emulsion, 13, 14*f*, 15
 - salt-dependence of mean particle diameter and creaming stability of primary and secondary emulsions, 19, 20*f*
 - secondary emulsion, 13, 14*f*, 15
 - tertiary emulsions, 14*f*, 15
 - thermal processing, 19
 - See also* Delivery systems
 - Multilayer emulsions, structured delivery systems, 10, 11*f*, 12
 - Multilayers
 - assembly, 36, 39
 - disassembly, 36, 38
 - food biopolymer, 42
 - release of active ingredients from foods, 43
 - zeta potential of emulsion droplets vs. layer number, 42
 - See also* Biopolyelectrolyte multilayers
 - Multiple emulsions, structured delivery systems, 10, 11*f*
 - Myristic acid (MA)
 - material, 171
 - solubilized quantity in emulsion, bulk oil, and aqueous micelle solution, 173, 175*t*
 - time variation of solubilized quantity in emulsion, 172–173, 174*f*
 - See also* Long-chain fatty acids
- N**
- NaCl concentration, influence on ζ -potential, mean particle diameter, and creaming stability of primary and secondary emulsions, 19, 20*f*
 - Nanodispersions
 - actives encapsulated in, 190*t*
 - benefits, 188–195
 - bioavailability of nutrients, 193–195
 - coenzyme Q10 formulation, 188*t*
 - controlled release, 191
 - ease of dispersion, 189
 - experimental design of, with coenzyme Q10, 194–195
 - liposomes to, 186–188
 - protection of ingredients, 192–193
 - targeting, 189, 190*f*, 191
 - water-dispersible, 187
 - See also* Soy lecithin based nanotechnology
 - Nanoemulsions
 - curcumin encapsulation in, 208, 210
 - emulsions with different formulations, 205*t*
 - encapsulation of polyphenols in, 207–208, 210
 - high-pressure homogenization, 204, 205*f*
 - HPLC chromatograms of epigallocatechin gallate (EGCG), and EGCG aqueous solution, 207*f*
 - nanoencapsulation, 203–204, 207
 - optical microscope images, 206*f*
 - oxidation of EGCG nanoemulsion and EGCG aqueous solution, 208*f*
 - preparation process, 205*f*
 - UV spectra of curcumin, prepared by high-pressure homogenization, 209*f*
 - See also* Polyphenols

- Nanoencapsulation
 emulsions, 202–203
 milk phospholipids as potential, 137, 140–141
 milk proteins as potential, systems, 132–137
 nanoemulsion, 203–204, 207
 techniques, 201–202
- Nano-laminated coatings
 applications of laminated edible coatings, 22–23
 electrostatic attraction driving layer-by-layer (LbL) deposition, 23
 formation of laminated edible coatings, 23, 26
 future research, 31
 LbL technique coating macroscopic objects, 23, 24*f*
 possible components for assembling multilayered edible films or coatings, 23, 25*f*, 26
 possible multilayered edible film, 26, 27*f*
 preliminary studies for forming, 26, 29
 schematic of coating hydrogel surface with lipid droplets, 26, 28*f*
 turbidity of anionic hydrogels in contact with emulsion containing whey protein coated droplets at various pH values, 29, 31*f*
 turbidity of emulsions over time, 26, 29*f*
 ζ -potential and mean particle diameter of droplets in contact emulsion from surfaces of hydrogels, 29, 30*f*
- Nanoparticles, caseins encapsulating and delivering bioactives, 132
- Nanoscale. *See* Aroma release
- Nanostructures. *See* Zein
- Nanotechnology. *See* Soy lecithin based nanotechnology
- Nanotubes, self-assembly of amphiphilic molecules, 154
- Natural polyelectrolytes, adsorbing substance for layers, 23
- Non-ionic polysaccharides, biopolymers, 7, 7*t*
- Non-ionic surfactants, building blocks, 5–6, 7*t*
- Nonylphenol ethoxylates, surfactants, 118*f*
- Nutraceuticals
 improving public health, 99
See also Soy protein; Soy protein hydrogels
- Nutrients, protection by nanodispersions, 193
- ## O
- Obesity
 health concern, 68
See also Fat
- Oil droplets, oil-in-water (O/W) emulsion containing, 170
- Oil-in-water (O/W) emulsions
 advanced delivery tool, 170
 average diameter vs. pH during acidification, 164*f*
 charged polysaccharides controlling bulk properties, 158–159
 charged polysaccharides high methoxyl pectin (HMP) and soy soluble polysaccharide (SSPS), 159
 determining photon transport mean free path (1*), 160
 diameter vs. polysaccharide added to sodium caseinate emulsions, 161, 162*f*
 diffusing wave spectroscopy (DWS), 160

- experimental, 160–161
 - hydrodynamic diameter of
 - emulsion droplets and charged polysaccharide concentration, 162
 - parameter $1/l^*$ changes by DWS and ultrasonic attenuation, 162–163
 - rearrangement of emulsion droplets in space, 163
 - stabilization by protein systems, 158
 - ultrasonic spectroscopy, 159–160
 - values of $1/l^*$ by DWS and ultrasonic attenuation, 163*f*
 - values of $1/l^*$ by DWS and ultrasonic attenuation for control, and emulsions containing HMP, 165, 166*f*
 - values of $1/l^*$ by DWS and ultrasonic attenuation for control, and emulsions containing SSPS, 165, 166*f*
 - Oil-in-water (O/W) microemulsions
 - advanced delivery tool, 170
 - determination of surfactant molar composition at O/W interface, 123–125
 - nonylphenol ethylene oxide surfactants from, 120*t*, 121*t*
 - oil penetration and microemulsion formation, 127, 128*f*
 - role of surfactant solubility at O/W interface, 126, 127*f*
 - type, 117–118
 - See also* Microemulsions
 - Orange oil
 - coacervation, 273, 274
 - effect of antioxidant on, oxidation, 279, 281*f*
 - effect of type of wall material in coacervation of oxidative stability, 279, 280*f*
 - effects of crosslinking on oxidation
 - of, during storage, 276, 277*f*, 278*f*
 - emulsification and retention of, during spray drying, 222, 225, 228
 - flavor release from coacervates, 279, 282, 283*f*
 - headspace comparison of flavor release due to matrix effects, 282, 284*f*
 - infeed solids and oil load
 - influencing retention of, during spray drying, 216*t*
 - low molecular weight
 - carbohydrates and retention of, during spray drying, 221*t*
 - scanning electron microscopy (SEM) of spray-dried powders with, encapsulated with glucose syrup and modified starch, 227*f*
 - shelf life stability of encapsulated, 217, 219*f*
 - See also* Carrier properties; Coacervation; Spray-dried powders
- P**
- Palmitic acid (PA)
 - material, 171
 - solubilized quantity in emulsion, bulk oil, and aqueous micelle solution, 173, 175*t*
 - time variation of solubilized quantity in emulsion, 172–173, 175*f*
 - See also* Long-chain fatty acids
 - Pancreatic lipase, lipolysis, 79
 - Particle sizes
 - nanoparticle dispersion of
 - caseinate/gum arabic and salt concentration, 136–137, 139*f*

- stable dispersions in pH range of 5.4 to 3.0, 136
zein, 146, 147*f*
- Particle sizing distribution, hydrophobin in water, 92, 93*f*, 94*f*
- Particle uptake, small intestine, 186
- Percolation, droplets merging and reforming, 118
- pH
influence on mixed interfacial biopolymer films, 61–63
influence on ζ -potential, mean particle diameter, and creaming stability of primary and secondary emulsions, 17, 18*f*
nanoparticles of sodium caseinate/gum arabic, 136, 138*f*
- Phase separation, structural design principle, 8–9
- Phosphatidyl choline (PC), surface elastic modulus vs. interfacial tension of mixtures of, and digalacto diacylglycerols, 82–83
- Phosphatidylserine, encapsulation in nanodispersions, 190*t*
- Phospholipids, structural component of liposomes, 187
- Photon transport mean free path (1*)
diffusing wave spectroscopy, 160
See also Oil-in-water (O/W) emulsions
- Phytosterol esters, encapsulation in nanodispersions, 190*t*
- pKa values, charged amino acids, 56*t*
- Plant oils, lipids, 5, 7*t*
- Plants, galactolipids, 82
- Polyelectrolyte multilayer
adsorption onto protein varying with degree of charging, 64
influence of background electrolyte, 61–63
number of charged segments, 60–61, 62*f*
varying charge of polyelectrolyte, 58–59
- See also* Biopolyelectrolyte multilayers; Mixed interfacial biopolymer films
- Polyelectrolyte-protein complex
SCF calculations and methodology, 49–51
self consistent field (SCF), 48–49
theoretical modeling, 48
- Poly(lactic-*co*-glycolic acid) (PLGA), encapsulation, 144
- Poly-L-lysine hydrobromide (PLL)
assembly of multilayers, 39
infrared spectra of 10 layer pectin/PLL multilayer, 40, 41*f*
swelling ratio vs. pH for 10 layer pectin/PLL, 40, 41*f*
See also Biopolyelectrolyte multilayers
- Polyphenols
chemical structures of curcumin, 202*f*
chemical structures of tea catechins, 200*f*
curcumin, 201, 202*f*
emulsion as encapsulation technique, 202–203
emulsions with different formulations, 205*t*
encapsulation of, in nanoemulsions, 207–208, 210
encapsulation techniques, 201–202
epigallocatechin gallate (EGCG), 199, 200*f*
health benefits, 199
HPLC chromatograms of EGCG nanoemulsion and EGCG aqueous solution, 207*f*
mechanisms of instability in emulsions, 203*f*
mouse ear inflammation model for testing anti-inflammation activity of nanoemulsified, 208–209
nanocurcumin emulsion administration on growth of

- transplant human prostate cancer cell in male mice, 210, 211*t*
 - nanoemulsion as encapsulation technique, 203–204, 207
 - optical microscope images of emulsions, 206*f*
 - oral administered curcumin nanoemulsion on 12-O-tetradecanoylphorbol-13-acetate (TPA)-induced edema of mouse ears, 208, 210*f*
 - oxidation of EGCG in nanoemulsion vs. aqueous solution, 208*f*
 - possible pathway for EGCG oxidation, 200*f*
 - process for preparing nanoemulsions, 205*f*
 - tea catechins, 199–201
 - UV spectra of curcumin nanoemulsion prepared by high-pressure homogenization, 209*f*
 - Polysaccharides
 - adsorption behavior to protein at interface, 63
 - charged, and properties of protein-stabilized emulsions, 158–159
 - functional ingredient in foods, 47
 - See also* Oil-in-water (O/W) emulsions
 - Poly(vinyl alcohol) (PVA)
 - surface-active polymers, 238, 240*f*
 - surface composition of PVA/dextran with encapsulated bovine serum albumin (BSA), 242*f*
 - Powders
 - in-situ coating of, 238–239
 - See also* Spray-dried powders
 - Powders, spray-dried, coating material as release barrier, 214–215
 - Primary emulsion
 - electrostatic deposition, 13, 14*f*, 15
 - freeze drying, 21–22
 - freeze-thaw cycling, 19, 21
 - lipid oxidation, 22
 - pH influence on ζ -potential, mean particle diameter, and creaming stability, 17, 18*f*
 - salt-concentration of mean particle diameter and creaming stability, 19, 20*f*
 - thermal processing, 19
 - Production, soy lecithin based nanodispersions, 195–196
 - Prostate cancer cells, nanocurcumin emulsions on growth of transport human, in mice, 210, 211*t*
 - Protection of ingredients, nanodispersions, 192–193
 - Proteins
 - daily diet, 99
 - emulsifying properties, 228
 - emulsions stabilized by, 72, 73*f*
 - factors affecting structure, 145
 - fat content of model emulsions vs. emulsions stabilized by, 73–74, 75*f*
 - functional ingredient in foods, 47
 - interfacial rheology of, system, 70, 71*f*
 - roles in foods, 90
 - stabilizing oil-in-water (O/W) food emulsions, 158
 - viscoelasticity of cream layers stabilized by, 72–73, 74*f*
 - See also* Hydrophobins; Oil-in-water (O/W) emulsions; Soy protein
- R**
- Real time monitoring. *See* Oil-in-water (O/W) emulsions
 - Release barrier, coating material as, for core compounds, 214–215
 - Release profile, fragrances, 191, 192*f*
 - Retinol
 - hydrophobic nutrient, 107, 109

- transmission electron micrograph
 - of soy protein microspheres
 - with, 112*f*
 - Riboflavin
 - cumulative amounts in dialysis fluid, 107, 111*f*
 - nutrient encapsulation, 106–107
 - photomicrograph of soy protein microspheres, 108*f*
 - Rumen environment, ingredient protection, 193
 - Rupture force, beads with alginate and soy protein isolate, 102, 103*f*
- S**
- Salt concentration
 - influence on ζ -potential, mean particle diameter, and creaming stability of primary and secondary emulsions, 19, 20*f*
 - nanoparticle dispersion of caseinate/gum arabic, 136–137, 139*f*
 - Satiety, emulsions and, 81–84
 - Secondary emulsion
 - electrostatic deposition, 13, 14*f*, 15
 - freeze drying, 21–22
 - freeze-thaw cycling, 19, 21
 - lipid oxidation, 22
 - pH influence on ζ -potential, mean particle diameter, and creaming stability, 17, 18*f*
 - salt-concentration of mean particle diameter and creaming stability, 19, 20*f*
 - thermal processing, 19
 - Self-assembly
 - directed, 9–10
 - spontaneous, 9
 - Self consistent field (SCF)
 - calculated density profiles of biopolymers, 56, 57*f*, 58
 - calculations and methodology, 49–51
 - flexibility assumption for polyelectrolyte chains, 64
 - formation of mixed interfacial layers, 48–49
 - free energy of system, 51
 - hard core potential, 50
 - local electric potential, 50
 - polyelectrolyte binding to protein
 - above iso-electric point, 63
 - short range interactions, 51–52, 54
 - See also* Mixed interfacial biopolymer films
 - Self-organization
 - scanning electron micrograph of zein-oleic acid film, 153*f*
 - tertiary structures by zein, 155
 - zein-fatty acid organization, 151, 154–155
 - See also* Zein
 - Sensory analysis, aroma release, 248–249
 - Sensory perception
 - fat, 69–70
 - fat content of model emulsions vs. actual fat content of emulsions, 75*f*
 - Small intestine
 - absorption, 184, 186
 - absorptive surface features, 185*f*
 - uptake of particles, 186
 - See also* Soy lecithin based nanotechnology
 - Sodium caseinate
 - absorbance of, gum arabic, and their mixtures vs. NaCl and CaCl₂ concentration, 136–137, 139*f*
 - absorbance vs. pH of, and mixture of, with gum arabic, 136, 138*f*
 - diameter vs. polysaccharide added to, emulsions, 161, 162*f*

- See also* Milk proteins-polysaccharide; Oil-in-water (O/W) emulsions
- Sodium chloride, nanoparticle dispersion of caseinate/gum arabic, 136–137, 139*f*
- Solid lipid nanoparticles, structured delivery systems, 11*f*, 12
- Solubilization
- lipophilic molecules in micelle solutions, 170
 - mechanisms, 178
 - model of, of lipid into emulsion droplets, 177*f*, 178
- See also* Long-chain fatty acids
- Soy lecithin based nanotechnology
- actives encapsulated in dispersions, 190*t*
 - affinity of targeted nanodispersions to mucin-coated sepharose, 190*f*
 - antiperspirant production, 191, 192*f*
 - benefits of nanodispersions, 188–195
 - coenzyme Q10 nanodispersion formulation, 188*t*
 - controlled release, 191
 - ease of dispersion, 189
 - experimental design, 194, 194*f*
 - food and health markets, 186
 - fragrance sniff test of two antiperspirants, 192*f*
 - increased bioavailability, 193–195
 - liposomes to nanodispersions, 186–188
 - nanodispersions containing coenzyme Q10, 194–195
 - production and economic considerations, 195–196
 - protection of ingredients, 192–193
 - release profile of fragrances, 191, 192*f*
 - small intestinal absorption, 184–186
 - targeting with nanodispersions, 189, 191
- Soy protein
- bead preparation with soy protein isolate (SPI) powder, 102
 - beads, 101–102
 - cumulative amounts of riboflavin in dialysis fluid, 107, 111*f*
 - emulsification-gelation technique to microspheres, 104–105
 - extrusion for beads, 101–102
 - extrusion methods to microspheres, 102, 104, 105*f*
 - fluorescence photomicrographs of, microspheres by extrusion and emulsification/internal cold gelation, 105*f*
 - functional food ingredient, 100
 - hydrophilic nutrients, 106–107
 - hydrophobic nutrients, 107, 109
 - microspheres, 102, 104–105
 - morphology of microspheres, 104–105
 - nutrient encapsulation and release in gastrointestinal tract, 105–109
 - photographs of, beads by extrusion, 103*f*
 - photomicrograph of, microspheres incorporating riboflavin, 106, 108*f*
 - retinol encapsulation, 107, 109, 112*f*
 - riboflavin encapsulation, 106–107, 108*f*, 111*f*
 - stabilizing oil-in-water emulsions, 107, 109
 - TNO intestinal model (TIM1), 106–107, 110*f*
 - transmission electron microscopy of internal structure of, emulsion microspheres incorporating retinol, 107, 109, 112*f*
 - Young's modulus and rupture force of beads with alginate and SPI, 103*f*
- Soy protein hydrogels
- calcium cross-linked, 100–101

- cold-induced gelation of soy protein, 100
- scanning electron micrographs of, cold-set gels, 101*f*
- Soy soluble polysaccharide (SSPS)
 - charged polysaccharide, 159
 - diameter vs. pH during acidification of emulsions with, 164*f*
 - diameter vs. polysaccharide to sodium caseinate emulsions, 161, 162*f*
 - interaction with charged casein patches, 165
 - values of $1/(\text{photon transport mean free path}) [1/l^*]$ vs. SSPS concentration, 163*f*
 - values of $1/l^*$ of control emulsions and emulsions with, 165, 166*f*
 - See also* Oil-in-water (O/W) emulsions
- Spontaneous self-assembly, structural design principle, 9
- Spray-dried powders
 - coating material as barrier for release of core compounds, 214–215
 - coating material as release barrier, 214–215
 - differential scanning calorimetry (DSC) characteristics of, with orange oil and different wall materials, 224*t*
 - emulsification capacity, 222, 225, 228
 - infeed solids and oil load influencing retention of orange oil, 216*t*
 - influence of molecular weight of carbohydrates on orange oil retention during spray drying, 221*t*
 - moisture content and glass transition and melting characteristics, 221*t*
 - moisture/sorption isotherms of, with orange oil and different wall materials, 223*f*
 - scanning electron microscopy (SEM) of, with orange oil encapsulated with glucose syrup and modified starch, 227*f*
 - See also* Carrier properties
- Spray drying
 - aqueous two-phase systems (ATPS) for encapsulation, 239, 241–242, 244
 - ATPS concept for encapsulation of live probiotics, 242, 243*f*, 244
 - bovine serum albumin (BSA) in formulations with and without coating, 238, 240*f*
 - dynamic surface tension analyses of PVA, insulin and PVA/insulin, 238, 240*f*
 - emulsions, 235, 238
 - encapsulating food ingredients, 234
 - in-situ coating of powders, 238–239
 - poly(vinyl alcohol) (PVA)/dextran system, 241–242
 - schematic of encapsulation in ATPS, 241*f*
 - surface composition of spray-dried powders of casein micelles and lactose, 236*f*
 - surface composition of spray-dried protein/rapeseed oil/lactose emulsions, 237*f*
 - surface composition of spray-dried sodium caseinate/rapeseed oil/lactose emulsion, 237*f*
 - surface formation in, 234–235
 - survival rate of *Lactobacillus plantarum* in methyl cellulose/dextran, 242, 243*f*, 244
 - time-of-flight secondary ion mass spectrometry (ToF-SIMS), 234

- transmission electron microscopy (TEM) of particle containing casein micelles and lactose, 236*f*
- X-ray photoelectron spectroscopy (XPS), 234–235
- Starches
 - amorphous state of carbohydrate matrix, 216–217, 220
 - hydrolyzed, characterization, 215–216
 - modified, as alternative to gum arabic, 225
 - See also* Carrier properties
- Structural design principles
 - biopolymers, 6, 7*t*
 - building blocks, 5–6, 7*t*
 - delivery systems, 10–12
 - directed assembly, 10
 - directed self-assembly, 9–10
 - electrostatic interactions, 8
 - hydrogen bonding, 8
 - hydrophobic interactions, 8
 - lipids, 5, 7*t*
 - major food-grade structural components, 7*t*
 - molecular interactions, 6, 8
 - phase separation, 8–9
 - spontaneous self-assembly, 9
 - surfactants, 5–6, 7*t*
 - See also* Delivery systems
- Structured solids, zein, 148, 150–151
- Sunscreen actives, encapsulation in nanodispersions, 190*t*
- Surface-active lipids, adsorbing substance for layers, 26
- Surface composition, spray-dried protein/oil/lactose emulsions, 235, 237*f*
- Surface formation
 - composition analysis, 235, 236*f*
 - spray drying, 234–235
- Surface rheology
 - hydrophobin gels, 92, 96*f*
 - measurements, 92
- Surfactants
 - building blocks, 5–6, 7*t*
 - emulsions stabilized by, 72, 73*f*
 - fat content of model emulsions vs. emulsions stabilized by, 73–74, 75*f*
 - glycolipids, 81–84
 - nonylphenol ethoxylates, 118*f*
 - role of, solubility at oil-in-water (O/W) interface, 126, 127*f*
 - viscoelasticity of cream layers stabilized by, 72–73, 74*f*
 - water-in-oil (W/O) and O/W microemulsions with nonylphenol ethoxylates, 120*t*, 121*t*
 - See also* Microemulsions
- T
 - Targeting, nanodispersions, 189–191
 - Tea catechins, polyphenol compounds, 199–201
 - Tertiary emulsion, electrostatic deposition, 14*f*, 15
 - Thermal processing, primary and secondary emulsions, 19
 - Time-of-flight secondary ion mass spectrometry, surface analysis, 234
 - Titration method, microemulsions, 118, 122–123, 126*f*
 - Tocopherols, encapsulation in nanodispersions, 190*t*
 - Tocotrienols, encapsulation in nanodispersions, 190*t*
 - Topography, atomic force microscopy (AFM) images of zein on hydrophilic and hydrophobic surfaces, 148, 150*f*, 152*f*
 - Trehalose
 - crystallization of, vs. hydrolyzed starch, 220
 - differential scanning calorimetry (DSC) characteristics of spray-

- dried powders with orange oil and different wall materials, 224*t*
- encapsulation of fish oil, 222
- extent of crystallization of orange oil powder encapsulated with, 222
- moisture/sorption isotherms of spray-dried powders with orange oil and different wall materials, 223*f*
- replacing glucose syrup, 220, 221*t*
- Turbidity**
- anionic hydrogels in contact with emulsions at different pH, 29, 31*f*
- emulsions over time, 26, 28*f*
- monitoring adsorption of droplets to hydrogel surfaces, 26, 29*f*
- U**
- Ultrasonic spectroscopy, food emulsions, 159–160
- V**
- Villi, small intestine's absorptive surface, 185*f*
- Vitamins, encapsulation in nanodispersions, 190*t*
- Volatile components, flavor, 191, 247
- W**
- Water-in-oil (W/O) microemulsions
- nonylphenol ethylene oxide surfactants from, 120*t*, 121*t*
- type, 117–118
- See also* Microemulsions
- Whey proteins, potential nano-encapsulation systems, 133, 135
- X**
- Xanthan system, *in vivo* release of ethyl butyrate, 253–254
- X-ray photoelectron spectroscopy (XPS), surface analysis, 234–235
- Y**
- Young's modulus, beads with alginate and soy protein isolate, 102, 103*f*
- Z**
- Zein
- adsorption kinetics, 149*f*
- adsorption to carboxylic and methylated surfaces, 150*f*
- adsorption to hydrophobic and hydrophilic surfaces, 146–148
- AFM (atomic force microscopy) and section analysis of, deposited on hydrophilic surface, 150*f*
- AFM and section analysis of, deposited on hydrophobic surface, 152*f*
- applications of zein-based structured solids, 155
- coating ability, 145
- cooperative assembly of silicate-surfactant mesophases in water, 154*f*
- development of zein-oleic acid structures in response to solvent character, 153*f*
- diagram of tertiary structure, 147*f*
- nanotubes, 152, 154
- polypeptide groups, 145–146
- prolamine in corn endosperm, 143, 145

- scanning electron microscopy
 - (SEM) of zein-oleic acid film, 153*f*
- self-organization and characterizing
 - tertiary structures, 155
- small-angle x-ray scattering
 - (SAXS) for size and shape, 146
- structure, 145–146
- structured solids, 148, 150–151
- structure model of zein films, 152*f*
- TEM image of "tube", 154*f*
- topography of, deposits, 148
- transmission electron microscopy
 - (TEM) image of critical point freeze-dried, 146, 147*f*
- tubes, 151
- zein-fatty acid organization, 151–152, 154–155
- Zwitterionic surfactants, building blocks, 5–6, 7*t*

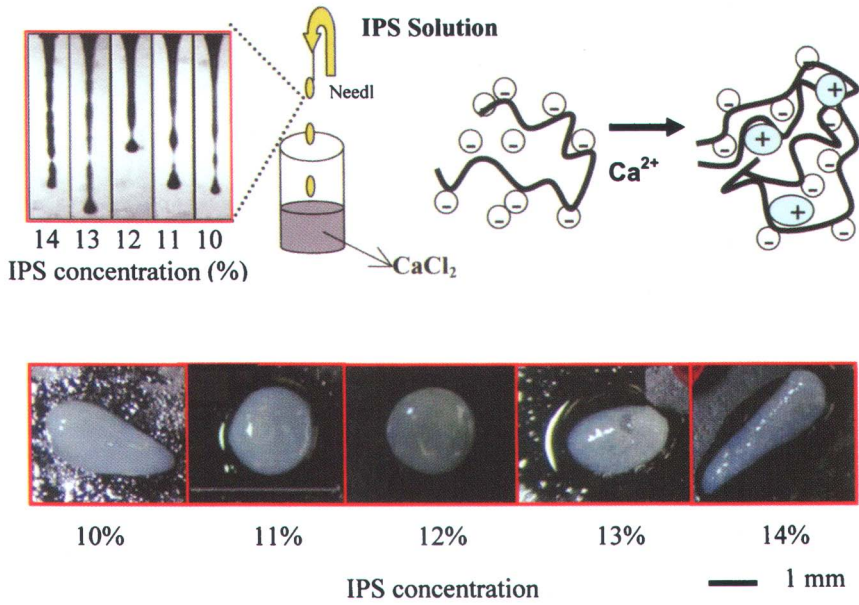


Figure 6.2. Photographs of soy protein beads prepared by extrusion at various protein concentrations.

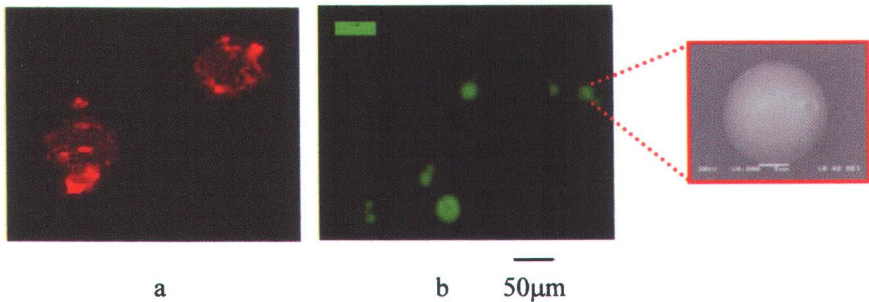


Figure 6.4. Fluorescence photomicrographs of soy protein micro-spheres prepared by extrusion (a) and emulsification/internal cold gelation (b), Insets show scanning electron microscopic image of micro-spheres in photograph b.